P l u t o n i u m   F u t u r e s —
T h e   S c i e n c e

Topical Conference on Plutonium and Actinides
Santa Fe, New Mexico (USA)
August 25–27, 1997

Sponsored by
Los Alamos National Laboratory
in cooperation with the
American Nuclear Society

Pu Futures '97

				Pu	Am	Cm	Bk
Pa	U	Np		Plutonium	Americium	Curium	Berkeli
rotactinium	Uranium	Neptunium		(145)	(145)	(247)	(247)
	238.029	237.0482					

Los Alamos
NATIONAL LABORATORY

Conference
Transactions

Plutonium Futures—The Science Conference

General Chairs:
>   *Bruce Matthews, Los Alamos National Laboratory*
>   *Paul Cunningham, Los Alamos National Laboratory*

Organizing Committee and Reviewers:
>   *Kyu C. Kim, Los Alamos National Laboratory*
>   *K. K. S. Pillay, Los Alamos National Laboratory*
>   *Gerd M. Rosenblatt, Lawrence Berkeley National Laboratory*
>   *Edward D. Arthur, Los Alamos National Laboratory*
>   *Allen Hartford, Jr., Los Alamos National Laboratory*
>   *Amy Longshore, Los Alamos National Laboratory*

Program Chairs:
>   *Kyu C. Kim. Los Alamos National Laboratory*
>   *K. K. S. Pillay, Los Alamos National Laboratory*

Program Committee:
>   *Gregory R. Choppin, Florida State University*
>   *Richard A. Bartsch, Texas Tech University*
>   *Rodney C. Ewing, University of New Mexico*
>   *Darleane Hoffman, University of California, Berkeley*
>   *Lawrence Berkeley National Laboratory*
>   *Lawrence Livermore National Laboratory*
>   *John R. Huizenga, University of Rochester*
>   *Abdul Fattah, International Atomic Energy Agency*
>   *J. M. (Mal) McKibben, Westinghouse Savannah River Company*
>   *Ann Gibbs, Westinghouse Savannah River Company*
>   *Nancy Trahey, National Institute of Standards and Technology*
>   *William G. Sutcliffe, Lawrence Livermore National Laboratory*
>   *Major Thompson, Westinghouse Savannah River Company*

An Affirmative Action/Equal Opportunity Empoyer

Plutonium Futures—The Science

Topical Conference on Plutonium and Actinides
Santa Fe, New Mexico (USA)
August 25–27, 1997

Conference Transactions

Los Alamos

NATIONAL LABORATORY

Los Alamos, New Mexico 87545

Contents

Presentations

Plenary Session

Materials Science

Transuranic Waste Forms

Nuclear Fuels/ Isotopes

Separations

Transuranic
Waste Forms

Isotopes/Nuclear
Fuels

Separations

Detection and
Analysis

Novel
Plutonium
Actinide
Compounds and
Complexes

Plutonium Futures—The Science Conference

Preface

S. S. Hecker
Director
Los Alamos National Laboratory

Plutonium is at once one of the most dreaded materials in the eyes of the public and the most fascinating of all elements scientifically. An artificial element discovered in 1941 by Glenn T. Seaborg and coworkers at the University of California, Berkeley, plutonium was immediately attractive as an atomic explosive during the Manhattan Project because of its large cross section. In fact, the special nuclear properties of ^{239}Pu make it a key ingredient of modern nuclear weapons and make it very attractive as a nuclear reactor fuel. Another isotope, ^{238}Pu, is an excellent heat source for thermoelectric generators because of its copious radioactive alpha-particle decay.

With the end of the Cold War, the world faces a surplus of weapons-usable plutonium. Today, the challenge is to dispose of the surplus plutonium and prevent the proliferation of nuclear weapons. The United States is working closely with Russia in developing suitable disposal options. The United States is pursuing a dual-track approach of burning surplus plutonium as mixed oxide fuel or disposing it through vitrification and burial. A corollary challenge is to deal with the legacy of 50 years of nuclear materials and weapons production–that is, stabilizing production residues and scrap, disposing of radioactive wastes, and cleaning up the production sites. Again, this will have to be accomplished while protecting the plutonium and ensuring the health and safety of workers and protecting the environment. Moreover, we face the challenge of how to manage the accumulating plutonium inventories being produced in nuclear power plants around the world. The industrialized nations of the world will have to weigh carefully the benefits of plutonium-containing nuclear fuels versus the potential proliferation problems associated with reprocessing plutonium from spent fuel.

Clearly, many of these issues will require political solutions since public acceptance is such a strong driver in the democracies of the world. However, it is also time for the scientists and engineers to refocus their scientific attention to developing a better fundamental understanding of plutonium, its compounds, and its interaction with humans and the environment. The special nuclear properties of plutonium are widely appreciated. Much less understood is the fact that plutonium also has a most unusual electronic structure. Specifically the close proximity of the 7s, 6d, and 5f electrons in valence orbitals generates a strong competition among these configurations. In the solid state, plutonium sits on the edge between 5f electrons being localized (magnetic) or delocalized (bonding). Combined with the asymmetry of f-electron orbitals, this makes plutonium extremely sensitive to changes in temperature, pressure, and chemical alloying—resulting in multiple allotropes and anisotropic structures and properties. Plutonium also has a great propensity for oxygen and hydrogen. The aqueous chemistry of plutonium is complicated by the existence of multiple oxidation states with similar reduction potentials, and the strong tendency for the aqueous cations to complex with a wide variety of anions. Similarly, the chemistry of insoluble or immobile plutonium species in the environment is also complex—sorption, hydrolysis, precipitation and complexation processes all play an important role. In addition, we find the combination of nuclear and electronic processes complicate the behavior even further. Nuclear induced self-irradiation effects in plutonium influence the properties of solid and liquid phases, with important implications to biological systems.

In these conference transactions we aim to enhance the dialog among scientists on the fundamental properties of plutonium and their technological consequences. Moreover, we hope that this conference will stimulate the next generation of scientists and students to study the fundamental properties of plutonium. We are encouraged by the great response we received to our call. The papers cover the entire spectrum of plutonium behavior. The contributors come from the scientific community across the world, with many excellent papers by authors from several countries. I am pleased that the Los Alamos National Laboratory was able to sponsor this conference in cooperation with the American Nuclear Society. Our hope is that a renewed scientific interest in plutonium and the actinides can be generated, which in turn, will allow us to make great strides in solving the Cold War legacy problems and allow us to take full advantage of the benefits of the enormous energy potential of plutonium for the benefit of mankind.

Plutonium Futures—The Science

Abstract

Compiled by
Amy Longshore
*Los Alamos National
Laboratory*

Los Alamos National Laboratory in cooperation with the American Nuclear Society sponsored the international conference *Plutonium Futures—The Science* on August 25–27, 1997 at the Hilton Hotel in Santa Fe, New Mexico, USA. The conference hosted scientists, engineers, and students from Department of Energy national laboratories, other federal and international institutions, universities, and industry to discuss our current understanding of plutonium and actinide sciences and to rejuvenate the science needed for solving important national and international issues, including the safe storage/ultimate disposal of surplus weapons materials and the management of large inventories of actinides from civilian nuclear power generation. The technical basis for addressing these issues requires capabilities in plutonium and actinide science and technology. The scientific program comprised plenary session presentations followed by oral and poster presentations of papers covering topics on materials science, transuranic waste, isotopes/nuclear fuels, separations, environmental and biosphere chemistry, detection and analysis, and novel plutonium/actinide compounds and complexes. The document is a collection of extended abstracts from papers presented during the plenary, oral, and poster sessions.

Plenary Talks

The Role of Plutonium in Energy Production Outside the United States

A. E. Waltar
Advanced Nuclear & Medical Systems

Few events in history have borne more potential impact for the human condition than the discovery of plutonium. Proponents of this vastly powerful substance hail it as the energy source that can fuel the world for countless centuries. Opponents decry it as "unnatural" and are clamoring for the world to rid itself of this "dangerous" substance.

Ironically, it is within the United States, the nation in which this substance was discovered and first harnessed for energy production, that the most vocal dissonant voices are being heard. A hard-core anti-nuclear subculture has been highly successful in manipulating the media and even major political movements into believing that the U. S. would be better off to rid itself of plutonium at the earliest possible date.

Yet despite what happens in the U. S., the value of plutonium has not gone unnoticed in the rest of the world. Plutonium will be used in ever increasing quantities to provide the prodigious quantities of electricity required to fuel an increasing global population. Modern communications have allowed this growing population to become more and more aware of the quality of life that electricity can provide. These world citizens are not to be denied.

Nearly 20% of the electricity generated around the world currently comes from nuclear power. Whereas most of the population believes this energy is generated solely from uranium, the fact is that approximately one-third of it is generated by plutonium— simply due to the buildup of plutonium in the normal isotopic balance of nuclear reactor operations. With the higher burnups now being attained in commercial light water reactors, the fraction of electricity generated by plutonium will continue to increase.

As a direct result of the plutonium produced during normal power reactor operations, over 60 metric tons (MT) of plutonium is currently being discharged in spent fuel from the global commercial nuclear power industry each year. According to IAEA projections, this will rise to over 100 MT/year early in the next century, reaching some 400 MT/year by 2050. The total accumulated plutonium in spent nuclear fuel is now about 100 MT, and is projected to rise to some 10,000 MT by the year 2050.

Given the enormous energy potential of this fuel, it has always been the goal of the scientific community to recycle this spent fuel to extract the useable plutonium (and uranium) setting aside the fission products for burial or future beneficial use. With only a few exceptions, this is precisely the path being followed by most modern countries outside the U. S. Mixed (Pu, U) Oxide (MOX) fuel was first tested in light water reactors in the 1960s in Belgium, and has since been utilized in France, Germany, and Switzerland. Some 22 reactors in Europe are currently loaded with sizeable quantities of MOX fuel, with about twice this many reactors scheduled for MOX loadings within the next 10 years. Three MOX fuel fabrication facilities are already in operation in Europe. Concrete plans for burning MOX are being implemented in Japan, and strong interest has been shown in South Korea and Russia, the latter interest being generated mainly by the desire to burn weapons-return plutonium.

The use of recycled plutonium for energy production will undoubtedly continue to generate controversy, both within and outside of the United States. However, the fact remains that this material is currently the only known material that has

the technical maturity to provide the energy needs to a growing world population for literally a millennia— and to do so in a manner compatible with preserving our environment. Consequently, it is essential that the scientific community find effective ways to help take the mystery out of plutonium and provide assurances to a skeptical public that the continued development and utilization of plutonium will provide them a far better quality of life than any other known source of energy. A denial of the proper utilization of plutonium will most assuredly result in more reliance on fossil fuels, with the attendant crucially needed for a wide variety of other uses.

What are the consequences of the United States permanently turning its back on the commercial utilization of plutonium for the generation of electricity? Would this significantly alter the approach the rest of the world may take? If experience to date with the U. S. denial of reprocessing has any bearing on this question, the answer is that it will have very little lasting effect, internationally. In fact, the U. S. stand on reprocessing could well be argued to have been counterproductive to the stated U. S. non-proliferation goals, since the U. S. soon became known as an unreliable supplier. This spurred both France and the U. K. into an aggressive program to become self-sufficient, and their closed nuclear system is now fully operational.

Consequently, a denial of the benefits of plutonium by the U. S. will, at a minimum, result in further erosion of U. S. influence on nuclear matters on the international scene. It will also (1) eventually place the U. S. in a strong dependency on other nations for energy resources, and (2) gradually force our country into a third-world status. The full consequences of such a scenario would please very few thinking Americans!

Plutonium is currently being recognized outside of the United States as a most precious commodity. The fundamental question is whether the U. S. has the courage to regain leadership in this field, or whether we will elect to be a bystander. The fate of our nation awaits that answer.

Options for Plutonium Utilization:
Sustainable Energy Development, Safeguards,
and Nuclear Safety

Introduction

V. M. Mourogov
International Atomic Energy Agency, Austria

In the 50 years since its discovery, plutonium has left its undeniable mark on the history of civilization. Although it made an ominous beginning as the fuel for the world's first atomic bomb which ended World War II, plutonium has a key role in supplying vast amounts of electricity to a large segment of the world's population. Even today, nuclear power constitutes 17% of all electricity generated and the contribution through fissioning of plutonium approaches 50% near the end of a typical commercial fuel cycle. Despite this impressive progress, the future of plutonium, as an energy source, has become clouded in many countries. Key issues relate to safety, waste disposal, non-proliferation concerns, economics, and public acceptance. The issue of public acceptance is an integrated response to the other factors and must be faced constructively if the potential of plutonium is to be harnessed for the long-term benefit of humanity.

Properties of Plutonium

A nuclear weapon can be made from essentially any grade of plutonium. Consequently, it is essential that all plutonium be effectively safeguarded. However, plutonium is far less dangerous to the human body than widely believed. No measurable ill-health effects have been noticed in the world's population due to the ten tons of vaporized plutonium dispersed into the atmosphere from weapons testing. Workers exposed to plutonium in accidents at Los Alamos and Rocky Flats in the U.S. have shown no adverse health effects. Although negative health effects have been observed in workers who received high plutonium doses at the Mayak facility in Russia, it must be noted that these negative effects are far less significant than those from smoking.

Use of Plutonium in the Civilian Sector

The first MOX fuel was used in the 1960s in Belgian PWRs. Since that time, MOX has been used in commercial quantities in light water reactors in France, Germany, and Switzerland. To date, the total energy production from irradiated MOX assemblies amounts to ~11 GWy. There are now plans to use MOX in Japan, Britain, Republic of Korea, and Russia. Some challenges associated with the multirecycling of MOX in light water reactors include the buildup of minor actinides.

The heavy water moderated Fugen reactor in Japan has been successfully operating with MOX fuel since 1979.

France, Russia, and Japan have accumulated experience on the use of MOX fuel in fast reactors. The CAPRA program in France was undertaken to exploit the flexibility of fast reactors to burn or to breed starting from a large variety of plutonium vectors. In the U.S., the Integral Fast Reactor (IFR) was under development by Argonne National Laboratory (ANL) from 1984 to 1994. The program was canceled by the government despite strong objections from the scientific community. One of the key attributes of the IFR system is that no separated plutonium exists at any point of the fuel cycle. The system also has some impressive passive safety characteristics. Heavy metal cooled fast reactors have been

proposed by some leading Russian scientists due to special advantages such as chemical compatibility with air, very high boiling temperature, near natural circulation capability, and near zero coolant void coefficient of reactivity.

A joint program of Canada, Korea, and the U.S. called "DUPIC" defines a method for inserting spent fuel from PWRs directly into CANDU reactors for further burning.

MHTGR reactors may have the maximum capability of any reactor type to eliminate plutonium in a single cycle. For achieving a "deep" plutonium burn, substitutes for uranium, such as Th, SiC, $MgAl_2O_4$, ZrO_2, etc are also under investigation for thermal and fast reactor fuels. Substantial interest has been generated in the development of Accelerator-Driven Systems (ADS). However, such proposals are still in a highly undeveloped stage. A note of caution would be in order on this issue. If the world proceeds under the assumption that plutonium should be eradicated, a time will surely come when our planet is left with only natural uranium and depleted uranium. Without plutonium it will be nearly impossible to utilize the remaining uranium.

Since the end of the Cold War, attention is being focused on alternatives to remove plutonium from the weapons stockpiles. While Russia has long preferred the option of burning it in the form of MOX in fast and thermal reactors, there has been a raging debate on this alternative in the U.S. Ex-weapon plutonium disposition issues were deeply discussed at the international meeting held in Paris in October 1996 on "Safe and Effective Management of Weapons Fissile Materials No Longer Required for Defense Purposes" and recently at the IAEA International Symposium on "Nuclear Fuel Cycle and Reactor Strategies: Adjusting to New Realities" held in Vienna in June 1997.

Nuclear Technology and Sustainable Development

Energy is an essential input for sustainable development of the world population. Although projecting energy needs over long time frames such as a century is difficult, the International Nuclear Societies Council (INSC) has conducted global studies on this subject. The results indicate that by the year 2050 the energy demand would rise to 2.6 times that in the year 2000, even if the standard of living in developing countries rises only to half that enjoyed by the developed world. Without the use of plutonium, it is inconceivable to sustain nuclear energy production over such long time frames. The Los Alamos National Laboratory is developing an integral modeling capability taking into account several more variables in making projections about plutonium stocks. Initial results indicate that the advent of fast reactors can lead to significant reductions in nuclear proliferation concerns mainly because plutonium can then be well protected within reactors.

Nuclear technology has been playing an important role in sustainable development over the past five decades. The applications include medical diagnostics, nuclear therapeutics, agricultural advances, food preservation, and a wide variety of other industrial applications. As one measure of the impact of nuclear science and technology in our world, a 1991 study revealed that radioisotopes accounted for 257 billion dollars and provided 3.7 million jobs in the U.S. alone. Commercial nuclear electricity added another 73 billion dollars and 400,000 jobs. If the general public could be made aware of the benefits already being delivered by nuclear science, public acceptance may improve. In this context, plutonium should be viewed as a necessary link in providing the large quantities of energy required to sustain a hungry and thirsty world for the next century and beyond.

Conclusion

The following points must be borne in mind in formulating policies with regard to the use of plutonium:

- Nuclear technology must be viewed globally

- Energy needs will grow substantially

- Greater care in plutonium utilization could lead to greater benefits

- Effective plutonium management policy cannot be based on fear

- National sovereignty is not the most appropriate approach in dealing with nuclear waste management issues

- Nuclear technology has been providing significant benefits beyond energy production

- Nuclear waste generally considered as an undesirable component of the nuclear fuel cycle could also be converted into a vital resource at a future point in time

Whatever policy options are chosen regarding plutonium management, they would have a far reaching impact on the future of human civilization in the coming centuries.

Materials Science

Materials Science of Plutonium and Americium with Group IV Elements: Compounds and Solid Solution Relevant to Nuclear Applications

The science of immobilizing materials for nuclear applications has been an important topic for several years and many different studies have been performed and reported on this topic. The interest has varied from determining physical properties of many types of materials to modeling long-term performances of the materials suggested for immobilization hosts. With respect to the latter, it is critical to have valid, fundamental information of the materials science of the particular materials as well as short-term experimental results. Our experimental efforts have been aimed at addressing the science of different materials having some potential for such nuclear applications with a particular aim of addressing and acquiring information that would be required for estimating long-term evaluations of performance.

Several ceramic-type materials have been discussed as potential hosts for immobilization of actinide materials. One of the most recognized materials, Synroc, is based on mixtures incorporating Al, Ba, Ca, Ti, and Zr for the host. This material was discussed in the late seventies and several varieties have been subsequently developed; one of these has been the well-known zirconolite. Zirconolite is essentially a ceramic having a nominal composition of $CaZrTi_2O_7$, which contains two of the Group IV elements. Efforts with these materials usually support the use of variable compositions and phases to maintain maximum flexibility for applications with different elements and oxidation states.

Our efforts have been developed more along the line of fundamental chemistry of simpler (e.g., binary) compounds between actinide and other inorganic ceramic-like materials. One area of interest has been the materials science of oxide compounds formed with the actinides and the Group IV elements, Ti, Zr, and Hf. In the particular studies reported here, we concentrated on materials formed between either Pu and Am and Zr or Hf, with the focus being on oxide pyrochlores and solid solutions of oxides of these elements. Special aspects of the work dealt with the role of the actinide's oxidation state in determining the products obtained and differences in the oxidation state behaviors of Pu and Am in these ceramics as compared to other immobilization hosts that have been proposed.

Oxide pyrochlores of the general type, $A_2B_2O_7$, where A and B are metallic cations of different oxidation states, exhibit a variety of interesting physical properties. The lanthanide pyrocholore, $La_2Zr_2O_7$, which belongs to the $A_2^{3+}B_2^{4+}O_7$ family, is known to exhibit low-leachability in water, significantly lower than some glass matrices that have been discussed for immobilization materials. Some of the materials we shall discuss concern compounds of this class. We have determined that the oxidation state of the actinide is especially critical in the particular products formed, and that oxidation or reduction of the actinide can totally change the product(s) and their physical nature.

In this regard, we have employed several synthetic approaches and evaluated the products by different techniques, one of the major ones being x-ray powder diffraction.

The presentation will include a discussion on the crystal structures and the role they play in the properties of the products, the importance and control of oxidation states in the formation of specific materials and their properties, an overall consideration of these materials, and their potential applications for nuclear applications.

P. E. Raison
R. G. Haire
Oak Ridge National Laboratory

T. Sato
T. Ogawa
Japan Atomic Energy Research Institute
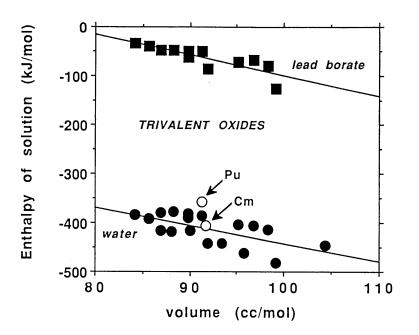
Thermochemistry of Crystalline and Amorphous Phases Related to Plutonium Containment

The incorporation of actinides and radioactive fission products into solid glassy and ceramic materials is crucial to their containment. This paper focuses on thermodynamic aspects of such materials. Vitrification (placing radionuclides into a borosilicate, aluminosilicate, phosphate, or other matrix prepared by melting) results in predominantly glassy log of material whose durability is governed both by its intrinsic thermodynamic properties and by the environment in which it sits. Because actinides have a profound influence in modifying and disrupting the molecular-level structure of a glass, a discussion of glass structure and thermodynamics is presented which culminates with an assessment of what is known about the thermochemistry, phase separation, and crystallization of lanthanide- and actinide-containing glasses.

Figure 1 compares the enthalpies of solution of trivalent lanthanide and actinide oxides in water at 25°C and in molten lead borate near 700°C.

Crystalline waste forms consist of host phases (perovskite, zirconolite, pyrochlore, zircon) which incorporate actinides. Both zirconolite and zircon are being investigated as hosts for plutonium. The thermodynamics of these families of related phases is reviewed, with emphasis on systematic trends which can be used to estimate the energetics of actinide incorporation. Much more thermochemical study of these phases is needed and is being started. Table 1 gives thermochemical data currently available.

Prospects for using oxide melt solution calorimetry to study the energetics of incorporation of Pu into ceramic and glassy waste forms are discussed.

A. Navrotsky
University of California at Davis

Figure 1. Enthalpy of solution of trivalent lanthanide oxides in molten $2PbO \cdot B_2O_3$ at 700°C and enthalpy of solution of lanthanide and actinide oxides in water at 25°C, each plotted against molar volume.

Table 1.
Thermodynamic
properties of
crystalline phases
related to actinide
and fission product
containment.

Phase	Composition	Formation from Oxides	
		ΔH°_{298}(kJ/mol)	ΔS°_{298}(J/mol•K)
perovskite	$CaTiO_3$	-81.5	+4.6
zircon	$ZrSiO_4$	-25.9	-7.7
monazite	$LaPO_4$	?	
titanite (sphene)	$CaTiSiO_5$	-106.8	-1.0
strontium orthosilicate	Sr_2SiO_4	-212.4	
strontium metasilicate	$SrSiO_3$	-143.3	
strontium titanate	$BaTiO_3$	-135.1	+3.3
barium titanate	$BaTiO_3$	-152.3	-16.0
calcium zirconate	$CaZrO_3$	-31.3	+10.4
strontium zirconate	$SrZrO_3$	-75.9	+8.4
barium zirconate	$BaZrO_3$	-123.9	+2.0
lanthanum zirconate	$La_2Zr_2O_7$	-136.1	
barium orthosilicate	Ba_2SiO_4	-285.3	
barium metasilicate	$BaSiO_3$	-147.6	
strontium zirconium silicate	$SrZrSi_2O_7$	-127.5	
strontium zirconium silicate	$Sr_7ZrSi_6O_{21}$	-1112.9	
cerium aluminate	$CeAlO_3$	+110.4[a]	
cerium aluminate	$CeAl_{12}O_{19}$	+151.6[a]	
yttrium aluminate	$YAlO_3$	-23.6	
yttrium aluminate	$Y_3Al_5O_{12}$	-115.4	
lanthanum aluminate	$YAlO_3$	-63.2	

[a] From CeO_2 and Al_2O_3 with evolution of O_2.

Point Defects in the Solid Solutions of Actinide Oxides $(M,An)O_{2+x}$ and Properties of Fuels (An=Np, Pu, Am, or Cm)

Introduction

M. Beauvy
C. Duriez
T. Gervais
J. Larroque
J. M. Bonnerot
Commissariat à l'Energie Atomique, France

The mixed oxides of uranium and plutonium have been used with success for more than 30 years as fuels in the nuclear power reactors in France. The behavior of the standard fuels of the Fast Breeder Reactors with about 20 at.% of plutonium has been studied since the beginning of the 1970s, and more recently, the MOX $(U_{>0.92}Pu_{<0.08})O_{2+x}$ has been used in the Pressurized Water Reactors (PWR). The properties of these fuels had been measured in our laboratory, and now they are relatively well known. Today, new oxide fuels of plutonium or other actinides are proposed to burn more plutonium or to transmute the actinides with high radiotoxicity for a long time. The measurements of the basic properties of these new "fuels" are under investigation but these studies must be correlated to our general knowledge on the mixed oxides of actinides.

New Studies on the Actinide Oxide Compounds

Among the new fuels of plutonium or actinides studied and developed for tomorrow are the MOX $(U_{<0.92}Pu_{>0.08})O_{2+x}$ for the PWR, the mixed oxides with more than 40 at.% of plutonium for the FR, and the mixture of actinide oxides with inert oxide for the transmutation (actinide = Np, Pu, Am, or Cm).

The crystallochemical analysis of the solid solution $(U,Pu)O_{2+x}$ has been done for all the compositions of the oxide fuels. The nature of the bondings between the atoms in the crystals have been considered, and the agreement with the results of thermodynamic measurements has been analyzed. New equipments for measurements of the thermophysical properties on the actinide compounds have been developed in our laboratory. The measurements of specific heat, thermal diffusivity, and mechanical properties at high temperature are in progress on these fuels, and some preliminary results will be presented to validate the crystallochemical analysis.

Point Defects in the Solid Solution $(U,Pu)O_{2+x}$ and Properties of Fuels

The structure of the actinide dioxides AnO_2 is cubic-fluorite type, and the bondings between the atoms in the crystal are usually considered to be with a strong ionic character. The limits for the saturation of substitutions of the cations (Pu/U), oxygen vacancies, and interstitial oxygens in the mixed oxides $(U,Pu)O_{2+x}$ have been determined from the crystal cell parameters measured on the fuel pellets and from the ionic radii of the elements. In the hyperstoichiometric mixed oxide $(U,Pu)O_{2+x}$, there is practically no possibility for the oxygen to be on interstitial site in purely ionic crystal. In the stoichiometric mixed oxides $(U,Pu)O_2$, there are different sites for the substitutional atoms of plutonium making different clusters with the uranium atoms and the oxygen atoms, and therefore, several sublattices can be found in the crystals. Considering that the distribution of the point defects is homogeneous in these crystals, the composition limits of the oxide for the saturation of each type of cluster in the lattice have been evaluated. These limits in content of plutonium among the cations are multiples of 6.25 or 20 at.%. They will be compared with the U-Pu-O phase diagram and with the results of the analysis of the effect of plutonium content on physical and transport properties of the mixed oxides. The oxidation states of the cations and the thermodynamic data

for $(U_{>0.8}Pu_{<0.2})O_{2+x}$ will be also considered in this discussion. The effect of the heterogeneity of the composition of the oxide in the pellet on the properties of fuel will be described from the distribution of the point defects in the crystals.

Point Defects in the Solid Solutions and Properties of (M,An)O$_{2+x}$

The same analysis has been done for the mixed oxides of actinides $(M,An)O_{2+x}$ where An is the actinide (U, Np, Pu, Am, or Cm) and M is another element (for instance Y and Ce). These solid solutions are proposed for the transmutation of the actinides or in the CAPRA program. The results of thermophysical properties of the solid solutions measured at high temperature in our laboratory are used to confirm the conclusion of the crystallochemical analysis.

Conclusion

Crystallochemistry and thermodynamics must be used simultaneously to analyze the properties of plutonium or actinide oxide fuels. The atom density and the radius of the atoms in the ionic solid solution $(M,An)O_{2+x}$ are not compatible with ideality for this solid solution. Different point defects and clusters must be considered successively to characterize all the compositions of a mixed oxide, and therefore, there are several mechanisms to explain the variation of the properties of these fuels.

Transuranic Waste Forms

Immobilization of Pu-Rich Wastes in Synroc

Zirconolite-rich Synroc is a ceramic host for the immobilisation option for the final disposition of weapons grade Pu. Some of the Pu considered for immobilisation contains significant impurities whose role in the waste form chemistry and processing must be understood.

The incorporation of pure Pu in zirconolite utilising processing atmospheres ranging from oxidising to reducing is reasonably well understood on the basis of detailed compositional, x-ray absorption and x-ray diffraction data. Pu can enter the Ca site at levels of up to ~0.5 formula units (~ 30 wt % PuO_2), in either the +3 or +4 states. However only Pu^{4+} can enter the Zr site and then only at levels of ~0.15 formula units.[1] At higher levels of Pu, mixtures of different zirconolite structures form, sometimes together with pyrochlore, and these phases are distributed on a sub-micron scale, depending on the firing temperature.

The main "impurity" in the Pu of interest in the present work is U, and detailed data on the co-incorporation of Pu and U are being collected. Two approaches are being examined, based on previous work: (a) to maximise the actinide content of the zirconolite (~0.5 formula units), the actinides should be incorporated in the Ca site and (b) to maximise the pyrochlore phase abundance for the minimum amount of actinide, it is clear that the actinides need to be incorporated in the Zr site, with the total tetravalent actinide content being approximately 0.5 formula units. Examination of the general viability of a pyrochlore-based ceramic as well as having small amounts of pyrochlore present in zirconolite-based ceramics is an implicit aim of (b). Other "impurity" elements which have been demonstrated in the present work to have significant solubilities in zirconolite include Ga, Al, Fe, Mg, Cr, Ni, and Ta. The effects of F and Cl are discussed.

The solubility of the neutron poisons Hf and Gd has been shown to be extensive (0.7 and 1 formula unit respectively)[2] and that of Sm is now shown to be very similar to that of Gd. The inclusion of various non-actinide impurities accompanying the Pu in zirconolite is then considered and data on co-incorporation of Pu, U, and neutron poisons will be given.

There are process advantages in using the multi-phase zirconolite-rich Synroc, notably in minimising the zirconolite grain size to avoid microcracking effects attendant upon radiation damage and to allow chemical flexibility in terms of waste/precursor ratio. Some of the impurity elements mentioned above can also partition into the non-zirconolite phases.

The incorporation in zirconolite-rich titanate ceramics of Pu as a nitrate solution or as high-fired PuO_2 has been demonstrated[3] but not previously reported in the open literature; details will be given.

The excellent aqueous durability of zirconolite at 90°C in deionised water and over a range of pH values has been reported previously,[4] and recent data[3] obtained on zirconolite-rich titanate ceramics at 200°C in deionised water, a silica-rich water, and a brine will be summarised.

The practicality of immobilising Pu-rich wastes by the Synroc process will be discussed, in terms of feedstocks, redox constraints, mode of hot-pressing, etc.

E. R. Vance
A. Jostsons
M. W. A. Stewart
R. A. Day
B. D. Begg
M. J. Hambley
K. P. Hart
ANSTO
Australia

B. B. Ebbinghaus
Lawrence Livermore National Laboratory

References

1.   E. R. Vance et al., in *Scientific Basis for Nuclear Waste Management XVIII*, T. Murakami and R. C. Ewing, Eds. (Materials Research Society, Pittsburgh, PA, 1979), p. 767.

2.   E. R. Vance et al., in *Scientific Basis for Nuclear Waste Management XIX*, W. M. Murphy and D. A. Knecht, Eds. (Materials Research Society, Pittsburgh, PA, 1996), p. 41.

3.   E. R. Vance et al., "Incorporation of High-Fired Plutonium Oxide in Zirconolite-Rich Synroc," ANSTO report C469 (1997).

4.   P. J. McGlinn et al., in *Scientific Basis for Nuclear Waste Management XVIII*, T. Murakami and R. C. Ewing, Eds. (Materials Research Society, Pittsburgh, PA, 1995), p. 847.

Amorphous Zirconium Hydrosilicate (AZHS)—
A Prospective Material for Pu Fixation

The disposal of Pu must be considered in its different forms: metallic Pu from weapons pits; Pu in spent fuel; and Pu-containing residues, ashes, and solutions. Therefore, more than one option for the disposition of Pu must be considered: Pu "burn-up" in MOX fuel; Pu immobilization in a ceramic matrix; and Pu vitrification. Regardless of the strategy adopted for the disposition of Pu, a necessary first step is to create a stable and environmentally safe interim form for Pu. This paper discusses a possible approach toward Pu stabilization.

A zirconium-silicate gel can be used for the durable fixation of Pu and actinides from solution, in particular, when they are accompanied by significant admixtures of non-radioactive elements. This gel is prepared by mixing methanol solutions of $(C_2H_5O)_4Si$ and Zr-actinide nitrates. The amorphous zirconium hydrosilicate (AZHS) of variable chemical composition, as a result of gel solidification, may be considered an unusual Pu-host-phase. However, this approach is based on the results of a detailed examination of a natural zirconium-silicate material "gel-zircon," which was studied by transmission electron microscopy (TEM), electron microprobe energy-dispersive x-ray spectroscopy (EDS), x-ray diffraction (XRD), U-Pb age dating, and other methods.[1] Previous studies have shown that gel-zircon is a chemically durable solid of the following composition (wt %): Zr-20.9 to 26.5; Si-8.0 to 10.4; U-3.6 to 12.8; Fe-0.7 to13.8; and Al- 0.5 to 2.0 plus water. Naturally occurring "gel-zircon" is stable despite an age of more than 400 million years. "Gel-zircon" is assumed to be the result of natural gel precipitation under metasomatic conditions, and therefore, is a metastable material which, over time, may crystallize. However, the high concentration of U in "gel-zircon" may cause the competing process of amorphization to occur due to radiation damage caused by α-decay. We propose that the equilibrium between crystallization and metamictization is one of the reasons for the long-term stability of "gel-zircon." The results of a "gel-zircon" leaching study are also discussed.

We suggest the use of AZHS as a synthetic analogue of "gel-zircon" for the durable fixation of weapons-grade Pu and actinides for the goal of long-term intermediate storage. The advantages include:

1. AZHS can accommodate not only Pu, but also other elements in a broad range of concentrations (in the range of a few wt % or more), which is important for industrial scale technologies.

2. AZHS can be used as a starting material for the synthesis of a crystalline ceramic based on two host phases, zircon and zirconia, for the final disposal of excess weapons Pu in deep geological formations.

3. AZHS has a natural analogue, which is apparently stable over the long-term.

4. Preliminary experiments show that the synthesis of AZHS may be carried out by the sol-gel method, possibly *in situ* in tanks or canisters under relatively low temperatures (<200°C).

Reference

1. K. B. Helean, B. E. Burakov, E. B. Anderson, E. E. Strykanova, S. V. Ushakov, and R. C. Ewing, "Mineralogical and Microtextural Characterization of "Gel-Zircon" from the Manibay Uranium Mine, Kazakhstan," *MRS Symposium Proceedings Scientific Basis for Nuclear Waste Management XIX* (in press).

B. E. Burakov
V. G. Khlopin Radium Institute, Russia

K. B. Helean
University of New Mexico

E. B. Anderson
V. G. Khlopin Radium Institute, Russia

R. C. Ewing
University of New Mexico

A. F. Smetannikov
V. G. Khlopin Radium Institute, Russia

New Ceramics for Tetravalent Actinides: $Th_4(PO_4)_4P_2O_7$. Leaching Tests for U^{4+} and Pu^{4+}
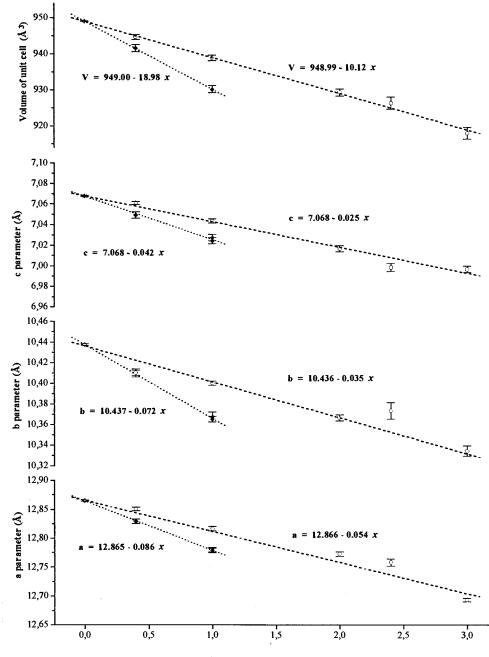
The chemistry of tetravalent uranium and thorium phosphates have been completely re-examined. It appeared that most of the well-known compounds, described in the literature, do not exist or have been wrongly identified.[1-4] In the ThO_2-P_2O_5 system, the thorium phosphate $Th_3(PO_4)_4$ cannot be synthesized and must be replaced by the thorium phosphate-diphosphate $Th_4(PO_4)_4P_2O_7$ (TPD),[4] which crystal structure as well as some of its physico-chemical properties like solubility in various media has been already studied.

The replacement of Th^{4+} by smaller ions like U^{4+} and Pu^{4+}, in TPD structure has been investigated. The solid solutions $Th_{4-x}U_x(PO_4)_4P_2O_7$ and $Th_{4-x}Pu_x(PO_4)_4P_2O_7$ using ^{238}U and ^{239}Pu have been synthesized with the following x values: $0 \le x \le 3.2$ for uranium and $0 \le x \le 1.0$ for plutonium. The evolution of the cell parameters (Figure 1) confirms that plutonium (r= 0.96 Å) and uranium (r = 1.00 Å) take the place of thorium (r=1.04Å) in the str ucture at the tetravalent state. For plutonium, the upper value of x calculated from the evolution of the cell parameters is equal to 1.7.

Attemps to get cerium (IV) compounds considering cerium as a surrogate for plutonium have failed. Indeed, Ce^{4+} is reduced to Ce^{3+} during the heat treatment which leads to a mixture containing $CePO_4$ (monazite structure) and TPD. Polyphase systems have been also obtained for several trivalent rare-earths.

Leaching tests on the thorium-uranium phosphate-diphosphate $ThU_3(PO_4)_4P_2O_7$ have been achieved in water. Uranium has been measured in aqueous solution by Laser-Induced Time-Resolved Spectrofluorometry (LITRS) in the uranyl form. The concentration of uranium at equilibrium after 24 days of contact of water with the solid is near $10^{-6}M$. The determination of ^{239}Pu in the same conditions for $Th_3Pu(PO_4)_4P_2O_7$ is under progress. Other series of leaching tests have been performed with the thorium phosphate-diphosphate doped with ^{241}Am, ^{235}Np, ^{236}Pu, and ^{244}Cm at tracer scale.

The pressure and temperature to get the sintering of TPD have been also determined. A sample axially pressed at 0.5 GPa at room temperature then heated up to 1250°C for 12 hours gives a pellet mechanically strong with a density equal to 95% of the calculated value.

N. Dacheux
R. Podor
V. Brandel
J. F. LeDû
B. Chassigneux
M. Genet
Nuclear Physics Institute, France

Figure 1. Evolution of the cell parameters and the volume in terms of *x* value.

$V = 949.00 - 18.98\ x$

$V = 948.99 - 10.12\ x$

$c = 7.068 - 0.042\ x$

$c = 7.068 - 0.025\ x$

$b = 10.437 - 0.072\ x$

$b = 10.436 - 0.035\ x$

$a = 12.865 - 0.086\ x$

$a = 12.866 - 0.054\ x$

x in $Th_{4-x}Pu_x(PO_4)_4P_2O_7$ (solid diamonds) and in $Th_{4-x}U_x(PO_4)_4P_2O_7$ (open circles)
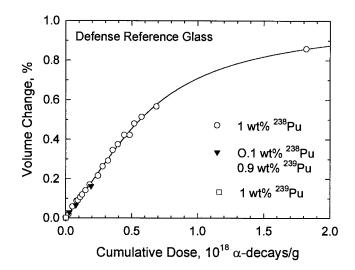
References

1. P. Benard, D. Louër, N. Dacheux, V. Brandel, M. Genet, *Chem. Mater.* **6**, 1049 (1994).

2. N. Dacheux, V. Brandel, M. Genet, *New J. Chem.* **19**, 1029 (1995).

3. V. Brandel, N. Dacheux, M. Genet, *J. Solid State Chem.* **121**, 467 (1996).

4. P. Benard, V. Brandel, N. Dacheux, S. Jaulmes, S. Launay, C. Lindecker, M. Genet, D. Louër, M. Quarton, *Chem. Mater.* **8**, 181 (1996).

Self-Radiation Effects in Glass and Ceramic Waste Forms
for the Stabilization and Disposition of Plutonium

W. J. Weber
N. J. Hess
Pacific Northwest National Laboratory

S. D. Conradson
Los Alamos National Laboratory

J. D. Vienna
Pacific Northwest National Laboratory

A challenge facing the world community is the stabilization and disposition of both the plutonium residues/scraps located throughout the world's weapons complexes and the excess plutonium recovered from the dismantling of several thousand nuclear weapons under the first and second Strategic Arms Reduction Treaties. One of the options under consideration is the incorporation of the plutonium in specially formulated glass or ceramic waste forms for disposition. The long-term performance and durability of such waste forms are an important consideration because the fissile ^{239}Pu and its fissile daughter, ^{235}U, present considerable environmental risk if released. Self-radiation damage from α-decay of the ^{239}Pu, which releases a 5.16 MeV α-particle and a 0.086 MeV ^{235}U recoil nucleus can significantly affect the structure and properties of such waste forms. The purpose of this paper is to report the results from recent studies of self-radiation effects in a suite of glasses and a ceramic due to α-decay of the incorporated short-lived ^{238}Pu isotope.
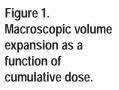
Density, XANES/EXAFS, and diffuse x-ray scattering measurements were performed on a suite of compositionally identical Pu-doped (1 wt %) waste glasses prepared with different α-activities by varying the ^{239}Pu/^{238}Pu isotopic ratio. The resulting α-activities in these glasses, which were prepared in July 1982, range from 1.9×10^7 to 4.2×10^9 Bq/g, and the accumulated dose ranges from 8.7×10^{15} to 1.8×10^{18} α-decays/g. Similar measurements have been carried out on a Pu-zircon (8.1 mole% ^{238}Pu was substituted for Zr) prepared in August 1981; the α-activity and accumulated dose in the zircon are 5.6×10^{10} Bq/g and 2.6×10^{19} α-decays/g, respectively. The macroscopic volume expansion of the glasses is shown in Figure1 as a function of accumulated dose. These r esults suggest that for this range of α-activities there is no significant effect of the α-activity (i.e., dose rate) on the macroscopic density change in waste form glasses. Self-radiation from α-decay in the Pu-zircon results in the simultaneous accumulation of point defects and amorphous domains that eventually lead to a completely amorphous state.[1] The macroscopic volume expansion of the zircon is much larger than in the glasses as a result of a radiation-induced crystalline-to-amorphous transformation, reaching a saturation value of almost 17%.[1]

Figure 1.
Macroscopic volume expansion as a function of cumulative dose.

Initial results from the XANES measurements at the Pu and U L_{III}-edges and Zr K-edge indicate that plutonium and uranium occur in more highly oxidized valence states in the waste glasses than in the Pu-zircon. Analysis of the Pu and U L_{III}-edges EXAFS at these absorption edge show a general trend of increasing structural disorder with increasing accumulated dose. However, analysis of the Zr K-edge EXAFS suggests that there is some densification of the waste glass at an intermediate length scale, a result supported by the pair distribution function from the diffuse x-ray scattering measurements. The Zr K-edge EXAFS of the Pu-zircon sample displays contraction of the oxygen shell concomitant with expansion of the next nearest neighbor silicon shell. Both the Pu dopant and the U-recoils that accumulate in the structure of the Pu-zircon exhibit the 4+ valence state, despite the amorphous nature of the highly damaged sample.

Results of recent stored energy measurements and TEM analysis of the Pu-containing glasses also will be presented. In addition, based on this and previous studies, a predictive model of self-radiation effects in [239]Pu-containing zircon as a function of geologic storage time and temperature has been developed and will be discussed.

Reference

1.   W. J. Weber, *J. Mater. Res.* **5**, 2687–2697.

Isotopes/
Nuclear Fuels

Nuclear Pu-Based Fuels for the Future

Introduction

H. Bernard
French Atomic Energy Commission, France

In 1996, commercial nuclear reactors throughout the world safely generated 17% of the world's electricity production, consuming more than 10,000 tons of UO_2 fuel and consequently producing 100 tons of plutonium. Separated from its intimate UO_2 matrix, this plutonium can be reused in power reactors.

Plutonium recycling in MOX fuels loaded in LWRs and FRs is economical, ecological, and in agreement with nuclear nonproliferation concerns. To date, more than 500 tons of MOX are loaded in 20 European reactors: MOX recycle is an industrial reality.

Specific developments are under way to manage Pu inventories, to reduce the potential radiotoxicity source of spent fuel (Pu and minor actinides burning such as MOX fuels in LWR, mixed oxide fuels or americium targets in FR...), and to tranform U. S. and Russian weapons-Pu (W-Pu) into MOX fuel.

Description of Actual Work

In addition to the increase in the number of reactors loaded with MOX and of the number of MOX subassemblies present in each core, an important R&D program has been launched with 3 main objectives:

Improvement of Current MOX Fuel Performances

LWRs: The major objective here is to safely increase the fuel burnup up to 60 GWd/t while keeping at the same high level the operational flexibility and reliability of the reactor. Compared with commercial fuels, an improved fuel should better resist waterside corrosion, better retain the fission products, and limit the pellet cladding interaction effects.

Ongoing research in the following areas includes: new cladding alloys more resistant to water corrosion, advanced microstructure fuels with large grain sizes, and intragranular precipitates and intergranular viscoplastic phases. Fuels containing a high content of burnable absorber (erbium or gadolinium oxide) and composite fuels (large particles dispersed in a metallic-CERMET-or ceramic-CERCER-matrix) are also studied.

FRs: The objective is to reach 20 at. % peak burnup safely with a fuel residence time of about 2000 equivalent days at nominal power (approximately 6 years), which represents a structural damage of about 180 dpa.

Cladding and wrapper steels that can reach the objective are examined. Advanced versions of austenitic alloys are promising candidates. For wrapper tubes, attention is focused on ferritic-martensitic and Oxide Dispersion Strengthened (ODS) steels.

Innovative Fuel Development

These new fuels cover a wide range of Pu contents, from 0 to 100%, depending on the reactor type.[1] Though still oxide-based, new LWR and FR fuels will be evolutionary ones, designed for achieving high burnups.

New FR fuels designed for an increased Pu consumption and the use of variable Pu isotopics (CAPRA, SPIN,...) are nonconventional: mixed oxide or nitride with very high Pu content, nonfertile fuels.

Adapting of Current MOX Fuel to W-Pu

The main objective is two fold: confirmation of the technical feasibility of a MOX fuel fabrication (the tranformation of the alloyed W-Pu into sinterable PuO_2 powder before manufacturing the MOX pellets), and verification of satisfactory irradiation behavior in existing power plants.

Results

The first destructive examination results obtained from the MOX high burnup program (GRA 4) show that after four irradiation cycles, the behavior of the MOX fuel remains essentially the same as it was after three cycles. The fission gas release is in particular similar to that of three cycles but probably due to the low heat rate experienced by the rod during the fourth cycle. In the pellet center, pore coalescence in Pu agglomerates generates large cavities surrounded by metallic precipitates. Grain size is equivalent to that of the surrounding UO_2 matrix. In colder regions, Pu agglomerates become highly porous with a fine grain structure similar to that of the UO_2 rod rim region at high burnup. High xenon concentration is measured in close vicinity to Pu rich zones whereas it is no longer detected by EMPA in the agglomerates.

Within the framework of KAP (Knowledge Acquisition Program) and for the first time, three experimental subassemblies will be loaded in the SUPERPHENIX core in mid-1997. Successfully manufactured in 29 months (May 1994 to October 1996) by COGEMA/Cadarache, the CAPRA 1A and 1B subassemblies are designed for plutonium burning and the NACRE for [237]NP transmutation (SPIN program). The CAPRA subassemblies are characterized by an ~30% plutonium content and a heterogeneous pin bundle in which two-thirds of the pins are fissile and the remaining third dummy. The CAPRA 1B subassembly uses plutonium recovered from MOX spent fuel instead of the standard Pu (used in CAPRA 1A). NACRE is a standard subassembly with the exception of 2% neptunium, which is added to the fuel.

Beyond the reference process for the TOMOX facility to be build in Russia for the W-Pu conversion into MOX fuel, initial experiments carried out in ATALANTE by a joint French-Russian team have produced 200 g of PuO_2 powder using the pyrometallurgical process in molten salts. The sintering capability of that powder will be examined during the next few months by manufacturing MOX pellets in the LEFCA Laboratory in Cadarache.

Reference

1. H. Bernard, P. Millet, J. Rovault, "Nuclear Fuels for the Future: Recycling in PWR MOX Fuels and in Fast Reactor CAPRA Fuels," EUROMAT Conference, Bournemouth, United Kingdom, October 21–23, 1996, p. 141–148.

Concepts for Advanced MOX Fabrication Technology

Introduction

W. Stoll
Institute for Industrial Environment, Germany

Most of the present MOX fuel is fabricated in analogy to standard UO_2-fuel via the classical ceramic route. All attempts so far to replace the expensive, mechanically complicated, and multistep process by simpler approaches could not find their way into large-scale technology. Also complete process automation is reliable only in the fabrication steps, where the severe abrasive properties of oxide powder and alpha-radiolysis do not interfere with low-tolerance moving mechanical equipment. All plants still require hands-on maintenance, so that major fractions of fission products cannot be tolerated in the starting material. For any closed fuel cycle, therefore, a decontamination from fission products up to 6 orders of magnitude is required, while the physics requirements would dictate one or two orders and those for specific neutron absorbing nuclides only.

Concept Description

Modern pharmaceutical pellet fabrication, when applied to the MOX-fabrication process, still delivers fuel very similar in properties to the classical route, but allows an almost continuous flow through the process and avoids all mechanical positioning of the ceramic parts. The process envisaged and already partly tested starts with a UO-2/PuO2-powder milling step, at which the Pu-fraction is high, but not above 38 wt %. A powder of this composition can be achieved via a comilling process, in which the forces of self-agglomeration in fine powders are suppressed with a milling aid. As an alternative the solutions of U-VI and Pu-VI can be mixed and coprecipitated as complex ammonium-carbonates, filtered, dried, and calcined, so as to arrive at a homogenous mixed crystal powder. It is one of the peculiarities of the hexavalent actinides, that in an ammonium-carbonate system they exhibit a selective anionic behavior. So the Di-ammonium-pentacarbonates are relatively water soluble, while the tetraammonium-three-carbonates are less soluble, the difference being more than two orders of magnitude. This would open the possibility, to separate U, Pu, and some minor actinides from fission products while undergoing two dissolution-precipitation cycles, as they are necessary for the starting powder anyway, and achieve a decontamination factor of up to 500. A separation process of this quality could either stand alone for later remote fuel fabrication or serve as an extra purification step after a single purex-cycle in reprocessing. To achieve a sufficient powder flowability, it is essential to mix the resulting dry master-blend with a free flowing UO-2 as a matrix material down to the desired Pu-U-ratio. A press feed of this type does not require binder or lubricant over and above the milling aid added, if the right compound was chosen. As a further deviation from the classical process, a rotting pellet press is fed, which presses pellets with a l/d below one, preferentially below 1/2. Those "coin"-type pellets show no measurable hourglassing and shrink during sintering to dimensions within narrow tolerances. Because they are of relatively high pressing density, they are stable enough to allow pooring instead of stapling in sintering boats. For sintering this is done in a slowly rotating molybdenum-tube-furnace with cold ends, heated by direct current, using a reducing atmosphere of argon-8% hydrogen in a countercurrent flow. Over a vibrating tilted table the coin-pellets are separated from broken parts and powder and arrayed over a wire-cage feeder into columns. Those columns are fed upwards into vertically aligned cans.

The whole process would in principle also allow the introduction of fission products, provided they do not interfere with the cladding stability and chemistry. It has proven to be of particular value to introduce getter substances in the form of sintered bodies (uranium-metal in open zircaloy-tube-inserts at the fuel rod end) to keep the stoichiometry close to or slightly below two also after extended burnups and to compensate for other corrosive impurities and fission products, particularly halogens. With those precautions also, Pu recovered as oxide via salt refining (electrochemically or over selective dissolution processes) could be tolerated. It was possible as well to utilize fuel powder coming from a redox-process, in which only thermally removable fission products have been removed before.

Results

While the process as a whole has not yet been exercised in current fabrication plants, almost all steps have been used in an isolated manner in different approach documents. The "coin"-pellet concept was once demonstrated as feasible in an irradiation of hot-presses pellets in the Garigliano-BWR (Italy), while the complex ammonium-carbonate-precipitation and also the comilling process was exercised in the German plant for a longer time. The stable dimensions of the flat pellets have been demonstrated in fabricating pellets for a critical facility (SNEAK), where narrow tolerances were required, while the partial decontamination in the salt refining process was demonstrated in Russia (Dimitrowgrad, Fast Breeder fuel), where the beneficial effect of U-metal as a getter had been proven over long burnups.

It should be kept in mind that the very narrow specifications for the micro-distribution of Pu in U are a consequence of the acceptance-specifications of reprocessors in view of the poor solubility of PuO_2 in nitric acid and their relatively mild dissolution conditions. If however a reprocessing of the irradiated MOX-fuel was not envisaged, the much looser specifications, allowing a higher fraction of coarse PuO_2 particles to be present in the ceramic, could simplify the fabrication process even further and considerably shorten the comilling step, if not avoiding it completely, depending on the starting grain size of the PuO_2.

Inert Matrix Non-Fertile Fuels for Plutonium Transmutation in PWRs

F. Vettraino
ENEA, Italy

C. Lombardi
A. Mazzola
Polytechnic of Milan, Italy

About 100 MT of excess plutonium are going to be originated from warheads dismantling under the START I and II agreements (50 MT by each side—U. S. and former Soviet Union), and about another 200 MT are already stockpiled from commercial spent-fuel reprocessing. The latter, also called civilian or reactor grade plutonium (RG-Pu), is accumulated at a rate of 60 to 70 MT/year and, by the year 2000, will come to a total world inventory of 1600 to 1700 MT.

Therefore, there is a pressing need in finding novel and more secure methods to deal with all kind of excess plutonium in the aim of rendering it ultimately unusable for proliferation purposes.

Three main technology alternatives in weapons Pu disposition have been addressed: reactor (LWRs); direct immobilization (vitrification or ceramics); and deep borehole entombment.

Most recently attention has been concentrated only on the first two options (U.S.), and the reactor alternative is referred basically to MOX fuel utilization in LWRs.

Three generic fuel types could be used to burn plutonium in LWRs:

1) uranium-based mixed oxides (MOX) $(U,Pu)O_2$

2) thorium-based mixed oxides $(Th,Pu)O_2$

3) inert matrix fuels (IMF), in which PuO_2 is dispersed in a neutron transparent ceramic inert carrier

The mixed-oxide $(U,Pu)O_2$ fuels have been thoroughly studied and used, and a rather wide operational use is now available on a commercial basis. In fact this option has been indicated by the U.S. DOE as the reference for disposing its WG-Pu. The main drawback for this solution is that new plutonium is continuously generated during the fuel irradiation so that a significant fraction (70%) of the loaded plutonium is still present in the spent fuel, although denatured. The $(Th,Pu)O_2$ fuel option is interesting because it potentially increases the Pu consumption with respect to $(U,Pu)O_2$ due to the lack of ^{238}U. From calculations emerge the total plutonium consumption, which, compared to MOX, can be higher by a factor >2 and the fissile plutonium burnt fraction increases a factor of 1.6. Moreover, there exists experience, although limited on $(Th,U)O_2$ fuels, that indicates a good behavior under irradiation and a rather high stability for the resulting exhausted fuel, so that it is likely to be appropriate for direct disposal. A major disadvantage, however, for Th-fuel is the breeding of ^{233}U, eventhough the high gamma activity of the separated uranium mixture, coming mainly from ^{232}U, should highly discourage this proliferation pathway.

On the other side, inert matrix fuel is a completely novel fuel concept that finds justification because, for weapons Pu transmutation in LWRs, the precisely required fuel is not immediately available and even for the MOX option, processes and facilities have to be set up before reaching the operational stage. The dimension of such a delicate task and the perspective of finding even more effective and ultimate solutions from both the security and safety standpoints, are sufficient reasons for putting attention on new fuel concepts such as IMF.

Inert matrix fuel is a non-fertile oxide fuel consisting of PuO_2, either weapon-grade or reactor-grade, diluted in a mixed compound of inert oxides such as stabilized ZrO_2, Al_2O_3, MgO, and $MgAl_2O_4$. Its primary advantage is the no-production of new plutonium during irradiation, because it does not contain uranium (*U-free* fuel) whose ^{238}U isotope is the departure nuclide for breeding ^{239}Pu.

The physics investigations presently under way and aimed at enlighting the best core layouts possible when using inert matrix U-free fuel in commercial PWRs, operating in a once-through cycle scheme, show that IMF has a quite high Pu burning capability: >93% of fissile plutonium and 74/85% of total RG-/WG-Pu is burnt at end of fuel life.

The calculations evidentiate also that radiotoxicity levels in inert matrix spent fuel do not appear to increase with respect to standard unreprocessed spent fuel.

This new fuel will have a plutonium-relative content comparable to one used in standard MOX fuel for PWRs and is expected to respond to the following basic requirements: good chemical compatibility, acceptable thermal conductivity, good nuclear properties, good stability under irradiation, high dissolution resistance, and long-term chemical stability.

As result of these good properties, after discharge from reactor and adequate cooling time, the spent fuel is outlooked to be sent, as a HLW, directly to the final disposal in deep geological formations without requiring any further reprocessing treatment *(once-through solution)*.

Moreover the expected very limited solubility under the current fuel reprocessing techniques, coupled to the quality-poor residual Pu in the spent fuel, will make inert matrix fuel a potentially strong anti-proliferation product.

An R&D programme on IMF, starting from simulate fuel sample fabrication and characterization, is presently under way at ENEA as a cooperation activity between ENEA-Nuclear Fission Division and Polytechnic of Milano, Italy.

The fuel pellets similar to those currently employed in commercial PWRs will come from the ceramic mixed powders technology or from the Gel Supported Precipitation (GSP) microsphere process.

Simulate fuel pellets based on inert oxides such as $ZrO_2(CaO)$, $MgAl_2O_4$ and a mixture of Al_2O_3-ZrO_2-MgO, mixed with ceria as a plutonium oxide substitute, have been fabricated via the GSP wet route, and compliance with basic nuclear grade specification such as for density and grain size has been achieved.

The characterization tests on these pellets and granules dealing with thermo-physical properties, Ion Irradiation Damage, corrosion and disssolution resistance are under way and first results indicate that IMF is a highly stable material.

The main weakness for the IMF is that no operational experience is available, and it has to be thoroughly tested before becoming a commercial application. Notwithstanding this drawback, this option has the advantage of quasi-total incineration of plutonium, and the development of an innovative fuel concept with a flexible design could have fallout for other applications too (MAs burning, Pu-based fuel for accelerator-driven systems, HEU fuels).

Development of Coated Particle Plutonium Fuel in Russia

Introduction

Since April 1993, General Atomics (GA) and the Russian Federation Ministry for Atomic Energy (MINATOM) have been participating in a joint cooperative program to develop the Gas Turbine Modular Helium Reactor (GT-MHR) for disposition of surplus weapons-grade plutonium and subsequent commercial applications.[1, 2] Framatome joined the conceptual design effort in 1996, and Fuji Electric in 1997.

Coated particle plutonium fuel offers advantages throughout the fuel cycle, including superior diversion and proliferation resistance, improved economics associated with deep burning of highly-enriched fuel, and nearly ideal final waste form characteristics provided by highly corrosion-resistant coatings and graphite.[3, 4]

GT-MHR plutonium fuel is being developed at the Russian Research Center-Kurchatov Institute and the A. A. Bochvar All-Russian Scientific Institute of Inorganic Materials (ARSRIIM) in Moscow, the Scientific and Industrial Association-Lutch in Podolsk, and the Siberian Chemical Complex (SSC) in Seversk, with participation of other Russian organizations. In a complementary activity, OKBM in Nizhni Novgorod is completing a conceptual design for the reactor and plant.

The fuel conceptual design phase, completed in October 1997, calls for production of plutonium oxide kernels and demonstration of TRISO coating and compacting processes. Also included are a conceptual design of a bench-scale fabrication line for later production of fuel compacts with coated plutonium particles and for studies of establishing fuel fabrication facilities at SSC.

Fuel Design and Performance

Design plutonium burnup is 750,000 MWd/t at < 1300°C. The particle design is based on a TRISO-coated plutonium particle manufactured at Oak Ridge National Laboratory and successfully irradiated in the Peach Bottom gas-cooled reactor. The irradiation was at peak temperatures up to 1440°C, peak burnup of 747,000 MWd/t.[5, 6]

The kernels have a multi-layer TRISO coating, which consists of a 110-μm low-density buffer layer with 50% void volume, a 35-μm inner pyrolytic carbon layer, a 35-μm silicon carbide layer, and a 40-μm outer pyrolytic carbon layer. The coating layers form a miniature pressure vessel essentially impermeable to gaseous and metallic fission products. The coated particles are bonded together with a carbonaceous matrix into cylindrical compacts, which are stacked in blind fuel holes of a nuclear-grade graphite fuel element.

Fuel Manufacturing

For the plutonium fuel, coating and compacting processes are taken directly from those used for uranium fuel, but the kernel is unique to this application.

Plutonium oxide kernels satisfying GT-MHR requirements were produced at ARSRIIM earlier this year. As the Peach Bottom irradiation indicated, it is important to maintain the O/Pu ratio below about 1.7. Otherwise, excess oxygen,

V. M. Makarov
A.A. Bochvar All-Russian Scientific Research Institute of Inorganic Materials, Russia

A. S. Shenoy
General Atomics/ San Diego

M. B. Richards
D. W. McEachern
General Atomics / Los Alamos

liberated during the fission process, can cause particle failure by the kernel migration phenomenon (amoeba effect).

The process used to produce the 200 mm-diameter kernels having 97% theoretical density and O/Pu < 1.7 is an internal gelation process. The process steps are described in Table 1.

Lutch has constructed and is testing a TRISO-coater and compacting equipment designs to be used in the bench-scale manufacturing line now being designed for ARSRIIM.

Conclusions

Plutonium oxide kernels meeting specifications have been produced in Russia. Adaptation of coating and compacting processes used earlier in Russia and the U.S. for uranium fuel are being re-established in Russia for use with plutonium fuel. The GA/MINATOM/Framatome/Fuji cooperative program is demonstrating the benefits of international cooperation in developing this promising fuel form at approximately 1/3 the cost of a similar program in the United States, while also employing Russian military/industrial staff and facilities in new, post-cold war activities.

Table 1. Fabrication of plutonium oxide fuel kernels.

Process Step	Description
1. Preparation of concentrated solution	Dissolve in dilute HNO_3 and evaporate, plutonium nitrate stabilize to Pu^{+4}.
2. Neutralization and hydrolysis of plutonium nitrate solution	Partially neutralize with strong ammonia solution and add ammonia donors for gelation.
3. Production of gel spheres	Form mono-sized spheres in vibrating nozzles and gel in heated trichloroethylene.
4. Washing of gel spheres	Wash in ammonia; use solution electrical conductivity as end point.
5. Drying and calcination	Dry in humid atmosphere; calcine in air.
6. Sintering	@>1600°C in O_2 free H_2 in fluidized bed.
7. Quality control	Diameter, sphericity, density, O/Pu, impurities.

References

1. M. P. LaBar, W. A. Simon, and A. S. Shenoy, "Status Update: Disposition of Surplus Russian Weapons Grade Plutonium with the GT-MHR," Fourth Annual International Policy Forum: Management and Disposal of Nuclear Weapons Materials (AIPF:MDNWM), Lansdowne, Virginia, February 11–14, 1997.

2. D. Alberstein, W. A. Simon, A. S. Shenoy, V. N. Mikhailov, B. V. Budylin, F. M. Mitenkov, and N. N. Ponomarev-Stepnoi, "Increasing International Support for Disposition of Surplus Weapons Grade Plutonium with the GT-MHR," The Third AIPF:MDNWM, San Diego, California, March 19–22, 1996, General Atomics document GA-A22368.

3. M. B. Richards, "Disposition of Spent Nuclear Fuel Using the Modular Helium Reactor," *Energy–The International Journal* **21**(4), 333–341 (1996).

4. M. B. Richards, D. Alberstein, and A . J. Neylan, "PC-MHR Spent Fuel—An Ideal Waste Form for Permanent Disposal," in *Proceedings of The 4th International Conference on Nuclear Engineering*, American Society of Mechanical Engineers (New Orleans, Louisiana, 1996), Vol. 5, pp. 1–4.

5. P. Barr, N. Pollitt, G. B. Redding, A. Sorenson, and P. Svensson, *Proceedings of a Symposium on the Use of Plutonium as a Reactor Fuel*, (International Atomic Energy Agency, Vienna, Austria, 1967) SM-88/38, pp. 391–4177.

6. W. J. Scheffel, "Design and Operational Evaluation for the Plutonium Test Element (FTE-13)," 1972, Gulf General Atomic Company document Gulf-GA-B12271.

Separations

Recovery of Plutonium or Conversion of Plutonium-Containing Materials to Glass Using a GMODS Dissolution Glass

C. W. Forsberg
Oak Ridge National Laboratory

Introduction

A new general-purpose process is proposed to (1) recover plutonium from complex plutonium-containing mixtures of metals, ceramics, amorphous solids, halides, and organics or (2) convert complex plutonium mixtures into glass for storage or disposal. Plutonium operations generate a variety of scrap and residues. Replacement of multiple small existing processes with a general-purpose process has the potential for large economic savings, reduced occupational exposure with larger-scale automated processing, and improved safety.

Process Description

A new process with capabilities for plutonium separation or conversion of plutonium-containing materials to glass has been invented. The dual capabilities (Figure 1) are a consequence of similar front-end processing requirements for (a)plutonium separations pr ocesses using nitric acid and (b) conversion of plutonium-containing materials to glass. The new process for both applications (1)r emoves troublesome halogens, sulfur, and noble metals from the feed and (2)converts the other elements to oxides in a borate fusion melt. The solidified melt is soluble in nitric acid and produces a feed for standard nitric-acid-based separations technologies such as Purex and ion exchange. In effect, the process is a front-end treatment step to convert complex feeds into a chemical form allowing easy recovery of plutonium with aqueous separation technologies. As a glass-making process, the resultant borate fusion melt is converted to a borosilicate glass.

For both plutonium separations or glass production the front-end processes (Steps 1A–D) are identical. Feeds are sent to a glass melter (Step 1A) with a molten glass containing at least 2 mol PbO per mole B_2O_3—the Glass Material Oxidation and Dissolution System (GMODS) dissolution glass. Oxides in the feed dissolve into glass and halides are converted to volatile lead halides and exit via the off-gas system (Step 1B). In the molten glass, the PbO oxidizes metals to metal oxides and organics to carbon oxides with byproduct production of lead. The metal oxides dissolve into the glass, and the carbon oxides exit the melter as gases. The noble metals are extracted into the molten lead metal. The product of these chemical reactions is a lead-borate fusion melt with all elements dissolved in the glass as oxides.

The lead-metal reaction product separates from the glass and sinks to the bottom of the melter. Lead is reoxidized in an external loop (Step 1C) to PbO and is fed back to the melter during the processing of the next batch of feed. Noble metals may be recovered from the lead (Step 1D).

To recover plutonium, carbon is added to the melter (Step 2A) to reduce the PbO in the melt to lead metal that separates from the glass. The B_2O_3 melt containing dissolved oxides is cooled and becomes the feed to conventional nitric-acid-dissolution separation processes such as Purex and ion exchange. Published work[1] indicates that plutonium separation (Step 2C) from a nitric acid, boric acid solution is straightforward. Boron-oxide fusion melts that are *solidified as glasses* are soluble and easily dissolved in nitric acid (Step 2B), whereas many feeds are not. In the glass structure slow-to-dissolve oxides (PuO_2, etc.) are in solution with soluble B_2O_3 and thus are not as difficult to dissolve as are crystalline forms.

To convert plutonium and other feed components to glass for storage or disposal, carbon and glass frit are added to the lead-borate glass (Step 3). The carbon reduces the PbO to lead metal, which then separates from the melt. The glass frit converts the melt to a borosilicate glass.

Experimental Activities

Tests[2] in lead-borate glass demonstrated the dissolution of UO_2, ZrO_2, Al_2O_3, Ce_2O_3, MgO, and other oxides. Oxidation-dissolution tests demonstrated the oxidation of the following metals and alloys (followed by the dissolution of their oxides into the melt): U, Ce, zircaloy-2, Al, stainless steel, and other metals. Oxidation-dissolution tests also demonstrated the oxidation of carbon and the resultant production of CO_2. Proof-of-principle tests revealed the conversion of chlorides to $PbCl_2$ and its escape into the off-gas system. Dissolution experiments have not yet been done on plutonium.

This dissolution glass has also become the preferred high-temperature solvent for determination of the thermodynamic properties of complex minerals.[3] In this application, it has been successfully used to dissolve complex minerals containing MgO, Al_2O_3, SiO_2, alkali oxides, alkaline earth oxides, MnO, MO (M = Co, Ni, Zn, Cd), Mn_2O_3, MnO_2, Fe_2O_3, Cr_2O_3, TiO_2, ZrO_2, rare earth oxides, GeO_2, Ga_2O_3, hydrous phases, carbonates, fluorides, and other compounds.

Conclusions

A general-purpose process for plutonium processing is proposed to replace multiple existing processes for plutonium recovery and conversion of plutonium-containing wastes to glass. This process has the potential for economic savings, reduced occupational exposure, and improved safety. Significant technical uncertainties remain.

References

1. W. W. Schulz, J. D. Navratil, and A. S. Kertes, *Science and Technology of Tributyl Phosphate: Volume IV- Extraction of Water and Acids* (CRC Press, Boca Raton, Florida, 1984).

2. C. W. Forsberg, E. C. Beahm, and J. C. Rudolph, "Direct Conversion of Halogen-Containing Wastes to Borosilicate Glass," in *Proc. Scientific Basis For Nuclear Waste Management XX*, (Materials Research Society, Pittsburgh, Pennsylvania, December 1996).

3. A. Navrotsky, "Progress and New Directions in High Temperature Calorimetry Revisited," *Phys. Chem. Min.* (in press).

Off-gas

NaOH ──▶ | **1B   Aqueous Scrubber**
$PbX_2 + 2NaOH \rightarrow Pb(OH)_2\downarrow + 2NaX$ | ──▶ *NaX (Halide)*

$Pb(OH)_2$

Off-gas
PbX_2 , CO_2
X=halide

Feed ──▶ | **1A   Feed Dissolution in Molten $2PbO:B_2O_3$ Glass**
Oxidation, Dehalogenation, and Oxide Dissolution
$yMe + z\,PbO \rightarrow Me_yO_z + zPb\downarrow$
$Pu + 2PbO \rightarrow PuO_2 + 2Pb\downarrow$
$MeX_y + (y/2)PbO \rightarrow MeO_{(y/2)} + (y/2)PbX_2\uparrow$
$C + 2PbO \rightarrow CO_2\uparrow + 2Pb\downarrow$

B_2O_3 ──▶

Plutonium Separations   *Conversion to Glass*

Pb   PbO

2A   Conversion to
Borate Fusion Melt
$C + 2PbO \rightarrow CO_2\uparrow + 2Pb\downarrow$ | ── Pb ──▶ | **1C   Lead**
Oxidation
$2Pb + O_2 \rightarrow 2PbO$ | ◀── Pb ── | **3   Silicate Glass**
Formulation
$C + 2PbO \rightarrow CO_2\uparrow + 2Pb\downarrow$
Frit Addition

Pb   Pb
(noble metals)

2B   Conventional
Aqueous Nitric Acid
Dissolution | **1D   Noble Metal**
Recovery
(Optional) | *Borosilicate*
Glass

Noble Metals

2C   Conventional
Separations Process
(Purex etc.) | ──▶ *Pu(NO₃)₄*

2D   Conventional
Waste Solidification | ──▶ *Borosilicate Glass*
or Other Waste Form

Feed = Input to Process
Lead Oxidation = Process
Pu(NO₃)₄ = Process Output

Figure 1. Flowsheet for recovery of plutonium or conversion to glass.

Recovery of Surplus Weapons-Usable Plutonium
for Mixed Oxide Reactor Fuels

Introduction

T. R. Johnson
R. D. Pierce
C. C. McPheeters
*Argonne National
Laboratory*

The DOE strategy[1] for disposition of surplus weapons-usable plutonium allows for both immobilizing it in a glass or ceramic waste form and using it as mixed oxide (MOx) fuel for commercial reactors in a once-through fuel cycle. In either case, the plutonium is ultimately disposed of in a high-level waste repository. About 6 T of the 50 T of surplus plutonium resides in the plutonium-rich residues at Rocky Flats Environmental Test Station (RFETS). Processes being developed at Argonne National Laboratory (ANL) can be used to separate plutonium from these residues in a MOx-usable form, or to immobilize it in a ceramic waste form. The low-plutonium waste from these processes can be more easily characterized than the untreated residues. Ease of characterization is a significant advantage in light of Environmental Protection Agency (EPA) regulations aimed specifically at transuranic (TRU) waste disposal in the Waste Isolation Pilot Plant (WIPP).[2] All of the process steps have been demonstrated on a laboratory scale, some on an engineering scale, and key process steps are currently being tested at ANL-West in full-scale equipment.
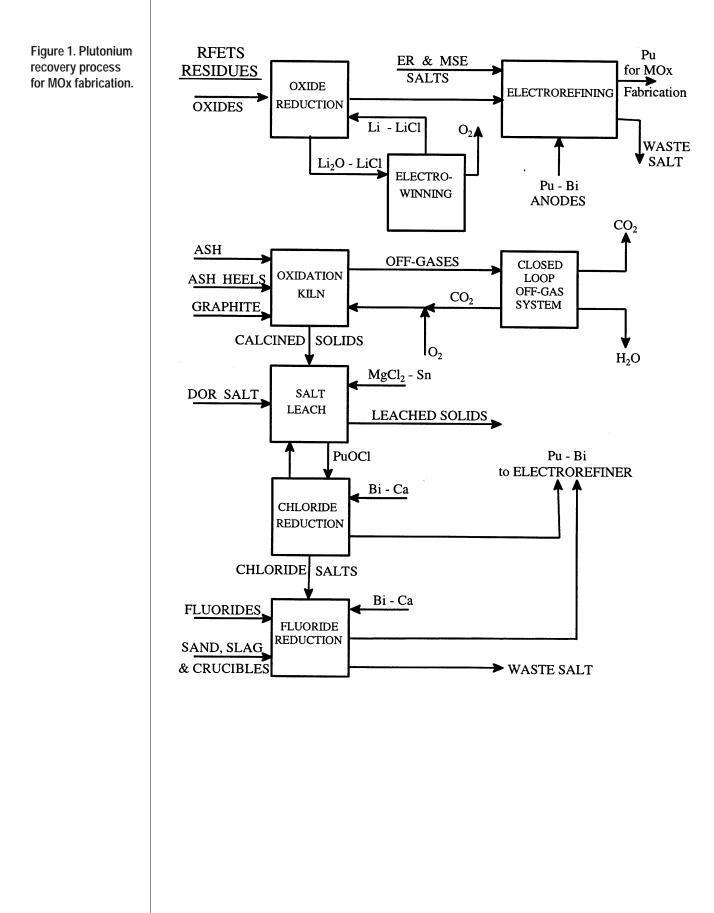
Process Overview

The basic process shown in Figure 1 recovers plutonium from most of the RFETS residues and wastes and produces waste forms with known characteristics, but this paper focuses on treatment of the Pu-rich residues listed in Table I. This process recovers more than 99% of the plutonium in a form suitable for conversion to MOx fuel. If the goal is immobilization, the process can be modified to sorb plutonium from the molten electrorefiner salt into a zeolite and then immobilize it in a ceramic waste form.

In this process, PuO_2 in the oxide residues is reduced to metal by lithium in LiCl. This plutonium and plutonium recovered from the other residues are anodically dissolved in the electrorefiner and deposited in cathodes in a form convertible to MOx fuel. The plutonium in the Electrorefining (ER) and Molten Salt Extraction (MSE) salts is also deposited in these cathodes. In the electrowinning step, Li_2O produced in the reduction step is converted to lithium metal, which is recycled.

The other process steps shown in Figure 1 are used to treat the other residues. Ash, ash heels, and graphite residues are oxidized in a rotary kiln, and the combustion gases flow through a Closed Loop Off-Gas System before being vented. Calcined solids from the kiln are contacted with a molten salt consisting of direct oxide reduction (DOR) salt and $MgCl_2$. By reaction with $MgCl_2$, PuO_2 is preferentially leached from the solids and dissolved in the salt as PuOCl. The PuOCl-laden salt is circulated between the leach vessel and the chloride reduction vessel, where the PuOCl is reduced by a Bi-Ca alloy. The plutonium produced is dissolved in the bismuth. Salts from the chloride reduction step are then mixed with the fluoride residues plus the sand, slag, and crucibles to form a molten chloride and fluoride salt pool. Similar to the chloride reduction, containers with Bi-Ca alloy are immersed in the mixed salts to reduce PuF_4. The Bi-Pu products from both salt reduction steps are transferred to the electrorefiner where the plutonium is extracted anodically.

Figure 1. Plutonium recovery process for MOx fabrication.

RFETS
RESIDUES

OXIDES

OXIDE REDUCTION

ER & MSE SALTS

ELECTROREFINING

Pu for MOx Fabrication

WASTE SALT

Li - LiCl

O_2

Li_2O - LiCl

ELECTRO-WINNING

Pu - Bi ANODES

ASH

ASH HEELS

GRAPHITE

OXIDATION KILN

OFF-GASES

CLOSED LOOP OFF-GAS SYSTEM

CO_2

CO_2

O_2

H_2O

CALCINED SOLIDS

$MgCl_2$ - Sn

DOR SALT

SALT LEACH

LEACHED SOLIDS

PuOCl

CHLORIDE REDUCTION

Bi - Ca

Pu - Bi to ELECTROREFINER

CHLORIDE SALTS

FLUORIDES

FLUORIDE REDUCTION

Bi - Ca

SAND, SLAG & CRUCIBLES

WASTE SALT

Table 1. Plutonium-
rich residues at
Rocky Flats.

Residue Group	Total Weight (kg)	Plutonium Content (kg)	Principal Components
Oxides	2000	1600	Impure PuO_2
Ash and Ash Heels	21000	900	Al, Mg, Ca, and Si oxides; some chlorides and fluorides; C
Graphite	27000	200	Graphite pieces, CaF_2
ER, MSE, and DOR Salts	21000	1100	Ca, Na, K, and Mg chlorides
Fluorides; Sand, Slag, and Crucibles	8000	2000	Pu and Ca fluorides, MgO and CaO

Lithium Reduction

Studies[3] of the reduction of nuclear fuel oxides at ANL have shown that lithium is an effective reductant in the presence of LiCl. The salt dissolves and transports lithium to the oxide surfaces and dissolves the Li_2O reaction product. For example,

$$PuO_2 + 4(Li)_{LiCl} \rightarrow Pu + 2(Li_2O)_{LiCl}.$$

Above a critical Li_2O concentration, PuO_2 is reduced only to Pu_2O_3. However, at the preferred operating temperature of 650°C, complete PuO_2 reduction can be achieved at Li_2O concentrations up to 5 mol %.

The lithium reduction process has been successfully demonstrated[4] in engineering-scale equipment using 9.8 kg of high-fired UO_2 pellets with a nominal PuO_2 content of 0.7 wt %. Complete reduction of the actinides was demonstrated, and the electrowinning of lithium from Li_2O was also successfully carried out. It is estimated that crushed fuel pellets can be completely reduced in a stirred reactor in less than 2 h. The product metal particles can be separated from the salt in a hydroclone. Work is in progress to install this process at ANL-West to treat DOE oxide fuels.

Electrorefining

The ANL electrorefiner differs in several respects from the electrorefiner that is used for plutonium purification. The electrorefiner currently being used at ANL-West to treat irradiated metal fuels from Experimental Breeder Reactor-II operates at 500°C and has anodes that are steel baskets containing clad fuel sections. Actinides in the fuel sections are anodically dissolved into a molten LiCl-KCl electrolyte and deposited on cathodes. Steel cathodes collect only uranium, while cathodes of cadmium in a ceramic crucible collect a mixture of uranium and plutonium.

$MgCl_2$ Leaching

When samples of RFETS ash and ash heels were exposed to a salt containing $MgCl_2$ in the presence of zinc, the contained plutonium was selectively leached from the solids and dissolved in the salt as PuOCl,

$$PuO_2 + MgCl_2 + 1/2 Zn = PuOCl + MgO + 1/2 ZnCl_2.$$

Typically 98% of the plutonium was dissolved in a single contact with salt in these laboratory tests. The PuOCl was then easily reduced from the salt solution by calcium. In the proposed process, tin rather than zinc would be used.

Process Wastes

As shown in Figure 1, the kiln off-gases, mainly CO_2 and H_2O, undergo phase changes in the off-gas system before release.[5] The CO_2 is absorbed into a K_2CO_3 solution that is first filtered and then heated to regenerate K_2CO_3 from the $KHCO_3$ and release CO_2. The small amounts of inert gases, such as nitrogen, that build up in the system are released through membranes. The vented gases and discharged water will contain virtually no particles or pollutants. The CO_2 absorption system is similar to one that has been used commercially to extract CO_2 from combustion gases.

The only solid waste is a combination of salts from the electrorefining and fluoride salt reduction steps and the $MgCl_2$-leached solids. Its plutonium content will be less than 0.2%, and its volume will be less than half the volume of the untreated residues. Waste composition and the characteristics required for waste performance assessments can be determined more easily and reliably than for the residues.

Conclusions

The new EPA rule[2] requires that performance and compliance assessments must be made for any TRU waste destined for WIPP and describes in some detail the requirements for the computer models for these assessments. The waste characteristics that must be determined include "solubility, formation of colloidal suspensions containing radionuclides, production of gas from the waste, shear strength, compactability, and other waste related inputs to the computer models." These characteristics can be more easily determined after treatment by the proposed process than for the RFETS residues in their present condition.

References

1. "Record of Decision for the Storage and Disposition of Weapons-Usable Fissile Materials: Final Programmatic Environmental Impact Statement," U.S. Department of Energy (January 14, 1997).

2. Environmental Protection Agency, "Criteria for the Certification and Recertification of the Waste Isolation Pilot Plant's Compliance with 40CFR Part 191 Disposal Regulations," *Federal Register,* Vol. 61, No. 28 (February 9, 1996), pp. 5224–5245.

3. C. C. McPheeters, R. D. Pierce, and T. P. Mulcahey, "Applications of the Pyrochemical Process to Recycle of Actinides from LWR Spent Fuel," *Progress in Nuclear Energy* **31**(1/2), 175–186 (1997).

4. E. J. Karell, R. D. Pierce, and T. P. Mulcahey, "Treatment of Oxide Spent Fuel Using the Lithium Reduction Process," in Proceedings, *DOE Spent Nuclear Fuel and Fissile Material Management*, (Reno, Nevada, June 1996).

5. M. K. Clemens, P. A. Nelson, and W. M. Swift, "Removal of Carbon Dioxide in Closed Loop Off-Gas Treatment Systems," *J. Envir. Sci. Health* **A31**(7), 1801 (1996).

Aqueous Processes for the Conversion of Metallic Plutonium into an Oxide Powder Suitable for MOX Fuel Fabrication

B. Zakharkin
L. Borisov
VNIIM, Russia

P. Brossard
P. Bros
CEA/DCC, France

A. Boesch
E. Capelle
CEA/DAM, France

Abstract

Several processes have been proposed to convert weapons-grade plutonium into PuO_2 suitable for MOX fuel manufacturing. Among those, Russian and French research teams underwent detailed studies of aqueous chemistry procedures that are compatible with a PUREX-type purification step. These are:

- dissolution in a HNO_3 - HF mixture
- dissolution in a HNO_3 - HCOOH mixture
- air oxidation into PuO_2 and dissolution in HNO_3 using electrogenerated Ag(II)

This paper describes the three processes and gives the main results which have led to the choice of the reference scheme to be used in the TOMOX facility design.

Summary

The joint Russian-French AIDA/MOX program launched in 1992 covers several technical topics. The aim was to define a general scheme to convert the excess dismantled weapons plutonium into MOX fuel to be irradiated in existing Russian reactors.

One of these topics concerns the transformation of metallic plutonium into sinterable plutonium dioxide powder (or uranium-plutonium dioxide).

Starting with a metallic plutonium having up to 5 % at. of Ga, the final powder should meet precise specifications in terms of chemical and radiochemical purity, grain size, and specific area.

The first stage of the joint work consisted of choosing the processes that should be investigated. Using the experience of each team and the tight safety and waste management criteria, some processes were quickly discarded. One can recall:

- conversion by hydridation-oxidation steps because of the handling difficulties presented by the plutonium hydride and the necessary mixing of H_2 and O_2 in a gas phase at a high temperature

- dissolution in sulfamic acid because the procedure can lead to highly pyrophoric residues and gives liquid waste difficult to handle (presence of sulfate)

Also, the dissolution in hydrochloric acid was, after a short study, abandoned because of the pyrophoric residues formation and corrosion problems.

Thus, three methods have been studied in detail as part of this joint research.

Dissolution in a Mixture of Nitric and Hydrofluoric Acids

Although the catalytic influence of HF upon the metallic plutonium dissolution has been known for a long time, only recently has it been shown that the

complexing properties of fluoride ion can greatly enhance the dissolution kinetic. Indeed the work done by the VNIIM Institute gives tremendous results confirmed by few experiments done by the French ATALANTE Laboratory in MARCOULE. At boiling temperature ($\approx 105°C$) a $HNO_3 = 7$ M; $HF = 0.4$ M mixture dissolves Ga alloyed plutonium at a rate of about 315 mg/mn/cm^2, which is about six to seven times the best results ever obtained with sulfamic acid. The dissolution, even with surface oxidized samples, forms less than 0,2 % of residues showing no pyrophoric behavior. The gas phase composition is found to be about $NO_2 \approx 23\%$, $NO_2 \approx 46\%$, $N_2O \approx 2\%$, $N_2 \approx 30\%$ and $H_2 < 0.5\%$.

Following the dissolution and after a cooling down to 60°C, aluminum nitrate is added to the medium in quantities sufficient to complex all the fluoride ions. The solution is then suitable for a Purex-type purification stage.

Dissolution in a Mixture of Nitric and Formic Acid

Pure carboxylkacids do not r eact with metallic plutonium. However it was found that in the presence of formic acid, nitric acid readily dissolved δ-phase plutonium. The catalytic loop (involving nitrous acid) that induces the classical passivation scheme in pure nitric acid is blocked by the presence of HCOOH. Mechanisms are not well understood but certainly involve an absorption of HCOOH at the surface of the sample and a reaction with HNO_2. Anyhow the dissolution occurs very quickly even at low temperature. For example, with a mixture of $HNO_3 \approx 3.2$ N and $HCOOH \approx 5.3$ M at 30°C, a dissolution rate of 140 mg/mn/cm^2 is obtained with a residue accounting for about 7% of the initial mass.

This residue was found to be not pyrophoric and to dissolve easily with silver(II). It is thought to be simply PuO_2.

The mean gas evolution is the following: $CO_2 \approx 70\%$, $NO \approx 15\%$, $N_2 \approx 10\%$, and $H_2 \approx 3\%$, the hydrogen being produced mainly during the first few minutes of the dissolution.

Excess formic acid is simply eliminated by boiling and the plutonium nitrate solution can be sent to a PUREX-type process for Ga and Am purification and conversion into oxide.

Air Controlled Oxidation and Dissolution in Silver(II)

The plutonium oxide dissolution in nitric acid using electrogenerated Ag(II) is a well-known process used at an industrial scale at the LA HAGUE reprocessing plant in France. The ability of metallic plutonium to "burn" in the presence of oxygen to give PuO_2 is also a well-known fact. The idea of combining these two stages was not difficult to put forward as a possible conversion process. Many runs were undertaken to determine the best conditions for the Pu oxidation in air:

• preheating of the furnace under an argon atmosphere to above 500°C so that there will be no induction time

• supply of a calibrated air flow taken, for example, from the glovebox and containing up to 15000 ppm of H_2O

• the oxidation starts immediately accompanied by a 100°C temperature rise. The rate is governed by the oxygen flowrate and is linearly dependent with the surface area of the sample. Kinetic up to 40 mg/mn/cm^2 can be achieved

The resulting compound is a mixture of PuO_2, Ga_2O_3, and metallic gallium. It is not pyrophoric and can readily dissolve in nitric acid using electrogenerated silver(II).

This dissolution procedure is used on an industrial scale at the LA HAGUE Plant in France to dissolve aged plutonium oxide powders. It does not need any basic research and is fully compatible with a PUREX-type process.

Taking altogether the advantages and drawbacks of each of the three studied methods, the scientific committee of the joint program has proposed the dissolution in nitric-hydrofluoric acids to be the reference process for the conception and designs of the TOMOX facility. The process offers the best kinetic, and hundreds of kg of alloyed plutonium have already been treated. Its drawbacks, that will be addressed in the coming months, are the fluoride ions management and the safety problems linked to the possible precipitation of PuF_4, which is a strong neutron source. Air calcination of the alloyed plutonium followed by dissolution in HNO_3 using silver(II) is proposed as an alternative process.

Magnetic Separation for Nuclear Material Applications

Introduction

Magnetic separation is a physical separation process that exploits differences in the magnetic susceptibility of materials.[1,2] When particles encounter a nonuniform magnetic field, those that are paramagnetic are attracted toward the highest field gradient while those that are diamagnetic are repelled from the highest field gradients. Because all actinide compounds and many fission products are paramagnetic, magnetic fields containing magnetic field gradients can be used to extract these materials from residues, environmental sources, or field samples. Los Alamos National Laboratory is evaluating magnetic separation for a variety of actinide applications.

Description of the Actual Work

Although numerous magnetic separation methods exist, we have concentrated on development of two distinct methods: high gradient magnetic separation (HGMS) and magnetic roll separation (MRS). These two methods are complementary in the materials that can be treated. Analytical models describing both magnetic separation processes have been developed. The models can provide guidance towards optimization of testing parameters which is crucial for nuclear material operations.

HGMS is being developed for the extraction and concentration of actinides and actinide-containing particulates from 100 microns down to submicron sizes. For the work presented here, a high-performance superconducting magnet is being designed for single particle retrieval from extremely dilute field-collected samples. This case is significant where only one particle may exist in a host material and retrieval of the particle is crucial. Separator parameters that are significant and can be controlled and optimized for a specific situation include matrix material, applied magnetic field strength, flow velocity, solids density, and surfactant.

MRS is applicable to dry powders containing particles greater than 75 microns. It offers improved processing rates for residues compared to open gradient magnetic separation (OGMS), which was previously demonstrated.[3,4] Because MRS is based on permanent magnet technology, it is somewhat easier to implement especially in a glovebox environment. We have investigated MRS for the separation of plutonium or uranium from materials such as sand/slag/crucible (SS&C), graphite, or gravel, which are generated in actinide processing and testing operations.

Magnetic Roll Separation Results

A systematic approach to address actinide processing residues was undertaken, which included laboratory-scale feasibility, optimization of separation variables, and development of an analytical model to predict separator performance. Feed samples were sieved to provide a uniform particle size and to define the MRS particle size performance limits. An increased magnetic field intensity was obtained by an advanced magnet design and coupled with the use of thin Kevlar belts.

Table 1 summarizes the MRS results for the magnetic fraction from two residues generated in actinide processing and testing operations. From our studies, we have demonstrated that MRS is most effective for particles in a size range of 100mm to 4 mm. Lar ge particulate gravel spiked with an uranium surrogate

L. A. Worl
D. Hill
D. Padilla
C. Prenger
E. Roth
Los Alamos National Laboratory

Matrix	Separation Method	Actinide	Particle Size Range	% Actinide	In Total Bulk %	CR[a]
MgO Sand	OGMS	Pu	88–841 mm	66	23	2.9
SS&C	OGMS	Pu	88–841 mm	73	22	2.7
SS&C	MRS	Pu	106–841 mm	76	37	1.8
Graphite	MRS	Pu	106–841 mm	85	4	4.4
Gravel	MRS	Pr[b]	2.5–4.25 mm	100	9	11.0

[a] CR, the Concentration Ratio, is an indication of the performance. The CR is defined as the ratio of the actinide concentration in the magnetic stream divided by actinide concentration in the initial feed stream. The higher the concentration ratio, the better the separation and volume reduction.
[b] Pr_2O_3 used as uranium surrogate.

(Pr_2O_3) conveyed the best results, where optimized tests achieved a 100% separation. These results were used to validate and develop the analytical model. Plutonium residues with strongly diamagnetic properties, such as graphite, were shown to be highly separable, 85% of the plutonium was collected in 4% of the bulk mass. Residues with discrete particles composed of paramagnetic and diamagnetic components (e.g., SS&C residues where plutonium can be included within the diamagnetic slag) made a separation more difficult. If the contaminants are physically liberated in the feed material, a high degree of separation can be achieved.

HGMS Results

We have previously completed a comprehensive series of HGMS experiments with radioactive materials. Our results have been used to develop a model that describes the HGMS process.[5] Extension of this model to submicron, dilute species is currently being investigated. The principal forces governing particle behavior are magnetic, viscous, gravitational, and electrostatic. The performance of the high gradient magnetic separator is then modeled using a force balance on an individual paramagnetic particle in the immediate vicinity of a magnetic capture site.

Several HGMS tests have been conducted where we have investigated advanced matrix material designs with water samples spiked with a submicron-sized plutonium surrogate. From the results, higher extractions were observed with a finer matrix material. These results support theoretical calculations showing that the maximum magnetic attractive force occurs when the matrix element diameter is the same order as the particle diameter. We will extend these results to further enhance HGMS applicability for signature particle collection from a wide variety of samples.

In summary, we have shown that magnetic separation can be used to concentrate actinides from extraneous sources yielding more efficient recovery and treatment operations. For these reasons, efficient physical separation processes can provide cost-effective separation alternatives.

References

1. W. J. Lyman, "High-Gradient Magnetic Separation" in *Unit Operations for Treatment of Hazardous Industrial Wastes*, D. J. De Renzo, Ed. (Noyes Data Corp., Park Ridge, New Jersey, 1978) pp. 590–609.

2. L. R. Avens, D. D. Hill, F. C. Prenger, W. F. Stewart, T. L. Tolt, and L. A. Worl, "Process to Remove Actinides from Soil Using Magnetic Separation," The Regents of the University of California, Office of Technology Transfer, Alameda, California, U.S. Patent No. 5538701 960723, 1996.

3. L. R. Avens, U. F. Gallegos, and J. T. McFarlan, *Separation Science and Technology*, Los Alamos National Laboratory report LAUR-89-3410, 25 (13–15), (1990), pp. 1967–1979.

4. J. M. Hoegler, W. M. Bradshaw, U. S. DOE report ORNL TM-11117 (1989).

5. F. C. Prenger, W. F. Stewart, D. D. Hill, L. R. Avens, L. A. Worl, A. Schake, K. J. deAguero, D. D. Padilla, and T. L. Tolt, "High Gradient Magnetic Separation Applied to Environmental Remediation," Cryogenic Engineering Conference, Albuquerque, New Mexico, July 1993, U. S. DOE report, Los Alamos National Laboratory report LA-UR-93-2516.

Actinides in the Environment

Actinides in the Environment:
Some Perspectives from an Aqueous Chemist

J. Bruno
QuantiSci SL, Spain

Introduction

Anthropogenic inputs of the actinides in the various environmental compartments have increased greatly since the Manhattan project. This is particularly true of plutonium which was basically non-existent in the Earth crust prior to 1940. The assessment of the environmental impact of these elements is dependent not only on the amounts that are being transported through the various compartments but also on the chemical form in which they are present. In this context, chemical thermodynamics and kinetic methods are critical to understand the behavior of the actinides, predict the environmental consequences, and assist on the planning of nuclear waste management strategies. This presentation will focus on the latest developments concerning the aqueous chemistry of the actinide elements by comparing the behavior of uranium and plutonium in the various environmental compartments.

Description of Work

The experience from laboratory work on the chemical thermodynamics and kinetics of the actindes will be presented. The validity and limitations of laboratory data applied to natural systems will be discussed by using the data from recent studies on selected natural systems (Poços de Caldas, Cigar Lake, El Berrocal, Oklo, and Palmottu). The recent developments on the application of kinetic and thermodynamic modeling techniques to the behavior of U and Pu in the environment will be presented.

Investigations of Microbial Systems in Radioactive Environments

A multi-technique approach has been used to investigate microbial systems in radioactive environments. Epifluorescence microscopy, optical density, scanning electron microscopy, microfiltration, and liquid scintillation counting methods have been used to study (1) microbial populations in inoculated, actual radioactive waste/brine mixtures and pure brine solutions, (2) the effects of ^{238}U, ^{232}Th, ^{239}Pu, ^{243}Am, and ^{237}Np to a bacterial species with respect to radiologically or chemically induced changes to cell morphology or bacterial growth, and (3) the association of ^{238}U, ^{232}Th, ^{239}Pu, ^{243}Am, and ^{237}Np with the bacterial cell wall. Studies of this type are crucial from the standpoint of bacteria in contact with radioactive materials in the environment because it is necessary to understand how bacteria may participate in (1) actinide retardation or transport, (2) biological transformation of organic or inorganic materials in radioactive waste containers, and (3) gas generation due to bacterial metabolic activity.

In tests of actual TRU waste under high-ionic-strength conditions at Los Alamos National Laboratory, 54 test containers have added actual solidified inorganic process sludge, pyrochemical salts, and various cementitious waste materials used in various aspects of actinide research or processes. These waste forms are the type that could be destined for storage under high-salt environmental conditions. In order to elucidate the microbiologically influenced transformations of the TRU waste in the test containers, a mixed inoculum was added to all of them. The inoculum was composed of muck pile salt, hypersaline lake brine, and sediment slurry taken from a high-salt environment. The mixed inoculum was verified as containing microorganisms with various metabolic capabilities.

Epifluorescence microscopy with 4',6-diamidino-2-phenylindole dihydrochloride (DAPI) staining was used to enumerate total bacterial populations within the brine solution, as a function of time. Those results showed that the total bacterial cell numbers decreased, perhaps due to cell lysis and death. It is plausible, however, that the bacteria were removed from the brine fluid column through aggregation or sorption to waste and test container surfaces. For any viable bacteria present, sorption to sludge material is feasible because this material could provide a source of carbon, nitrogen, sulfur, and phosphorus, essential nutrients for bacterial survival, which are all present in the solid sediment (or material) in the test containers.

In the second study reported here, total bacterial counts from both a mixed and a pure culture were obtained in order to construct growth curves (cell numbers versus incubation time) of the cultures exposed to various concentrations of actinides. Any appreciable radiological or chemical effects from the actinides appear as variations in the growth curves. Turbidimetric (optical density) measurements agreed well with the microscopy results.

Through the images obtained, changes to cellular morphology can be observed and represent another piece of evidence regarding the effect of Pu on the cells. In this study we observed that the morphology of the cells changed such that the rods seen initially became shorter and more coccoid in appearance with increasing Pu concentration. The overall bacterial size, from random sampling observations, was reduced in specific cases. Comparisons of filtered, inoculated control (without added actinide) and actinide-containing inoculated experiments demonstrate the association of actinide with the bacteria.

M. E. Pansoy-Hjelvik
B. A. Strietelmeier
Los Alamos National Laboratory

J. B. Gillow
C. J. Dodge
Brookhaven National Laboratory

R. J. Sebring
S. M. Kitten
P. A. Leonard
R. Villarreal
I. R. Triay
Los Alamos National Laboratory

A. J. Francis
Brookhaven National Laboratory

H. W. Papenguth
Sandia National Laboratories

Scanning electron microscopy experiments enabled us to more closely study the association of plutonium with a bacterial isolate. The bacterium a facultative anaerobic halophile, was grown under denitrifying conditions in this study, with succinate as the carbon source. Two plutonium concentrations, 10^{-6} and 10^{-5} M, were used, supplied as both the perchlorate salt and as plutonium: EDTA (1:1 complex) to determine the effect of different Pu speciation on the association with the cell, and to ensure solubility of the plutonium in the high-ionic-strength media. The bacteria were grown at 30°C for about 2 days to mid-log-phase in tubes containing SEM grids (carbon/formvar coated nickel) and Pu-containing media. The cultures were then fixed with glutaraldehyde and the grids were removed from the media and subjected to three different washing treatments, one with osmium tetroxide and two without. The grids were then analyzed (uncoated) by scanning electron microscopy with an energy-dispersive x-ray spectrometer to determine Pu association with the cells and with other elements.

The consortium of methods used in these studies will be utilized in several future studies which examine the association of actinides with bacteria in an applied potential field for the electrokinetic remediation of contaminated sites and in column studies which examine the chemical and physical factors which control the transport of bacteria.

Mediation of Actinide Mobility and Potential Actinide Remediation by Microbes in the Environment

Introduction
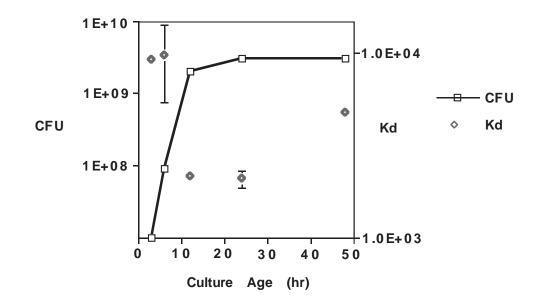
Prediction of actinide migration in the environment and effective remediation of actinide-contaminated sites are dependent on identifying and characterizing the important physical, chemical and biological processes which affect actinide mobility in the environment. Microorganisms are known to populate the environments where actinide contamination has occurred and where nuclear waste repositories are proposed.[1] Metals and radionuclides cannot be degraded in the same way as toxic organics; however, they can be transformed by microorganisms to another chemical form.[2] These biotransformations can profoundly affect the solubility, transport, and toxicity of metals and radionuclides in the environment. These biological processes can potentially be used to separate, concentrate, or immobilize metals and radionuclides in the environment. There are many mechanisms by which microbes may transform metals and radionuclides, most of which are just beginning to be understood in sufficient detail to provide the scientific foundations for *in situ* (and *ex situ*) remediation. However, there is increasing recognition of the role that these processes play in the geochemical cycling of iron, manganese, and trace metals (including contaminants) in the environment and the potential of these processes for remediation of contaminated ground water, soils, and sediments.

Two processes carried out by microbes which may affect actinide mobility in these environments are production of metal complexants and mediation of metal redox state. Metal complexation and metal reduction is well known to affect the biogeochemical cycling of iron and trace metals in the environment and to be involved in the acquisition of required metal nutrients by microorganisms. Because of the similar characteristics of Fe(III) and the tetravalent actinides, these processes are potential contributors to the mediation of actinide mobility and risk. In earlier work we demonstrated that isolated microbial siderophores were able to effectively solubilize Fe from hematite[3] and Pu from a solid hydrous Pu(IV) oxyhydroxide matrix.[4] We have also demonstrated that iron reducing *Bacillus* species are able to solubilize Pu from the same hydrous Pu solid matrix, presumably by a reductive dissolution mechanism.[5] Here we extend these studies to further evaluate the effects of microbial complexants and microbially mediated redox reactions on the speciation of plutonium and uranium.

Results and Discussion

Bacterial cell surfaces contain a variety of acidic functional groups, most of which can function as complexants for metals. Biosorption, the immobilization of metallic elements by bacteria (or other biological systems) may be applied similarly to ion exchange or activated carbon adsorption to remove metals from solution. Alternatively, adsorption of metals to mobile bacteria in the subsurface may enhance metal transport under some conditions. To begin to characterize the interactions between soluble Pu species and bacterial cell surfaces, we examined the biosorption of 10^8 to 10^9 M ^{239}Pu in J13 well water, pH 8, to a *Pseudomonas sp.* isolated from surface soil samples collected at the Nevada Test Site. The sorption ratio (gm/ml) for Pu to this *Psuedomonas* isolate is shown as a function of the growth phase for the bacteria in Figure 1.

J. R. Brainard
S. Thompson
L. Hersman
Los Alamos National Laboratory

As the figure demonstrates, the sorption is related to the physiological state of the organism. Rapidly growing log phase cultures, exhibit 3 to 5 times stronger sorption than stationary phase cultures. Notably, the sorption ratio for Pu on the *Psuedomonas sp.* is 10^4 greater than for Pu on Yucca Mountain tuff, suggesting that the presence of bacterial surfaces in the environment may play an important role in mediating actinide transport.

Uranium contamination in aerobic environments is found primarily in the U(VI) oxidation state. This oxidation state tends to be fairly mobile in the environment, due to the relatively high stability and solubility of uranyl carbonate complexes. Separation of uranium from contaminated soils is an important remediation need. Although the uranium mining industry makes use of oxidative strategies to improve solubilization of uranium from reduced ores, this strategy is of limited value for solubilization and separation of oxidized uranium phases from soil. As an alternative strategy, we have examined the potential of reducing conditions to promote uranium solubilization from contaminated soils. Figure 2 compares the fraction of uranium, iron, and aluminum solubilized from U-contaminated Fernald soil (~550 ppm) in the presence of indigenous microbes by anaerobic incubation with 0.05M nitrilotriacetate (NTA), tryptic soy broth (TSB), and the combination of NTA and TSB.

A seven day anaerobic incubation in the presence of the chelator NTA solubilized greater than 90% of the iron and uranium contained in these soil samples. These results suggest that micobially mediated reduction may be involved in the solubilization of uranium under these conditions. Although the mechanism for solubilization is presently under investigation, it is likely that the reductive dissolution of iron oxyhydroxides in the soil, liberates sorbed contaminant species, such as uranium in this case.
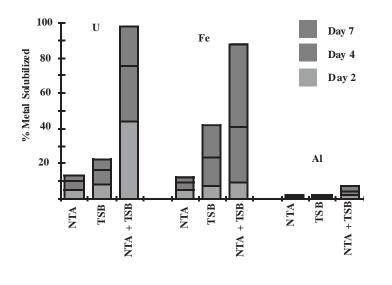
Figure 2. Solubilization of U, Fe, and Al from Fernald soil under reducing conditions. NTA- nitrilotriacetate, TSB-tryptic soy broth.

References

1. J. K. Fredrickson, F. J. Brockman, B. N. Bjornstad, P. E. Long, S. W. Li, J. P. McKinley, J. V. Wright, J. L. Conca, T. L. Kieft, and D. L. Balkwell, *Geomicobiol. J.* **11**, 95 (1993). T. L. Kieft, J. K. Fredrickson, J. P. McKinley, B. N. Bjornstad, S. A. Rawson, T. J. Philps, F. J. Brockman, and S. M. Pfiffner, *Appl. Environ. Micobiol.* **61,** 749 (1995).

2. Bolton and Gorby, *Bioremediation* **3**(10), 1–16 (1995).

3. L. Hersman, P. Maurice, and G. Sposito, *Chemical Geology* **132,** 25–31 (1996).

4. J. R. Brainard, B. A. Strietelmeier, P. H. Smith, P. J. Langston-Unkefer, M. E. Barr, and R. R. Ryan, *Radiochinica Acta* **58/59,** 357–363 (1992).

5. P. A. Rusin, L. Quintana, J. R. Brainard, B. A. Strietelmeier, C. D. Tait, S. A. Ekberg, P. D. Palmer, T. W. Newton, and D. L. Clark, *Environ. Sci. Technol.* **28,** 1686–1690 (1994).

Actinide Solubility and Speciation in YM and WIPP Aquifers: Experimental Data and Predictions Based on Thermodynamic and Geochemical Modeling

Thermodynamic codes used to calculate risk assessments of proposed nuclear waste repositories and actinide transport through the geosphere should be capable of predicting solubility, stability, and speciation of actinide complexes in aqueous systems. Agreement between geochemical calculation and experimental results can validate the thermodynamic database used for the modeling. The solubilities of U, Np, and Pu were measured in Yucca Mountain (YM) ground waters and WIPP brines and compared to solubility calculations to establish consistent and thorough integration of the experimental and predicted data into an internally consistent model.

Yucca Mountain ground waters are low in ionic strength and contain primarily sodium bicarbonate and very little other dissolved solids. The water from well J-13 (total carbonate of 0.0028M) has been recommended as a reference water for YM. Solubilities of Np and Pu in J-13 water were determined in solid-liquid phase equilibria achieved from under- and oversaturation at three different temperatures (25, 60, and 90°C). The solubility limiting Np and Pu solid phases were characterized by powder x-ray diffraction and diffuse reflectance spectroscopy. Unlike previously reported, the formation of solid Np and Pu carbonates is found to be unimportant in J-13. In the presence of low Na^+ or K^+ concentrations, as in the near-field of Yucca Mountain, less complexation and therefore less formation of the carbonates, $MAnO_2(CO_3)$ and $M_3AnO_2(CO_3)_2$, is expected. Neptunium formed mainly Np_2O_5; and plutonium formed Pu(IV) oxides or hydroxides. The Np solubilities ranged from about 1 mM at pH 6 to 5.5×10^{-6} at pH 8.5; plutonium was less soluble than Np, between 5×10^{-8} at pH 6 and 3×10^{-9} at pH 8.5.

WIPP brines are highly concentrated in NaCl and $MgCl_2$ and chloride complexation plays a significant role in the speciation of actinides. We determined the solubility of U(VI) and Pu(VI) in concentrated NaCl solutions and WIPP brines, and found an increase of U and Pu solubility by about one order of magnitude compared to those found in inert electrolyte solutions, such as $NaClO_4$. Solid carbonate phases were identified to be stable only at high CO_2 partial pressure. When lowering the CO_2 partial pressure, U(VI) and Pu(VI) oxides or hydroxides were formed resulting in a lower solubility.

Mathematical modeling codes, such as EQ3NR, are used to calculate aqueous speciation, adsorption/desorption, and precipitation/dissolution.[1] They require a large geochemical database of thermodynamic constants for all components expected in the system under study. Thermodynamic data for neptunium species and minerals in the composite database were derived from Lemire[2] to produce the species distributions under solution conditions representative for the proposed Yucca Mountain and WIPP repositories. A simple species distribution showing only the carbonate complexes under carbonate concentrations representative of those found in UE-25p#1 and J-13 ground waters are shown in Figure 1. In the J-13 water $NpO_2(CO_3)^-$ is predicted to be the dominant species even at pH = 9. There is never enough carbonate present to increase the concentration of the biscarbonato species $NpO_2(CO_3)_2^{3-}$ to 50% of the total neptunyl concentration. Hydrolysis species, such as $NpO_2(OH)$, are predicted to be unimportant, even at pH values near 11.0 (not shown in Figure 1). We also observe that the carbonate J-13 would not be high enough to allow formation of the tris complex $NpO_2(CO_3)_3^{5-}$. As the ionic strength decreases along the abscissa, we see the
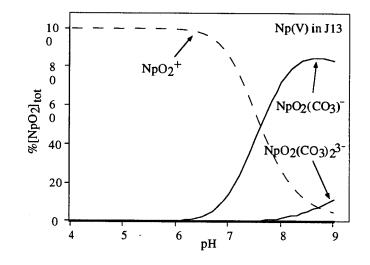
D. R. Janecky
D. W. Efurd
Los Alamos National Laboratory

C. D. Tait
W. Runde
G. T. Seaborg Institute for Transactinium Science, Lawrence Livermore National Laboratory

appearance of a large number of additional species such as $Np(OH)_5^-$, $Np(OH)_4$ (aq), NpF^{3+}, etc. The thermodynamic data for these complexes is still only poorly characterized and in need of further study to properly model this ground water environment.

A model, based on the Pitzer activity coefficient formalism,[3] was developed to describe and predict the solubility of An(VI) (An = U, Pu) in highly concentrated NaCl aqueous solutions. For this purpose spectroscopic data and osmotic coefficients of U(VI) and Pu(VI) are used to parameterize the interaction between actinide(VI) complexes and electrolyte ions. Stability constants of Pu(VI) chloro complexes were implemented in the thermodynamic database. In parallel, Specific Interaction Theory (S.I.T.)[4] has been integrated into the codes as another option as activity model. Both models obtained are compared with S.I.T. and are tested against experimental An(VI) solubility and speciation data in complex brine solutions.

References

1)   D. L. Clark, S. D. Conradson, S. A. Ekberg, N. J. Hess, D. R. Janecky, M. P. Neu, P. D. Palmer, C. D. Tait, *New J. Chem.* **20**, 211–220 (1996).

2)   R. J. Lemire, "An Assessment of the Thermodynamic Behavior of Neptunium in Water and Model Groundwaters from 25 to 150°C," Atomic Energy of Canada Limited report AECL-7817, (1984), p. 53.

3)   Pitzer, *Activity Coefficients in Electrolyte Solutions* (CRC Press, 1991).

4)   I. Grenthe, J. Fuger, R. J. M. Donigs, R. J. Lemire, A. B. Muller, C. Nguyen-Trung, H. Wanner, *Chemical Thermodynamics of Uranium,* (Elsevier Science Publishing Company Inc., North-Holland, 1992) Vol. 1.

Detection
and Analysis

Advantages and Limitations of Oxidation State Analogs

G. R. Choppin
Florida State University

In strong acid solutions Pu(III), Pu(IV), Pu(V)O_2^+ and Pu(VI)O_2^{2+} can coexist in equilibrium although in most solutions only two or three of these oxidation states are present in observable amounts. In neutral/alkaline oxic solutions, the presence of the IV, V, and VI states must be considered. Plutonium solution behavior is complicated further by the kinetics of redox since the electron exchange reactions between the III and IV states and between the V and VI states are quite rapid whereas the redox reactions between the III, IV and the V, VI states are much slower due to the necessity of forming or breaking the metal-oxo bonds. In process chemistry or in stored waste systems the redox behavior may be further complicated by reactions of the plutonium species with the products of radiolysis.

In order to develop new and improved methods for separation systems or for treatment of nuclear waste which includes plutonium, it is necessary to have a good understanding of the initial distribution of oxidation states and of any perturbations of these which may occur during the separation/treatment. It is also important in environmental systems in which plutonium has been released to natural waters to understand the role of the different oxidation states. Unfortunately, the complexity of the redox reactions of plutonium greatly complicates the interpretation in terms of redox speciation of the plutonium data that is obtained from most analyses.

To gain better insight into these systems many groups have used oxidation state analogs in which metal ions that have very similar chemical behavior to the plutonium species of interest are used to mimic the plutonium behavior. Hopefully the chemical behavior would be almost identical for a particular plutonium state and its oxidation state analog. In this review, the degree of similarity that can be obtained by careful choice of oxidation state analog is discussed.

For oxidation state III there is a very good coorelation in the behavior of Pu(III) and that of other trivalent 4f and 5f elements such as Am(III), Nd(III), Eu(III), Gd(III). These analogs can be obtained as radioisotopes for use in tracer studies but, the 4f element cations also allow a variety of other techniques to be employed at higher concentrations. For example, Nd(III) has hypersensitive spectral absorption bands which are sensitive to changes in complexation, symmetry, etc.. Eu(III) has excellent fluorescence characteristics which can be used to monitor the number of coordinating donor sites on a ligand, the residual number of waters of hydration in the inner sphere, and the number of species present (from the excitation spectrum). Gd(III) is an excellent relaxation agent in NMR studies and can provide information on structural characteristics of anions complexed to the Gd cation. All of these 4f cations allow study at the millimolar level to provide results that can be applied to tracer behavior. By contrast, changing the concentration of Pu in a system from tracer to millimolar may change the redox speciation.

PuO_2^+ and PuO_2^{2+} are closely related to the chemical behavior of the much more stable species NpO_2^+ and UO_2^{2+}. The lower specific activity of U and Np allows use of a much broader variety of techniques. Again, techniques requiring millimolar concentrations can be utilized to gain more extensive information on the systems under study. These analog cations also can be used at tracer level concentrations without concern that their oxidation state specification may be modified.

The tetravalent plutonium species is one in which the oxidation state analog approach has somewhat less success. In general, Th(IV) is the best oxidation state

analog for Pu(IV) but its complexation is somewhat weaker, as its hydrolytic tendency. The use of Th(IV) as a model requires slight adjustment to fit Pu(IV) behavior.

Details on the similarities and behavior and on the types of laboratory techniques which can be used with the oxidation state analogs will be discussed. The value of the use of data from "natural analog sites" (i.e., regions of near surface uranium and thorium deposits) is also to be included in this discussion. The advantages and limitations on such laboratory and field data will be the primary concern of the presentation.

Spectroscopic Study of Chelation Between Pu and Modified Siderophores

The efficient and preferential removal of Pu from aqueous solutions by chelating resins and solvent extraction agents containing functional groups commonly found in natural siderophores[1] has been demonstrated over a wide range of solution composition.[2] During the course of testing the uptake of ^{242}Pu by 1,2-hydroxypyridinone resin (1,2-HOPO resin) and 1,2-HOPO octylcarboxamide extractant, we found that these types of chelating agents can effectively remove low concentrations of both Pu(IV) and Pu(VI), although the agents were originally designed for removal of Pu(IV). It is well known that among the common oxidation states, Pu(IV) species have the strongest complex-forming ability due to the higher ratio of formal charge to ionic radius.[3] Therefore, it is possible for organic ligands in the system to reduce Pu(VI) to Pu(IV) first, and then form more stable Pu(IV) complexes. We realized that there was a potential for the reduction of Pu species by binding groups such as 1,2-hydroxypyridinone in our systems. Furthermore, the reduction prior to the complexation can consume a portion of the chelating agent and affect the overall separation efficiency. A better understanding of the chelation mechanism between the complexing agents and Pu can help optimize use of these agents in Pu separations. In the current study, we sought to characterize the oxidation states of Pu in the chelated complex using x-ray absorption near-edge structure (XANES) spectroscopy and UV/VIS spectroscopy in order to obtain information on these complexes at a molecular level.
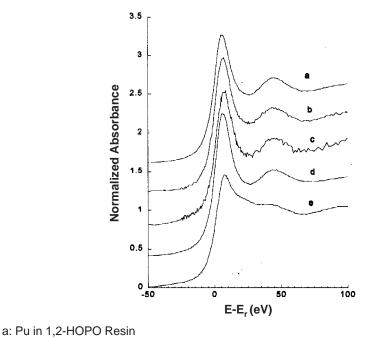
XANES is generally applicable to characterizing the bonding geometry and valence of selected elements in a given compound or complex. This technique can be applied to both liquid and solid phases. Figure 1 shows the Pu L_2 edge XANES spectra for different samples containing Pu and chelating agents along with XANES of reference solutions of Pu(IV) and Pu(VI), respectively. The results indicate that the Pu in both 1,2-HOPO resin and 1,2-HOPO octylcarboxamide extractant is predominantly in the IV oxidation state, despite initial introduction of PuO_2^{2+} into solutions with the chelating agents.

The Pu(VI) aqua species have a sharp absorption peak at 832 nm with a molar extinction coefficient of 440 in solution of dilute nitric acid (Figure 2a), which allows one to detect Pu(VI) at concentrations as low as 5×10^{-6} M with a conventional spectrophotometer. To find out the sequence of the complexation and reduction reactions between Pu(VI) and 1,2-HOPO chelating agents, we have conducted a different set of experiments using UV/VIS spectroscopy. In these experiments, we first sorbed Pu(VI) on 1,2-HOPO resin by mixing Pu(VI) solution (concentration at 6.7×10^{-5} M) with 1,2-HOPO resin and stirred the mixture for 1 hour. The absorption (Figure 2b) and a-liquid scintillation counting data showed that nearly 100% of the PuO_2^{2+} was sorbed onto the resin within 15 minutes. The subsequent extraction of Pu from the resin was carried out using 1 M HEDPA (1-hydroxyethane-1, 1-diphosphonic acid). The analysis (combination of both absorbance and a-liquid scintillation counting measurements) of Pu in the supernatant solutions indicated that 96% of the Pu removed from the 1,2-HOPO resin was Pu(VI) (Figure 2c). The absorption band is shifted to 840 nm due to the complexation of Pu(VI) with HEDPA. These results indicate that 1,2-HOPO chelating agents can form complexes with both Pu(IV)[2] and Pu(VI) ions. However, the Pu(VI)-1,2-HOPO complexes will convert to the more stable Pu(IV)-1,2-HOPO complexes over time.

P. Zhao
V. V. Romanovski
D. C. Hoffman
C. E. A. Palmer
D. W. Whisenhunt Jr.
G. T. Seaborg Institute for Transactinium Science, Lawrence Livermore National Laboratory
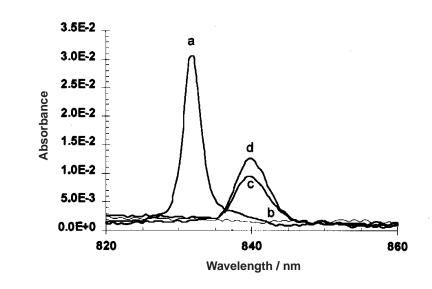
P. G. Allen
D. K. Shuh
J. J. Bucher
N. M. Edelstein
Lawrence Berkeley National Laboratory
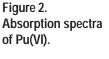
D. J. White
J. Xu
K. N. Raymond
University of California, Berkeley

Figure 1. Pu L$_2$ x-ray absorption near-edge structures spectra..

Figure 1. Pu L$_2$ x-ray absorption near-edge structures spectra..

a: Pu in 1,2-HOPO Resin
b: Pu in 1,2-HOPO Octylcarboxamide/Octanol extracted from 1 M HNO$_3$/5 M NaNO$_3$
c: Pu in 1,2-HOPO Octylcarboxamide/Octanol extracted from 1 M HNO$_3$
d: 1×10^{-3} M Pu(IV) in pH 7 buffer solution
e: 2×10^{-3} M PuO2^{2+} in 0.5 M HNO$_3$

In this study, we have characterized the oxidation states of Pu in Pu(VI)-1, 2-HOPO-chelation reactions using both UV/VIS spectroscopy and XANES. The initial products of the chelation were shown to be Pu(VI) complexes. However, by the time of the XANES measurement, the chelation products were identified as Pu(IV) complexes. These results should help to determine optimum conditions for Pu separations using 1,2-HOPO chelating agents.

Figure 2. Absorption spectra of Pu(VI).

a: 6.7×10^{-5} M PuO$_2$$^{2+}$ in 0.5 M HNO$_3$
b: Supernatant from solution "a," after mixing with 1,2-HOPO resin for 15 minutes
c: Supernatant from mixing Pu(VI)-1,2-HOPO resin with 1 M HEDPA for 30 minutes
d: Reference solution: 2.9×10^{-5} M PuO$_2$$^{2+}$ in 1 M HEDPA
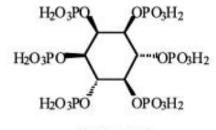
References

1. K. N. Raymond, D. J. White, J. Xu, T. R. Mohs, "Sequestering Agents for the Removeal of Actinides from Waste Streams," in Proceedings from the ESP's 1997 Technical Exchange Meeting, Pacific Northwest National Laboratory report PNNL-SA-28461 (1997), pp. 2.15–2.20.

2. D. C. Hoffman, V. V. Romanovski, A. C. Veeck, P. Zhao, "Evaluation and Testing of Sequestering Agents for Removal of Actinides from Waste Streams," in Proceedings from the ESP's 1997 Technical Exchange Meeting, Pacific Northwest National Laboratory report PNNL-SA-28461 (1997), pp. 2.21–2.24.

3. J. M. Cleveland, *The Chemistry of Plutonium,* American Nuclear Society (1979), p. 92.

Immobilization of Plutonium in Geomedia by Phytic Acid

Residual actinide-containing materials from production, device fabrication, experimentation, and remediation efforts are present in a multitude of forms throughout the complex of Department of Energy facilities. Purposeful and accidental discharges of these materials have caused subsurface contamination. The mobility of these actinides in the subsurface varies both with the hydrology and geology and with the chemical speciation of the particular actinide. Actinide oxides such as PuO_2 are rather insoluble and immobile, but highly mobile species such as NpO_2^+ or the triscarbonato complexes of the hexavalent actinides could be transported by groundwater. In addition, colloidal transport of radioactive species into the surrounding environment must be considered.

Since the total exclusion of groundwater from a site cannot be guaranteed over the lifetime of long-lived radionuclides, a better, more broadly applicable approach to protecting the surrounding environment might be the *in situ* conversion of mobile radionuclides to thermodynamically stable, insoluble mineral forms. Examination of the thermodynamic literature and consideration of the types of naturally occurring f-element minerals leads to the conclusion that actinide-phosphate mineral phases have optimum thermodynamic stability. We are developing a process to immobilize actinides in geomedia by treatment with a ubiquitous natural product, myo-inositolhexakisphosphoric acid or phytic acid. Phytic acid forms insoluble salts with many metal ions, including the f-elements. Our previous laboratory studies have shown that f-element-phytate complexes decompose under environmental conditions to yield phosphate mineral phases that retain trivalent and hexavalent actinides well, even in the presence of a simulated groundwater containing chelating agents.[1]

Phytic Acid

Our prior work lead us to consider the possibility of using salts of phytic acid as degradable cation exchangers for the actinides. First, a calcium salt of phytic acid, found to have the stoichiometry $Ca_{4.5}H_3(C_6H_6(PO_4)_6) \cdot 6.5\ H_2O$, was precipitated from neutral solutions of phytic acid containing between 1 and 6 moles Ca^{2+} per mole of phytate. Then batch experiments with actinide spiked soil samples from Fernald were used to compare the relative effectiveness of $Ca_{4.5}H_3(C_6H_6(PO_4)_6) \cdot 6.5\ H_2O$ and the mineral hydroxyapatite for decreasing the solubility of UO_2^{2+}, NpO_2^+, and Am^{3+} in a groundwater-soil slurry. The results of these experiments demonstrate that $Ca_{4.5}H_3(C_6H_6(PO_4)_6) \cdot 6.5\ H_2O$ is a good ion exchange material for actinide ions with large selectivity for f-elements over Ca^{2+} and distribution coefficients (ml solution/g PO_4) that are higher than those of hydroxyapatite, resulting in lower solution concentrations of the actinide ions. In addition, salts of phytic acid will decompose to form actinide phosphates, unlike hydroxyapatite.

M. P. Jensen
S. R. Friedrich
J. J. Hines
M. A. Schmidt
K. L. Nash
Argonne National Laboratory

Finally, we demonstrated the effectiveness of phytic acid in reducing the solubility of plutonium and americium. Using radiotracer techniques, we followed the fate of PuO_2^{2+}, Pu^{3+}, and Am^{3+} complexes of citric acid or EDTA in a simulated groundwater containing 0.1 M NaCl, 0.0005 M HCO_3^-, 0.01 M Ca^{2+}, and 45 ppm $Ca_{4.5}H_3(C_6H_6(PO_4)_6) \cdot 6.5\ H_2O$ or an equal concentration of the soluble dodecasodium salt of phytic acid between pH 6 and 8. The later was studied because it could be delivered to contaminated soils as a solution. In the presence of Ca^{2+}, the dodecasodium salt precipitated within hours, often reducing the dissolved actinide concentration to values below our limit of detection (3×10^{-10} M for Pu and 5×10^{-12} M for Am) despite the presence of citric acid or EDTA. After a month, calcium phytate salts, regardless of the method of preparation, had reduced the dissolved concentration of Pu or Am in all cases by at least an order of magnitude to less than 10^{-7} M or 10^{-9} M, respectively. Actinide solubility, in general, was reduced more by phytate salts at pH 7 and 8 than at pH 6, and the calcium salts of phytic acid were at least as effective as $H_xPO_4^{x-3}$ per mole of phosphate in removing Am^{3+} from solution.

Reference

1.   M. P. Jensen, K. L. Nash, L. R. Morss, E. H. Appelman, M. A. Schmidt, in *Humic and Fulvic Acids: Isolation, Structure, and Environmental Role*; J. S. Gaffney, N. A. Marley, S. B. Clark, Eds. (American Chemical Society, Washington, DC, 1996), ACS Symposium Series 651, pp. 272–285.

Characterization of Actinide Materials by Elemental and Molecular Imaging

G. J. Havrilla
J. R. Schoonover
F. Wesner
C. Worley
Los Alamos National Laboratory

M. Sparrow
P. J. Treado
University of Pittsburgh

Introduction

Imaging technology provides a powerful means to convey material characteristics very rapidly. Elemental and molecular imaging in the meso-scale regime offers new capabilities to characterize not only conventional materials but actinide containing materials as well. The meso-scale regime falls between the micro region which is below 10 microns and the bulk region which is above 3 mm. Spectral probes with spatial resolution of 100 microns or less can detect elemental and molecular features over large areas covering up to several square centimeters or more. The purpose of combining both elemental and molecular imaging is to provide comprehensive characterization of materials. Integrating the ability to characterize heterogeneous elemental composition with spatially resolved molecular speciation is a powerful analytical approach because complementary information is acquired which cannot be obtained separately. X-ray microfluorescence (XRMF), micro-Fourier transform infrared (FTIR), and micro-Raman imaging spectrometries are utilized in this work. These complementary techniques are employed because they have the potential to be integrated within a single analytical instrument that may be deployable in the field to provide *in situ* analysis of actinides.

Several actinide-containing materials which include Rocky Flats ash residue, MOX fuel and MOX fuel surrogates, and STTP filters have been investigated. The Rocky Flats ash residue has been characterized on a bulk level, however studies have shown that this material is quite heterogeneous. MOX fuel pellets and surrogates have been studied for both plutonium distribution and gallium removal. STTP filters exhibit significant heterogeneity and provide unique challenges for both elemental and molecular imaging techniques.

Experimental

The x-ray microfluorescence data is collected on a Kevex Omicron equipped with a rhodium x-ray tube which can operate at a maximum of 50 watts (50 kV and 1mA). Apertures are placed in front of the x-ray beam to provide x-ray spot sizes from 50 microns to 3 mm in diameter. Typically there is no sample preparation required other than to ensure that the radioactive material is contained. The Raman microscope employs an Ar+ laser coupled to an infinity-corrected microscope via holographic relay optics to excite the sample. The Raman scattered image is collected by the microscope objective and can be directed to a remote spectrograph via a fiber optic bundle for microspectral analysis. For image analysis, the image is presented to a high-performance liquid crystal tunable filter (LCTF). The LCTF scans the Raman spectrum and high-fidelity images are collected at each scan increment. As a result, hundreds of thousands of Raman spectra can be collected very rapidly where the number of Raman spectra is limited by the number of pixels on the CCD camera. The infrared microscope consists of a Nicolet 20SXBO FTIR spectrometer interfaced to a Spectra-Tech Research IRplan microscope. The detector is a HgCdTe element with a low-energy cutoff near 700cm $^{-1}$. IR imaging is accomplished using a filtered globar source, Spectra-Tech Analytical microscope, and an InSb focal plane array.

Results
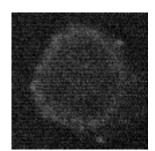
The Rocky Flats ash residue elemental map is shown in Figure 1. Although there is a significant radiation background, the x-ray induced plutonium x-ray at 14.279 keV can be detected without interference. The elemental maps of the other elements shown illustrate the heterogeneous nature of the ash residue. Molecular characterization of the plutonium species will provide important information required for designing treatment strategies for this residue material.
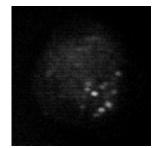
MOX fuel and surrogates provide interesting challenges in characterizing the distribution of elements in the fuel pellets and the removal of gallium from the feed oxide material. The gallium removal is a critical step since gallium is a known alloying metal. Analyses of samples obtained from gallium removal research studies show that under reducing conditions the gallium volatilizes and migrates out of the pellet. XRMF elemental maps show that the gallium appears to follow the thermal gradient within the pellet. In addition to elemental images, we are investigating the use of Raman imaging to identify the molecular species involved with the gallium removal. This analytical work is providing data to understand the gallium removal mechanism and determine the optimum conditions for maximum gallium removal.
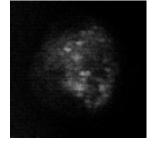
Homogeneous distribution of plutonium is a critical parameter for MOX fuel pellets. Alpha-autoradiography is currently used to determine plutonium homogeneity in European MOX fuel. The primary limitation of this approach is that it relies solely on exposed film standards and not on a quantitative measurement. XRMF is being developed to make a quantitative measurement of plutonium homogeneity. In addition to detecting plutonium, iron contamination and residual gallium can be detected as well. This is a significant advantage of XRMF over autoradiography by detecting non-radioactive elements.

STTP filters offer a heterogenous mixture of chlorides, oxides, carbonates, and other species. Although these can be identified using XRD, sample sizes are small and some species may not be crystalline and therefore not observable with XRD. Micro-FTIR and micro-Raman spectrometries provide molecular species identification associated with visibly observed particles and elemental maps.

Figure 1. XRMF elemental maps of chlorine, iron, and plutonium from Rocky Flats ash residue using 300 micron aperture.

Plutonium

Electron Localization in the Series of Actinide Metals and Pu₃X (X=Al, Ga, In, Tl) Compounds

M. Pènicaud
Commissariat à l'Energie Atomique, France

Introduction

It is known[1,2] that the series of actinide metals, corresponding to the progressive filling up of the *5f* electronic subshell, must be split in two. In the first sub-series, from Pa to Pu, the *5f* electrons bind in the manner of *d* electrons in transition metals. In the other sub-series, starting with Am, the *5f* electrons are localized, similarly to electrons in deep atomic layers, and like the *4f* electrons of lanthanides do not take part in metallic bonding.

The localization of *5f*-electrons in Am was obtained[3] by semi-relativistic and spin-polarized calculations. In our opinion, however, this is not definitive because a final theory should treat spin-polarization simultaneously with spin-orbit coupling[4] and correct the local density approximation (LDA) for localization effect.

Here are results obtained with our fully relativistic muffin-tin orbital (MTO) band calculation method.[5] We present a theoretical calculation of the equilibrium volumes of the whole series of actinide metals available to make bulk measurements, i.e., from Ra to Es. Localizing completely or not the *5f*-electrons, we have tried to reproduce the transitions in volume between α-Pu (19.86 g/cm³), δ-Pu (15.92 g/cm³), and Am (13.67 g/cm³). Special attention has been focused on finding the electronic structure of einsteinium metal in accordance with its low density (8.84 g/cm³).

The theoretical equilibrium volumes of Pu₃X (X=A1, Ga, In, Tl) compounds in the AuCu₃ structure, which are found too low with the LDA scheme,[6] will be also calculated.

Relativistic MTO Method. Treatment of Localized Electrons

We have obtained quite good agreement between MTO calculations and experimental equilibrium volume from Ra to a-Pu.[7] We do have bonding *5f*-electrons up to α-Pu and the band theory may be applied. In these calculations, *6s, 6p1/2, 6p3/2* were treated as band states, and for the exchange-correlation terms the Kohn-Sham parametrization[8] was taken.

From Am, *5f*-electrons become localized. It is well known that LDA fails to describe properties of systems with localized *d* and electrons. In this case, LDA overestimates the band character of electronic states.

Several different attempts (SIC-LDA,[9,10] LDA+U,[11] SRC[12]...) were made to overcome these limitations and repair LDA by introducing some corrections for localized states, but they proved not completely satisfactory and are difficult to use, specially in the fully relativistic case. Moreover, we should point out that α-Pu, δ-Pu, and Am are all found experimentally to be non-magnetic, and we cannot employ the same method as that used[9,10] for the isostructural transition between the low density, magnetic, γ-Ce and the high density, non-magnetic, α-Ce. Here, we have chosen a simpler procedure which gave good results for the equilibrium volume of the lanthanide metals.[13] Since LDA is known to overestimate the extent of the localized orbitals and hence the effects of interatomic hybridization and overlap, we neglect these terms in the matrix elements. We reproduce the localized character of electrons by removing the coupling between their states and other angular momenta. To do this using the MTO method, we only have to cancel the corresponding matrix elements in our "structure constants."[5]

Equilibrium Properties and Electronic Structures

In Figure 1, our calculated equilibrium Wigner-Seitz atomic radii are compared with the experimental values. The agreement is good for MTO calculation with delocalized *5f* to α-Pu. The treatment with full-unhybridized *5f* is obtained by canceling the matrix elements between *f* and angular momenta *s, p, d* and those between the *5f5/2* and *5f7/2* states. When bonding begins to be caused by *5f*-electrons with Th, this treatment fails.

Best agreement for Am and Cm... is obtained by unhybridized *5f* where we allow the coupling of *5f5/2* and *5f7/2* again. We also use the Hedin-Lundqvist[14] exchange-correlation instead of Kohn-Sham.[8] In addition, for δ-Pu the coupling of *5f5/2* with *s, p, d* states is allowed, the coupling of *5f7/2* with *s, p, d* is still forbidden, and we obtain the exact experimental value of the equilibrium atomic radius. This is in accordance with the recent x-ray and high-resolution UV photoemission study which found the localization of δ-Pu *5f*-electrons half-way between Am and α-Pu.[15]

For Es we obtain excellent agreement with the experimental equilibrium volume if we cancel the coupling of the *5f* states with the *s, p, d* and the coupling of *6d* states with the *s, p*. In this case also the Hedin-Lundqvist exchange-correlation was used.

The theoretical equilibrium volumes of Pu_3X (X=A1, Ga, In, Tl) compounds will be also calculated, as for δ-Pu, with unhybridized *5f7/2* electron-states.

The various total and partial densities of states will be presented and the corresponding electronic structures discussed.

Finally, we have shown that it is possible to take account rather correctly of the partial localization of electronic states through their unhybridization. This is a first approach to correct LDA for localized states in the case of non-magnetic, highly relativistic metals and compounds.
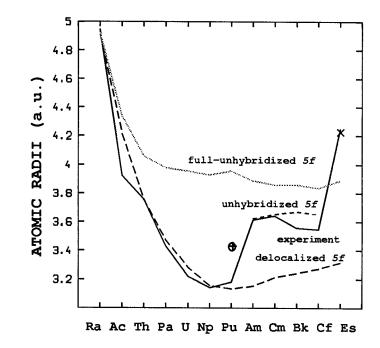
**Figure 1.
Comparison of experimental and calculated (in fcc structure) equilibrium atomic radii.
(+) experimental and (o) calculated, with unhybridized *5f7/2* electron-states, values for δ-Pu.
(x) calculated value for Es with unhybridized *5f* and *6d* electron-states. Full-unhybridized *5f* are obtained by cancelling also the coupling between *5f5/2* and *5f7/2* electron-states.**

References

1. E. A. Kmetko and H. H. Hill, in *Plutonium 1970 and Other Actinides*, W. N. Miner, Ed. (Metallurgical Society of AIME, New York, NY, 1970), p. 233.

2. A. J. Freeman and D. D. Koelling, in *The Actinides: Electronic Structure and Related Properties*, A. J. Freeman and J. E. Darby, Eds. (Academic Press, New York, NY, 1974), Vol 1.

3. H. L. Skriver, O. K. Andersen and B. Johansson, *Phys. Rev. Lett.* **41**, 42 (1978).

4. I. V. Solovyev, A. I. Liechtenstein, V. A. Gubanov, V. P. Antropov, and O. K. Andersen, *Phys. Rev. B* **43**, 14414 (1991).

5. M. Penicaud, in *Shock Waves in Condensed Matter 1983*, J. R. Asay, R. A. Graham, G. K. Straub, Eds. (Elsevier Science Publishers, Amsterdam, Holland, 1984), p. 61.

6. J. D. Becker, J. M. Wills, L. Cox, B. R. Cooper, *Phys. Rev. B* **54**, R17265 (1996).

7. M. Penicaud, J. *Alloys and Compounds* **213/214**, 410 (1994).

8. W. Kohn and L. J. Sham, *Phys. Rev.* **140**, A1133 (1965).

9. Z. Szotek, W. M. Temmerman and H. Winter, *Phys. Rev. Lett.* **72,** 1244 (1994).

10. A. Svane, *Phys. Rev. Lett.* **72,** 1248 (1994).

11. I. V. Solovyev, P. H. Dederichs, V. I. Anisimov, *Phys. Rev. B* **50,** 16861 (1994).

12. N. E. Zein, *Phys. Rev. B* **52,** 11813 (1995).

13. B. I. Min, H. J. F Jansen, T. Oguchi, and A. J. Freeman, *J. Magn. Magn. Mater.* **61,** 139 (1986).

14. L. Hedin and B. I. Lundqvist, *J. Phys. C* **4,** 2064 (1971).

15. J. R. Naegele, L. E. Cox, J. M. Ward, in Proceedings of the 23èmes Journées des Actinides, Schwarzwald, Germany, 1993 (unpublished).

Coordination Chemistry of Actinide Ions (U, Np, Pu) Under Highly Alkaline Conditions

From a historical perspective, the chemistry of actinide ions under strongly acidic conditions is relatively well known, while actinide chemistry under strongly alkaline conditions, such as those found in aging waste tanks within the DOE complex, is poorly understood. Highly alkaline conditions can favor actinide ions in high oxidation states such as V, VI, and even VII. We have used EXAFS, single crystal x-ray diffraction (XRD), Raman and multinuclear NMR spectroscopy to determine the molecular structures of a variety of limiting transuranic complexes under highly alkaline solution conditions. The coordination chemistry, molecular structures, and ligand exchange dynamics will be discussed. In particular, the structure of Np(VII) in 2.5 M NaOH solution was determined. It has long been proposed in the Russian literature that Np(VII) contained the unusual $NpO_4(OH)_2^{3-}$ ion. Using a combination of EXAFS and ^{17}O NMR spectroscopy, we have shown that Np(VII) actually consists of a trans dioxo ion, $NpO_2(OH)_4(OH_2)_x^-$, whose full characterization will be discussed.

Single crystal x-ray diffraction and EXAFS spectroscopy of Np(VI) ions under alkaline conditions revealed $NpO_2(OH)_4^{2-}$ complexes. Strong bonding of equatorial OH^- ligands result in a lengthening of the An=O bond and large shifts (100 cm^{-1}) to lower energy in the Raman-active v_1 stretch of these species. ^{17}O NMR spectroscopy on NpO_2^{2+}, and NpO_2^{3+} ions in 2.5–3.5 M OH^- reveals a water assisted chemical exchange between An=O and An-OH units, and is confirmed by Raman spectroscopy on ^{18}O-enriched samples (Scheme I).

D. L. Clark
S. D. Conradson
D. W. Keogh
M. P. Neu
P. D. Palmer
R. D. Rogers
W. Runde
B. L. Scott
C. D. Tait
G. T. Seaborg Institute for Transactinium Science, Lawrence Livermore National Laboratory and Los Alamos National Laboratory

Scheme I
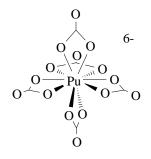
It is widely held that knowledge of uranium chemistry can act as a guide for the behavior of more highly radioactive actinide elements neptunium and plutonium. For example, under highly alkaline conditions, the uranyl ion (UO_2^{2+}) is known to precipitate as insoluble uranate salts such as $Na_2U_2O_7$. One might predict therefore, that neptunium and plutonium will also be insoluble under highly alkaline conditions. However, our work shows that the corresponding neptunyl ions (NpO_2^+ and NpO_2^{2+}) are extremely soluble in 2–3.5 M NaOH and LiOH solution due to formation of anionic species, $NpO_2(OH)_4^{n-}$ (n = 2, 3). This finding is significant because it demonstrates that actinide ions can have significant solubilities under conditions relevant to alkaline radioactive wastes in the U.S., and may impact low-level waste streams at sites such as Hanford and Savannah River. This work also demonstrates the importance of understanding the chemistry of actual transuranic elements.

In addition to our work in hydroxide solutions, there are opposing views on the nature of carbonato complexes of Pu(IV). One view favors the stepwise formation of complexes of general formula $Pu(CO_3)_n^{4-2n}$,[1–3] while an opposing view favors mixed hydroxo-carbonato complexes such as $Pu(OH)_2(CO_3)_2^{2-}$.[4] The identity of the

limiting complex in high carbonate solution is still unknown, and its identity is crucial to the understanding of the complex equilibria in this system.[5] We determined the molecular and solid-state structure of the limiting complex $Pu(CO_3)_5^{6-}$ in 2 M Na_2CO_3 using a combination of XRD and EXAFS spectroscopy.

The solution UV-Vis-NIR, diffuse reflectance of single crystals, and EXAFS solution spectra show that the same limiting anion is present in both solution and the solid-state. The identity and molecular structures of the other Pu(IV) complexes that can form in carbonate solution at lower pH will also be discussed.

References

1.   Kim, Lierse, Baumgartner, *ACS Symp. Ser* **216**, 319 (1983).

2.   Lierse, *Ph. D. Thesis*, T.U. Munich, 1985 .

3.   Nitsche, Silva, *Radiochim. Acta* **72**, 65–73 (1996).

4.   Yamaguchi et al., *Radiochim. Acta* **66/67**, 9–14 (1994).

5.   Capdevilla, Vitorge, Giffaut, *Radiochim. Acta* **74**, 93 (1996).

Polymeric Plutonium(IV) Hydroxide: Formation, Prevalence, and Structural and Physical Characteristics

Plutonium(IV) hydrolyzes more readily than any other oxidation state or species of Pu. The first hydrolysis product is $PuOH^{3+}$, the monohydroxide complex.[1,2] Subsequent hydrolysis could be stepwise, but in reality, even with very dilute Pu, further hydrolysis to form "polymerized" Pu(IV) is extremely rapid. The strong and fast hydrolysis make the thermodynamically and kinetically stable product a pervasive Pu species. The best description of this material is that it consists of oxo-bridged Pu that may be hydrated to some variable extent. Given the potential for variable degree and forms of oxo bridging between Pu atoms, a tremendous range of "apparent molecular weights" exist for the Pu(IV) polymer. The wide variation in formation, size, and other physical properties of Pu(IV) colloids, and our current poor understanding of them, make them troublesome and unpredictable. We present here the first molecular structural studies of polymeric Pu(IV) hydroxides, and extensive characterization of colloidal Pu(IV) materials formed and observed under a variety of conditions.
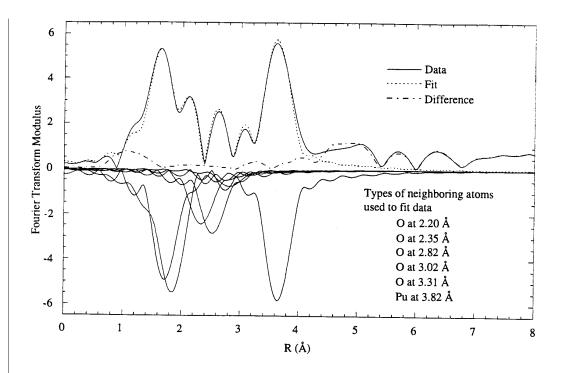
We prepared polymeric Pu(IV) hydroxide in nitrate solution using known procedures,[3,4] and with the addition of saturated sodium chloride and the strongly complexing ligand, citrate. Interestingly, Pu-containing colloids did not form under similar conditions (pH, ionic strength, added base) in pure saturated sodium chloride or citrate solutions.

We used a variety of techniques to characterize the colloids, including: optical absorption spectroscopy (UV/Vis) to confirm polymer formation; dynamic light scattering (LS) and field flow fractionation (FFF) to determine the size and extent of aggregation; scanning and transmission electron microscopy (SEM, TEM) to study the morphology and crystallinity; and extended x-ray absorption fine structure (EXAFS) to determine the molecular structure and Pu coordination geometry.

Dynamic LS and FFF indicate the colloidal products have hydrodynamic radii on the order of 20 to 200 Å. SEM and TEM images show these materials are "polymer-like," with amorphous morphologies. Parallel analyses of aged materials and of products from slightly different syntheses show that the polymer can become crystalline. Both x-ray and electron diffraction analysis have shown that the crystalline polymer consists of very small crystallites of PuO_2.[4] These crystallites can aggregate and become up to micron size in solution.

Extended x-ray absorption fine structure (EXAFS) spectra of the colloids prepared in nitrate solution reveal structural features similar to that of PuO_2; specifically, two dominant near-neighbors to the Pu absorber: O at 2.33 Å and Pu at 3.84 Å (all ± 0.02 Å).[5] In addition, there are O at the unusually short distance of 2.20 Å, and at 2.82 Å, 3.02 Å, and 3.31 Å (Figure 1). The product from nitrate, saturated sodium chloride had identical EXAFS and optical absorbance spectra. In contrast, the material prepared in citrate and nitrate had an optical absorbance spectrum similar to both the mononuclear Pu(IV) citrate complex and the colloidal hydroxide. The EXAFS spectrum contained features similar to the other two colloids, but there were significant differences--no O at 3.31 Å, additional O at 3.72 Å, additional Pu at 4.45 Å, and variation in the number of Pu and O atoms. These data suggest that the short hydroxide or oxide bridges are intrinsic to colloidal Pu(IV) materials, but there is substantial variation in the longer bridges, the Pu sublattice or Pu-bridge-Pu structural subunits, and terminal ligands in the coordination sphere.

M. P. Neu
R. K. Schulze
S. D. Conradson
J. D. Farr
G. T. Seaborg Institute for Transactinium Science, Lawrence Livermore National Laboratory and Los Alamos National Laboratory

R. G. Haire
Oak Ridge National Laboratory

Figure 1. Fourier transform of the EXAFS spectrum of colloidal Pu(IV) hydroxide. Shells of neighbor atoms used to fit the experimental data are plotted with negative amplitude.

Types of neighboring atoms used to fit data
O at 2.20 Å
O at 2.35 Å
O at 2.82 Å
O at 3.02 Å
O at 3.31 Å
Pu at 3.82 Å

Using the spectroscopic data collected on the 'simple' samples (above) as a basis, we have observed polymeric Pu(IV) hydroxide in a number of complex matrices, including in brine solution in contact with actual TRU waste, in spent ion exchange resin (initially Pu(IV) chloride),[6] and in plutonium solubility experiments (initially Pu(VI) carbonate). Implications of these findings to general plutonium chemistry, environmental speciation, and waste issues will be discussed.

References

1. K. A. Krause and F. Nelson, *J. Am. Chem. Soc.* **72**, 3901 (1955).

2. S. W. Rabideau and R. J. Klien, *J. Phys. Chem.* **64**, 6145 (1960).

3. a. M. H Lloyd and R. G. Haire, *Radiochim. Acta* **25**, 139 (1978).

   b. I. R. Triay, D. E. Hobart, A. J. Mitchell, T. W. Newton, M. A. Ott, P. D. Palmer, R. S. Rundberg, and J. L. Thompson, *Radiochim. Acta* **52153** 127 (1991).

4. This work and previously reported by R. G. Haire, M. H Lloyd, M. L. Beasley, and W. O. Milligan, *J. Electron Microscopy* **20, 8** (1971).

5. L. A. Morales, S. D. Conradson, M. P. Neu et al., unpublished results.

6. Presented at this conference by D. K. Veirs et al.

Actinide Compounds and Complexes

The Los Alamos Tunable Light Source
for Transuranic Photoelectron Spectroscopy: First Results for δ-Pu

A. J. Arko
J. J. Joyce
L. E. Cox
Los Alamos National Laboratory

Photoelectron Spectroscopy represents perhaps the most direct and detailed tool for experimentally determining the electronic structure of a material. This is especially true when this tool is used in conjunction with a tunable light source where it is possible to select any desired photon energy, owing to the fact that the cross section for photon absorption is a strong function of both electron orbital symmetry as well as photon energy. Resonant photoemission is particularly useful since the 5f signal at the 5d absorption edge (at resonance) is dramatically enhanced, while just below the edge it is almost totally suppressed (anti-resonance). By collecting spectra at resonance and anti-resonance it is possible to deconvolute the orbital symmetry of the various spectral features. One cannot help but see the importance of this approach when trying to determine the 5f electronic structure.

Inasmuch as synchrotrons represent the premier machines for providing a tunable source of light, it is unfortunate indeed that the safety aspects related to transuranic research preclude the measurement of these materials at synchrotrons. This stems from the fact that in photoelectron spectroscopy the specimen cannot be encapsulated. Indeed, the surface of the material must be cleaned *in situ* to expose a clean surface in this surface sensitive technique, thus resulting in material removal which threatens contamination of an expensive machine.
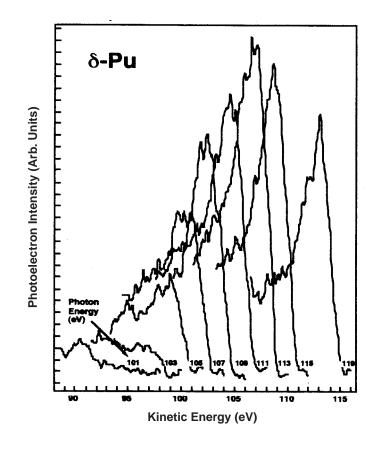
We have overcome many of the difficulties described above by building the first-of-a-kind tunable light source in the laboratory, designed specifically for transuranic research. It is based on a laser plasma light source whereby we focus a powerful pulsed (200 Hz max.) KrF laser light onto a target material such as Au. A plasma is created at the focal spot (about 50 mM diameter) which upon recombination radiates in the soft x-ray region as a pseudo-continuum. We presently collect about 10^{-4} steradians of this light and monochromate it with a Hettrick Scientific variable groove spacing monochromator which has a maximum resolving power of about 1000 at 100 eV photon energy. The usable energy range is from 30 eV to 150 eV photon energy, providing presently about 10^9 photons per second at the sample at maximum resolving power. An upgrade to this monochromator is on order which will increase the throughput by at least an order of magnitude with no loss of resolving power. We are thus able to mimic a synchrotron in the laboratory, albeit at somewhat lower intensities even after the upgrade, and simultaneously satisfying the ES&H issues.

An almost equally important innovation is the method of surface preparation which allows us to clean the transuranic specimen *in situ* with minimum contamination of the spectrometer. This involves cleaning via KrF laser ablation. Pulses of KrF light are diverted into a sample preparation chamber and focused onto the heavily oxidized specimen. The thick oxide is readily removed and the sample is transferred into the spectrometer chamber via a load lock. During transfers additional oxide develops on the surface due to diffusion from the bulk which is cleaned off with only a few laser pulses with the sample inserted into a tube to contain the contamination. The sample is first cooled to 77K to prevent further migration of oxygen to the surface.

Using these techniques we have obtained the worlds first resonant photoemission data on any material outside a synchrotron, but more significantly, these data are on δ-Pu shown in Figure 1. Here we show a series of moderate resolution spectra (≈10 eV wide each, with $\Delta E \approx 500$ meV) ranging from anti-resonance (hν = 101 eV)

through resonance (hν = 113 eV). Note how the 5f signal is almost completely suppressed at anti-resonance, and dramatically enhanced at hν = 113 eV. The small oscillations in the data represent statistical noise and are to be ignored. Each spectrum was collected in a mere 5 minutes to avoid eventual oxygen contamination of the sample. High resolution scans at resonance indicate a sharp 5f feature at E_F consistent with itinerant states, but better statistics await the new monochromator. This represents exciting prospects for future work which will involve surface studies related to hydride formation.

The Actinide Extraction Properties of 1,3 Para-Tert-Butyl-Acid-Diethyl Amide Substituted Calix[4]Arene

The calix[n]arene[1] class of compounds has received considerable attention in recent years due to their ability to selectively complex metal ions.[2] Functional modification to both the lower and upper rims is necessary to improve the extraction characteristics in terms of selectivity, efficiency, and chemical immobilization. We have initiated a research programme to modify the calix[4]arene class of compounds to prepare new and improved toxic and radioactive metal ion extractants.[3-4] The compounds are functionalised to negate the use of anions or phase transfer agents to assist in the extraction process. In this way minimal sample pre-treatment is required to apply the excellent extraction properties to either analytical or waste treatment operations.

Thirty elements, the lanthanides are counted as one, were used to assess the extraction properties of the acid-amide, as a function of pH, by solvent extraction and also through immobilisation onto polystyrene divinyl benzene beads.[5] Complexation data were obtained from metal:ligand solvent extraction ratios,[6] NMR spectroscopy, crystallography, and molecular modelling. Following the simulant experiments low-level radioactive waste was passed through a separation column to determine the selectivity and efficiency of uranium extraction.

The extraction properties of the 1,3 para-tert-butyl-acid-diethyl amide calix[4]arene (referred to as acid-amide), see Figure 1, are as expected pH dependent. The first pKa was determined to be 2.2 indicating why no extraction of metal ions occurs below pH 2. Divalent UO_2^{2+} begins to extract prior to trivalent ions possibly due to a reduced ligand deprotonation requirement necessary for overall charge neutrality and solvent extraction. The extraction efficiencies for these ions in simulant solutions generally increase from pH 3 to pH 6 whereupon extraction remains high >90%. Th^{4+} does not extract over the pII range 3–9, which is not surprising as the acid-amide has only three anionic functionalities. The results also indicate that complexes with more than one ligand per metal ion do not form. As the lanthanides are readily extracted above pH 3, it would be expected that the acide-amide would likewise extract Am^{3+}. No studies have been performed with Pu.

G. P. Nicholson
M. J. Kan
G. Williams
AWE
Aldermaston,
United Kingdom

P. D. Beer
P. Schmidt
University of Oxford,
United Kingdom

M. G. B. Drew
P. D. Sheen
University of Reading,
United Kingdom

Figure 1. 1,3 para-tert-butyl-acid-diethyl amide calix[4]arene (acid-amide).

The acid-amide extracts uranyl with a metal:ligand ratio of 1:1 as determined by both solvent extraction and NMR titration. Molecular modelling has not established the likely co-ordination environment, and no crystallography data are available. For trivalent actinides, the use of crystallography data obtained for the lanthanides[3] may be applicable. The crystal structures of europium and samarium complexes show a centrosymmetric dimer of 2 Eu (Sm) : 2 acid-amide ligands, in agreement with the solvent extraction metal:ligand ratio of 1:1 for La. The acid-amide has fully deprotonated, as determined by metal oxygen bond lengths, and provides an oxygen-rich environment with the lanthanide bound to the lower rim of the cavity, with co-ordination number 8. However for Lu, the smallest lanthanide, the crystal structure shows a monomeric 1 Lu : 1 acid-amide with co-ordination number 7, again in agreement with the solvent extraction metal:ligand ration of 1:1. It would be expected that Am would form a dimeric species as its behaves simularly to larger lanthanides.

Immobilisation of the acid-amide caused extraction to occur under slightly more acidic conditions than by solvent extraction. The extraction experiments consisted of a single pass, under gravity, through the column. Column separation experiments with untreated low-level waste solutions, containing a vast excess of predominantly Ca and Mg, showed that >95% of the uranium was removed in a single pass through the column at pH 3–7. These results not only demonstrate fast extraction kinetics but also the lack of interference from ions in excess, e.g., Ca:U approximately 10^4. As the pH approaches neutral the extraction contribution from the resin bead becomes significant. Optimisation of support material would allow the high selectivity achieved to be applied at neutral pH and therefore ideal for many environmental applications. As the extraction process is pH dependent, recovery of extracted metal ions is facile, 1 M nitric acid is used to strip the columns, which are then ready for re-use.

References

1. C. D. Gutsche, *Calixarenes, Monograph in Supramolcular Chemistry*, J. F. Stoddart, Ed. (Royal Society of Chemistry, Cambridge, United Kingdom, 1989).

2. R. Ludwig *Japan Atomic Energy Research Institute Review* **95-022** (1995).

3. P. D. Beer, M. G. B. Drew, A. Grieve, M. J. Kan, P. B. Leeson, G. P. Nicholson, M. I. Ogden, G. Williams, *Chem. Common,* 1118 (1996).

4. P. D. Beer, M. G. B. Drew, M. J. Kan, P. B. Leeson, M. I. Ogden, G. Williams, *Inorganic Chem.* **35**(8), 2202-2211; (1996).

5. Method of using a low boiling point solvent to coat the bead in tri-butyl phosphaste followed by slow evaporation.

6. H. S. Du, D. J. Wood, S. Eshani, C. M. Wai, *Talanta* **40**(2), 173–177 (199x).

Materials Science

The Activities of the V.G. Khlopin Radium Institute, Russia, in the Field of Pu and Actinide Immobilization

E. B. Anderson
V. G. Khlopin Radium Institute, Russia

The scientific and technological approaches of the V. G. Khlopin Radium Institute, Russia, to the problem of Pu and actinide immobilization are presented. Principal considerations set by the Ministry of Atomic Energy of Russian Federation (MINATOM RF) include:

1. Weapons-grade Pu cannot be considered as a waste, and the Pu should be employed as a fuel;

2. For Pu and actinide immobilization, the most environmentally stable forms must be utilized: fuel burning (weapon-grade Pu), burning by transmutation (actinides, civilian Pu), disposal in a deep geological formation (actinides and possibly civilian Pu);

3. Immobilization of actinides should be considered separately from other HLW, based on existing Russian technology of HLW partitioning;

4. The most stable materials have to be developed for durable incapsulation of spent fuel and solidified HLW.

Therefore, the Radium Institute is involved in a broad range of goals which sometimes are apparently contradictory. However, our extensive radiochemical, mineralogica,l and technological experience allows us to combine these different approaches in order to create multi-use materials. The basis of this work is as follows:

- crystalline ceramic consisting of durable host phases is the most stable and the most attractive material for HLW immobilization

- zircon, $ZrSiO_4$, and zirconia, ZrO_2, are the most durable host-phases for Pu and actinides[1–2]

- zirconia is suggested as a very stable material for Pu ceramic fuel[3]

- a two phase ceramic material based on zircon and zirconia is also considered for Pu ceramic fuel[1]

- during fuel reprocessing in Russia, a very large amount of zirconium from zircaloy cladding comes with the actinide fraction of HLW. This source of zirconium could be used for the synthesis of crystalline ceramic based on zircon and zirconia

- zircon and zirconia are phases having natural mineral analogues, and they are geochemically compatible with granitoid rocks of Nizhnekanski massif investigated as a site for a HLW repository.[4] These minerals could be used as a ceramic material for additional incapsulation of solidified HLW and even for spent fuel

- the Radium Institute has all its experience in the "real" synthesis of crystalline ceramics based on zircon and zircona[1,5] according to existing Russian technologies. Some other durable host-phases (spinel, $MgAl_2O_4$, and $Y_3Al_5O_{12}$) possible for Pu and actinide transmutation are also considered. As a conclusion, the broad field of crystalline synthesis is described. The Radium Institute at present carries out a joint research program with the University of New Mexico for the synthesis of crystalline ceramics based on zircon and zirconia doped with Pu and other actinide simulants, followed by detailed examination of these ceramics under irradiation and leaching conditions.

References

1. B. E. Burakov, E. B. Anderson, B. Ya. Galkin, V. A. Starchenko, V. G. Vasiliev, "The Crystalline Host-Phases for Immobilization of Weapons Plutonium and Waste Actinides," in *Disposal of Weapons Plutonium* (Kluwer Academic Publishers, 1996), pp. 85–89.

2. R. C. Ewing, W. Lutze, W. G. Weber, "Zircon: A Host-Phase for the Disposal of Weapons Plutonium," *J. Mater. Res.* **10** (2), 243–246 (1995).

3. D. F. Carrol, "The System PuO_2-ZrO_2," *J. Of Am. Cer. Soc.* **46** (4), 194–195 (1963).

4. B. E. Burakov, E. B. Anderson, S. I. Shabalev, "The Search of the Optimum Forms for HLW Consolidation, Geochemically Compatible with Granitoid Rocks, NATO Workshop, Krasnoyarsk, 1996 (in press).

5. B. E. Burakov, E. B. Anderson, V. S. Rovsha, S. V. Ushakov, R. C. Ewing, W. Lutze, and W. J. Weber, Synthesis of Zircon for Immobilization of Actinides," in *Scientific Basis for Nuclear Waste Management XIX* (Mat. Res. Soc. Proc. 412, 1996), pp. 33–39.

Calculated Structural Relaxation in Pu-Ga

Introduction

Small additions of Ga (Al, In, or Tl) to Pu stabilize the high-temperature (nominally fcc) δ phase of Pu to room temperature, and the possible existence and nature of this stabilization down to the lowest temperatures continues to be a question of fundamental interest. EXAFS data[1] show structural disorder in the alloy while pair-distribution functions derived from neutron scattering[2] suggest otherwise. Indeed, the possible metastability of the alloy at room temperature has not been resolved.[3,4]

First-principles calculations with large supercells can be used to predict lattice relaxation from fcc and to obtain interatomic potentials to study thermo-elastic effects in dilute Pu-Ga alloys. Thus, we aim to use the relaxation information (forces and total energies as a function of configuration) both directly and indirectly to model structural and vibrational disorder in the alloys at finite temperatures.

Methods

A 32 atom supercell, equivalent to 2×2×2 fcc unit cells, with a Ga atom at the center is the starting configuration. The supercell volume is fixed at the LDA theoretical atomic volume of δ Pu, 17 $Å^3$ per atom.[4] Using the full-potential LMTO method[5] and the local density approximation, the Hellman-Feynman forces on the nearest-neighbor (Pu) atoms to Ga in a $Pu_{31}Ga$ supercell are calculated. Starting with an fcc lattice, atomic positions are adjusted to minimize the forces using the Broyden linear-projection technique.

The LMTO basis set includes the 6s, p, d, 7s, p, and 5f partial waves for Pu and 3d, 4s, p for Ga. Two sets of energy parameters are used with the lower energy being appropriate for the Pu semi-core states. The Hamiltonian matrix includes elements connecting the bases associated with each energy set—allowing full hybridization among the orbitals. Ten high-symmetry k-points in the irreducible wedge—corresponding to 216 points per atom in the full zone—are sampled, and a Gaussian function of 10 mRy width is associated with each eigenvalue.

Results

The nearest-neighbor shell surrounding the Ga atom relaxes inward by approximately 1% of the starting bond length, 2.86 Å. The Pu atoms in the third shell relax away from the Ga atom by 0.1%, though constrained by symmetry to move in the planes of the supercell faces. The Pu atoms in the second neighbor shell around Ga are fixed since they are equidistant between pairs of Ga atoms. The nearest-neighbor shell around these atoms relaxes anisotropically with four of their nearest neighbors moving outward (and toward the Ga) by 1%.

The relaxation energy is approximately 0.1 mRy/atom. The EXAFS data[1] for Pu-3.3 at. % Ga imply an inward relaxation of the Pu shell surrounding a Ga atom of 4%. The neutron pair-distribution function measurements[2] of Pu-2 at. % Ga show no such lattice relaxation.

J. D. Becker
Los Alamos National Laboratory

B. R. Cooper
West Virginia University

J. M. Wills
L. Cox
Los Alamos National Laboratory

References

1.   L. E. Cox, R. Martinez, J. H. Nickel, S. D. Conradson, and P. G. Allen, *Physical Review B* **51**, 751 (1995).

2.   G. H. Kwei, A. C. Lawson, B. S. Cort, R. Martinez, and F. A. Vigil, in progress.

3.   P. H. Adler, *Metall. Trans. A* **22**, 2237 (1991).

4.   J. D. Becker, J. M. Wills, L. Cox, and B. R. Cooper, *Phys. Rev. B.* **54**, 17265 (1996).

5.   J. M. Wills and B. R. Cooper, *Phys. Rev B* **36**, 3809 (1987).

Electronic Structure and Theory of Bonding in δ-Pu

O. Eriksson
J. M. Wills
Los Alamos National Laboratory

The failure of explaining the exotic physical and chemical properties of δ-Pu using current theories for the actinides is pointed out. In particular we demonstrate that the standard model of these systems, stating that the 5f electrons are completely delocalized for the early actinide metals (α-Th → α-Pu) and completely localized for the latter elements (Am → Lr), does not explain the equilibrium volume, structural properties, and elasticity of δ-Pu. Instead we propose that δ-Pu is unique in the sense that it signals strongly correlated electron behavior with a ground state which is much more complex than what the standard model of the actinides stipulates. We present results from our recent theoretical efforts trying to describe this unique Pu allotrope. In particular we demonstrate that the two different electron configurations of the standard model of the actinides (delocalized and localized) are almost degenerate for Pu. We do this by means of calculations based on the local approximation of density functional theory (DFT) and a modification (constraint) of it, which enables calculations of localized electron states.

Normally DFT calculations amount to minimizing the total energy expression E_{LDA} (n(r)) with respect to the electron density, n(r), thus giving a good estimate of the ground state energy of the system. In order to treat localized electrons, it has in the past been demonstrated that one has to perform a constrained DFT calculation where the electron density is divided into two parts $n(r)=n(r)_f+n(r)_{rest}$. Minimization of the density functional can now be done as usual although an additional constraint is put on the one 5f electrons, namely that they should be atomic like, lack hybridization with all other electron states, and have an integer occupation. One may thus evaluate a constrained density functional as $E_{LDA,C}(n(r_f, n(r)_{rest})$ which due to the constraint always is higher in energy compared to $E_{LDA}(n(r))$. However, due to the constraint one may now form a Russel-Saunders ground state of the atomic like 5f electrons and gain a substantial amount of electron-correlation energy, E_{corr}. The localized solution thus has an energy $E_{LDA,C}(n(r)_f, n(r)_{rest})+E_{corr}$, where the value of the latter term is known from experiments and always lowers the energy. One now has a direct way of evaluating accurately the total energy of the delocalized configuration, through $E_{LDA}(n(r))$, and compare it with the energy of the localized configuration, through $E_{LDA,C}(n(r)_f, n(r)_{rest})+E_{corr}$.

We have performed such comparisons for U, Np, Pu, and Am and find in agreement with the experiment that the delocalized state of U, and Np are lower in energy compared to the localized solution. For these two metals we thus correctly reproduce the equilibrium volume, bulk modulus, and structural properties. For Am we find that the delocalized solution is lower in energy and also here we reproduce the volumes, bulk modulus, and structure. Plutonium presents an extremely intricate situation since we find that the delocalized and localized solutions are almost degenerate in energy (within the accuracy of our calculations).

The calculated properties (volume and structure) of the delocalized solution of Pu are in almost perfect agreement with observed data of α-Pu. However, the near degeneracy of the localized and delocalized solutions makes in tempting to associate the electronic structure of δ-Pu with a hybrid state, where the 5f electrons are allowed to fluctuate between two different solutions forming a complex electronic ground state. Based on constrained DFT calculations, as described above, we have investigated the total energy of such a state and find it to be close in energy with the energy of α-Pu. This is consistent with the experiment since a few atomic percent of impurities added to α-Pu stabilize the δ-allotrope, proving the near degeneracy of these two phases.

Gallium Interactions with Zircaloy Cladding

The current accepted approach for disposition of weapons-grade plutonium in the U.S. includes both immobilization and MOX fuel conversion options. The MOX fuel conversion option requires an in-depth analysis of the effects of gallium on fuel performance and its compatibility with fuel components. MOX fuels from the processed spent fuels of LWRs have been used in Europe during the last three decades, and the performance and the cladding compatibility of these fuels have been studied extensively. However, there is no data available about the possible effect of the MOX fuel converted from weapons-grade plutonium on fuel performance and cladding compatibility. Since the U.S. weapons-grade plutonium has small amounts of gallium,[1] the effect of this reactive element to fuel components needs to be understood before using these fuels commercially.

Currently, there are ongoing studies at the national laboratories to clarify some of the issues regarding gallium. We are presently investigating the effects of gallium from weapons-grade plutonium MOX fuel on cladding materials, particularly zircaloy, during reactor irradiation. The methodology used for this study and some preliminary observations are presented in this paper. It is hoped that an upper limit on Ga concentration in the MOX fuel pellet can be established so that the cladding is little affected during burnup.

Although the precise chemical form of gallium in MOX fuel is not known,[2,3] one can assume that gallium is present in elemental or oxide form (Ga_2O_3).[4] In any event, the Ga released from the pellet will interact with the cladding while the cladding is also being irradiated with fission fragments, neutrons, and beta- and gamma-rays. If gallium is present as an oxide, the irradiation conditions will probably lead to breakup of the molecule, so that Ga may still diffuse into the cladding. Clearly, the Ga-cladding interaction will not be under thermal equilibrium conditions. The irradiation of the cladding, especially by the fission fragments, will probably lead to enhanced diffusion and possibly to enhanced chemical reactions.

It is estimated that each ppm of Ga in the fuel corresponds to about 5×10^{16} Ga atoms/cm^3. Since a pellet is about 1 cm^3 surrounded by about 3 cm^2 of cladding, if all the Ga were released, the cladding would be impacted by about 10^{16} Ga atoms/cm^2 per ppm in the fuel. Thus, 100 ppm would give roughly 10^{18} Ga atoms/cm^2.

To approximate the situation, Ga ions are implanted to fluences in the 10^{16} to 10^{18}/cm^2 range into Zirc-II and Zirc-IV[5] to a shallow depth of about 400 Å (100keV ions) while the tar gets are maintained at typical cladding temperatures, 375°C. If there were no diffusion nor sputtering, a 10^{17} fluence would give a peak concentration of 40% in Zr (corresponding to a standard deviation in the projected range of 229 Å). The Ga depth profile may then be measured approximately using Rutherford backscattering (RBS) of energetic He ions. Since the mass of Ga is less than that of Zr, the sensitivity will only be in the percent range. Even so, major effects may be observed. Perhaps, the Ga totally indiffuses or totally outdiffuses or forms a well-defined compound layer.

The depth profile measurements are to be supplemented with scanning electron microscopy (SEM) for morphology, transmission electron microscopy (TEM) for microstructure measurements, and electron microprobe (EM) measurements of especially the lateral distribution of Ga as well as for the identification of possible

R. R. Hart
J. Rennie
Texas A&M University

K. Ünlü
C. Ríos-Martínez
The University of Texas at Austin

compounds. Laterally, it may be possible to determine whether Ga diffuses to grain boundaries.

Following studies of hot implants of Ga into zircaloy, we plan to go to the next level of complexity and bombard the implanted targets with Zr ions to simulate knock-ons produced by the fission fragments without introducing additional chemical complexities. This will also be done while maintaining the targets at cladding temperatures. As a maximum it is estimated that fission fragments deposit about 13 watts/cm^3 in the first 10 microns of the cladding. A significant fraction of this power is deposited via nuclear stopping which produces knock-on recoiled atoms. A 1 microamp/cm^2 ion beam of Zr ions will deposit 2.6×10^4 watts/cm^3 in 765 Å. This gives a ratio of about 2000. Thus, 3 years of fuel burnup may be simulated in about 1/2 day of ion beam irradiation. That is, a similar number of dpa are produced. Again, RBS and electron beam measurements will be performed to see the effects of knock-ons on the implanted Ga.

At this preliminary stage of the study, gallium ions with implantation doses of 10^{16} to 10^{18} atoms/cm^2 have been implanted into polished Zirc-II and Zirc-IV samples. Sample temperatures were maintained at 375°C (typical operational cladding temperature) during the implantation. From SEM studies, there were no observable effects such as blisters, pits, etc. on the surface of these samples up to fluences of 10^{17} atoms/cm^2. Although it is not conclusive, following a fluence of 10^{18} atoms/cm^2 electron microprobe measurements indicate that gallium is concentrated in a micrograin boundary-like structure. Further analysis and structural determinations with TEM are currently ongoing. When this study is completed, it will aid in understanding pellet cladding interactions in general and in understanding the effects of possible corrosion and/or liquid metal embrittlement problems that may be initiated by the presence of gallium.

References

1. T. B. Lindemer, "Assessment of Gallium Effects in Processing and Performance of U-Pu Oxide LWR Fuels," *Fissile Materials Disposition Program,* Oak Ridge National Laboratory report ORNL/MD/LTR-38.

2. "Nuclear Fuels Technologies, Gallium Evaluation Test Plan, Fissile Materials Disposition Program," Los Alamos National Laboratory report LA-UR-96-920.

3. "Nuclear Fuels Technologies, Fiscal Year 1996 Research and Development Test Matrices, Fissile Materials Disposition Program," Los Alamos National Laboratory report LA-UR-96-856.

4. I. A. Sheka, L. S. Chaus, and T. T. Mutyevera, *The Chemistry of Gallium*, (Elsevier, 1996).

5. Material Safety Data Sheet (Zirconium base alloys), (Teledyne Wah Chang, Albany, New York, 1995).
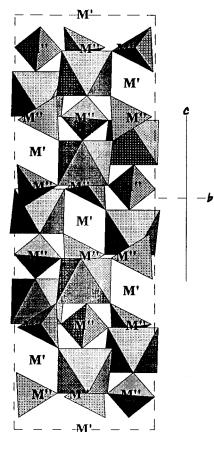
Synthesis and Characterization of Solids in the $Na_{1-x}K_xCe_{2-y}U_y(PO_4)_3$ System

H. T. Hawkins
D. K. Veirs
J. A. Danis
W. H. Runde
Los Alamos National Laboratory

B. E. Scheetz
The Pennsylvania State University

Members of the $NaZr_2(PO_4)_3$ structural family ([NZP]) possess desirable properties that would permit their application as host materials for the actinides. These properties, which include negligible thermal expansion, high thermal stability, compositional flexibility, and radiation damage resistance, arise from the three-dimensional structure of $NaZr_2(PO_4)_3$. This framework structure, which may be represented by the general structural formula $M'M''\square\square\square M'''\square A_2(XO_4)_3$, offers three distinct crystallographic sites that permit the accommodation of a variety of cations. These sites include the A site (an octahedral site normally occupied by Zr^{4+}), the X site (a tetrahedral site normally occupied by P^{5+}), and two interstitial sites, M' and M'', which may or may not be occupied by Na^+. As the oxidation states of the ions occupying the A and the X sites increase, the stability of the structure and the number of structural variations possible for a particular composition increase; as the oxidation states of the ions occupying A and X decrease, the stability of the framework is compromised and the structure collapses.[2]

The isovalent substitution of the larger Th^{4+} for Zr^{4+} results in a loss of symmetry in the [NZP] unit cell with a concomitant increase in the coordination of the A site; this effect has been observed for $KTh_2(PO_4)_3$.[3] However, the effect of U^{4+}, Np^{4+}, and Pu^{4+} substitution for Zr^{4+} on the [NZP] unit cell has not been rigorously addressed. An examination of the literature reveals inconsistencies in the identification of compounds with identical stoichiometries.[4-7]

Compounds in the solid solution series $Na_{1-x}K_xCe_{2-y}U_y(PO_4)_3$ have been prepared through reaction of constituent oxides/nitrates under hydrothermal conditions and by the solid state reaction of constituent oxides/carbonates at elevated temperatures. We will use a multi-method approach to fully characterize these compounds and to examine the effect of U^{4+} and Ce^{4+} (analog for Pu^{4+}) substitutions on the [NZP] unit cell. The extent of solid solution formation in the $Na_{1-x}K_xCe_{2-y}U_y(PO_4)_3$ system will be explored with Rietveld refined powder x-ray diffraction data and transmission electron microscopy (TEM). When appropriate, the compounds will be characterized by both single crystal x-ray diffraction and EXAFS spectroscopy to determine the coordination environments and oxidation states, respectively, of the U and/or Ce ions. Implications of our findings to the application of [NZP] compounds as host materials for the actinides will be discussed.

Figure 1. Projection of the $NaZr_2(PO_4)_3$ structure along the *c*-axis normal to the *a*-axis of the R3c unit cell. The structure is rhombohedral with Na^+ occupying large octahedral cavities (M') between adjacent ZrO_6 and PO_4 polyhedra. M'' sites are vacant, but may be occupied by Na^+ upon substitution of a heterovalent cation for Na^+, Zr^{4+}, or P^{5+}. The figure was drawn with ATOMS for WINDOWS (version 3.2© 1995 Eric Dowty).[1]

References

1. H. T. Hawkins, B. E. Scheetz, and G. D. Guthrie, Jr., "Scientific Basis for Nuclear Waste Management XX," W. J. Gray and I. R. Triay, Eds. (Mater, Res. Soc. Proc. to be published in 1997).

2. J. Alamo, *Solid State Ionics* **63-65**, 547–561 (1993).

3. B. Matkovic, B. Prodic, M. Sljukic, and S. W. Peterson, *Croatica Chem. Acta* **40**, 147–160 (1968).

4. C. E. Bamberger, R. G. Haire, G. M. Begun, and L. C. Ellingboe, *Inorg. Chim. Acta* **94**, 49–56 (1984).

5. C. E. Bamberger, *Handbook on the Physics and Chemistry of the Actinides*, A. J. Freeman and C. Keller, Eds. (Elsevier Science Publishers, B. V., 1985), pp. 289–303.

6. A. A. Burnaeva, Yu. F. Volkov, A. I. Kryukova, I. A. Korshunov, and O. V. Skiba, *Radiokhim.* **34**(5), 12–21 (1993).

7. F. Nectoux and A. Tabuteau, *Radiochem. and Radioanalyt. Lett.* **49**(1), 43–48 (1981).

Hot Isostatic Pressing (HIP) Synthesis of Pu-bearing Zircon

Introduction

Zircon ($ZrSiO_4$) has been extensively reviewed as a potential host-phase for the disposition of excess plutonium and other actinides.[1-3] It is a well-characterized material[4] in which actinides can substitute for Zr in the structure,[5] and has been shown to be resilient to radiation damage from natural radioisotope content,[6] ion bombardment,[7] and ^{238}Pu doping.[8, 9] Naturally occurring zircons have been found with U/Th concentrations of up to 5,000 ppm. Zircon is also exceedingly resilient to weathering and leaching on geologic time scales and is chemically refractory.
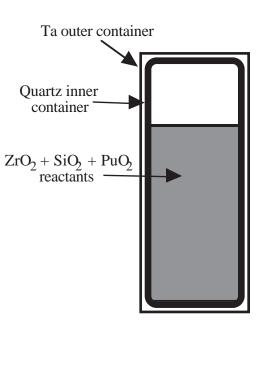
The zircon structure is adopted by the actinide orthosilicates ($ASiO_4$, where $A^{4+} =$ Ac, Th, Pa, U, Np, Pu, Am), all of which have been synthesized in small quantities.[10] Both pure end-member $PuSiO_4$[10] and $(Zr,Pu)SiO_4$ with up to 10 wt % Pu[11, 12] have been synthesized, which suggests that extensive substitution of Pu for Zr in the zircon structure may be possible, allowing for substantial waste loading.

Despite the tremendous amount of research that has been done on using zircon as a potential host phase for Pu disposition, synthesis techniques have not been developed for the large-scale production of Pu-bearing zircon. In order to assess the feasibility of using zircon to immobilize actinides, the solid solubility of actinides in zircon must be determined, and a containment system for high-temperature high-pressure solid state syntheses and process parameters must be developed so that pilot scale fabrication of actinide-bearing zircon can be demonstrated.

Description of Work

The containment system currently being tested for use in a Hot Isostatic Pressing synthesis process consists of an inner quartz container in contact with the reactants, a special sealant to join the parts of quartz containers without fusion inside gloveboxes, and a TIG-welded tantalum outer container (Figure 1). This containment system has the advantages of being both relatively easy to assemble and non-reactive relative to the mixed oxide precursors.

Finely ground equi-molar zirconia and quartz powder mixtures in 80-gram batches were processed at temperatures between 1,450 to 1,500°C and pressures between 4,000 to 10,000 psi for a duration between 2 and 8 hours. Products were then analyzed by x-ray powder diffraction for determining the extent of reaction. Possible reactions between the reactants and containment vessels were also investigated.
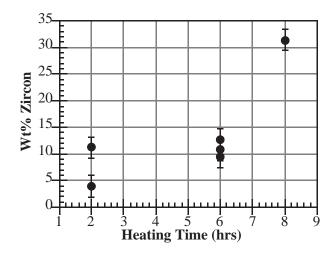
J. Y. Huang
D. R. Spearing
Los Alamos National Laboratory

Ta outer container

Quartz inner container

$ZrO_2 + SiO_2 + PuO_2$ reactants

Results
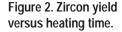
Preliminary results indicate that detectable zircon formation begins after about 2 hours. After 8 hours, > 30 wt % zircon has been synthesized (Figure 2). Some reaction between the quartz and tantalum containers is evident, yet there appears to be little or no reaction between the inner quartz container and reactants. Continuing tests are in progress to increase product yeild and to determine the optimal conditions for the safe fabrication of actinide-bearing zircon.

Figure 2. Zircon yield versus heating time.

References

1. R. C. Ewing, W. J. Weber, and W. Lutze, "Crystalline Ceramics: Waste Forms for the Disposal of Weapons Grade Plutonium," *Disposal of Weapons Grade Plutonium,* E. R. Merz and C. E. Walter, Eds. (1996), pp. 65–83.

2. R. C. Ewing, W. Lutze, and W. J. Weber, "Zircon: a Host-Phase for the Disposal of Weapons Plutonium," *Journal of Materials Research* **10**(2), 243–246 (1995).

3. W. J. Weber, R. C. Ewing, and W. Lutze, *Materials Research Society Symposium* (1996), pp. 25–32.

4. J. A. Speer, "Zircon," *Orthosilicates* 2 ed., P. H. Ribbe, Ed. (1982), pp. 67–112.

5. J. A. Speer, "The Actinide Orthosilicates," *Orthosilicates* 2 ed., P. H. Ribbe, Ed. (1982), pp. 113–136.

6. S. Ellsworth, A. Navrotsky, and R. C. Ewing, "Energetics of Radiation Damange in Natural Zircon ($ZrSiO_4$)," *Physics and Chemistry of Minerals* **21,** 140–149 (1994).

7. R. C. Ewing, W. J. Weber, and J. F. W. Clinard, "Radiation Effects in Nuclear Waste Forms for High-Level Radioactive Waste," *Progress in Nuclear Energy* **29,** 63–127 (1995).

8. W. J. Weber, "Radiation-Induced Defects and Amorphizations in Zircon," *Journal of Materials Research* **5,** 2687–2697 (1990).

9. W. J. Weber, R. C. Ewing, and L. M. Wang, "The Radiation-Induced Crystalline-to-Amorphous Transition in Zircon," *Journal of Material Research* **9**(3), 688–698 (1994).

10. G. Keller, "Untersuchungen über die germinate und silikate des typs ABO_4 der vierwertigen elemente thorium bis americium," *Nukleonik* **5,** 41–48 (1963).

11. G. J. Exarhos, "Induced Swelling in Radiation Damaged $ZrSiO_4$," *Nuclear Instruments and Methods in Physics Research* **B1,** 538–541 (1984).

12. W. J. Weber, "Self-Radiation Damage and Recovery in Pu-Doped Zircon," *Radiation Effects and Defects in Solids* **115,** 341–349 (1991).

Glass and Glass-Ceramic Waste Forms Developed to Immobilize Actinides

D. A. Knecht
S. Johnson
K. Vinjamuri
T. P. O'Holleran
S. Frank
S. V. Raman
B. A Staples
Lockheed Martin
Idaho Technologies
and Argonne National
Laboratory-West

Introduction

The Idaho Chemical Processing Plant (ICPP), which is a part of the Idaho National Engineering Laboratory (INEL), has stored and reprocessed irradiated nuclear fuel since 1953 to recover uranium-235 and krypton-85 for the U.S. Department of Energy (DOE). The resulting acidic high-level liquid radioactive waste (HLLW) has been converted to a granular solid material using a fluidized-bed calcination process. The calcined waste is stored in near-surface, stainless-steel bins within concrete vaults. The major component (wt %) in ICPP HLW alumina calcine includes alumina (82-95), and the major components in zirconia calcines and zirconia calcines blended with other sodium-bearing process and decontamination wastes include fluorite (41-44), zirconia (17-19), calcia (12-13), alumina (914), alkali oxides (5-7), borate (2-4), and cadmium oxide (0-7). Fission product content is typically less than 1 wt %.

As described in the *Record of Decision on the Storage and Disposition of Weapons-Usable Fissile Materials Final Programmatic EIS*, both mixed oxide nuclear fuel and immobilization in glass or ceramic will be pursued in the disposition of plutonium. Glass and glass-ceramic waste forms have been prepared from ICPP HLW compositions that produce durable waste forms suitable for immobilization of plutonium. The purpose of this paper is to describe recently prepared glass ceramic samples containing plutonium or cerium as a plutonium surrogate as part of an evaluation of the technical feasibility of using waste compositions in ICPP HLW calcines as a host for plutonium.

Description

Durable glass-ceramic forms for immobilizing ICPP HLW have been prepared using surrogate alumina, zirconia, and zirconium-sodium blended calcines with a borosilicate frit and other additives such as titania and metallic Ti and Al powders.[1] Major crystalline phases included fluorite, zirconia, and zircon. Sphene and other titanates were formed with added titanium, and calcium-aluminum silicates were formed with the added aluminum. MCC-1 leach rates decreased with lower borate concentration, normalized elemental leach rates of <1 g/m² day were attained.

Glass-ceramic waste forms have also been developed that are suitable for immobilization of plutonium.[2] Several surrogate Idaho HLW alumina, zirconia, and zirconia-Na calcines were used to prepare glass-ceramic forms with calcine loadings of 22 to 60 wt %. These glass-ceramic waste forms were prepared by melting at 1050 to 1450°C with subsequent devitrification by heat treatment, by using a hot isostatic press (HIP) at high pressure and 1050°C, or by sintering at 1150 to 1400°C. The waste forms contained 6 to 18 wt % cerium oxide as a plutonium simulant and 3 to 10 wt % samarium oxide (neutron absorber). Waste forms in which the cerium oxide was replaced with 10 to 20 wt % plutonium have also been produced. Calculations using the Microshield code predicted that glass-ceramic waste forms containing 22 to 60 wt % of radioactive calcine would exhibit radiation doses of 100 to 600 rem/hr at 1 m, that would be considered to be self protecting for nuclear nonproliferation according to DOE orders.

Results and Discussion

Glass-ceramic forms were prepared by melting or sintering different formulations of non-radioactive surrogate zirconia and alumina calcine, cerium oxide as a plutonium surrogate, samarium oxide as a neutron absorber, and additives. The additives included varying amounts of compounds of Si, Na, B, Ca, Ti, and Zr. Loadings of cerium dioxide were equivalent to 20 wt % plutonium dioxide. Preliminary results indicate that cerium is incorporated in mainly the crystalline matrices of glass-ceramic forms with elemental release rates measured by PCT as less than $0.5 \ g/m^2$ day. The crystalline phases included corundum, zircon, zirconia, and ceria. An aluminosilicate glass phase contained from undetectable to low levels of cerium.

Plutonium glass-ceramic waste forms were also prepared with up to 20 wt % plutonium dioxide by melting and sintering, and plutonium is observed to be incorporated mainly in the crystalline phases.

This paper will present details of the microstructure and product characteristics of these materials.

References

1 .   D. A. Knecht, P. C. Kong, and T. P. O'Holleran, "Proposed Glass-Ceramic Waste Forms for Immobilizing Excess Plutonium," Proceedings of the Spring 1996 ANS Meeting, Reno, Nevada (June 1996).

2.   T. P. O'Holleran et al., "Glass-Ceramic Waste Forms for Immobilizing Plutonium," in *Scientific Basis for Waste Management XX,* W. Gray and I. Triay, Eds. (Mat. Res. Soc. Proc., to be published, 1996.)

Phase Separation in Borosilicate Glasses with P, F, and S and the Influence on Glass Durability in Aqueous Environments

Phase separation associated with P, F, and S, and their mixtures was studied using a single baseline composition, Pu10S-2, for vitrification of PuO_2 containing scrape and residues. Single component solubility in the Pu10S-2 was determined: 3.33 wt % P_2O_5, 3.43 wt % F, and 0.70 wt % SO_3. At the solubility limits, no liquid-liquid phase separation was detectable in the annealed samples at slightly above glass transition temperature for 24 hours. The phase separation was determined by visual examination for glass opalescence. Table 1 summarizes the results of phase separation study for all glasses with and without P, F, and S, or their mixtures.

Transmission electron microscopy (TEM) was used to characterize the microstructure of Pu10S-2-PF2 (with 2.24 wt % F and 3.14 wt % P_2O_5) glass that exhibited phase separation. A diffusive ring pattern from selected area diffraction (SAD) analysis demonstrated that the separated phase was amorphous. The matrix and the separated phase were analyzed using electron energy dispersive x-ray spectroscopy (EDXS). The EDXS results showed that the dispersed phase was rich in both P, F, and Na. In addition, Ce (simulant for Pu) exclusively partitioned to the dispersed phase as well as Gd. The results in Table 1 demonstrate that the mixture of P and F promotes glass phase separation, and even the concentrations of

H. Li
Y. L. Chen
J. D. Vienna
Pacific Northwest National Laboratory

Glass ID	P_2O_5 (wt%)	F (wt%)	SO_3 (wt%)	Phase Separation
Pu10S-2	0.00	0.00	0.00	N
Pu10S-2-P1	*3.33* [a]	0.00	0.00	N
Pu10S-2-P2	3.90	0.00	0.00	Y
Pu10S-2-P3	4.90	0.00	0.00	Y
Pu10S-2-F1	0.00	*3.43*[a]	0.00	N
Pu10S-2-F2	0.00	3.87[b]	0.00	Y
Pu10S-2-S1	0.00	0.00	*0.71*[a]	N
Pu10S-2-S2	0.00	0.00	1.66	Na_2SO_4 droplets
Pu10S-2-PF1	3.23[b]	3.34[b]	0.00	Y
Pu10S-2-PF2	3.14[b]	2.24[b]	0.00	Y
Pu10S-2-PF3	2.17[b]	3.36[b]	0.00	Y
Pu10S-2-PS1	3.25[b]	0.00	1.66[b]	Y

[a] The values represent the solubility limits in the Pu10S-2 baseline glass at 1350°C.

[b] The values are based on nominal concentrations of these components. Phosphate concentration in the glass is considered to be the same as the nominal concentration because of little loss due to volatilization, fluorine concentration in glass may be either close to (if the concentration is less than the solubility) or slightly less than (if the concentration is slightly greater than the solubility) the nominal concentration, and the actual sulfate concentration in glass should be much lower than the nominal concentration based on its weak EDXS signal (made by TEM), which can be attributed to high volatility of sulfate at glass melting temperature.

P_2O_5 and F do not exceed their solubility limits in the glass. Glass phase separation associated with P and S was also observed in this study. Without the presence of P, crystalline Na_2SO_4 droplets were found in the glass. However, by incorporating both P and S in the glass, no Na_2SO_4 droplets were detectable under an optical microscope; glass exhibit opalescence. The phase separation in glass with both P and S was identified in low-level waste (LLW) glasses by Raman spectroscopy and solid state ^{31}P-NMR.[1,2] The results of previous studies showed that P and S interacted with each other and promoted separation of both species from the glass network. Combining the previous results with those from this study, it can be also concluded that the mixture of P and S promotes glass phase separation.

The effects of phase separation on glass dissolution and the releases of Ce (simulant for Pu) and Gd were investigated in this study using the product consistency test (PCT) method. All PCTs were conducted in deionized water at 90°C, and the time duration varied from 7 days to about 6 months. For short-term PCTs (7 days and 1 month), the effect of phase separation on glass network dissolution was negligible. However, the 6-month PCT results showed that phase separation of P and S in combination significantly increased the glass network dissolution; the effect was the most as compared with the effects of phase separation of either P and F in combination or P. The network dissolution of glasses with separated single P phase was the lowest and its effect on glass durability was negligibly small.

The PCT results further showed that colloidal particles with a size less than 45mm and gr eater than 40 Å were more likely to form in leachates containing P (released from the glass) than in leachate without P. Those colloids were found to contain Ce as well as Gd. The concentration of Ce and Gd containing colloids increased as test time increased. Liquid state ^{31}P-NMR spectroscopy indicated that the colloids may be attributed to Ce and Gd complexation with P.[3] The results obtained from this study suggest that the transportation of radionuclides, which released from glass, in water may be limited by the formation of colloids rather than by their solubility limits in water.

References

1 .   H. Li, J. G. Darab, D.W. Matson, P. A. Smith, P. Hrma, "Phosphate-Sulfate Interaction in Low-Level Simulated Nuclear Waste Glass," Mat. Res. Soc. Proc., W. M. Murphy and D. A. Knecht, Eds. (MRS, Pittsburgh, Pennsylvania, 1996),Vol. 412, pp. 221–148.

2.   C. Rong, K. C. Moon, H. Li, P. Hrma, H. Cho, "Solid-State NMR Investigation of Phosphorus in Aluminoborosilicate Glasses," (submitted to *J. Non-Crystalline Solids*1997).

3.   H. Li, J. D. Vienna, Y. L. Chen, L. Q. Wang, J. Liu, "Phase Separation in Simulated Plutonium Glasses with Phosphate and Fluorine and the Effect on Glass Corrosion," in *Water. Mat. Res. Soc. Proc* (MRS, Pittsburgh, Pennsylvania, in press, 1997).

Glass Melter Development for Plutonium Immobilization

In the aftermath of the Cold War, the United States has taken the lead in technology development for fissile materials disposition to promote global non-proliferation. In support of this mission, the U. S. Department of Energy's (DOE) Office of Fissile Materials Disposition (OFMD) has been charged with providing technical support for evaluation of options for the disposition of the excess fissile materials manufactured under the nation's defense programs.

One option for plutonium disposition is immobilization using the can-in-canister concept. In this process, plutonium will be immobilized in either a glass or ceramic form and placed in small stainless-steel cans. Several of these cans will then be placed in a rack which will be positioned in a large stainless-steel canister. The large canister will then be filled with high-level radioactive waste glass which will surround the small plutonium bearing cans and act as a high-radiation, non-proliferation barrier.

Currently there are two waste form options being considered for the immobilization of plutonium: a lanthanide borosilicate glass (LaBS) and ceramic based on a synroc composition. To facilitate the down selection between these waste forms by September 30, 1997, data is needed regarding the processing and performance of these forms.

Platinum lined, bottom pour glass melters are attractive candidates for processing the LaBS glass for several reasons. High processing temperatures (~1500°C) are required to achieve the necessary plutonium loading in the glass, and at these processing temperatures, platinum is likely the best glass contact material. Additionally, platinum is not readily wetted by molten glasses so material hold-up in the melter upon draining will be minimized. This is an important attribute from criticality and material accountability perspectives. Platinum melters are also routinely used in the commercial glass industry so there is a great deal of process knowledge and data available for consultation.

Platinum melters can be heated in essentially three ways: indirect heating, direct resistance heating, and induction heating. All three of these methods adequately provide the necessary heat for glass melting, and there is essentially little to differentiate between the three methods. Induction heated melters were selected and are being developed for this application primarily because of the availability of commercial units of the size necessary for the production process. This helps minimize development efforts and provides additional process knowledge and confidence.

Testing in two induction melters is under way to provide data for the down-selection process. A scaled melter system is being evaluated using surrogates for plutonium by Westinghouse Savannah River Company (WSRC). The system includes: a feed system; an inductively heated, platinum vessel with stirring capability; an inductively heated bottom drain spout; and an integrated off-gas system. The goals of the testing are to demonstrate the processability of the LaBS glass in an integrated system, test and determine the optimal configuration for starting and stopping the glass pour, evaluate the compatibility of variable feed streams with melter operation, and evaluate the corrosion behavior of the materials of construction of the system.

A tilt pour induction heated melter is being tested at Lawrence Livermore National Laboratory (LLNL) jointly by LLNL, WSRC, and Pacific Northwest National Laboratory (PNNL) researchers to evaluate the dissolution kinetics of

J. Marra
K. Marshall
R. Schumacher
M. Speer
J. Zamecnik
R. B. Calloway, Jr.
J. Coughlin
R. Singer
Westinghouse Savannah River Company

J. Farmer
W. Bourcier
D. Riley
B. Hobson
Lawrence Livermore National Laboratory

M. Elliott
Pacific Northwest National Laboratory

plutonium in the LaBS glass. This melter utilizes a platinum liner in a graphite crucible and discharges the glass by tilting and pouring into a stainless-steel can. There is some hold-up of the product upon pouring, thus, the melter is not considered a configuration suitable for production. This melter does, however, provide a suitable test bed to investigate the dissolution behavior of plutonium in the LaBS glass in kilogram melt scale quantities. The objectives of this testing are to examine the effects of plutonium oxide particle size, stirring, and residence time of the dissolution rate of the oxide into the glass.

In this paper, an overview of the can-in-canister concept and the glass immobilization option will be provided. Additionally, a summary of the melter selection criteria resulting in the selection of platinum, bottom pour melters will be presented. Finally, results of the testing at WSRC and LLNL utilizing this melter technology will be discussed.

A Statistically Designed Matrix to Evaluate Solubility, Impurity Tolerance, and Thermal Stability of Plutonium-Bearing Glasses

In support of the Department of Energy's (DOE) Office of Fissile Material Disposition (OFMD) Program, Westinghouse Savannah River Company (WSRC) is evaluating a unique lanthanide borosilicate glass to immobilize excess plutonium and other heavy metals. The lanthanide borosilicate (LaBS) glass system met all FY 1996 programmatic planning objectives. Those objectives were focused on demonstrating 10 wt % Pu solubility[1] and meeting preliminary product performance criteria.[2] Although 10 wt % Pu solubility was demonstrated with product performance exceeding high-level waste glasses based on PCT results, the LaBS system was not optimized.

In FY97, the programmatic focus shifted from "pure" plutonium feeds to both "pure and impure" feed streams. The impure feed streams are primarily comprised of two major elements: plutonium and uranium. These streams also include "minor" concentrations of Ca, Mg, Ga, Zn, Fe, Cr, Ni, Na, Ba, Mo, Ga, Cl, and F. The FY 1997 research and development efforts are focusing on technical issues regarding the tolerance of the LaBS glass to Pu, U, and other feed impurities while maintaining thermal stability after a specific heat treatment. Glass formulations not only have to meet both solubility and thermal stability requirements but also address product performance and processing requirements as well. A simultaneous optimization of these parameters was the focus of this work.

A statistically designed matrix was developed to address two technical issues: (1) the solubility of plutonium, uranium, and other minor components into the LaBS glass system and (2) the thermal stability of the glass after a specific heat treatment. This heat treatment schedule will closely resemble the expected heating and cooling cycle of the small internal cans within the can-in-canister alternative. In this alternative, small cans of a Pu-bearing glass or ceramic waste form would be placed in a DWPF canister and high-level waste glass poured around the small cans. This concept was successfully demonstrated using a simulating Pu-glass waste form while DWPF performed "cold" qualification runs.

The purpose of the designed matrix was to demonstrate solubility and thermal stability for candidate glasses that would be processed by melting expected feed streams with an appropriate frit material. The test matrix was designed based on the expected feed streams, oxide ranges of frit components, and the relative proportions of feed to frit that bounded a compositional envelope that would identify compositional spaces in which the criteria were met. The glasses fabricated targeted feed loadings between 5 and 15 wt % which translated into Pu and U loadings ranging from 2.5 to 15 wt % and 0 to 7.5 wt %, respectively. The compositional region evaluated also targeted an "others" loading between 0 and 3.3 wt %. The "others" consists of minor components such as Ca, Mg, Cl, Ga, Fe, Cr, Ni, F, K, Na, Mo, Ta, Ba, W, and Zn at their maximum concentration from all feed streams. The purpose of using the maximum concentration regardless of feed stream was to simulate a "worst case scenario." Studies evaluating individual feed streams as identified by Vienna and Diaz are reported elsewhere. It is anticipated that a compositional region will be defined in which the expected Pu-feed streams can be processed to produce a homogeneous, thermally stable glass that meets preliminary product performance criteria.

D. K. Peeler
T. F. Meaker
T. B. Edwards
D. S. McIntyre
Westinghouse Savannah River Company

References

1. J. D. Vienna, D. K. Peeler, T. F. Meaker, D. L. Alexander, H. Li, and M. J. Schweiger, "Plutonium Dioxide Dissolution Kinetics," Pacific Northwest National Laboratory report PNNL-11346 (September 1996).

2. N. E. Bibler, W. G. Ramsey, T. F. Meaker, and J. M. Pareizs, "Durabilities and Microstructures of Radioactive Glasses for Immobilization of Excess Actinides at the Savannah River Site," Westinghouse Savannah River Company.

Dissolution Studies of Plutonium Oxide in LaBS Glass

Introduction

As part of the international agreement between the United States and Russia, a significant amount of plutonium requires disposition. One of the disposition paths is to immobilize it and dispose of it in a geological repository. The two favored immobilization forms are glass and ceramic. The plutonium, as an oxide, would be reacted with the glass or ceramic to form a homogenous material. The resulting solid product would then be encased in High-Level Waste (HLW) glass for the can-in-canister option. The HLW glass gives a radiation barrier to increase proliferation resistance. The glass canister would then be disposed of by geological emplacement.

The immobilized form has a number of important criteria to meet. These include:

- Significant actinide solubility

- Easily handled and processed in a glovebox environment

- The product should be as durable as spent fuel at a minimum

- The PuO_2 feed should be incorporated into the matrix without a significant amount of unreacted material

Both the glass and ceramic immobilized product need to meet all of these criteria. The ceramic option is described in other papers being presented at this conference. This paper discusses how glass meets criteria 1 and 4.

Description

The proposed glass formulation is a lanthanide boro-silicate (LaBS) glass. The formulation is shown in Table 1.

The initial production of the LaBS glass was done on the laboratory scale at Pacific Northwest National Laboratory (PNNL), Westinghouse Savannah River Company (WSRC), and Lawrence Livermore National Laboratory (LLNL). These mixes were static or with very little agitation (near static runs). They showed solubility of plutonium in the neighborhood of 10 wt % Pu.

D. Riley
W. Bourcier
Lawrence Livermore National Laboratory

J. Vienna
T. Meaker
Pacific Northwest National Laboratory

D. Peeler
J. Marra
Westinghouse Savannah River Company

Table 1. Base LaBS composition.

Oxide	Weight %
SiO_2	25.80
B_2O_3	10.40
Al_2O_3	19.04
ZrO_2	1.15
Gd_2O_3	7.61
La_2O_3	11.01
Nd_2O_3	11.37
SrO	2.22
PuO_2	11.39

Plutonium dissolution in the melt was also studied at LLNL using the Tilt-Pour furnace in the Plutonium Facility (Building 332). This furnace has the capability of making glass volumes of about 2 liters (about 10 kilograms of glass). The furnace has a platinum crucible and can stir the glass. After the completion of the dissolution, the product is poured into a stainless-steel mold. The glass can be recovered from the molds. The Tilt-Pour Furnace was used to determine the effects of stirring, plutonium oxide particle size and residence time on the dissolution rate, and solubility of plutonium in glass. These runs were a joint effort of LLNL, WSRC, and PNNL.

Results

In this paper the results of the static, near static, and agitated runs will be discussed. The results will include the information about the dissolution rate as a function of particle size, residence time, Pu concentration, and stirring. These results will greatly aid in the design and operation of the glass melter for whatever design is chosen. They will also help set the requirements for the feed pretreatment prior to the glass melter.

Schoepite Weathering in the Presence of Calcium and Phosphate Bearing Water: Pathways and Products

The environmental fate of uranyl minerals plays an important role in radioactive waste management and risk assessment. Uranium is known to occur in a wide variety of uranyl mineral phases at contaminated sites worldwide as the result of direct disposal or *in situ* formation. Once present in the environment, uranyl mineral phases can control the release of uranium for transport in the geosphere and biological uptake into the food chain and can govern the release of transuranic elements and fission products from spent nuclear fuel in a repository setting.

The uranyl oxide hydrate schoepite, $[(UO_2)_8O_2(OH)_{12}](H_2O)_{12}$,is widely recognized as a major nuclear fuel corrosion product and as a uranium solubility limiting phase in oxidizing environments.

Experience in natural uranium mineralogy and nuclear fuel disposal research indicates schoepite as a metastable phase in the presence of common soil solution constituents. Environmental chemistry has a profound effect on the fate of uranyl minerals in terms of weathering reactions, rates, and pathways. In the presence of alkali, alkaline earth, and transition metal cations, schoepite is known to transform to the respective metal uranyl oxide hydrates through the exchange of metal cations for interlayer water.

In a previous study, the authors have observed the rapid and extensive transformation of schoepite when contacted with solutions bearing calcium and phosphate at room temperature.[1] In a 0.01 M Ca, 0.01 M PO_4 system, schoepite disappeared entirely between 1 day and 1 week of contact, and was replaced with several uranyl phosphate phases and the isostructural mineral phase becquerelite. Table 1 lists uranyl minerals relevant to schoepite weathering in Ca-PO_4 systems along with current structural formulae. Evidence from x-ray powder diffraction (XRD) data reveal wide variations in the crystallinity of newly formed phases.

The objectives of this work are to further examine the transformation of schoepite in the U-Ca-PO_4 system, describe weathering sequences in terms of reaction pathways and products using XRD and electron microscopy, and interpret results in light of recent work on the structural hierarchy of inorganic uranyl mineral phases.[2] Synthetic samples of schoepite and becquerelite were contacted in batch with solutions containing calcium and phosphate at concentrations ranging from 0.01 M down to 0.0001 M in order to observe the effects of these solution components alone or in combination on the schoepite transformation sequence. The solid phase was sampled periodically and analyzed using XRD. Dissolved concentrations of uranium were also monitored throughout using kinetic phosphorimetry.

A. G. Sowder
Clemson University

S. B. Clark
Washington State University

R. A. Fjeld
Clemson University

Solid Phase	Structural Formal[2]
schoepite	$[(UO_2)_8O_2(OH)_{12}](H_2O)_{12}$
becquerelite	$Ca[(UO_2)_3O_2(OH)_3]_2(H_2O)_8$
autunite	$Ca[(UO_2)(PO_4)]_2(H_2O)_{10}$
meta-autunite	$Ca[(UO_2)(PO_4)]_2(H_2O)_6$
chernikovite (HUP)	$H[(UO_2)(PO_4)](H_2O)_4$

Table 1. Structural formulae for select uranyl minerals.

Results of transformation studies indicate competing pathways for schoepite alteration that are extremely sensitive to the presence and concentration of soil solution constituents. In a simple system bearing 0.01 M concentrations of calcium and phosphate, schoepite undergoes ion-exchange reactions evident in the rapid formation of well-ordered, highly crystalline becquerelite and incongruent dissolution in the formation of autunite. At lower calcium and phosphate concentrations, the transformation of schoepite is less pronounced, becquerelite formation is not indicated, and autunite appears as the sole weathering endpoint. Transformation kinetics appear to be much more rapid within structural families (e.g., schoepite to becquerelite) than between structural families (e.g., schoepite to autunite).

The weathering of schoepite to secondary minerals is of interest because as weathering progresses, alteration products tend to decrease in solubility. The uranyl phosphate minerals, particularly the autunites, are extremely insoluble in the environment. They frequently define the last vestiges of uranyl mineralization in weathered uranium ore deposits prior to outright dispersal of uranium in the surrounding geologic media. Moreover, uranyl phosphates are encountered as prominent forms of uranium at contaminated sites worldwide. Accordingly, where present, the uranyl phosphates can dramatically impact risk assessment and remediation efforts since their low solubilities may reduce the ecological and human health impact of uranium in soils while severely inhibiting the effectiveness of soil clean-up strategies.

References

1. A. G. Sowder, S. B. Clark, R. A. Fjeld, *Radiochim. Acta* **74**, 45–49 (1996).

2. P. C. Burns, M. L. Miller, R. C. Ewing, *Can. Mineral.* **34**, 845–880 (1996).

Alpha Radiation Damage in Plutonium Encapsulating Materials

Weapons-grade plutonium is encapsulated by various materials which act as barriers in pits that are being stored as well as in service in the U.S. weapons stockpile. The materials are subject to continuous irradiation by alpha particles that are emitted from plutonium with energies up to 5 MeV. It is calculated that the flux of alpha particles is more than 10^{15} alphas/cm^2 year which corresponds to 10^{17} alphas/cm^2 in 100 years. The importance of understanding the effects of alpha particles on the properties of these materials over a long period of time is evident. In this study polished stainless-steel samples are implanted with He-3 ions with various energies and fluences to simulate the actual effects of alpha radiation. Depth distributions of the He-3 are determined by the neutron depth profiling (NDP) method which utilizes thermal-neutron-induced charged particle interactions. Surface conditions of the samples are investigated by scanning electron microscopy (SEM) in order to look for any observable blisters or pits due to implantation. Transmission electron microscopy (TEM) is used to monitor possible microstructural changes and bubble formation caused by He-3. A similar study is planned for beryllium metal. A summary of the method used and some of the preliminary results are reported in this paper.

Helium behavior in materials has been an important subject for materials research during the last 40 years. This interest is a consequence of the search for fusion reactor first wall materials that can withstand the high alpha fluences that may be generated in future fusion reactors. The aim of these studies is to obtain information on the relation of the helium fluence and depth distribution on the microstructural and surface changes in various materials. Therefore, a wealth of data is available in the literature about helium behavior in materials.[1,2]

When helium is introduced into materials, it tends to nucleate into small gas clusters at lattice defects. If the helium fluence is increased, the small gas clusters combine and form gas bubbles. Gas bubbles recombine and create a pressurized cavity beneath the material surface. When the pressure of the cavity is high enough, it can form blisters, and the rupturing of these blisters causes surface flaking or exfoliation.[3] Pressurized helium gas bubbles inside materials may also cause cracks and crack propagation into the bulk which can compromise the structural integrity of materials.

To simulate the helium effects on materials used in weapons-grade plutonium encapsulation, a 140 kV ion accelerator is used to implant the He-3 ions. NDP measurements are done using the NDP facility at the University of Texas 1-MW TRIGA MARK-II research reactor.[4] The charged particle reaction ^{3}He(n,p)^{3}H with a thermal cross section of 5,330 barns is used to obtain depth profile data. The residual energy of the outcoming proton is measured, and the corresponding depth at which the reaction took place is determined using the stopping power for the sample material. SEM is used for the observation of surface conditions before and after implantation. A number of test samples have currently been measured by NDP and SEM, and the preliminary results show that implantation doses up to 10^{16} He-3 ions/cm^2 do not cause significant surface damage of samples. The implantation range for 140 keV He-3 ions has been measured to be 400 nm which compares favorably with results of the TRIM code. Unimplanted and implanted samples for TEM observation have been prepared using a jet-thinner, and TEM micrographs of unimplanted samples have been obtained. The TEM analysis of implanted samples is currently under way.

K. Ünlü
M. Saglam
C. Ríos-Martínez
University of Texas at Austin

R. R. Hart
J. D. Shipp
Texas A&M University

The NDP, SEM, and TEM analyses are complemented by *in situ* Rutherford backscattering and channeling analysis of a He-4 implanted single crystal Fe sample to determine the concentration of lattice defects generated by the He-4 as a function of depth.[5] Since Fe is a major component of stainless steel, this will give information on bulk crystalline damage of stainless steel. The simulation of the actual energy distribution of the alpha particles emitted from plutonium will be done by implanting more energetic alpha ions as the study progresses. The completion of the study will provide a better understanding of the correlation between implantation dose, depth distribution, and surface and microstructural effects on stainless steel and beryllium metals.

References

1. S. E. Donnelly, "The Density and Pressure of Helium in Bubbles in Implanted Metals: A Critical Review," *Radiat. Eff.* **90**, 1 (1985).

2. H. Ullmaier, "Helium in Metals," *Radiat. Eff.* **78**, 1 (1983).

3. D. Fink, "Helium Implantation and Thermal Annealing Behavior," *Radiat. Eff.* **106**, 231 (1988).

4. K. Ünlü, B. W. Wehring, "Neutron Depth Profiling at the University of Texas," *Nucl. Instr. and Meth. Phys. Res. A* **353**, 402 (1994).

5. R. Hart, *Radiat. Eff.* **6**, 1 (1979).

Development of a Ceramic Form
for Immobilization of Excess Plutonium

Introduction

R. Van Konynenburg
B. Ebbinghaus
F. Ryerson
H. Shaw
P. Curtis
*Lawrence Livermore
National Laboratory*

Between 8 and 50 metric tonnes of excess plutonium are currently planned to be immobilized in a glass or ceramic waste form in the U.S. The immobilized Pu would then be encased in HLW glass (the "can-in-canister" alternative), which would provide a radiation barrier to enhance the proliferation resistance of the material. Associated with the plutonium are about 15 metric tonnes of uranium (primarily ^{238}U) and a variety of other impurities (primarily Ga, Mo, Al, Mg, Si, and Cl) totaling about 1 metric tonne or less. Immobilization of this material is complicated by the fact that the uranium content in the various feed streams varies widely, from 0 to about 95%.

The proposed ceramic form is composed of about 90% zirconolite ($CaZrTi_2O_7$) and/or pyrochlore ($CaPuTi_2O_7$) with about 10% other phases, typically hollandite ($BaAl_2Ti_6O_{16}$) and rutile (TiO_2). The form is a variation of Synroc-C, which contains nominally 30% zirconolite, 30% perovskite ($CaTiO_3$), 30% hollandite, and 10% rutile and noble metal alloys. Zirconolite and perovskite are the actinide host phases in Synroc-C, with zirconolite being the more durable phase. The pyrochlore structure is closely related to zirconolite and forms at higher actinide loadings. Thus, this mineral is of interest for plutonium disposition in ceramic. Pyrochlore has the advantage that it is cubic rather than monoclinic like zirconolite. Cubic minerals swell isotropically when radiation damaged. As a result, differential strain in the microstructure will be minimal, leading to significantly less microcracking of the form after thousands of years in a repository. Zirconolites and pyrochlores containing uranium and/or thorium exist in nature and have demonstrated actinide immobilization for periods exceeding 100 million years.

Description

The ceramic form being developed for Pu disposition should have the following characteristics:

- a high solid solubility of actinides and neutron absorbers

- extraction of the plutonium for reuse in weapons is difficult

- easily handled and processed in a glovebox environment

- a product at least as durable in a repository environment as borosilicate glass and spent fuels

- incorporation of the PuO_2 feed into the ceramic minerals without a significant amount of unreacted material

- tolerance to feed impurities without significantly affecting the durability or processability

- no adverse effect of the heating cycle due the encapsulation of HLW glass

Work being performed at Lawrence Livermore National Laboratory (LLNL) to address each of these characteristics will be presented and discussed.

The ceramic forms have been fabricated using primarily cold pressing and sintering techniques. Product phase assemblages and compositions were determined by x-ray diffraction, SEM, and microprobe analyses. Selected samples were sent to Argonne National Laboratory for further characterization and durability testing. The bulk of the development work at LLNL was performed on surrogate samples using Ce as an analog for Pu. Once the process parameters were fairly well defined, verification samples were prepared with plutonium. Samples sizes vary from small test samples, roughly 3 g net mass, to large process-prototypic samples, roughly 300 g net mass.

Results

Tests with cerium have shown that about 0.15 formula units can be substituted on the Zr site. Greater cerium contents form an ordered pyrochlore of the approximate composition $CaCe_{0.5}Zr_{0.5}Ti_2O_7$. A two-phase region between $CaCe_{0.5}Zr_{0.5}Ti_2O_7$ and $CaCeTi_2O_7$ has also been identified. Initial results with plutonium-loaded samples confirm that at least 11 wt % Pu^{4+} can be accommodated in the zirconolite phase under oxidizing conditions.

Significant amounts of Ga, Mo, and W have been incorporated into ceramic phases. Ga is incorporated in the Ti site in zirconolite or the Al site in hollandite. Small amounts of Mo and W are also incorporated into the zirconolite phase. Initial tests using a <20 micron diameter, calcined PuO_2 powder as a starting material have shown that between 80% and 85% of the PuO_2 was dissolved in the ceramic matrix after heating at 1300°C for 4 hours. The same tests using $Pu(NO_3)_4$ solution showed essentially complete dissolution of the actinide into the ceramic matrix. Detailed tests on impurity tolerances and actinide oxides dissolution kinetics are currently in progress.

Limited studies on alternate minerals for the incorporation of actinides confirmed that the zirconolite/pyrochlore-rich Synroc is easier to fabricate. Alternate mineral forms tested included zircon ($ZrSiO_4$), monazite ($CePO_4$), uraninite (UO_2), and baddeleyite (ZrO_2).
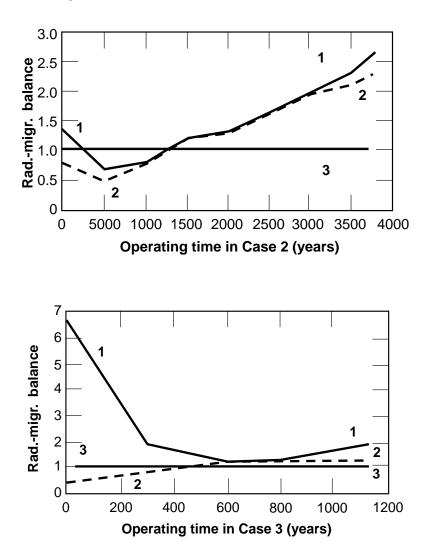
Good densification is achieved by the use of sintering aids and appropriate processing conditions, temperature, atmosphere, etc. BaO is the preferred sintering aid and is incorporated into the hollandite phase the final form. Other sintering aids tested were SrO, MgO, and SiO_2.

Transuranic Waste

The Raw Material and Waste Activity Balance in the Projected Nuclear Power of Russia

Under discussion is the management of long-lived high-level wastes in the nuclear energy sector of Russia, the development of which on a large scale in the next century is motivated by the need for arresting the increasing consumption of fossil fuels. The prerequisites for the nuclear power growth consist in the design of naturally safe reactors and development of a transmutational nuclear fuel cycle (NFC) technology. The choice of operations in such a cycle and of their quantitative characteristics, is aimed at minimizing the wastes to approach the radiation balance with the natural uranium extracted and put to use. The paper discusses the way the approximation to the balance between the raw material and waste activity is influenced by introduction of the transmutational NFC (in Case 2), inclusion of transmutation reactors into the energy mix (Case 1), partial disposal of actinide wastes into outer space, and by recycling of protactinium (Case 3). It is shown that such a balance can be sustained for a considerable time in Cases 2 (Fig. 1) and 3 (Fig. 2) or throughout the operation stage of the future nuclear power (Case 1) (Fig. 3).
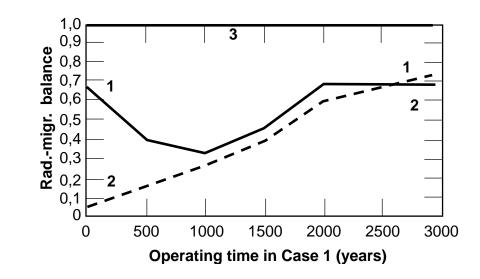
E. O. Adamov
I. Kh. Ganev
A. V. Lopatkin
V. G. Muratov
V. V. Orlov
Research and Development Institute of Power Engineering, Russia

Figure 1. Radiation balance with allowance for migration, $S=A_{RME}/A_{U+Th}$ in Case 2, with $K_{mig}=15$ and with the time of long-term monitored cooling of LHW, years:
1 – 0
2 – 200
3 – condition for balance ($S \leq 1$).
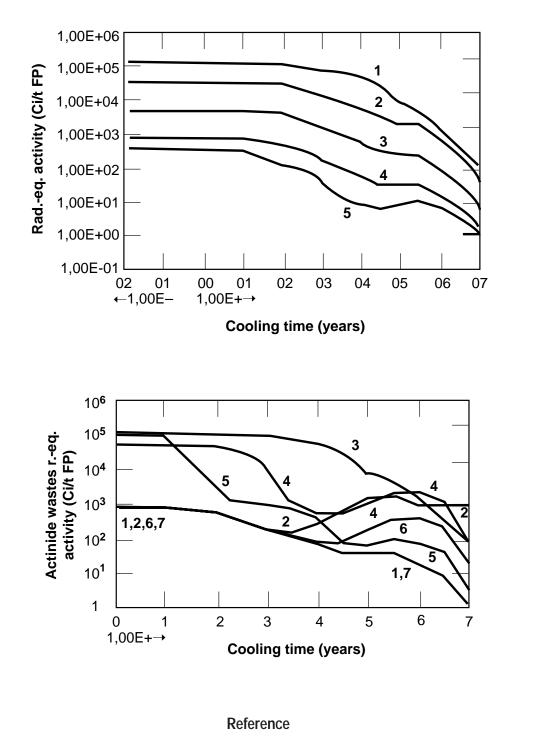
Figure 2. Radiation balance with allowance for migration, $S=A_{RME}/A_{U+Th}$ in Case 3, with $K_{mig}=15$ and with the time of long-term monitored cooling of LHW τ_0, years:
1 – 0
2 – 200
3 – condition for balance ($S \leq 1$).

Figure 3.

Acceptable separation of LHW elements. Reference 1 examines the effect of the degree of element separation in the course of BREST fuel reprocessing and hence of the portion ζ which goes to wastes, on the radiation-equivalent activity of actinide wastes. The cooling time before radiation balance is attained (in the range of 100 to 1000 years) depends mostly on ζ of such elements as Pu, Am, Cm (Figs. 4–5) and to a lesser degree, on Np, U, and Cf. Figure 5 offers a comparison of the above elements.

The data obtained suggest the following conclusions:

- there is no need for recycling californium with fast reactors and this element can be entirely disposed of

- from the viewpoint of the radiation balance, all neptunium can go to wastes and its recycling is unnecessary since the activity rise caused by 100% disposal of Np, with cooling time of $10^5 ... 10^6$ years (120...150 Ci/t of FP), would not exceed the actinide activity with cooling for 200 years (320 Ci)

- disposal of 100% of uranium is impermissible due to a significant increase in the actinide activity within $(1...3) 10^5$ years (1000...1300 Ci/t of FP); if 10% of uranium is disposed of, however, the activity will not exceed the level corresponding to 200-year cooling, wherefore given uranium recycling, separation of, e.g., 98 to 99% of uranium is a tolerable level, with 1 to 2% of this element dumped

- recycling is advisable in case of plutonium with the greatest possible separation of this element; its desirable portion in wastes is 0.01%

- americium needs recycling with 0.01 to 0.1% sent to wastes, otherwise the activity of actinides becomes unacceptably high with monitored cooling for 200 years

- disposal of 100% of curium is desirable in order to reduce the neutron activity of the fuel in recycling, but it cannot be tolerated due to the high activity of actinides in the period ranging between zero and 1 to 3 thousand years, it is advisable to recycle Cm with 1 to 2% contribution to wastes or to introduce intermediate cooling the recycling process

Figure 4. Radiation equivalent activity of BREST actinide wastes. Equilibrium closed NFC of BREST reactors. Contribution to wastes: U,Np,Am,Cm,Cf–1%, Th,Pa,Bk–100%, and Pu:
1 – 100%
2 – 10%
3 – 1%
4 – 0.1%
5 – 0.01%

Figure 5. Radiation equivalent activity of BREST actinide wastes. Equilibrium closed NFC of BREST reactors. Contribution to wastes: Th, Pa, Bk–100%, and other elements are as follows:
1–100% Cf,
0,1% U, Pu, Np, Am, Cm
2–100% U,
0,1% Pu, Np, Am, Cm, Cf
3–100% Pu,
0,1% U, Np, Am, Cm, Cf
4–100% Am,
0,1% U, Pu, Np, Cm, Cf
5–100% Cm,
0,1% U, Pu, Np, Am, Cf
6–100% Np,
0,1% U, Pu, -, Am, Cm, Cf
7– 0,1% U, Pu, Np, Am, Cm, Cf

Reference

1. E. O. Adamov, I. Kh. Ganev, A. V. Lopatkin, V. G. Muratov, V. V. Orlov, "LHW Management in Phasing Out Large-Scale Nuclear Power in Russia," RDIPE Report, 1996, Atomnaya Energiya, in press, 1997.

Statistical Signal Processing and Artificial Intelligence Applications in the Nondestructive Assay of U/Pu Bearing Materials

S. E. Aumeier
J. H. Forsmann
Argonne National Laboratory-West

Over the years, a number of techniques have been developed to determine the quantity and distribution of radiative isotopes contained in given assay samples through the measurement and analysis of penetrating characteristic radiations. An active technique of particular utility when assaying samples containing very small quantities of fissionable material or when high gamma ray backgrounds are encountered is the delayed neutron nondestructive assay (DN-NDA) technique.[1–4] Typically, analysis of the delayed neutron signal involves relating the gross delayed neutron count observed following neutron irradiation of an assay sample to total fissionable material present via a linear calibration curve.[1,3,4] In this way, the technique is capable of yielding the mass of a single dominant fissionable isotope or the total fissionable mass contained in a sample. Using this approach, the only way to determine the mass of individual fissionable isotopes contained in a sample is to correlate *total* fissionable mass to individual isotopics via calculations or other means, yielding an *indirect* measure of isotopics. However, there is isotope specific information in the temporal delayed neutron signal due to differences in the delayed neutron precursor yields resulting from the fissioning of different isotopes.

We present the results of an analysis to evaluate the feasibility of using Kalman filters[5] and genetic algorithms[6] to determine multiple specific fissionable isotopic masses contained in an assay sample from a cumulative delayed neutron signal measured following neutron irradiation of the sample. Delayed neutron measurement data were generated to simulate the ideal response of the leached fuel clad monitor located at Argonne National Laboratory—West (ANL—W).[7] The simulated measurement data were generated by calculating the cumulative delayed neutron count following the irradiation of a sample containing 5.9 g ^{238}U, 9.8 g ^{235}U, 16.9 g ^{239}Pu, and 3.1 g ^{240}Pu. Data were simulated for ~14 MeV neutron irradiation and irradiation with a moderated neutron beam with average neutron energy of ~200 eV, which yields a larger fissile/fertile fission ratio than the 14 MeV irradiation.

The simulated measurement data, with various levels of random noise superimposed, were analyzed using both the Kalman filter and genetic algorithm, details of which are beyond the scope of this summary. For both the genetic algorithm and Kalman filter, the 14 MeV and 200 eV data were processed simultaneously. The mass of ^{240}Pu is assumed known from coincidence measurements, and *a priori* masses were chosen to be 50% in error from correct values. The Kalman filter was executed in successive iterations on the same data set with the *a priori* for a given iteration taken to be the best estimate from the previous iteration with covariance matrix reset at each iteration to avoid filter saturation. Because of this, uncertainties for the Kalman filter estimates are biased and therefore not reported. To obtain an estimate of the uncertainty of each mass estimate and improve the accuracy of the estimates obtained using the genetic algorithm, batches of genetic algorithms were run for each case. The predicted mass was then taken to be the average of the individual estimates from the 50 batches and the uncertainty calculated as the standard deviation of the population of estimates about the mean. The genetic algorithm represented the masses of each isotope as a string of 11 binary bits on a chromosome.[6] The fitness (accuracy of mass estimate) of each chromosome was evaluated at each generation by comparing the calculated delayed neutron emission (calculated from a model developed using calibration data) resulting from the given mass estimates with the measured delayed neutron signal. The results of the

analyses are presented in Table 1 and show mass estimation accuracies better than 3% for the Kalman filter and better than 6% for the genetic algorithm with 10% Gaussian noise on the simulated measurement data.

Table 1. Mass estimates.[a]

Isotope	Kalman Filter Results N(0,2%) Noise on Measurement	Kalman Filter Results N(0,10%) Noise on Measurement	Genetic Algorithm Results[b] N(0,2%) Noise on Measurement	Genetic Algorithm Results[b] N(0,10%) Noise on Measurement
^{238}U	5.91 (0.2%)	5.97 (1.3%)	5.72 ± 0.37 (–3.1%)	5.73 ± 0.37 (–2.9%)
^{235}U	9.95 (1.5%)	9.68 (–1.2%)	9.98 ± 1.06 (1.8%)	9.41 ± 1.18 (–4.0%)
^{239}Pu	16.69 (–1.3%)	17.32 (2.5%)	16.71 ± 1.77 (–1.1%)	17.84 ± 1.96 (5.6%)
^{240}Pu	3.10 (0.0%)	3.10 (0.0%)	3.10 ± 0.00 (0.0%)	3.10 ± 0.00(5.6%)

[a] Percent deviation from actual in parentheses.
[b] 50 batches, 2500 generation; Mutation probability=65%, crossover probability =5%.

The results of the study demonstrate the feasibility of extracting isotope specific information from a cumulative delayed neutron measurement using statistical signal processing and artificial intelligence techniques, thus providing a direct measure or Pu content in an U/Pu bearing sample. Performance of the techniques using actual measurement data will be evaluated in the near future with success most likely depending strongly on the ability to acquire very accurate calibration data.

References

1.   T. Gonzani, "Active Nondestructive Assay of Nuclear Materials," NUREG/CR-0602, Monsanto Research Corporation (1981).

2.   G. Tessler, B. Beaudoin, W. Beggs, L. Freeman, A. Kahler, and W. Schick, "A Gauge for the Nondestructive Assay of Irradiated Fuel Rods," *Nuclear Technology* **82**, 275 (1988).

3.   T. D. Reilly, "The Measurement of Leached Hulls," Los Alamos National Laboratory report LA-7784-MS (1979).

4.   S. E. Binney, and R. I. Scherpelz, "A Review of the Delayed Fission Neutron Technique," *Nuclear Instruments and Methods* **154**, 413 (1978).

5.   A. H. Jazwinski, *Stochastic Processes and Filtering Theory*, (Academic Press, New York, New York, 1970).

6.   L. Davis, *Handbook of Genetic Algorithms*, (Van Nostrand Reinhold, 1991).

7.   S. E. Aumeier, W. P. Poenitz, and J. H. Forsmann, "Nondestructive Assay of Leached Cladding Hulls at ANL-W," *Proc. American Nuclear Society Spring Meeting*, Orlando, Florida, 1997 (in press).

Pu and Gd Chemistry of Zirconolite Polytypes in a Titanate Ceramic

A. J. Bakel
E. C. Buck
Argonne National Laboratory

B. Ebbinghaus
Lawrence Liverrnore National Laboratory
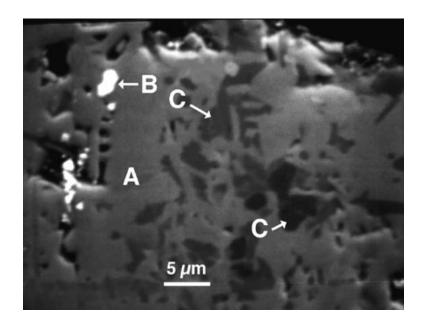
Introduction

Titanate-based ceramics are being developed as possible candidates for immobilizing excess plutonium from dismantled nuclear weapons. Evidence from testing of similar ceramics and natural analogues suggests that this material is very resistant to aqueous corrosion.[1–4] The purpose of our work is to describe the phase(s) present in these ceramics. In particular we are interested in the disposition of important elements such as Pu and Gd (to be incorporated into the wasteform as a neutron absorber). In concert with data from corrosion tests, this characterization will allow us to describe the release behaviors of important elements from this type of ceramic. This is particularly difficult and important due to the heterogeneous nature of the material.

Results and Discussion

A titanate ceramic was developed and produced at LLNL. Examination of the ceramic with scanning electron microscopy (SEM) and SEM/energy dispersive spectroscopy (SEM/EDS) shows the presence of several distinct phases. Figure 1 shows a SEM photomicrograph of one of the ceramic samples. The most common phase (A in Figure 1) contains Zr, Ca, Ti, and smaller amounts of Al, Pu, and Gd. Analytical electron microscopy (AEM) data indicates that this phase is probably a zirconolite. In addition, Pu-rich particles (B in Figure 1) probably undissolved $PuO_{2–x}$) are present in this ceramic. Ti-rich particles (C in Figure 1), possibly $TiO_{2–x}$, are also present with small amounts of Al and Zr. Gadolinium-rich phases, pyrochlore, and a Ca titanate (possibly perovskite) were also found in the ceramic by means of AEM analyses.

The substitution of Pu and Gd into zirconolite and related structures such as pyrochlore is being studied in several Pu-loaded ceramics and will be described in detail. Previous studies have shown that zirconolite has three crystallographic sites.[1] The first site can contain Ca, Th, U^{+4}, Pu^{+3}, and trivalent rare earth elements including Gd; the second site can contain Zr, Hf, Np^{+4}, Ce^{+4}, and Pu^{+4}; and the third site can contain Ti, Mg, Al, Mn, Fe, Nb, Ta, and W.

Figure 1. An SEM photomicrograph of a particle of the ceramic. The sample was mounted in epoxy, cross sectioned, and polished to 0.25 μm. The labels in the photograph correspond to phases described in the text.

We have analyzed the chemical compositions of individual particles with SEM/EDS. Using these data, we will describe substitution patterns in the phases. For example, if we find that the concentrations of Zr and Pu are inversely proportional in the population of zirconolite particles sampled, then it is reasonable to believe that Pu replaces Zr in the zirconolite structure. Any observed substitution patterns will be discussed in terms of crystal structure and the corrosion behavior of the ceramic.

Conclusion

Detailed characterization of ceramic samples will allow us to describe the disposition of Pu and Gd within the material. The release behavior of Pu and Gd from the ceramic will be strongly affected by the partitioning of these elements within various phases. The goal is to incorporate the Pu and Gd into a phase that is particularly resistant to corrosion. The first ceramic we examined was designed to incorporate both Pu and Gd into zirconolite. Several other phases are shown to contain Pu and/or Gd. The implications of the distribution on the release behavior of Pu and Gd from this ceramic material will be discussed.

References

1.   E. R. Vance, C. J. Ball, R. A. Day, K. L. Smith, M. G. Blackford, B. D. Begg, and P. Angel, "Actinide and Rare Earth Incorporation into Zirconolite," *J. Alloys Comp.* **213/214**, 406–409 (1994).

2.   V. M. Oversby and W. E. Ringwood, "Leaching Studies on Synroc at 95° and 200°C," *Rad. Waste Mgmt.* **2**, 223–237 (1982).

3.   G. R. Lumpkin, K. P. Hart, P. J. McGlinn, T. E. Payne, R. Giere, and C. T. Williams, "Retention of Actinides in Natural Pyrochlores and Zirconolites," *Radiochim. Acta.,* 469–474 (1995).

4.   P. J. McGlinn, K. P. Hart, E. H. Loi, and E. R. Vance, "pH Dependence of the Aqueous Dissolution Rates of Perovskite and Zirconolite at 90°C," *Mater. Res. Soc. Symp. Proc.* (1996).

Microwave Vitrification of Radioactive Sludge and Residue in Container

The vitrification technology of HLW in the ceramic melter EP-500 was put into practice in Russia, but not all types of radioactive wastes can be vitrified in this ceramic melter. Ferrocyanide-sulfide slurry and insoluble residues after their processing cannot be involved into a glass because of big concentrations of corrosion-aggressive components as regards to melter molybdenum electrodes (iron, nickel, sulfur).

Substantial amounts of these radioactive sludge and slurry have been accumulated in the storage tanks of the radiochemical industry such as PO "Mayak" (Ozersk) and Chemical Integrated Works (Krasnoyarsk). The above-mentioned wastes contain substantial amounts of plutonium (more 0,05% in kg of insoluble residue after chemical processing of ferrocyanide sulfide slurry). The simplest and most rational way of processing slurry and residues containing transuranium elements may be microwave heating in a container for storage of solidified waste where all stages of the process: water evaporation, denitration, calcination, and melting into glass take place in the above container.

Development technology is based on solidification of wastes in the container, applicable for storage, by heating it with the use of microwave energy.

A microwave pilot glass melter for ferrocyanide-sulfide slurry and insoluble residues was developed with the following characteristics:

- microwave power—5 kWt

- frequency—2450 MHz

- container volume—30 1

- melting temperature—up to 1050°C

The vitrification process in a stainless-steel container on simulated slurry and residue was checked. Orthophosphoric acid was used for flux glass-making. After mixing the acid with slurry, subsequent vitrification glasses with an ultraphosphate composition (with P_2O_5 content exceeding 55 to 60 mass %) are produced. Their glass making temperature does not exceed 900 to 950°C. Such glasses contain up to 2% mass of CeO_2 as plutonium surrogate and also more than 5 mass % of sulphate ion. Phosphate glasses obtained have low-melting with viscosity or 15 to 30 poise at 950 to 1050°C. This enables the obtaining of homogeneous glass within a bulk container.

The process of microwave vitrification of slurry and sludge in a container has the following merits:
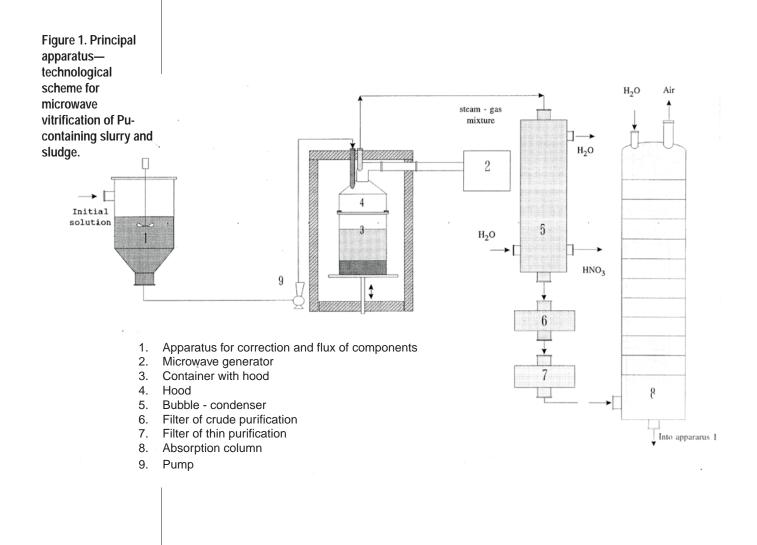
- simplicity and reliability because all stages beginning with water evaporation from sludge until glass melting are carried out in the container without the complicated operation of glass pouring

- compact facility consisting of container, stationary hood with slurry feed, and microwave energy feed, equipment for pressing container to hood, and for removing container within glass

G. B. Borisov
A. V. Nazarov
VNIINM, Russia

M. N. Molokhov
Research and Development Institute of Construction Technology and Residues (NIKIMT), Russia

Long-term tests of basic units are being carried out at the microwave pilot melter by the feeding of surrogate sluge.

At present, the microwave pilot melters are being developed for vitrification of Pu-containing slurry, insoluble residues as follows:

- with the microwave power of 5 kWt for "hot chamber" of Mining Chemical Integrated Works at the Krasnoyarsk site

- with the microwave power of 25 kWt for industrial use at MCW (see principal apparatus-technological scheme in Figure 1)

Figure 1. Principal apparatus—technological scheme for microwave vitrification of Pu-containing slurry and sludge.

1. Apparatus for correction and flux of components
2. Microwave generator
3. Container with hood
4. Hood
5. Bubble - condenser
6. Filter of crude purification
7. Filter of thin purification
8. Absorption column
9. Pump

Microscopic Analysis of Pu-Contaminated Incinerator Ash: Implications for Immobilization

E. C. Buck
Argonne National Laboratory

Introduction

In this paper, a nanometer-scale mineralogical study with analytical transmission electron microscopy (AEM) of plutonium-bearing incinerator ash from the Rocky Flats Environmental Technology Site (RFETS) in Colorado is described. The findings from this work may have implications for the present effort to immobilize plutonium waste.

Around 70% of the plutonium ash in the DOE weapons complex is stored at the RFETS.[1] The ash was formed from the combustion of contaminated wastes generated from plutonium processing. The RFETS incinerator ash composition has been determined by Blum et al.[1] The ash was formed at temperatures estimated to be between 200°C and 900°C and contains up to 14 wt % Pu.[2] Ash is a generic term used to describe the by-product of combustion and owing to the variability in the inorganic components.

Results
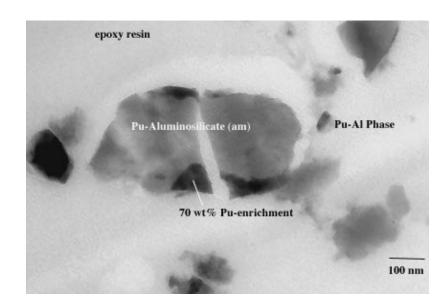
Samples of ash were examined with a combination of optical, scanning electron microscopy, and AEM. The ash exhibited a poikiloblastic texture with all the detectable plutonium as aphanitic particles surrounded by larger particles. The ash was crushed to release the Pu-bearing regions, and thin sections of this material were produced with ultramicrotomy for AEM. The combination of microscopy investigations determined the non-Pu-bearing particles to be SiO_2, K-feldspar ($KAlSi_3O_8$), fluorite (CaF_2), corrundum (Al_2O_3), chromite ($FeCr_2O_4$) diopside ($CaMg(SiO_3)_2$), anorthite ($CaAl_2Si_2O_8$), and amorphous aluminosilicates. Although most of the plutonium exists as a reduced plutonium oxide (PuO_{2-x}), a significant amount of the plutonium is present in other forms. Three types of Pu-bearing phases were observed, including a Pu-bearing aluminosilicate glass, various crystalline silicotitanate phases, and Pu-Al particles.
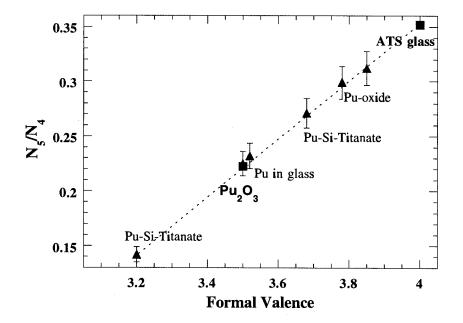
In some regions reaction with silicates has resulted in the formation of Pu-bearing glasses (Figure 1). The Pu is spread throughout the particle at about 23 to 25 wt %, but is enriched to about 75 wt % in some regions. These levels of Pu in glass have not been achieved in most waste glasses. The oxidation state of the Pu in the glass was determined using an electron energy-loss spectroscopy (EELS) method developed for rare earths.[3] The Pu oxidation state may be estimated from the ratio of the intensity of the Pu-N_5 to N_4 absorption edges, which correspond to the "white line" transitions $4d_{3/2} \rightarrow 5f_{5/2}$ (N_4) and $4d_{5/2} \rightarrow 5f_{7/2}$ (N_5). Samples of known Pu oxidation state were used to construct a calibration curve[4] for determining the oxidation state of Pu in the ash (Figure 2). The oxidation state of the trace level (< 100 ppm) of Ce present in ash particles was also obtained with the same method.[3]

The composition of two crystalline Pu-silicotitanates particles was determined to be $[(Pu^{+3.3}, Ce_{0.01}^{+3.1}, Ba_{<0.01})(Fe_{0.1}, Cr_{0.03})Ti_{0.8}, Al_{0.24})SiO_6]$ and $[(Pu^{+3.7}, Ce_{0.01}^{+3.4}, Ba_{<0.01})(Fe_{0.15}, Cr_{0.3})(Ti_{0.5}, Al_{0.2})SiO_5F]$. Electron diffraction indicated that the phases were structurally similar to chevkinite $[(Ca,REE,Th)_4(Fe,Mg)(Ti,Mg,Fe)_4Si_4O_{22}]$. The F-bearing phase may be related to rare-earth-bearing titanite which, in nature, incorporate 0.2 to 0.6 wt % F. Both chevkinite, the rare earth-Fe-Ti silicate, and titanite (ideally $CaTiSiO_5$) are known to occur, along with zirconolite polytypes

Figure 1. Transmission electron micrograph of a plutonium-bearing silica glass with ~20 wt % Pu and a region enriched to about 70 wt % Pu. An aluminum-plutonium particle is also visible in the thin section.

Figure 2. A calibration plot[3] using ATS glass[4] as the Pu^{4+} standard and cubic-Pu$_2$O$_3$ (actually Pu$_4$0$_7$) as the Pu$^{3.5+}$ standard. The ratios of Pu-N$_4$/N$_5$ for several phases found in the ash are shown.

[(Ca,REE,Th)(Zr,Hf)(Ti,Nb)$_2$O$_7$], in nepheline syenites and peralkaline granites.[6] These types of actinide-bearing silicotitanates might also occur in some waste forms for Pu-scrap immobilization. The Ce oxidation state in the two silicotitanate also varied; however, in each case the Pu was slightly oxidized relative to the Ce, which is consistent with cerium's greater oxidizing potential.

Discussion

This work demonstrates the utility of microscopy for obtaining information about low-level contaminants in environmental samples. Furthermore, with EELS, the oxidation state of the Pu and Ce in the discrete phases may be estimated. In some cases, incineration of Pu-bearing waste has resulted in the formation of phases which are similar to those currently being viewed as waste forms intended for Pu immobilization. Although the colloidal-size of the PuO$_{2-x}$ particles may present some concern regarding their stability over an extended period, the Pu-bearing phases observed, titanites and silicates, are known to be resistant to dissolution.[5,6]

References

1. T. W. Blum, R. G. Brehrens, V. J. Salazar, P. K. Nystrom, Los Alamos National Laboratory report LA-11747 (1989).

2. Typical RFETS ash composition for major elements (wt %) is Al = 4.3, Ca = 12.9, C = 6.9, Cl = 2.2, Cr = 2.6, Fe = 12.9, H = 0.5, K = 2.6, Mg = 8.6, Mn = 2.6, Ni = 2.6, Pb = 1.7, Pu 11.9, Si = 17.2, Na = 2.6, Ti = 4.3, and Zn = 3.4. F is also present.

3. J. A. Fortner, E. C. Buck, *Appl. Phys. Lett.* **68**, 3817–3819 (1996).

4. J. K. Bates, A. J. G. Ellison, *Mater. Res. Soc. Symp. Proc.* (1996).

5. E. C. Buck, A. J. Bakel, B. Ebbinghaus, and J. K. Bates, Scientific Basis for Nuclear Waste Management XX, Boston, Massachusettes, December 2–6, 1996.

6. R. Giere and C. T. Williams, *Contrib. Miner. Petrol.* **112**, 83–100 (1992).

Redox of Plutonium and Cerium in Vitrified Wastes

Introduction and Background

One method of stabilizing plutonium containing wastes is by vitrification. For example, PuO_2 containing material is mixed with glass frit and melted at temperatures of 1000°C or greater to form a stable waste form. The solubility of plutonium in the melt is a critical issue pertaining to its incorporation into the waste glass and is believed to be governed in part by redox chemistry.

For laboratory-scale experiments to industrial-scale melter evaluations, researchers require a non-radioactive surrogate for plutonium that emulates its behavior in the melt and in the final waste form. Although no single element can embrace the entire range of chemical and structural behaviors for plutonium, it has been suggested that cerium (Ce) may be the best candidate as a Pu-surrogate for the work that we shall discuss here.[1] Other reasonable candidates, depending on the anticipated melt redox chemistry include neodymium (Nd) and hafnium (Hf). Here we discuss the use of Ce as a possible Pu-surrogate for use in waste vitrification experiments.

In alkali/alkaline earth borosilicate glasses batched from less than ≈7 wt % plutonium oxide, Pu^{4+} has been identified as the predominant redox species[2,3] with Pu^{3+} accounting for the balance of the plutonium,[4] see Table 1. The glasses studied here are significantly different in composition, particularly in plutonium and lanthanide concentrations, from those previously studied and warrant investigation.

J. G. Darab
H. Li
M. J. Schweiger
J. D. Vienna
Pacific Northwest National Laboratory

P. G. Allen
J. J. Bucher
N. M. Edelstein
D. K. Shuh
Lawrence Berkeley National Laboratory

Table 1. Selected glass compositions from literature and this study and wt. % oxides.

Glass			Glasses 1 and 2		Glass 3
Composition:					
SiO_2	55.3	57.8	61.2	42.8	25.8
Al_2O_3			0.3	4.1	19.0
B_2O_3	13.2	11.1	9.5	13.2	10.4
Cs_2O				1.0	
K_2O			0.1	1.5	
Li_2O		4.4	9.9	4.1	
Na_2O	10.4	20.6	13.4	5.1	
CaO	2.8	5.5	5.3		
SrO					2.2
Fe_2O_3				4.7	
TiO_2	4.1		0.4		
ZnO	6.9				
ZrO_2					1.2
P_2O_5				2.1	
Gd_2O_3				11.3	7.6
La_2O_3					11.0
Nd_2O_3					11.4
PuO_2	7.4	0.6	2.0	10.0	11.4
Melt					
temperature	1250°C	1100°C	1000°C	1300°C	1500°C
duration	2+ hrs	4–8 hrs	12 hrs	2 hrs	4 hrs
atmosphere	oxygen	air	air	air	air
Reference	Karim, 1982	Karraker, 1982	Eller, 1985	This work	This work

Experimental

All of the glasses studied in this work were prepared at the Pacific Northwest National Laboratory (PNNL) according to procedures reported by Vienna et al.[5] Glass samples were shipped to Lawrence Berkeley National Laboratory (LBNL) where they were prepared and then sent to Stanford Synchrotron Radiation Laboratory (SSRL) where LBNL and PNNL collaborators performed X-ray Absorption Near-Edge Structure (XANES) spectroscopy.

Results and Discussion

Figure 1 shows a detail of the Pu L_{III} XANES region obtained from the Pu-containing glasses along with those obtained from the PuO_2 and Pu^{3+} (aq) reference materials. Note that the edge position of the glasses lines up close to that of the PuO_2 reference as well as that of the Pu^{4+} (aq) reference (not shown). This indicates that Pu^{4+} is the predominant species in these glasses, but that a small contribution from Pu^{3+} may also exist to varying degrees.

Figure 1b shows a detail of the Ce L_{III} XANES region obtained from the Ce-containing glasses along with those obtained from the CeO_2 and $Ce_2(SO_4)_3$ reference materials. The XANES peak observed at ≈5740 eV for the CeO_2 reference is characteristic to Ce^{4+} species in general,[6–8] and as such, can be used as a Ce^{4+} fingerprint. The complete lack of any XANES feature at ≈5740 eV for glass 3 indicates that an insignificant amount of Ce^{4+} is present. Some intensity is observed at ≈5740 eV for glasses 1 and 2, however, indicating that a small contribution of Ce^{4+} occurred in those samples.

The redox chemistry of various metal species in glass-forming oxide melts have previously been investigated at melt temperatures by Schreiber and coworkers[9–11] although, information concerning the redox chemistry of plutonium in such melts was not available. However, these researchers also demonstrated the comparability of the electromotive force series in aqueous solutions to those in silicate-based melts. Based on their results, the known aqueous redox potentials for the $Ce^{4+/3+}$ and $Pu^{4+/3+}$ couples in aqueous solution[11, 12] and the measured $[Ce^{4+}]/[Ce_{total}]$ ratio, the $[Pu^{4+}]/[Pu_{total}]$ ratio glass 3 was calculated to be ≈0.9. Thus, on a first principles basis, this analysis indicates that plutonium in the glass 3 should occur predominantly in the Pu^{4+} state, which is corroborated by Pu XANES results (Figures 1a and 1b). Based on these results, for the glass studied here and for other glass forming systems that may be more reducing, cerium would not be a good surrogate for plutonium because the measured $[Ce^{4+}]/[Ce_{total}]$ ratio remains relatively invariant at ≈0, whereas the $[[Pu^{4+}]/[Pu_{total}]$ ratio could vary significantly.

References

1.   J. Ryan, PNNL, internal communication (1996).

2.   P. G. Eller, G. D. Jarvinen, J. D. Purson, R. A. Penneman, R. R. Ryan, F. W. Lytle, R. B. Greeger, *Radiochemica Acta* **59**, 17 (1985).

3.   D. G. Karraker, *J. Am. Ceram. Soc.* **65**, 53 (1982).

4.   D. P. Karim, D. J. Lam, H. Diamond, A. M. Friedman, D. G. Coles, F. Bazan, G. L. McVay, *Scientific Basis for Nuclear Waste Management,* S. V. Topp, Ed. (Elsevier Science Publishing Co., Inc. New York, New York, 1982), pp. 67–73.

5.   J. D. Vienna, D. L. Alexander, H. Li, M. J. Schweiger, D. K. Peeler, T. F. Meaker, "Plutonium Dioxide Dissolution in Glass," Pacific Northwest National Laboratory report PNNL-11346.

6.   A. Bianconi, A. Marceli, H. Dexpert, R. Karnatak, A. Kotani, T. Jo, J. Petiau, *Phys. Rev. B* **35**, 806 (1987).

7. F. Le Normand, L. Hilaire, K. Kili. G. Krill, G. Maire, *J. Phys. Chem.* **92**, 2561 (1988).

8. M. R. Antonio, J. S. Xue, L. Soderholm, *J. Alloys & Compounds* **207/208**, 444 (1994).

9. H. D. Schreiber, G. B. Balazs, B. E. Carpenter, J. E. Kirkley, L. M. Minnix, P.L. Jamison, *Commun. Amer. Ceramic. Soc.* C-106 (1984).

10. H. D. Schreiber, *J. Geophys. Res.* **92**, 9225 (1987).

11. H. D. Schreiber, M. T. Coolbaugh, *J. Non-Cryst. Solids* **181**, 225 (1995).

12. L. J. Nugent, *Lanthanides and Actinides*, Inorganic Chemistry, Series Two, K. W. Bagnall, Ed. (University Park Press, Baltimore, Maryland, 1975), Vol. 7, pp. 195–219.
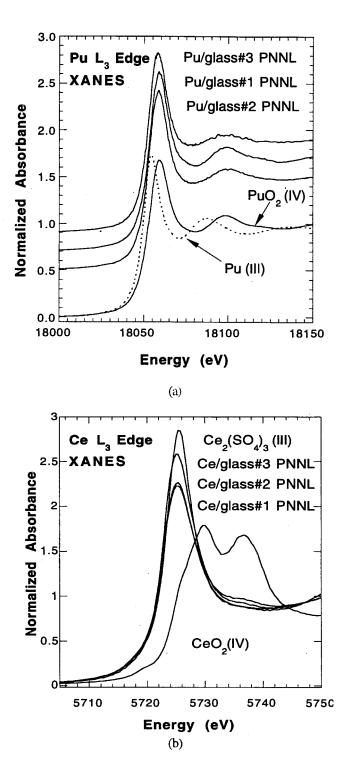
Figure 1. X-ray absorption near edge structure (XANES) spectra of (a) Pu and (b) Ce in the glasses studied here.

Plutonium Alteration Phases from Lanthanide Borosilicate Glass

A prototype lanthanide borosilicate (LaBS) glass containing 10 mass % plutonium was reacted with water vapor at 200°C for periods of 14 to 56 days. These tests, while not designed to replicate specific conditions that may be found in a potential geologic repository (e.g., Yucca Mountain), have been shown to accelerate alteration phase formation.[1] The surfaces of the glass samples, along with alteration phases, were examined with a transmission electron microscope (TEM). Tests of 14 days produced macroscopic (~20 mm) crystallites of a plutonium-lanthanide silicate. An extensive alteration layer was found on the glass surface containing amorphous aluminosilicate layered with bands of a cryptocrystalline plutonium silicate. After 56 days of testing, additional alteration phases were formed, including a strontium lanthanide oxide phase.

One of the options for disposal of surplus plutonium, particularly for impure residues that may be unfit for production of MOX fuel, is vitrification followed by geologic disposal.[2] Since geologic disposal requires a passive system to isolate the radiotoxic elements from the biosphere, it is important to understand the possible corrosion mechanisms of the waste form.

The LaBS glass, based upon Löffler-type glasses, is chemically durable and can dissolve substantial amounts of plutonium as well as the neutron absorbers gadolinium and hafnium.[3,4] The prototype LaBS formulation tested in this work, however, contained no hafnium but did contain zirconium, which is expected to behave in a chemically similar manner. The Argonne Vapor Hydration Test procedure was used and is discussed in detail elsewhere.[1]

Two types of TEM samples were prepared: (1) surface alteration crystals, which were about 20 mm across and affixed to the monolith surface, and (2) chips of glass, some of which held an intact surface alteration layer. The surface alteration crystals were found to be a plutonium lanthanide silicate. Electron energy loss spectroscopy revealed that the ratio of gadolinium to lanthanum in the alteration crystal was reduced more than a factor of two relative to the initial LaBS glass, although the gadolinium-to-plutonium ratio was nearly unchanged. The alteration surface layer, shown in Figure 1 for a 14-day test sample, contained bands of plutonium-rich silicates separated by amorphous aluminosilicates (probably hydroxides). The intralayer plutonium silicates were relatively depleted in lanthanide elements compared to surface crystals, although they produced similar electron diffraction patterns (Table 1). The compositional difference between the surface and intralayer crystals probably reflects solubility differences between the lanthanides and plutonium, the former being more readily transported to the surface of the glass as it alters.

J. A. Fortner
C. J. Mertz
D. Chamberlain
J. K. Bates
Argonne National Laboratory

Experimental d-spacings, surface crystal (nm)	Experimental d-spacings, intralayer crystallite (nm)	Nd_2SiO_5 JCPDS-ICDD 4–284 (nm)	La_2SiO_5 JCPDS-ICDD 40–234 (nm)	$PuSiO_4$ JCPDS-ICDD 43–1095 (nm)
0.489		0.4859	0.4418	0.4621
		0.4382		
0.387		0.3891	0.3805	
0.351	0.338	0.3413	0.3511	0.3452
	0.307	0.3180	0.2945	
	0.310	0.3128	0.2992	
0.286		0.2937	0.2850	
		0.2853	0.2831	
	0.275	0.2788		0.2766
0.260		0.2604	0.2652	0.2623
0.245	0.243	0.2467	0.2450	0.24415
0.224		0.2264	0.2202	0.21592
		0.2215	0.2192	
0.202	0.197	0.20046	0.2035	0.19860
	0.195		0.1984	
0.187	0.192	0.18678	0.1877	0.18305
0.176	0.170	0.17535	0.17699	0.17872
				0.17266
0.1652	0.166	0.16580	0.16555	0.16174

Plutonium has not been previously reported as a major component in silicate alteration phases on glass. Nevertheless, the occurrence of plutonium in alteration phases has been expected because of its low release rate in tests of high-level waste glass[6] and spent nuclear fuel.[7] Segregation was observed among the lanthanide elements lanthanum, neodymium, and gadolinium; also observed was separation of the lanthanides from plutonium. Corrosion tests (MCC- 1 and PCT-B) of the LaBS glass[8] indicate normalized release rates for lanthanides greater than for plutonium, with zirconium released at the lowest rate. Since gadolinium serves as a neutron absorber, its separation from the plutonium on a large scale may have implications for criticality. These combined data support the strategy of incorporating two neutron absorbers, gadolinium and hafnium, in the LaBS glass to provide for different corrosion scenarios.[3] The occurrence of a strontium lanthanide phase, which contained no detectable plutonium, provided impetus for strontium to be omitted from more recent LaBS formulations.[3]

References

1. D. J. Wronkiewicz et al., *Mat. Res. Symp. Proc.* **294,** 183 (1993).

2. National Academy of Sciences, "Management and Disposition of Excess Weapons Plutonium: Reactor-Related Options," NAS Panel on Reactor-Related Options for the Disposition of Excess Weapons Plutonium (National Academy Press, Washington, DC. 1995).

3. D. K. Peeler, private communication.

4. N. E. Bibler et al., *Mat. Res. Symp. Proc.* **412,** 65 (1996).

5.   JCPDS - International Centre for Diffraction Data PDF-2 Database JCPDS-ICDD
      International Centre for Diffraction Data (Newtown Square, Pennsylvania, 1996).

6.   J. A. Fortner and J. K. Bates, *Mat. Res. Symp. Proc.* **412**, 205 (1996).

7.   P. A. Finn et al., *Mat. Res. Symp. Proc.* **412,** 75 (1996).

8.   C. J. Mertz and S. F. Wolf, unpublished results.
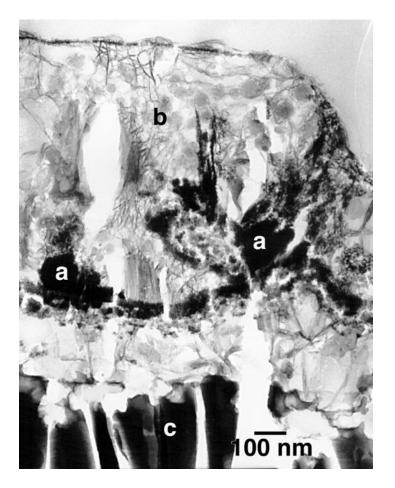
Figure 1. A TEM micrograph showing the alteration layer formed after a 14-day vapor hydration test. Visible are (a) plutonium-silicate alteration crystals, (b) amorphous aluminosilicate, and (c) unaltered glass.

Alternative Technology of HLW and Plutonium Immobilization within Mineral-Like Matrix by Means of Self-Propagating High-Temperature Synthesis (SHS)

E. M. Glagovsky
A. V. Kuprin
A.A. Bochvar All-Russia Research Institute of Inorganic Materials (VNIINM), Russia

At the present time, along with improving vitrification methods are being developed that allow mineral-like materials to be obtained. These mineral-like materials have more thermical stability than glasses and are able for a long time to keep their mechanically stability and chemical resistance with regard to natural aggressive components.

In particular, Synrock (Synthetic rock) is the process based on a hot isostatic pressing (HIP) by which, calcinates of HLW are solidified into titanate ceramics which is an analogue of rock-forming components on the base of titanium and zirconium compounds.

However, Synrock as a method of hot isostatic pressing of initial components and their further sintering demands complicated and expensive power-intensive equipment.

By synthesis of a mineral-like matrix, it is very important to observe such conditions of forming that would maximally ensure an isomorphous substitution of most parts of the radionuclides contained in HLW.

The alternative technology of HLW and plutonium immobilization developed by Russian scientists conforms to the above-mentioned terms.

SHS is a spontaneous solid-phase exothermal process with a high rate run and a low time for reaction products to be under high temperatures.

The essence of this process is in induced interaction of chemical elements and compounds that run under the mode of a self-propagating burning wave on account of the great amount of a chemical energy release.

The intensivity of the SHS process is flexible and adjusted (increase or decrease) by means of selection of batch components.

Merits of SHS include insignificant energy expenses, simplicity, reliability of equipment, short-term and high productivity.

- Main features of the SSHS process include the following:

- time of an initiation   0.05–5.0 s

- temperature at the front of burning   1500–3500 K

- velocity of a front burning spreading   1.0–100 mm/s

To obtain a highly-dense material, the SHS product is subjected to compacting, in particular, pressing on hydraulic presses with a residual poricity less than 0.2%.

At present, the process of HLW immobilization is designed by introducing HLW surrogates (rare-earth elements) into the titanate matrix.

Los Alamos Plutonium Facility Newly Generated TRU Waste Certification

K. Gruetzmacher
A. Montoya
B. Sinkule
M. Maez
Los Alamos National Laboratory

Introduction
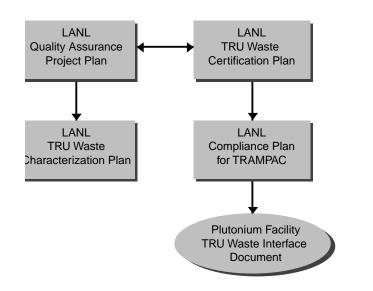
This paper presents an overview of the activities being planned and implemented to certify newly generated contact handled transuranic (TRU) waste produced by Los Alamos National Laboratory's (LANL's) Plutonium Facility. Certifying waste at the point of generation is the most important cost and labor saving step in the Waste Isolation Pilot Plant (WIPP) certification process. The pedigree of a waste item is best known by the originator of the waste and frees a site from many of the expensive characterization activities associated with legacy waste. Through a cooperative agreement with LANL's Waste Management Facility and under the umbrella of LANL's WIPP-related certification and quality assurance documents, the Plutonium Facility will be certifying most of its own newly generated waste.

Some of the challenges faced by the Plutonium Facility in preparing to certify TRU waste include the modification and addition of procedures to meet WIPP requirements, implementation of a computer-based TRU waste tracking system,[1] standardizing packaging for TRU waste, collecting processing documentation from operations which produce TRU waste, and developing ways to modify waste streams which are not certifiable in their present form.

Description of Work

The Plutonium Facility is the largest producer of newly generated TRU waste at LANL. The waste is to be sent to the WIPP and must be certified to Rev. 5 of the *Waste Acceptance Criteria for the Waste Isolation Pilot Plant* (WIPP WAC). NMT's compliance plan for the WIPP WAC and Transuranic Waste Characterization Quality Assurance Program Plan (QAPP) is the Transuranic Waste Interface Document developed to demonstrate compliance with the LANL site level certification program (Figure 1). Interim storage of newly generated TRU waste is provided by the LANL Waste Management Facility until the waste is shipped to WIPP. The Waste Management Facility also provides certification activities and loading facilities for all TRU waste and storage and repackaging facilities for legacy TRU waste.

TRU waste has been certified to Rev. 4 of the WIPP WAC for the past several years. The past 18 months have seen numerous changes in the certification requirements for WIPP, including Rev. 5 of the WAC, new quality assurance

Figure 1. LANL site specific WIPP compliance plans.

documents, transportation requirements, and the commitment of WIPP to open in November 1997. This has presented an evolving set of challenges to producers of newly generated waste as well as personnel who must prepare legacy waste for shipment to WIPP.

The Plutonium Facility currently produces 500 new containers of TRU waste per year and is anticipating an expanded mission and upgrades to the facility which will increase the waste production rate. The goal of the plutonium facility waste management group is to certify as much newly generated waste as possible for shipment to WIPP as it is produced. To this end, the Plutonium Facility's waste management personnel have an implementation plan to meet WIPP requirements; TRU waste procedures have been revised; packaging has been standardized to meet the wattage and plutonium equivalent (PE) Curie WAC limits; process documentation has been gathered to support acceptable knowledge (AK); and research and development activities have been planned for waste streams which consistently fail to meet the WAC and transportation requirements. Figure 2 shows waste streams and corresponding TRUPACT II Content (TRUCON) Codes.

- TRU Debris Waste

»	Absorbed Organics	LA 112
»	Graphite	LA 115
»	Combustibles	LA 116
»	Metal	LA 117
»	Glass and ceramics	LA 118
»	HEPA Filters	LA 119
»	Leaded gloves	LA 123
»	Salts	LA 124
»	Combustibles/Noncombustibles	LA 125
»	Inorganic Ash Waste	LA 130

- TRU Immobilized Liquid Waste

»	Cemented Inorganics	LA 114
»	Cemented Organics	LA 126

Results

Seventy-five percent of the TRU wastes generated by the Plutonium Facility from May 1, 1996 to November 1, 1996 meet the WAC and transportation[2,3] requirements pending approval of the Plutonium Facility Transuranic Waste Interface Document and appropriate verification of the drum contents by the LANL Transuranic Waste Certification Project. The vast majority of the remaining 25% fail due to wattage or PE Curie restrictions on americium-241 and plutonium-238 contaminated waste streams.

References

1. K. Smith, A. Montoya, R. Wieneke, D. Wulff, C. Smith, and K. Gruetzmacher, "Los Alamos Plutonium Facility Waste Management System," Waste Management '97, Tucson, Arizona, March 2–7, 1997.

2. DOE, TRUPACT-II Content Codes (TRUCON), U.S. Department of Energy document DOE/WIPP 89-004, Revision 8, Carlsbad Area Office (1994).

3. NRC, Safety Analysis Report for the TRUPACT-II Shipping Package, U.S. Nuclear Regulatory Commission docket 9218, Washington, D.C. (1994).

Waste Forms for Plutonium Disposition

S. G. Johnson
T. P. O'Holleran
S. M. Frank
M. K. Meyer
M. Hanson
Argonne National Laboratory-West

B. A. Staples
D. A. Knecht
P. C. Kong
Lockheed Martin Idaho Technologies Company

Introduction

The field of plutonium disposition is varied and of much importance, since the U.S. Department of Energy has decided on the hybrid option for disposing of weapons material. This consists of either placing the Pu into mixed oxide fuel for reactors or placing the material into a stable waste form such as glass.[1] The waste form used for Pu disposition should exhibit certain qualities: (1) provide for a suitable deterrent to guard against proliferation, (2) be of minimal volume, i.e., maximize the loading, and (3) be reasonably durable under repository-like conditions. This paper will discuss several Pu waste forms that display promising characteristics.

Results and Discussion
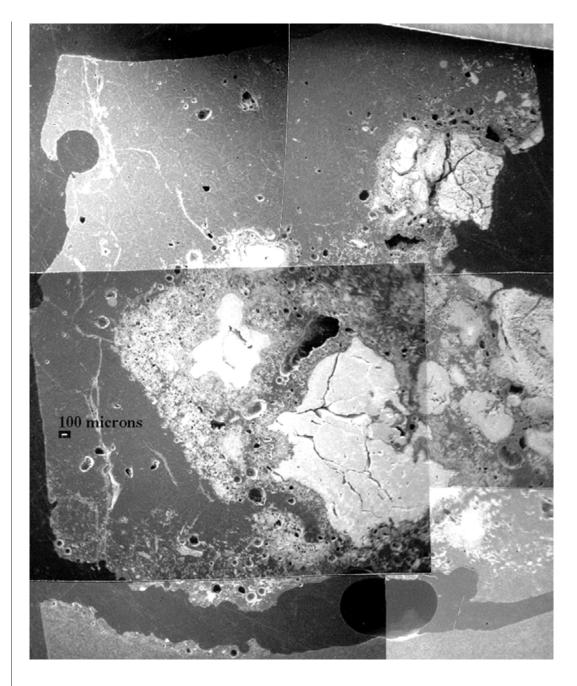
Our experiments are focused on two separate areas of interest in the plutonium disposition arena. The first involves taking metallic plutonium and placing it directly into a waste form with no prior processing. Most current waste form schemes call for a step involving oxidizing the metal to PuO_2. This is a process that requires additional facilities and subsequently adds further contamination sources to the overall process.

We have attempted to place Pu metal directly into a stable glass-ceramic form using only an ordinary furnace. This can be accomplished using conventional glass processing temperatures (1100°C) with reasonable casting times (72 hr) and with attractive plutonium loadings of 15 wt %. Our results indicate that stable Pu-containing phases are formed, such as cubic (fluorite structure), that incorporate high Pu loadings. This experiment was analyzed using x-ray diffraction (XRD), scanning electron microscopy (SEM), and performance testing methods. The low magnification SEM micrograph of a core sample from a crucible-sized experiment is featured in Figure 1. A small portion of the original Pu piece, now oxidized, is visible in the micrograph as are the various phases formed as the Pu dissolves into the glass. The XRD pattern confirms that no metallic plutonium is present.

The ability for the zirconia phase mentioned above to contain relatively high Pu-loadings, > 50 wt % makes it an attractive host for plutonium. An attempt to synthesize a phase pure c-zirconia that incorporates both Pu and Sm was undertaken. As a starting point the process parameters were first derived from surrogate experiments using CeO_2. Once this had been accomplished an experiment using PuO_2 was performed. This experiment involved two separate samples, one with PuO_2 and the second with PuO_2 and Sm_2O_3. These were analyzed using XRD, SEM, and performance tests. The XRD pattern is featured in Figure 2. This clearly shows a single c-zirconia type pattern that is different from PuO_2 and Sm_2O_3 in lattice parameter terms.

Figure 1. The SEM back scattered image from a waste glass used to dissolve and stabilize a piece of plutonium metal. The various regions of interest are discussed in the text. The Pu, if totally dissolved, would represent 15 wt % of the product. The magnification is 15X.

100 microns
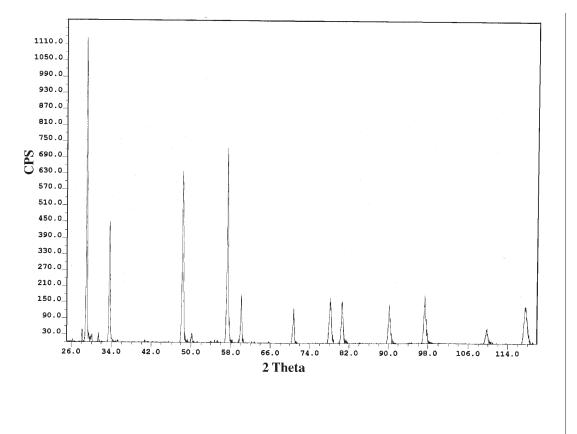
Figure 2. The XRD pattern of the pure phase zirconia with PuO_2, ZrO_2 and Sm_2O_3 constituents.

Reference

1. T. P. O'Holleran, S. G. Johnson, S. M. Frank, M. K. Meyer, N. Noy, E. L. Wood, D. A. Knecht, K. Vinjamuri, B. A. Staples, *Proceedings of the Fall 1996 Materials Research Society Meeting*, Boston, Massachusetts (1997).

Americium/Curium Bushing Melter Drain Tests

T. M. Jones
B. J. Hardy
M. E. Smith
Westinghouse Savannah River Company

Americium and curium were produced in the past at the Savannah River Site (SRS) for research, medical, and radiological applications. They have been stored in a nitric acid solution in an SRS reprocessing facility for a number of years. Vitrification of the americium/curium (Am/Cm) solution will allow the material to be safety stored or transported to the DOE Oak Ridge Reservation. Oak Ridge is responsible for marketing radionuclides for research and medical applications. The bushing melter technology being used in the Am/Cm vitrification research work is also under consideration for the stabilization of other actinides such as neptunium and plutonium.

Development of a melter system for the vitrification of the Am/Cm solution requires a reliable method for initiating and terminating glass pouring from the bushing melter. Glass flowrates from the melter are influenced by the temperature of the glass in the melter, the temperature of the drain tube, the inside diameter of the drain tube, and the hydraulic head of the glass. The drain tube assembly is the primary control for the glass flowrate and will be used to start and stop the flow of glass from the melter.

A series of melter drain tests were conducted at the Savannah River Technology Center to determine the relationship between the drain tube assembly operaing variables and the resulting pour initiation times, glass flowrates, drain tube temperatures, and stop pour times. Performance criteria such as ability to start and stop pours in a controlled manner were also evaluated. The tests were also intended to provide support of oil modeling of drain tube performance predictions and thermal modeling of the drain tube and drain tube heater assembly.

The Am/Cm Bushing Melter 1 was used in these tests. The melter was a Pt/10%Rh bushing vessel (insulated with castable refractory). This melter was 6.35 cm deep, 25.4 cm wide, and operated with a glass level of about 20.3 cm. The Pt/20%Rh drain tubes tested were welded directly to the melter bottom drain opening, and the drain tube heater assembly was mounted to the lower melter frame such that the drain tube extended within the center of the drain tube heater. Tubes and heaters tested ranged in length from 3.5 to 6 inches. The melter temperature ranged from 1300 to 1400°C, and the drain tube temperature was in the range of 1200 to 1350°C.

The Am/Cm melter drain testing provided opportunities to evaluate conditions necessary for successful glass pouring initiation and cessation in a controlled manner. As a result of difficulties encountered during early test pours, the principles and conditions necessary for successful drain tube heater operation and glass delivery were developed. The "cold glass plug" theory that suggests freezing the entire drain tube length of glass to prohibit glass flow with one pair of cooling air ports near the middle of the drain tube was shown to cause slow, unstable pour initiations. This resulted in cold glass stingers that failed to remain inside the canister and greatly increased the potential for plugging the drain tube and heater. The addition of another pair of cooling air ports near the tip of the drain tube and the revised practice of applying cooling air at these two heights of the drain tube at different times proved to be vital in controlling both pour stoppage and subsequent pour initiation. Per a request by the SRS plutonium immobilization program, a plutonium surrogate frit was also successfully melted and poured by using this dual cooling air technique. The next series of drain tube

heaters will focus on separation of the upper and lower drain tube zones for heating and cooling purposes.

The drain tests also provided an opportunity to validate the predictions developed by the viscosity oil modeling performance testing and thermal modeling. Drain tube lengths and inside diameters predicted by this modeling work were proven adequate in controlling the flowrates of glasses of two compositions. This information allowed for the proper sizing of the drain tube heater windings and dimensions of the insulating materials to yield functional heaters to initiate and control glass flow. The thermal modeling was also able to predict the time required to stop glass pouring under various conditions.

In conclusion, these drain tests were instrumental in the design of subsequent melter drain tube and drain tube heaters for the Am/Cm bushing melter, and therefore in the success of the Am/Cm vitrification and plutonium immobilization programs.

Stabilization of Recovered Ash
at the Lawrence Livermore National Laboratory

O. H. Krikorian
R. H. Condit
*Lawrence Livermore
National Laboratory*

Over 100 kilograms of plutonium ash residue material containing about 30 kilograms of plutonium has been generated over the past decades at the Lawrence Livermore National Laboratory. The material originated as research samples, metal adhering to crucibles and surfaces, chemical and metallurgical analysis samples, general box cleanups, and so on. The plutonium is mostly weapons grade but may include other isotopic mixes, and other actinides are present in some batches.

Most of the residues materials were first dissolved in hydrochloric acid and then precipitated using sodium hydroxide. The wash solutions were not completely washed away from the precipitates in order to minimize the generation of waste liquids. The precipitates were calcined at temperatures below 650°C and some portions may only have reached 400°C. The calcined ash material was retained in vented cans until 1992 when it was packaged in sealed cans with the intention of shipping it off site. Unfortunately, the shipment was delayed, and in 1994 several of the cans were found to be bulging.[1] This was attributed to radiolytic generation of gases from the calcined material which contained incompletely oxidized carbonaceous material and adsorbed water and water of crystallization in some salts. The gases included nitrogen, oxygen, hydrogen, carbon dioxide, nitrous oxide, and small amounts of hydrocarbons. We have offered an explanation for the chemical observations about the compositions of the gases and the solids based on whether the contents of the original package were oxidizing or reducing.[1]

After the discovery of the bulged cans, all the packages were punctured to allow escape of any gases generated and overpacked in cans having a carbon frit-filtered vent. A program of periodic inspection of these overpack packages has revealed little serious deterioration, although there has been occasional corrosion of some of the cans, possibly due to formation of nitric acid vapor from radiolysis of humid air. In any case, it would be highly desirable to stabilize all of the residue material so that it can be stored safely in sealed containers for many decades. The present effort is directed toward that goal.

The basic approach is to rewash the ash material with water or some solution yet to be developed and then recalcine the insoluble residue at 950 to 1000°C. Water washing removes sodium hydroxide, chlorides, nitrates, and other salts. These salts have constituted as little as a few percent of ash material in some samples and as much as 40% in others. The water washing seems to elute less than 0.1% of the plutonium from the insoluble portion and the wash solution could be discarded as TRU waste.

One benefit of washing away the soluble salts should be to decrease the amount of plutonium-containing residues. Also, the salts have melting points below 700°C. Molten slurries in the sintering mixture could interfere with the complete oxidation of carbonaceous material and would likely lead to the formation of clinkers and an inhomogeneous product. Finally, the salts have been found to be highly hygroscopic, sometimes deliquescent. After their removal, the residue should have reduced affinity for moisture. The process is being developed to be flexible because each batch of residue contains different concentrations of plutonium, between 5% and 60% PuO_2, and the other chemical constituents vary widely. This puts a special burden on the diagnostic tools and instrumentation of the processing. We have constructed a setup to permit the automatic titration of a

slurry of residue ash with acid, a step which should decompose the carbonates expected to be present, since they might solubilize plutonium as carbonate complexes. The leaching wash will be monitored using solution conductometry to establish the completion of elution of soluble salts. This allows us to limit the amount of liquid to what is necessary. Wash liquids will be processed using ion exchange columns when the concentrations of plutonium are above the discard limit.

Reference

1.   R. A. Van Konynenburg, D. H. Wood, R. H. Condit, and S. D. Shikany, "Bulging of Cans Containing Plutonium Residues—Summary Report," Lawrence Livermore National Laboratory report UCRL-ID-125115 (March 1996).

Analytical Technology Development for Transuranic Waste Characterization

C. Mahan
D. Wayne
D. Figg
D. Cremers
A. Koskelo
R. Drake
Y. Duan
J. Olivares
Los Alamos National Laboratory

Transuranic waste (TRU) is defined as waste containing greater than 100 nanocuries of radioactivity per gram waste (for elements > 92 amu and half-lifes of greater than 20 years). TRU wastes were generated primarily from plutonium reprocessing and fabrication, research and development activities, environmental restoration, and decontamination and decommissioning activities throughout the DOE complex. DOE plans to dispose of approximately 175,600 cubic meters of TRU waste in the Waste Isolation Pilot Plant (WIPP) site. Los Alamos National Laboratory (LANL) currently stores approximately 12,000 cubic meters of TRU waste (55,000 55-gallon drum equivalents). Hence, in order to fill the WIPP pipeline, LANL scientists are developing the capability to certify 3500 to 5500 drums/year of retrievable stored waste, in addition to the capability to characterize newly generated waste resulting from ongoing weapons activities. TRU waste characterization, including RCRA metal analysis is a primary component of compliance activities required to support the WIPP disposal activities.

Current methods of analysis used in the TWCP are costly, generate new waste as a result of the dissolution of the solid matrix, require considerable analytical resources to implement the associated QA program, and shorten the operational life expectancy of gloveboxes due to the strong acid concentrations used for sample digestions. Thus, analytical methods are needed that lower analysis cost, save time, minimize hazardous and mixed waste generation, and achieve regulatory compliance. LANL researchers are developing direct analysis techniques including laser induced breakdown spectroscopy (LIBS), laser ablation inductively coupled plasma mass spectrometry (LA-ICPMS), dc arc CID atomic emission spectroscopy (DC-AES), and glow discharge mass spectrometry (GDMS) to characterize the TRU waste in the original solid form. Advantages of these direct chemical analysis methods include rapid analysis turnaround times, reduced cost, no additional mixed wastes generated as a consequence of sample pretreatment, reduction of worker exposure to harmful reagents and radioactive samples, and decreased risk of sample contamination and analyte loss. In addition, LIBS can be performed *in situ*.

Analytical methods using Portland cement matrix are currently being developed for each of the listed techniques. Upon completion of the development stage, blind samples will be distributed to each of the technology developers for RCRA metals characterization. The round-robin testing will help determine which technique(s) hold the most promise for TRU characterization. The most promising technique(s) will continue development including, glovebox installations, re-engineering for mobile platforms if applicable, and placement into service. A brief description of the direct chemical techniques and methods development activities will be discussed.

DC-AES is a bulk solids analytical technique, which uses a solid state integrating detector to measure the spectral emission intensities produced when a sample is vaporized and excited by a dc arc. The CID detector represents relatively new technology, which has the potential to improve analytical performance over the traditional dc arc and conventional spectroscopic techniques. Samples are pulverized, mixed with graphite powder, and burned in the lower of two vertically mounted graphite electrodes. The detector chip is similar to a photographic plate in that it provides for continuous wavelength coverage and hence most elements in the periodic table can be determined if present in sufficient quantity.

LA-ICPMS uses a focused laser beam to ablate nanogram to microgram amounts of a sample into the plasma. The ablated material is transported by a stream of argon into the ICP-MS where the material is vaporized, dissociated, and ionized. A pellet is formed from the sample after the addition of cellulose. The laser (neodymium YAG laser, 266 nm) is rastered across the surface of the pellet. Two methods of signal normalization are currently under investigation. The first method involves adding a liquid phase internal standard to the samples prior to analysis. The sample is subsequently dried and pressed into a pellet. The second method for signal normalization relies on particle counting. Instead of internal standard addition, a portion of the ablated particle stream is diverted into a particle counter. Analyte calibration is accomplished using standard addition.

In the LIBS method, laser pulses are focused on the sample to generate a microplasma. The spectral emission from this plasma is measured to determine element concentrations. Initial results show excellent quantitative information for some elements. A LIBS instrument is in the process of being installed in a glove-box.

Glow discharge mass spectrometry (GDMS) is a direct sputtering analytical technique, wherein the surface of an electrically conducting sample is bombarded by Ar^+ ions. Sputtered sample atoms are ionized separately, via interactions with Ar^* metastables. The separation of atomization from ionization greatly reduces matrix dependency, and permits a wide range of standardization schemes for quantitative analysis. The GDMS can perform rapid quantitative major element analysis (weight % level) and trace analysis to the sub-ppb level in a single run by using multiple detection systems (Faraday cup, and post-acceleration detector operable in both analogue and ion-counting mode). The double focusing geometry and magnetic sector permit routine operation at resolutions > 4000. Non-conducting powders must be combined with a high-purity (> 99.995%) conducting metal powder (usually Ta), homogenized, and analyzed as a composite. Samples are baked in vacuo, pre-sputtered for 30 minutes, and quantitatively analyzed. Advantages of GDMS analysis include its high resolution (up to DM/M=12,000) capabilities, its ability to acquire quantitative data for all RCRA metals (and nearly all elements in the periodic table), and its wide (> 10^9) dynamic range. Standardization is easily accomplished through the use of both NIST standard reference materials and carefully prepared mixes of high-purity metal and metal oxide powders.

Results of quantitative analyses of TRU waste surrogates and figures of merit for each of the technologies will be discussed.

Liquidus Temperature and Durability of Pu Loaded Lanthanide Borosilicate (LaBS) Glass as a Function of Feed Stream Variation

T. F. Meaker
D. K. Peeler
C. M. Conley
J. O. Gibson
*Westinghouse
Savannah River
Company*

Introduction

In support of the Department of Energy's (DOE) Office of Fissile Material Disposition (OFMD) Program, an in-depth investigation of maximum loadings of individual feed streams containing Pu, U, and other minor components has been initiated. Successful dissolution of 10 elemental weight percent pure PuO_2 has been acheived in a lanthanide borosilicate glass (LaBS) in FY 1996.[1] The FMDP is now focusing on glass and ceramic compositions that can incorporate impure plutonium feeds. Liquidus temperature determination and product performance (as determined by the Product Consistency Test) will be determined as a function of Pu:U ratio, as well as, other minor components that have been identified in individual feed streams. The individual feed streams to be investigated are given in Table 1. It is believed that variations in feed streams (i.e., the Pu/U/minor component ratio) will have an affect on liquidus temperature and durability. The extent of that affect is unknown. Information gained from this study will be combined with the results of the plutonium variability study[2] and used in a down-select between ceramic and glass forms in September 1997. This paper will outline the results of how liquidus temperature is affected by the Pu:U ratio and if minor component concentrations have any affect. Homogeneity of 24-hour heat treated glasses will be determined by x-ray diffraction (XRD) and scanning electron microscopy with energy dispersive x-ray analysis (SEM/EDX).

Table 1. Identified individual feed streams for the Pu immobilization program.

Pu Source	% Pu	% U	Minor Components
Pure Pu	100.0	0	0
60/40-Pu/U	60.0	40.0	0
Impure Metal (A)	78.6	0	21.4% (Ca, Mg, Fe, Cr, Ni, K, Ta, W)
Pu Alloy	65.3	32.6	2.1% (Ca, Mg, Fe, Mo)
Impure Oxide (A)	47.1	0	52.9% (Ca, Mg, Cl, Fe, Cr, Ni, F, K, Na, Mo, Ba, W)
ZPPR Fuel	28.0	69.0	3.0% (Mo)

Procedure

Glass Formulation

Frit containing glass formers, uranium and minor components will be prepared similar to frit produced for the plutonium variability study.[2,3] PuO_2 will be mixed with frit and melted in the Shielded Cells Operation (SCO) Facility at the Savannah River Technology Center (SRTC). A processing temperature of 1500°C with a residence time of 4 hours will be used to vitrify the material. Samples will be prepared for XRD and SEM/EDX to determine homogeneity.

Liquidus Temperature Determination

Two to three grams of each glass will be subjected to 24 hour heat treatments at selected temperatures. Samples will be prepared for XRD and SEM/EDX do

determine homogeneity. The minimum temperature at which crystallization does not occur will be reported as the liquidus temperature for that particular glass.

Product Performance

Approximately 10 grams of only the pure Pu feed, 60/40-Pu/U feed and impure oxide feed glass samples will be ground and sieved according to the PCT procedure.[4] Triplicate samples will be held at 90°C for 7 days immersed in deionized water. This will allow for a comparison of the durability between Pu only glass and Pu with either U or minor components.

Results

Liquidus Temperature

Surrogate work with 20 to 25 wt % Th has shown uranium and/or minor components have little effect on liquidus temperature and durability. To date, the liquidus temperature of an 8 wt % elemental Pu LaBS glass has been determined to be between 1400° and 1450°C. That is, at 1450°C no crystals were observed by XRD. At 1400°C PuO_2 was detected by XRD. SEM/EDX results confirm the presence of devitrified Pu.

Product Performance

PCT results have shown that both surrogate (Th loaded glasses) and previously prepared Pu glasses (containing Pb and Ba) are 25 to 100 times more durable than typical high-level waste glass (up to 1000X more durable than environmental assessment (EA) glass) with respect to normalized Si and B release.[4,5] Similar results (high durability compared to EA glass) are expected with these glasses. However, allowing for the direct comparison of Pu only, Pu and U, and Pu and minor component glasses, any decrease (or increase) in durability between these three glasses should be a result of composition. Preliminary results of a long-term PCT test on a quenched Pu loaded glass and a heat treated Pu glass will also be presented.

References

1.   J. D. Vienna et al., *Plutonium Dioxide Dissolution in Glass*, Pacific Northwest National Laboratory report PNNL-11346 (September 1996).

2.   T. G. Edwards, *A Statistically Designed Plan for the Exporation of a Vitreous Pu Product Compositional Space as it Relates to Solubility and Thermal Stability,* Westinghouse Savannah River Company report SRT-ASG-97-1233 (January 1997).

3.   D. K Peeler, *Standard Laboratory-Scale Melting Procedures for Plutonium Containing LaBS Glasses,* Westinghouse Savannah River Company report SRT-GFM-97-0010 (January 1997).

4.   W. G. Ramsey, N. E. Bibler, T. F. Meaker, *Compositions and Durabilities of Glasses for Immobilization of Plutonium and Uranium,* Waste Management '95, Record 23828-23907, WM Symposia, Inc., Tucson, Arizona (1995).

5.   T. F. Meaker, *Effects of Heat Treatments on Crystallinity and Durability of Surrogate Plutonium Glasses*, Westinghouse Savannah River Company report SRT-CIC-95-0002 (1995).

Determination of Solubility Limits of Individual Pu Feeds into a Lanthanide Borosilicate (LaBS) Glass Matrix Without Preprocessing

Introduction

In support of the Department of Energy's (DOE) Office of Fissile Material Disposition (OFMD) Program, an in-depth investigation of maximum loadings of individual feed streams containing Pu, U, and other minor components has been initiated. Successful dissolution of 10 elemental weight percent pure PuO_2 has been acheived in a lanthanide borosilicate glass (LaBS) in FY 1996.[1] The FMDP is now focusing on glass and ceramic compositions that can incorporate impure plutonium feeds. Actual plutonium solubility will be determined in the presence of uranium, as well as other minor components that have been identified in individual feed streams. The individual feed streams to be investigated are given in Table 1. It is believed that variations in feed streams (i.e., the Pu/U/minor component ratio) may have an affect on maximum solubility. Programmatic concerns with large-scale blending requires investigation of individual feed streams. Information gained from this study will be combined with the results of the plutonium variability study[2] and used in a down-select between ceramic and glass forms in September 1997. This paper will outline the results of laboratory scale vitrification studies showing maximum loadings of individual feed streams with a constant frit. Homogeneity will be determined by x-ray diffraction (XRD) and scanning electron microscopy with energy dispersive x-ray analysis (SEM/EDX).

T. F. Meaker
D. K. Peeler
C. M. Conley
J. O. Gibson
Westinghouse Savannah River Company

Table 1. Identified individual feed streams for the Pu immobilization program.

Pu Source	% Pu	% U	Minor Components
Clean Metal (A)	98	0	2.0% (Ca, Mg, Ga, Zn)
Impure Metal (A)	78.6	0	21.4% (Ca, Mg, Fe, Cr, Ni, K, Ta, W)
Pu Alloy	65.3	32.6	2.1% (Ca, Mg, Fe, Mo)
Clean Oxide	98.5	1.1	0.4% (Al)
U/Pu Oxide Pu/U Cmpds	33.4	60.4	6.3% (Ca, Mg, Fe, Ni, K, Na, Mo, Ta, Ba, W)
Impure Oxide (A)	47.1	0	52.9% (Ca, Mg, Cl, Fe, Cr, Ni, F, K, Na, Mo, Ba, W)
Impure Oxide (T)	86.4	0	13.6% (Ca, Mg, Cl, Fe, Cr, Ni, F, K, Na, Mo, Ba, W)
ZPPR Fuel	28.0	69.0	3.0% (Mo)

Procedure

Frit containing glass formers, uranium, and minor components will be prepared similar to frit produced for the plutonium variability study.[2,3] PuO_2 will be mixed with frit and melted in the Shielded Cells Operation (SCO) Facility at the Savannah River Technology Center (SRTC). A processing temperature of 1500°C with a

residence time of 4 hours will be used to vitrify the material. Samples will be prepared for XRD and SEM/EDX to determine homogeneity.

Results

Although the plutonium variability study is investigating an overall compositional space with respect to glass former and feed variations, this study will determine maximum loadings of individual feed streams with a single frit. This information, along with the compositional space determined by the variability study, will allow minor changes to be made to the concentrations of glass formers to ensure waste form criteria are met while achieving maximum loadings.

Surrogate work with 20 to 25 wt % Th has shown uranium and/or minor components have little effect on homogeneity within the bounds of the identified feed streams. To date, a 10 and 13 wt % (total loading) of a Pu/U mix has been incorporated in a lanthanide borosilicate (LaBS) glass. The Pu/U ratio was 1.5 (60/40 mix). This represents a theoretical blending of all streams not accounting for minor components. Furthermore, a 15 wt % loading of ZPPR fuel (Table 1) feed material and 12 wt % loading of Pu alloy (Table 1) feed material have been fully incorporated into the glass. These initial results show that Pu and U can be simultaneously incorporated into the glass matrix.

References

1.   J. D. Vienna et al., *Plutonium Dioxide Dissolution in Glass*, Pacific Northwest National Laboratory report PNNL-11346 (September 1996).

2.   T. G. Edwards, *A Statistically Designed Plan for the Exporation of a Vitreous Pu Product Compositional Space as it Relates to Solubility and Thermal Stability,* Westinghouse Savannah River Company report SRT-ASG-97-1233 (January 1997).

3.   D. K. Peeler, *Standard Laboratory-Scale Melting Procedures for Plutonium Containing LaBS Glasses,* Westinghouse Savannah River Company report SRT-GFM-97-0010 (January 1997).

Speciation and Surface Interactions of Actinides on Aged Ion-Exchange Resins

D. E. Morris
C. T. Buscher
Los Alamos National Laboratory

A. R. Wheeler
Furman University

R. J. Donohoe
C. D. Tait
Los Alamos National Laboratory

Introduction

The U.S. Department of Energy is presently faced with the stabilization and safe disposition of hundreds of metric tons of residue materials resulting from 50+ years of nuclear weapons production activities. These residues encompass a broad range of substrates and radionuclides and include both solid and liquid materials. Combustible residues constitute a significant fraction of the total residue inventory, and an important constituent within the combustible category is spent anion ion-exchange resins. These resins are typically utilized for the separation of plutonium from other radionuclides under strongly acidic nitric or hydrochloric acid solution conditions which favor the formation and partitioning of anionic Pu(IV) nitrate or chloride species. The spent resins are usually rinsed prior to storage as residues to reduce both acid and radionuclide concentrations, but significant radionuclide concentrations remain in these resins, and the long-term effects of concentrated acid and radiolysis on the resin integrity are relatively unexplored. Thus, new research is needed to assess the stability of these resin residues and address the need for further treatment to ensure stability prior to long-term disposal.

There have been numerous previous spectroscopic studies of plutonium and uranium solution speciation under ion-exchange process-relevant conditions,[1-4] and even some spectroscopic studies of plutonium speciation within the exchange sites of the anion-exchange resins.[5] However, similar speciation investigations on resins that have undergone aging effects as a result of chemical and radiolytic degradation have not been reported. In this study, we are examining the speciation and surface interactions of uranium and plutonium nitrato species on anion-exchange resins that have been "aged" under controlled conditions of elevated nitric acid concentration and temperature.

Experimental

Two anion exchange resins were selected for these studies: Dowex 11, which is a quarternary amine-derivatized polystyrene/divinylbenzene copolymer formulation, and Reillex HPQ, which is a methylated 4-vinylpyridine/divinylbenzene copolymer formulation. These resins are typical of those used in actinide processing applications. The resins are artificially aged by storage at ~ 50°C in nitric acid solutions ranging from 4 to 12 M for periods from several days to ~ 12 months. The effects of aging on the resins (in the absence of actinide species) is being assessed by Raman and luminescence spectroscopy. Aged and fresh resins are reacted with solutions of UO_2^{2+} or Pu(IV) in nitric acid of varying concentrations (0 – 12 M). Freshly loaded resins are also allowed to age in the presence of the actinide. The extent of loading and the speciation and interaction mechanism(s) of the actinide species on the resin are being determined using luminescence, photoacoustic, and Raman spectroscopies.

Results

The nitric-acid induced degradation of the anion-exchange resins is strongly dependent on the nitric acid concentration. At concentrations below 4 M, the resins appear to be indefinitely stable. At 12 M HNO_3, essentially complete degradation is observed within ~ 100 days. At intermediate concentrations (notably

those in the actinide processing regime), there are subtle changes in the vibrational spectroscopic data that clearly indicate a change in resin structure. However, the spectroscopic change suggests a quite specific, highly localized structural change. We do not observe changes in the nitrate stretching region of the vibrational spectra (~ 1350 to 1400 cm^{-1}) that would be consistent with nitration of the resin backbone.

Luminescence spectral data (continuous-wave and time-resolved) obtained for UO_2^{2+} on the resins as a function of nitric acid concentration (0 to 12 M) clearly indicate extensive uptake, even for nitric acid concentrations as low as 4 M. This suggests that anionic uranyl nitrate species exist even at these low HNO_3 levels in contrast to previously published interpretations of uranyl nitrate solution speciation results.[3,4] The luminescence data are complicated by the presence of a luminescence signal from the resin itself. However, the resin signal is overwhelmed by the uranyl signal at sufficiently high uranyl loading levels. In addition, the two luminescent signals do not appear to be simply additive, suggesting that there is some degree of electronic interaction between the uranyl in the resin exchange site(s) and the resin chromophore(s). At liquid nitrogen temperatures, the signals from the resin and the uranyl species become very well resolved, and the uranyl spectrum acquires its characteristic vibronic structure. Time-resolved spectral data were acquired to search for multiple uranyl exchange complexes on the resins, but these results are somewhat ambiguous. Aging effects in this system are still being assessed. Preliminary data analyses suggest that there are not significant changes in the speciation or uranyl on the resin with time.

New experimental studies for the Pu(IV) system on the resins using photoacoustic spectroscopy are under way, and the results will be discussed in detail as part of this report.

References

1.   P. G. Allen, D. K. Veirs, S. D. Conradson, C. A. Smith, S. F. Marsh, *Inorg. Chem.* **35**, 2841–2845 (1996).

2.   D. K. Veirs, C. A. Smith, J. M. Berg, B. D. Zwick, S. F. Marsh, P. G. Allen, S. D. Conradson, *J. Alloys Compounds* **213**, 328–332 (1994).

3.   L. Couston, D. Pouyat, C. Moulin, P. Decambox, *Appl. Spectrosc.* **49**, 349–353 (1995).

4.   C. Moulin, P. Decambox, P. Mauchien, D. Pouyat, L. Couston, *Anal. Chem.* **68**, 3204–3209 (1996).

5.   S. F. Marsh, R. S. Day, D. K. Veirs, "Spectrophotometric Investigation of the Pu(IV) Nitrate Complex Sorbed by Ion Exchange Resins," Los Alamos National Laboratory report LA-12070 (June 1991).

Application of Freeze Drying Technology to Liquid TRU Waste Minimization

Introduction and Background

Freeze drying technology (FDT) has been around for several decades as a separation technology. Most commonly FDT is associated with the processing of food, but the largest industrial scale use of FDT is in the pharmaceutical industry. Through a Cooperative Research and Development Agreement (CRADA) with BOC Edwards Calumatic, the industry leader in FDT, we are demonstrating the feasibility of FDT as a waste minimization and pollution prevention technology. This is a novel and innovative application of FDT. In addition, we plan to demonstrate the freeze dried residue is an ideal feed material for ceramic stabilization of radioactive waste and excess fissile material. The objective of this work is to demonstrate the feasibility of FDT to the separation of complex radioactive and non-radioactive materials including liquids, slurries, and sludges containing a wide variety of constituents in which the separation factors are in excess of 10^8. This is the first application of FDT where primary importance is given to the condensate. Our focus is applying this technology to the elimination of radioactive liquid discharges from facilities at Los Alamos and within the DOE complex; however, successful demonstration will lead to nuclear industry-wide applications.

Current conventional methods for separating undesirable substances from waste streams include distillation, ion exchange, precipitation reactions, or chelating agents, and require multiple passes, produce secondary waste (resins, chelating agent), and have resulted in much lower separation factors (Table 1). Freeze drying technology has the potential to decontaminate all aqueous waste streams from TA-55 and the CMR Building at Los Alamos by a factor of 10^8 or more. The high separation factors are obtainable only with FDT, hence only FDT can make this claim. No precipitating agents or ion exchange resins are required; therefore, secondary waste is not generated. Furthermore, only FDT can meet regulatory requirements now and into the future.

J. A. Musgrave
D. W. Efurd
J. C. Banar
S. Boone
Los Alamos National Laboratory

R. A. Podkulski
E. Renzi
P. Stewart
BOC Edwards Calumatic

Method	Theoretical Separation Factor	Separation Factor Obtained in Practice
Evaporation	10^3–10^4	200–300
Distillation	10^4	200
Precipitation	10^5	2500
Ion Exchange	10^6	2000–20,000
Freeze Drying	unknown	60,000,000

Table 1. Comparison of various separation methods.

What is Freeze Drying?

An aqueous solution can be separated into the solvent and solute components in the following manner. The solution is frozen; the frozen material is situated in the proximity of a condensing surface which is colder than the frozen solution ($T_{feed} > T_{condenser}$). A concentration gradient is established between the frozen radioactive solution in the sample chamber at left and the condenser surface due to the difference in the temperature dependent vapor pressure ($P_{feed} > P_{condenser}$) of the solvent at the two different locations. This concentration gradient drives the

transport of the non-radioactive solvent from the sample chamber to the condenser. A vacuum is usually applied to facilitate the diffusion of the sublimed solvent since the vapor pressures above the frozen solution can be quite low. Complete solvent removal is achieved by supplying enough heat to the frozen material to drive the sublimation process while removing enough heat at the condenser to maintain the concentration gradient.[1]

Application to Liquid Wastes

Through the efforts of this CRADA, a freeze drier has been designed and built specifically for the treatment of liquid wastes. This freeze drier is a prototype scale which will be used to conduct a variety of tests to assess this technology in waste treatment. Results from these tests will be used to scale the freeze dryer design to plant size and to make improvements on the freeze drying process and freeze dryer design.

FDT drastically reduces the volume of the waste since the volume of solute or solid component is smaller than the solution volume. Volume reduction factors greater than one thousand have been achieved in aqueous nitrate/nitric acid solutions containing dissolved and suspended solids, but the exact volume reduction of waste depends on the particular moisture content. Volumes may also be reduced through elimination of neutralization steps in transuranic (TRU) processing. Processing of Pu- and U-contaminated scrap often involves the dissolution of the scrap in nitric acid. These solutions are usually neutralized using sodium hydroxide for compatibility with subsequent process steps. A significant percentage of the waste generated and consequently stored at Hanford was the result of this chemical neutralization. If a process similar to those conducted at Hanford were carried out today, the application of FDT may eliminate the use of neutralizing agents and consequently greatly reduce the quantity of waste solids at later process steps. Integration of FDT into process lines may greatly increase process efficiency, and when combined with other more conventional methods of waste stream separations, FDT can potentially increase the effectiveness of these separations up to 10^{12}.

Application of FDT is not limited to radioactive liquid waste streams; FDT can be applied to plating waste solutions, separation of mixed wastes, and separation of Resource Conservation and Recovery Act (RCRA) metals from aqueous and nonaqueous waste streams. Treatment of mixed liquid wastes by FDT can render the waste into radioactive and hazardous waste components. Furthermore, FDT can be applied elsewhere in the DOE complex to treat newly generated wastes resulting from H and F canyon operations at Savannah River Site, and it can be used for the treatment of legacy wastes such as those at Rocky Flats and Hanford.

Reference

1.   J. D. Mellor, "Fundamentals of Freeze Drying," (Academic Press, London, England, 1978).

Silica Gel Treatment for Stabilization of Plutonium

Introduction

A. K. Nardova
E. A. Filippov
Russian Research Institute for Chemical Technology, Russia

E. G. Kudriavtsev
Ministry for Atomic Energy of Russian Federation, Russia

E. G. Dzekun
K. K. Korchenkin
A. N. Mashkin
"Mayak" Production Association, Russia

The Russian strategy for radioactive waste and plutonium management is based on the concept of the closed fuel cycle and the maximum possible utilization of the fission materials energy potential. Controlled fission means consuming the plutonium in power reactors as their fuel. This is a MOX process, in which Russia and other countries are currently engaged.

Several options are under consideration for the disposition of surplus Pu. One option is immobilization of plutonium in glass, followed by repository disposal. Due to thermodynamic instability of glass and glass-like compositions, these materials are not an optimal matrix for fixation of plutonium-239, which has the half-life of 24,000 years, and its doughtier, uranium-235, has a 700 million year half-life, and require the appropriate storage period. This causes the necessity of developing the alternative methods for immobilization actinides from solution into materials which have better chemical, thermal, and radiation stability.

The silica gel treatment process for stabilization of plutonium has been developed jointly by the Russian Research Institute for Chemical Technology and the Mayak Production Association.[1,2]

This paper summarizes the merits of the silica gel treatment option.

Results and Discussion

The silica get treatment process is the simple batch process involving adsorption of the radionuclides from solution onto pellets of silica gel, followed by a brief heating cycle. The process does not require exotic materials to be used.

If easy recovery of the adsorbed material is desired then the heating is conducted at relatively low temperatures, typically less than 350°C. If long term storage or permanent disposal is desired, then heating to 800 to 1,000°C converts the granules to dense, free-following particles suitable for packaging.

The solidified material is convenient both for temporary storage and for long-term storage and/or burial of the plutonium. The extraction of Pu from silica gel is made possible by the low calcination temperatures to which the saturated silica gel is subjected and is accomplished by desorption with acid.

The solid waste form for Pu storage is characterized by low dust generation rates and a good flowability coefficient. Transformation of the material from a form suitable for interim storage into one that is suitable for final burial can be done easily by calcination at a high temperature.

The maximum plutonium saturation levels of silica gel are 800 mg Pu 1 g SiO_2.
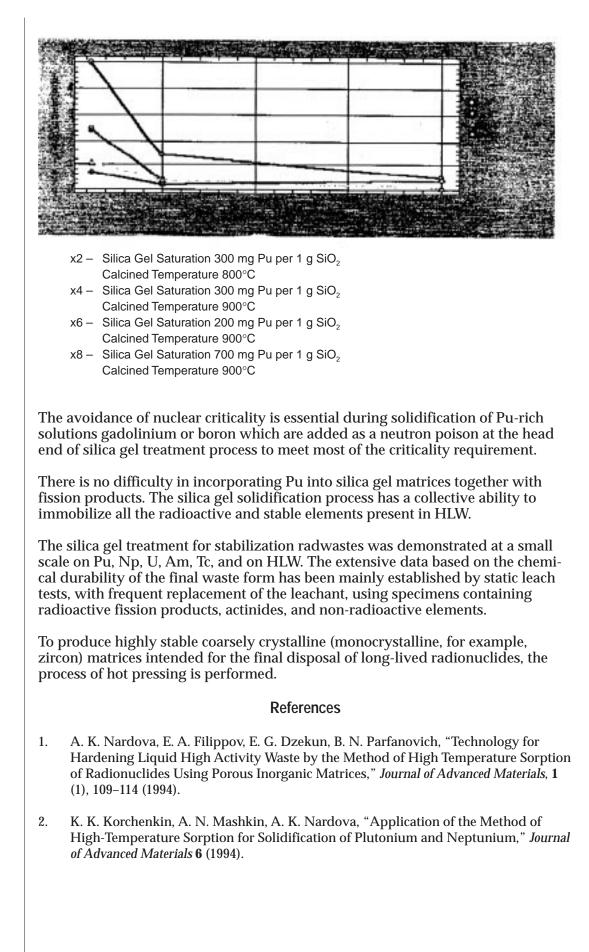
900°C calcined product did not leach with water of 3 M HNO_3 (Figure 1). 250 to 450°C calcined product is recoverable with 3 M HNO_3 at a temperature of 25°C.

Figure 1

x2 – Silica Gel Saturation 300 mg Pu per 1 g SiO_2
Calcined Temperature 800°C

x4 – Silica Gel Saturation 300 mg Pu per 1 g SiO_2
Calcined Temperature 900°C

x6 – Silica Gel Saturation 200 mg Pu per 1 g SiO_2
Calcined Temperature 900°C

x8 – Silica Gel Saturation 700 mg Pu per 1 g SiO_2
Calcined Temperature 900°C

The avoidance of nuclear criticality is essential during solidification of Pu-rich solutions gadolinium or boron which are added as a neutron poison at the head end of silica gel treatment process to meet most of the criticality requirement.

There is no difficulty in incorporating Pu into silica gel matrices together with fission products. The silica gel solidification process has a collective ability to immobilize all the radioactive and stable elements present in HLW.

The silica gel treatment for stabilization radwastes was demonstrated at a small scale on Pu, Np, U, Am, Tc, and on HLW. The extensive data based on the chemical durability of the final waste form has been mainly established by static leach tests, with frequent replacement of the leachant, using specimens containing radioactive fission products, actinides, and non-radioactive elements.

To produce highly stable coarsely crystalline (monocrystalline, for example, zircon) matrices intended for the final disposal of long-lived radionuclides, the process of hot pressing is performed.

References

1.   A. K. Nardova, E. A. Filippov, E. G. Dzekun, B. N. Parfanovich, "Technology for Hardening Liquid High Activity Waste by the Method of High Temperature Sorption of Radionuclides Using Porous Inorganic Matrices," *Journal of Advanced Materials*, **1** (1), 109–114 (1994).

2.   K. K. Korchenkin, A. N. Mashkin, A. K. Nardova, "Application of the Method of High-Temperature Sorption for Solidification of Plutonium and Neptunium," *Journal of Advanced Materials* **6** (1994).

Vitrification of Rocky Flats Incinerator Ash

T. S. Rudisill
J. C. Marra
D. K. Peeler
Westinghouse Savannah River Company

Introduction

Approximately 20,000 kilograms of incinerator ash generated during years of nuclear weapons production activities are currently stored at the Rocky Flats Environmental Technology Site (Rocky Flats). Although the continued storage is not of urgent concern, the Defense Nuclear Facilities Safety Board's 94–1 Recommendation[1] requires conversion to a form suitable for safe interim storage (or to an acceptable waste form) by the year 2002. Vitrification has been proposed as one treatment technology to stabilize the ash and produce a waste form which can be disposed of at the Waste Isolation Pilot Plant (WIPP).[2] Alternatively, vitrification could potentially allow disposal of the ash using a can-in-canister approach with the high-level waste glass produced at the Savannah River Site's Defense Waste Processing Facility (DWPF).

Description of Work

A series of small-scale vitrification experiments are currently in progress to develop and optimized glass formulations and processing conditions for the vitrification of Rocky Flats incinerator ash. Initially, scouting experiments were performed to demonstrate the feasibility of vitrifying a simulated ash using soda-lime-silicate and borosilicate glass formulations. The simulated ash was based on a composition reported by Johnson,[3] containing nominally 45 wt % glass formers (silicon and boron oxides), 20 wt % carbon, 15 wt % transition metals, 10 wt % alkali and alkaline earth elements, and 10 wt % actinides. Thorium and neodymium oxides were used as surrogates for plutonium and americium oxides, respectively. The experiments were performed in 100 ml alumina crucibles using melt temperatures from 1300 to 1500°C. Carbon was removed from the simulated ash using a slow temperature ramp or calcination at 800 to 900°C.

Based on the fabrication of x-ray amorphous glasses during the initial feasibility experiments and the simplicity of soda-lime-silicate glasses, a 60:30:10 (wt %) mixture of silicon, sodium, and calcium oxides was established as the baseline frit for additional experimentation. The focus of these experiments was the variability in the incinerator ash composition. The goal of the study was to identify the chemical components in the ash which have the greatest effect on glass formulation (liquidus temperature, viscosity, crystallinity, etc.) and to determine the loading limits for these species. The program consisted of 20 glass melts in which the concentration of key oxides (aluminum, calcium, chromium, copper, iron, magnesium, sodium, and potassium) were systematically varied from low to high concentrations while other components were held at average values. Hafnium and neodymium oxides were used as surrogates for plutonium and americium oxides in the surrogate ash. Carbon, added as graphite, was removed by holding the furnace temperature at 900°C for 3 hours. The melt temperature of 1350°C was then held for 4 hours before pouring the molten glasses onto a steel plate.

Results

Selected soda-lime-silicate glasses produced during the ash variability study were characterized by x-ray diffraction and Transmission Electron Microscopy (TEM). The glasses were selected based on good, average, and poor visual homogeneity. The results from x-ray diffraction showed that each glass was amorphous; however, TEM examination revealed small (50 to 100 nm), round crystalline precipitates in opaque regions of the glasses. The glass with the poorest homogeneity

contained the most crystals; however, the volume fraction was much less than 1%. There were no signs of amorphous phase separation in any of the glasses. Small metal spheres were found in many of the melts. X-ray fluorescence identified the spheres as a nickel-copper alloy reduced from the ash by residual carbon in the melt. The reduction of metals by carbon is also the likely source of the crystalline precipitates identified by the TEM.

Complete characterization of the glasses produced during the variability study has not been completed. Liquidus temperatures and viscosities of selected glasses will be measured to define the operating envelope for the soda-lime-silicate glasses. The durability of the glasses will also be compared to other waste forms using the Product Consistency Test[4] developed for DWPF glass. Although the durability of glasses produced from the simulated ash has not been measured, just the high-temperature treatment and immobilization generate a waste form which is acceptable for disposal at WIPP. The glasses are chemically stable and do not generate gas which is of primary concern to the WIPP Waste Acceptance Criteria.[5] In addition, the low concentration of plutonium in the glass and inherent difficulty of recovery reduce the attractiveness to the point where safeguards can be terminated based on provisions in DOE Order 5633.3B.[6]

Additional work planned for the soda-lime-silicate glasses includes radioactive experiments to measure the plutonium loading capacity in simulated ash and vitrification experiments with actual Rocky Flats incinerator ash to benchmark the work with surrogate materials. A parallel effort has also been initiated to develop a glass formulation with a processing temperature less than 1000°C. Implementation of a vitrification process at Rocky Flats may be constrained to temperatures below that required for fabrication of the soda-lime-silicate glasses.

References

1. J. T. Conway, "Recommendation 94–1 to the Secretary of Energy Pursuant to 42 U.S.C. [paragraph] 2286a(5) Atomic Energy Act of 1954, as amended," (Attachment), Letter from Defense Nuclear Facilities Safety Board to Secretary of Energy, Washington, DC (1994).

2. "Ash Residue End State Trade Study," Vol. 1, U. S. Department of Energy Idaho Operations Office report DOE/ID-10560 (1996).

3. T. C. Johnson, "Recovery of Plutonium from Incinerator Ash at Rocky Flats," Rocky Flats Plant report RFP-2520, Rockwell International (1976).

4. "Standard Test Methods for Determining Chemical Durability of Nuclear Waste Glasses: The Product Consistency Test," American Society for Testing and Materials ASTM Designation: C 1285–94 (1994).

5. "Waste Acceptance Criteria for the Waste Isolation Pilot Plant," U.S. Department of Energy document DOE/WIPP-069, Revision 5, Carlsbad Area Office (1996).

6. Department of Energy Order 5633.3B, "Control and Accountability of Nuclear Material," U. S. Department of Energy, Washington, DC (1994).

Integrated Nondestruction Assay Solutions for Plutonium Measurement Problems of the 21st Century

T. E. Sampson
T. L. Cremers
Los Alamos National Laboratory

The Safeguards Science and Technology Group (NIS-5) in partnership with the Nuclear Materials and Stockpile Management Program at Los Alamos National Laboratory is developing, designing, and implementing Nondestructive Assay (NDA) solutions to the Materials Control and Accountability (MC&A) problems associated with the new missions that will be found in the DOE complex in the dismantlement, disposition, residue stabilization, immobilization, and MOX fuel programs. These new solutions make extensive use of integration of several different NDA technologies and in most cases use robotics to reduce materials handling, reduce worker radiation exposure, increase throughput, and provide optimum safeguards for the materials. Issues associated with bilateral or international inspection of these materials are also being considered in these new systems. These systems are typified by the ARIES (Advanced Recovery and Integrated Extraction System) nondestructive assay system which is under construction at Los Alamos to measure the outputs of a weapon component dismantlement system.

The ARIES nondestructive assay system consists of four NDA instruments integrated with a central host computer and robotic sample handling. The four NDA instruments are (1) calorimeter, (2) gamma spectroscopy of plutonium isotopic composition, (3) Segmented Gamma Scanner (SGS), and (4) an active-passive neutron multiplicity counter. This suite of instruments is designed to measure all of the outputs of a pit dismantlement operation including both plutonium and enriched uranium. These instruments are all state-of-the-art designs which also have long proven capability in applications worldwide. The Safeguards Science and Technology Group at Los Alamos designed and fabricated all of these NDA instruments and also developed all of the software. This integrated approach at a single laboratory greatly facilitates system integration compared with efforts taking software and hardware from different sources.

The Los Alamos National Laboratory is redesigning and rebuilding its Nuclear Material Storage Facility (NMSF) to better adapt to the changing requirements for safe, secure storage of plutonium. The count room, incorporating a full suite of NDA instruments, is being designed with the principles of the ARIES NDA system in mind.

The NMSF is designed to handle two types of containers. The first container type is the standard DOE-approved container for long-term storage as specified by the 3013-96 standard. The vast majority of the material stored in the NMSF will use these containers. An automated NDA system as in ARIES is being proposed for the 3013 containers. The other container will be a larger container designed for storage of weapons components (pits) as Los Alamos continues its active role in stockpile surveillance as well as assuming a limited stockpile maintenance capability. We have specified additional instruments designed to measure all of the materials housed in either container.

In 1994 the Defense Nuclear Safety Board (DFNSB) issued an order (94-1) requiring that wastes from plutonium processing that were in storage be stabilized and repackaged in a form suitable for long-term storage. This program presents some challenges for nondestructive assay as the stabilized materials are likely to be highly impure. In spite of the impurities, it would appear that an instrument suite consisting of calorimetry, gamma ray isotopic analysis, and neutron multiplicity counting is nearly optimum for residue measurements in 3013 containers or other

containers with similar dimensions. There would appear to be few problems that this suite could not handle, although accuracy and precision, relative to values for product materials, will be degraded for many of the residues.

The ARIES NDA suite (without the SGS) is ideally suited to measure the input plutonium cans as well as the input uranium oxide, assuming packaging in a container similar to the 3013 container, for material entering a MOX plant, one of the United States' chosen plutonium disposition options.

The materials from an ARIES weapons dismantlement process and high purity stabilized 94-1 residues may be offered to the International Atomic Energy Agency (IAEA) for international inspection as excess fissile materials. The types of instruments and measurements represented in the ARIES NDA are very familiar to the IAEA. Neutron coincidence counting has been a mainstay of IAEA inspection techniques for many years. Plutonium gamma ray isotopic analysis measurements are also regularly used by the IAEA in conjunction with neutron coincidence counting. Calorimetry is now also becoming a very cost-effective option for some types of IAEA measurements. The IAEA is in the process of certifying calorimetry for use in the inspection of U.S. excess fissile materials.

An "ARIES-like" suite of NDA instruments including calorimetry, neutron multiplicity counting, and gamma ray isotopic analysis, in conjunction with robotic automation will find extensive use in solving the majority of the NDA problems of the future associated with weapons dismantlement, residue stabilization, long-term storage, disposition, and international inspection.

Stabilization of Plutonium Contaminated Wet Combustible Residues

N. C. Schroeder
M. Attrep, Jr.
S. B. Williams
*Los Alamos National
Laboratory*

The safe interim storage of plutonium contaminated wet combustible residues is problematic at many Department of Energy (DOE) sites. Wet combustibles are the laboratory trash accumulated from the processing of different plutonium streams and therefore consists of kimwipes, paper towels, polyethylene bags/tape, rubber gloves, and anti-C cotton coveralls. Organic wet combustibles produced from the machining of plutonium metal contain plutonium metal, volatile solvents (CCl_4), and cutting oils. The pyrophoric plutonium metal is the major hazard of this material. Nitrate wet combustibles result from the aqueous nitric acid processing of plutonium; nitrates in contact with organic materials may cause a potentially explosive condition resulting in over-pressurization and loss of containment of the storage vessels. Stabilization of these materials is also required for shipment and long-term geological disposition.

Los Alamos National Laboratory (LANL) was tasked with evaluating the proposed residue stabilization flowsheets. The major steps in the organic wet combustibles flowsheet consist of a low-temperature thermal desorption of the volatile organics and a steam oxidation of the plutonium metal to PuO_2. These steps are carried out in a 2 gallon Parr pressure reactor. Volatile organics are vaporized at 80°C at reduced pressure and trapped off line. Water is injected into the reactor and the steam oxidation of the metal is carried out at 110°C and 30 psi. This temperature corresponds to the maximum rate of plutonium metal corrosion by water vapor. Developmental work with cerium metal, a surrogate for plutonium metal, has shown > 98% conversion of the metal to the oxide in 1.5 hours for 100 to 500 g batches containing as much as 4% metal.

Two nitrate wet combustibles flowsheets consist of washing $Pu(NO_3)_4$ or PuO_2 from the combustibles with either water or 0.5 M KOH. The washing process may be augmented by sonication, heat, or the addition of detergent. Experiments with [141]Ce traced $Ce(NH_4)_2(NO_3)_6$ in moderately concentrated nitric acid mimic the behavior of $[Pu(NO_3)_6]^{2-}$ sorbed onto the combustible materials. These experiments show that > 75% of the $[Ce(NO_3)_6]^{2-}$ can be removed from the combustibles with three 10:1 v/w water washes. Likewise [141]Ce traced CeO_2 will be used to mimic the behavior of PuO_2.

Radioactive experiments with a maximum weight percent loading of 8% plutonium metal are being conducted in an inert atmosphere glovebox to evaluate the final process parameters for both the organic and nitrate wet combustibles.

The final stabilization treatments for these two waste streams are being developed and tested in order to evaluate the ease and efficiency of treatment, safety, and time of processing for these materials.

Colloids in TRU Waste Contaminated Saturated Brine

There has been continual interest in understanding the formation and stability of actinide intrinsic or actinide containing colloids, particularly in complex matrices relevant to waste isolation. These colloids are solid particulates less than 1 µm in size, which stay suspended in solution, and may be composed wholly of actinide species (intrinsic), or may be of another chemical composition and carry actinides as adsorbed or bound species (pseudo). Of specific interest here is the formation of Pu intrinsic colloids, pseudo colloids, and other non-actinide-associated colloids in waste environments composed of saturated brine. These complex matrices include those having high ionic strength, organic chelators, excessively high or low pH, or high concentrations of other dissolved species. The ultimate concern here is whether the colloidal particles have the ability to carry actinides, as in actinide intrinsic colloids and pseudo colloids, or have the potential, by the nature of their surface chemistry, to adsorb and further transport actinides. Factors of importance include the concentration, size distribution, chemical nature, and morphology of colloidal particles generated in saturated brine matrix waste forms of a variety of types, as these factors influence possible transport in environmental and waste situations.

We present studies of colloid and particle characterization from solution samples taken as part of the Waste Isolation Pilot Plant brine simulation experiment, the Source Term Test Program (STTP). The STTP consists of accelerated aging experiments of real TRU waste of various types in saturated brine solutions. The waste types include matrices of portland cement, envirostone, pyrochemical salts, combustibles, metals, and organic liquids. Characterization of the solution colloids is performed through extended x-ray absorption fine structure (EXAFS), dynamic light scattering, laser forward scattering, field flow fractionation (FFF), radiochemical measurements, electron microscopy/x-ray fluorescence, and other chemical speciation techniques. A survey of results indicates complex behavior of colloids in these high ionic strength brines. Light scattering analysis shows that absolute concentrations of colloids range from less than 10^6 up to 10^{11} particles/mL over the size range of 0.05 to 1.2 µm in diameter. The mean size of the number distribution is generally at the small sizes (0.1 µm or less), indicating a preponderance of small colloids. There are, in addition, substantial amounts of very small particulates less than 0.1 µm in size. Colloid characterization by electron microscopy and x-ray fluorescence analysis shows a variety of particle chemistries and morphologies. In general there are very few actinides associated with the solid particulates in the colloid regime, the solids carrying actinides being unstable as colloidal material and segregating out to the solid phase rather than the suspended phase of the waste matrix. In certain cases actinides are associated with colloids in brine-waste matrices having high amounts of organic wastes, including combustible materials and specific organic chelators. This is not unexpected, as organics in high ionic strength solutions tend to form agglomerate particles, and in certain cases, have a high ability to complex or bind actinides. These colloids will be discussed in the context of their solution concentration, morphology, and chemical nature. In other waste matrices, not necessarily having organic components, where actinides are found in higher concentration in the solution (up to 200 ppm), there is also evidence for actinide containing colloids. The specific nature of these colloids will also be discussed.

R. K. Schulze
M. P. Neu
J. D. Farr
S. D. Conradson
Los Alamos National Laboratory

Solution to the Problem of Recovery Transuranium Elements from Basin-Storage of Radioactive Waste and Equipment of Plants

N. E. Shingarjov
A. S. Polyakov
L. S. Raginsky
I. V. Mukhin
A. A. Bochvar All-Russia Research Institute of Inorganic Materials, Russia

At present, a great volume of radioactive waste (RW) has accumulated on the territory of radiochemical plants in Russia. In Ural alone, the quantity RW is estimated in 10^9 Ku, and in natural environment is ~ 1,3 10^8 Ku.[1] The special hazard RW is contained in the outdoor basin-storage of Russian radiochemical plants. Lake Karachay (PO "Mayak") contains 1,20 10^8 Ku radioactive waste. The basin-storage N 1, 2 for medium-level waste (10^{-5} to 10^{-1} Ku/l) and pulp-storage N 1, 2 for low-level waste (<10^{-5} Ku/l) were created by the Siberian chemical plant. Natural basin N 3, 4 was used too.[2] Complex work needs are fulfilled for site remediation and liquidation of the outdoor basin-storage.

This effort is a multilateral technological problem, including development of technology to extract transuranium elements, other technological processes, and equipment for its realization. The most difficult process is processing sludge of basin-storage, containing a preponderant quantity of radionuclides including transuranium elements, presence of which existing methods cannot be applied and long-term compaction of radioactive waste.

The leaching process for transuranium elements from sludge is very combined and requires a respectable rate of reagents,[3] therefore expediently reducing the volume of waste containing transuranium elements. It can be reached by the creation of the apparatus for classifying and compacting sludge.

The existence of basin-storage for long times has resulted in the formation of resistant compounds, which practically do not leach by use of classical methods of hydrometallurgical processing. At the first stage, realization of work on reducing the volume of tranuranium waste elements is expedient. It can be attained by developing equipment to classify and concentrate sludge.
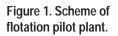
In order to realize this goal, a pilot plant is used to classify, compact, and wash sludge.
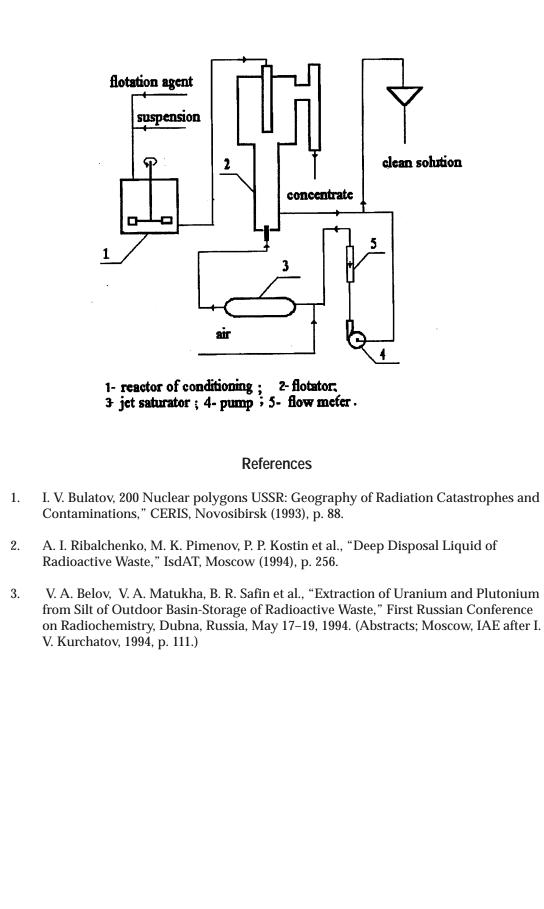
The separation sludge on the purified fraction and radionuclides concentrate was executed in the pulsed column. The tests have shown an opportunity to classify testing suspensions. The mode of operations determined, allowed the separation of up to 94% of purified fraction.

Using column flotation apparatus of a special design was investigated for flotation (seeFigure 1) compacting of suspension received during classification. The humidity was decreased 99.2% up to 93 to 94% as a result of spent experiments.

The volume of radioactive waste containing transuranic elements is reduced by 30 to 35 times during a complex run of the pilot plant.

Figure 1. Scheme of flotation pilot plant.

1- reactor of conditioning ;   2- flotator;
3- jet saturator ; 4- pump ; 5- flow meter.

References

1. I. V. Bulatov, 200 Nuclear polygons USSR: Geography of Radiation Catastrophes and Contaminations," CERIS, Novosibirsk (1993), p. 88.

2. A. I. Ribalchenko, M. K. Pimenov, P. P. Kostin et al., "Deep Disposal Liquid of Radioactive Waste," IsdAT, Moscow (1994), p. 256.

3. V. A. Belov, V. A. Matukha, B. R. Safin et al., "Extraction of Uranium and Plutonium from Silt of Outdoor Basin-Storage of Radioactive Waste," First Russian Conference on Radiochemistry, Dubna, Russia, May 17–19, 1994. (Abstracts; Moscow, IAE after I. V. Kurchatov, 1994, p. 111.)

The Waste Management System at the Los Alamos Plutonium Facility

Introducution

A computer-based transuranic (TRU) Waste Management System (WMS) is being implemented at the Plutonium Facility at Los Alamos National Laboratory (LANL). The WMS is a distributed computer processing system stored in a Sybase database and accessed by a graphical user interface (GUI) written in Omnis7, a client/server development tool. It resides on the local area network at the Plutonium Facility and is accessible by authorized TRU waste originators, Non-Destructive Assay (NDA) Laboratory personnel, radiation protection technicians (RPTs), quality assurance personnel, and waste management personnel for data input and verification. The WMS has changed the TRU paper trail into a computer trail, saving time and eliminating errors and inconsistencies in the process.

Description of Work

The Nuclear Materials Technology (NMT) Division as the landlord of the Los Alamos Plutonium Facility has recognized for many years that cradle to grave tracking of transuranic waste could be done most expeditiously by a computer network based real-time data generation and tracking system. Towards this goal, the WMS was conceived in 1991 and then launched in 1993 with a week-long meeting of users and programming personnel to determine the system requirements. Phased implementation of the WMS inside the Plutonium Facility began in August of 1995 with the submittal of waste information by the waste originator to the materials management and the waste management groups. Full implementation is anticipated in April 1997.

The Plutonium Facility is the largest generator of TRU waste at LANL, producing approximately 500 new containers of waste per year. The facility is anticipating an expanded mission and upgrades which will increase the waste production rate. The plutonium processing area in the facility has about 100 processes operating in over 300 gloveboxes and about 530 waste originators. TRU waste generated at the Plutonium Facility consists of solid (debris) waste and immobilized liquid (cemented) waste. The waste is primarily contaminated with plutonium isotopes and is destined for dispoal at the Waste Isolation Pilot Plant (WIPP).

The Waste Management System mirrors the old paper TRU waste data package system in that the final printed forms contain the same information as the old system. The old system consisted of 5 to 20 pieces of paper produced in the Plutonium Facility for each container of TRU waste, requiring a great deal of transcription of information from one piece of paper to another.

The WMS data is stored in a Sybase database which resides on a Sun Workstation. This program can be run using Windows and Macintosh operating systems. The implementation of the WMS required upgrades to networking capabilities throughout the Plutonium Facility so that originators could log on to the system in their own processing room and input the waste item information. This included the addition of new network lines and ports in the rooms and the purchase of new hardware and software.

Most information is selected from dropdown lists, check boxes or radio buttons. A dropdown list is a field on the window which may be expanded to a list of choices by using the mouse. A check box is a field that indicates a yes or no

K. Smith
A. Montoya
R. Wieneke
D. Wulff
C. Smith
K. Gruetzmacher
Los Alamos National Laboratory

selection. A radio button allows the selection of options which are mutually exclusive. One primary requirement of the system was that it be easy to learn and use.

Two of the major hurdles in the implementation of this system were the QA requirements for signatures and for an auditable trail of changes made to the data. These problems were resolved by requiring users to log onto the system and by setting up a table of authorities identifying who could change records, and tables to track changes.

Numerous benefits have already been realized using the WMS. Transcription and calculational errors and mistakes where decisions are made based on numerical comparisons have been eliminated. The need to enter the final data into a separate database has been eliminated. There is no longer a need to transfer hard copies of the data packages from a radiological controlled area to an uncontrolled area.

Personnel who participated in the phased testing of the system and provided feedback to the programmer became partners in the development and improvement of the WMS. This resulted in a vastly improved product that enhanced the WMS and in many cases caused personnel to re-think the way they had been performing work. Personnel who use the WMS frequently say that this part of their job has become a lot easier and less time consuming.

Enhancements to the WMS which are being considered for implementation at a future date include:

- electronic interface to NDA laboratory measurement instruments

- electronic transfer of data to the LANL Waste Management Facility

- capability for outside reviewers to approve data on-line

- incorporation of wattage and other WIPP limits into the WMS

- bar coding of waste items and containers for location tracking

Results

To date, implementation of this system has resulted in a 25% time reduction in paperwork for transuranic waste at the Plutonium Facility. We expect this time reduction to increase to 50% at full implementation. Transcription errors and calculational errors have been eliminated. Mistaken entries on paperwork have decreased. The need for a data clerk to enter the final data into a separate database has been eliminated.

Glass Encapsulation Technology for Pu-Bearing Wastes

Introduction and Background

A proposed method for the stabilization and ultimate disposal of low-concentration plutonium (Pu) bearing material is encapsulation in a glass matrix. This technology is being investigated for treatment of incinerator ashes, reduction residues (sand, slag, and crucible (SSC)), and graphite molds backlogged at the Rocky Flats Environmental Technology Site (RF). This technology offers rapid conversion to a safe and durable waste form with reduced safeguard requirements. Encapsulation may also be applicable to other Pu-bearing materials throughout the Department of Energy (DOE) complex and internationally.

The primary package being considered for this waste form is an 8 inch diameter by 10 inch tall Vollrath container constructed from 304L stainless steel. The target loading for each canister is 85 grams of fissile Pu. Different approaches were chosen for the two wastes investigated by PNNL. A homogeneous, sintered product containing less than 1 wt % Pu was selected for the ash waste stream. This was done to meet safeguards termination limit requirements while still being able meet the target Pu loading in each canister. A glass-encapsulated product containing less than 5 wt % Pu was chosen for the SSC. This product will have to satisfy safeguards termination limits requirements for Pu recovery. This requirement was met by evaluating Pu recovery using an acid dissolution benchmark developed at RF.

Results and Discussion

Glass frit compositions were developed for the ash and SSC waste streams by optimization of the glass properties. Glass property databases were used to narrow the compositions to three glass families: (1) Antimony-Vanadium-Phosphate (AVP),(2) Soda-Lime-Silicate (SLS), and (3) Alkali-Boro-Sificate (ABS). The viscosity-temperature relationship was determined to be a primary focus of glass development. Additionally, the reaction of glass with the waste was found to be important in frit development.

Figure 1 shows simulated SSC encapsulated in an AVP glass. The scale of particles are roughly 1/8 inch which corresponds to the crushed SSC in RF's backlog. The glass fully encapsulates each grain at 700°C in 1 h. Figures 2a and b show the encapsulation of ash in SLS glass after 2 h heat treatments. Figure 2a is the frit/ash mixture at 650°C where gasses from organic oxidation are still being evolved. The frit has not yet begun to sinter as can be seen by the sharp frit grains, leaving a path for oxygen and escaping gasses. Figure 2b is the same mixture at ~900°C. Here the ash is completely encapsulated in the molten glass. These samples were produced during the initial scoping studies. Subsequent development was done to reduce melting temperatures.

J. D. Vienna
M. L. Elliott
H. Li
J. K. Luey
Pacific Northwest National Laboratory

G. Veazey
R. Nakaoka
Los Alamos National Laboratory

Figure 1.
Encapsulation of MgO crucible chunks (~1/8 inch dimension) in AVP glass.

(a)

(b)
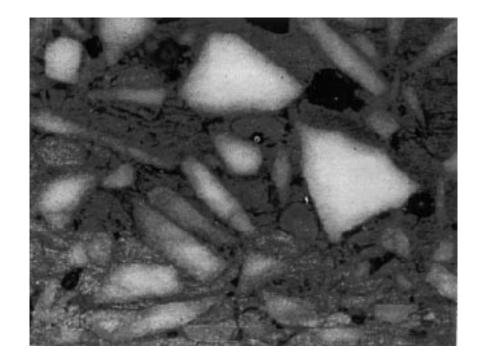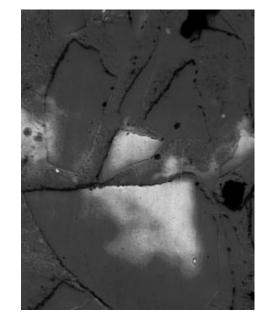
Figure 2.
Encapsulation of ash in SLS glass (a) typical below 700°C, (b) at 900°C.

Several large-scale experiments were completed to evaluate the processing (heating and cooling cycles) sequences, batch foaming, feed variability impacts, and materials interactions. Waste packages ranging from 1.0 liter to 8.2 liters (full-scale) were produced during experiments. The packages were sectioned and evaluated both physically and chemically. The glass waste forms were also evaluated for Pu recoverability. The heating and cooling requirements were found to be a strong function of the furnace design, glovebox cooling capabilities, and sample size.

Cathodic-Arc Deposited Erbia for Molten Plutonium Containment in Casting Operations

Plutonium forms a low melting point eutectic with many metals. This presents a problem in casting operations, because durable, lightweight metal molds cannot be used—the molten plutonium will attack and quickly destroy the mold. Graphite molds are commonly used, but only survive one or two castings before they must be disposed of as highly contaminated waste. If a durable, adherent, molten plutonium resistant coating could be deposited on a lightweight metal mold, such a mold might withstand many castings, thereby reducing the waste stream. Erbium oxide (erbia) is a good candidate for such a coating, since it is not attacked, nor wetted by molten plutonium. However, erbia is a brittle ceramic, and has a coefficient of thermal expansion which is quite different from most metals, making it difficult for the coating to adhere during the thermal shock of casting.

In this paper, we report the production of thin, highly adherent erbia coatings using a hybrid ion implantation and deposition process from a cathodic-arc derived erbium plasma. Such coatings, some as thin as 1 μm, have protected tantalum, 304L stainless steel, and niobium coupons during casting tests at Los Alamos.

In a cathodic-arc, a electrical arc of several tens to hundreds of amps is drawn in vacuum between a consumable cathode (erbium in this case) and a surrounding anode. This ejects a highly ionized, multiply charged metal-ion plasma from the cathode. By pulse biasing a nearby substrate to several tens of kilovolts negative potential, these positive ions can be accelerated toward the substrate and implanted in its surface. By operating the substrate pulsed bias at a lower duty cycle than the pulsed (or DC) cathodic-arc, simultaneous implantation and deposition can be achieved. In the presence of a few tenths of a millitorr of oxygen, the coating will be deposited as a ceramic metal-oxide. This process produces coatings of superior adhesion to the substrate, by developing a functionally graded interface over which the material properties smoothly change from those of the substrate to those of the coating material. This region, while less than 50 nm thick, greatly reduces the stresses which would develop at a sharp interface.

Highly adherent erbia coatings which successfully passed casting tests were produced by LANL and ISM Technologies, Inc., using two variations on the basic "recipe" described above. LANL coatings were produced with a pulsed cathodic-arc and pulse biased substrate in a four step process:

1. Argon ion sputter cleaning of the substrate.

2. High-voltage (20 kV) pulsed implantation of erbium ions.

3. High-voltage (20 kV) pulsed implantation and deposition of erbium and oxygen.

4. Medium-voltage (1 kV) deposition of erbia with a magnetically filtered arc.

Coatings by ISM Technologies, Inc. were produced with a DC cathodic-arc and pulse biased substrate in a three step process:

1. Erbium ion sputter cleaning of the substrate.

B. P. Wood
D. Soderquist
A. Gurevitch
K. Walter
Los Alamos National Laboratory
J. Treglio
ISM Technologies, Inc.

2. High-voltage (15 kV) pulsed implantation of erbium ions.

3. High-voltage (15 kV) pulsed with low-voltage (80 V) DC implantation and deposition of erbium and oxygen.

The ISM Technologies process is conceptually simpler and faster (due to the DC arc) than the LANL process, but produces coatings with a higher concentration of macroparticles—small (1 to 10 μm) droplets of erbium metal imbedded in the coating. These macroparticles can be pulled out of the coating, leaving pinholes behind in thin coatings. The magnetically filtered arc in the LANL process prevents most of these particles from reaching the substrate. ISM coatings were also sub-stoichiometric in oxygen (45% to 50% versus 60% for stoichiometric erbia).

Two casting tests were conducted. In each test, six 1- inch-diameter flat coupons were stacked with spacers in a graphite mold. The mold was preheated to 400°C, and 750 g of 1100°C plutonium was poured into the top of the mold. The mold was broken open the next day. The coatings were examined before and after the casting with an SEM. The surface of the plutonium which solidified against the coating was also examined with an SEM.

Conclusions reached as a result of two casting tests include the following:

•   Adequate sputter cleaning of the substrate prior to coating implantation/ deposition is essential for coating adhesion. It is necessary to re-sputter the substrate after any vacuum breaks which occur during the process.

•   Coatings as thin as 1 μm will provide protection against erosion by molten plutonium, but thicker coatings are more robust in repeated castings.

•   Pre-implantation of erbium metal will not produce adherent coatings without subsequent sputter cleaning.

•   The molten plutonium plucks off macroparticles larger than 5 μm in diameter, but leaves smaller particles behind. However, macroparticles seem not to be a problem as long as the coating is sufficiently thick (> 3 μm).

•   Coating stoichiometry is not critical. ISM coatings which were deficient in oxygen seem to work as well as stoichiometric LANL coatings.

These results suggest that durable, long-lived metal molds for near net shape casting operations can be produced with cathodic-arc derived erbia coatings. However, a number of questions remain to be answered by further research. Among these are:

•   Erbia coatings were subjected to two castings. Can they withstand 10 castings? 100 castings?

•   How resistant is an erbia coating to mechanical erosion by a directly impinging stream of molten plutonium?

•   Can these erbia coatings be deposited evenly upon real near net shape molds?
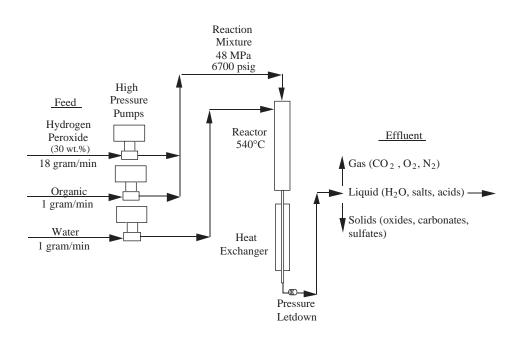
Hydrothermal Oxidation for Treatment of Plutonium Combustible Wastes

Introduction

Chemical reactions in high-temperature water (hydrothermal processing) allow new avenues for effective waste treatment and radionuclide separation. Successful implementation of hydrothermal technologies offers the potential to effectively treat many types of radioactive waste and reduce the storage hazards and the disposal costs, while minimizing the generation of hazardous secondary waste streams.[1-5] A major category of radioactive wastes includes combustible material such as organic solvents, rags, plastics, and paper that are contaminated with transuranics (TRUs) and strong oxidizers such as nitrates. In some cases these wastes are an acute safety hazard because of the production of flammable gases from organic decomposition initiated by radioactive decay. Experiments have demonstrated that hydrothermal processes can reduce the volume and remove the organic and nitrate components (> 99.999%) of most of the common combustible wastes generated by the nuclear industry.

Description of the Actual Work

A hydrothermal process unit was installed and tested in a plutonium glovebox for treatment of combustible wastes. A schematic is shown in Figure 1. Waste is slurried, pressurized, heated, and held at reaction temperature for a time sufficient to complete the desired chemical processes (oxidation, reduction, dissolution). Rapid oxidation occurs on the time scale of seconds to minutes, and produces simple products (ideally CO_2, H_2O, and N_2). The mixture is then cooled and depressurized, and the solid, liquid, and gaseous products are separated for disposal or further treatment. In the reactor, the organic components of the wastes are oxidized to carbon dioxide by reaction with the water and hydrogen peroxide. Nitrate contaminants also react with the organic material and are converted to nitrogen gas. Heteroatoms such as chlorine, sulfur, and phosphorus are oxidized and converted to acids or salts depending on the pH of the solution. Reaction temperatures and pressures are typically 550°C and 47 MPa psi. At temperatures above 500°C, reactions are rapid, and greater than 99% conversion can be achieved in seconds.

Figure 1. Schematic of hydrothermal processing

L. A. Worl
S. J. Buelow
L. Le
D. Padilla
J. Roberts
Los Alamos National Laboratory

Results

We have studied the reactions and treatment of a wide variety of organic wastes using non-radioactive simulants.[5] The results of these studies are given in Table 1. In general the total organic carbon (TOC) of the influent solutions was reduced to below detection limits in the hydrothermal processing effluents. In cases where chlorine heteroatoms were present, as in carbon tetrachloride, chloride is generated in the effluents and a titamnium liner was used to prevent corrosion of the stainless-steel reactor walls.

Table 1. Summary of waste treatment studies.

Waste Type	Composition	Reaction Conditions	Results*
Hydraulic jack oil	98% hydrocarbons, zinc, sulfur-related compounds, no silicone	550°C, 44 MPa, 60 seconds, 34 wt. % H_2O_2	25,000 ppm TOC reduced to < 5 ppm, effluent contained 300 ppm sulfate, pH~2.3
Vacuum pump oil	Olefin: $(CH_2)_n$ where $20<n<40$	550°C, 44 MPa, 60 seconds, 34 wt. % H_2O_2	40,000 ppm TOC reduced to < 5 ppm
Heavy mineral oil	Paraffin C_nH_{2n+2} where $n\sim34$	550°C, 44 MPa, 60 seconds, 34 wt. % H_2O_2	40,000 ppm TOC reduced to < 5 ppm
Tributyl phosphate	$(C_4H_9O)_3PO$	550°C, 44 MPa, 60 seconds, 34 wt. % H_2O_2	10,000 ppm TOC reduced < 5 ppm Effluent pH ~ 2
Diesel oil #2	Hydrocarbons: C_{15} to C_{25}	550°C, 44 MPa, 60 seconds, 34 wt. % H_2O_2	25,000 ppm TOC reduced to < 5 ppm
Toluene	C_7H_8	550°C, 44 MPa, 60 seconds, 34 wt. % H_2O_2	30,000 ppm TOC reduced to < 5 ppm
Carbon tetrachloride	CCl_4	450°C, 60 MPa, 80 seconds, titanium-lined reactor	CCl_4, 11,500 ppm reduced to < 0.5 ppm (>99.995% destruction)
Trichloroacetic acid	CCl_3COOH	500°C, 60 MPa, 30 seconds, titanium-lined reactor	CCl_3COOH, 1000 ppm reduced to < 1 ppm
Trichloroethylene	C_2Cl_3H	500°C, 60 MPa, 30 seconds, titanium-lined reactor	C_2Cl_3H, 1000 ppm reduced to < 1 ppm
1,1,1 Trichloroethane	CCl_3CH_3,	500°C, 60 MPa, 30 seconds, titanium-lined reactor	CCl_3CH_3, 1000 ppm reduced < 1 ppm
Cation exchange resin	$(C_8H_8SO_3)_n$, 50 - 100 mesh, 50 wt.% water	550°C, 44 MPa, 60 seconds, 34 wt. % H_2O_2	Effluent TOC < 1 ppm
General Lab Trash Mixture	18% cloth, 27.8% Tyvek, 18% plastic, and 18% rubber, 1/8" size	540°C, 40 MPa, 69 seconds, 30 wt. % H_2O_2	Effluent TOC < 5 ppm

* For all waste types, the TOC levels were below detection limit.

Experiments were also conducted with solid materials such as cation exchange resin and general lab trash. In these cases a viscosity enhancing agent was added to generate pumpable mixtures. A simulant of general lab trash consisted of 18% cloth, 27.8% paper, 18% tyvek, 18% plastic, and 18% rubber cryogenically shredded and passed through a screen. This mixture was slurried with water and reacted with hydrogen peroxide at 40 MPa and 540°C. In the gas phase, only oxygen and carbon dioxide were detected. The TOC in the effluent solution was below detection limits of 2 ppm. The solid Dowex 50Wx8 cation exchange resin was tested. The reaction at 550°C and 44 MPa for 1 minute produced carbon dioxide, water, and sulfuric acid. The results indicated that the global reaction is:
$(C_8H_8SO_3)_n + 21n\ H_2O_2 \longrightarrow 8n\ CO_2 + 25n\ H_2O + n\ H_2SO_4$.

In summary, recent experiments have shown that hydrothermal reactions can dissolve, oxidize, and separate metals, reformulate solids, and destroy organics and nitrates in radioactive simulants. Unlike traditional treatments that require the use of organic reagents, strong acids, or strong bases, hydrothermal processing uses oxidizers present in the wastes, such as nitrates, or simple oxidizers such as hydrogen peroxide. Hydrothermal oxidation is a treatment technology for the destruction of mixed wastes and TRU combustible wastes, yielding high cost savings and high return on investment. Testing of hazardous radioactive wastes at the Plutonium Facility are expected to begin in 1997.

References

1. R. Oldenborg, J. M. Robinson, S. J. Buelow, R. B. Dyer, G. Anderson, P. C. Dell'Orco, K. Funk, E. Wilmanns, and K. Knutsen, "Hydrothermal Processing of Inorganic Components of Hanford Tank Wastes," Los Alamos National Laboratory report LA-UR-94:3233 (1994).

2. P. C. Dell'Orco, B. R. Foy, E. G. Wilmanns, L. Le, J. Ely, K. Patterson, S. J. Buelow, "Hydrothermal Oxidation of Organic Compounds by Nitrate and Nitrite," *ACS Symposium Series* **179**, 608 (1995).

3. R. Oldenborg, S. J. Buelow, G. Anderson, G. Baca, R. Brewer, P. C. Dell'Orco, B. R. Foy, K. Knutsen, L. A. Le, R. McInroy, R. McFarland, S. Moore, J. M. Robinson, P. Rodgers, R. Shaw, and E. Wilmanns, "Evaluation of IPM Selection Criteria for Hydrothermal Processing," Los Alamos National Laboratory report LA-UR-94-1945 (1994).

4. B. R. Foy, P. C. Dell'Orco, E. Wilmanns, R. McInroy, J. Ely, J. M. Robinson, and S. J. Buelow, "Reduction of Nitrate and Nitrite Under Hydrothermal Conditions," in *Physical Chemistry of Aqueous Systems,* H. J. White Jr., J. V. Sengers, D. B. Neumann, and J. C. Bellows, Eds. (Begell House, New York, New York, 1995), pp. 602–609.

5. L. Le, S. J. Buelow, J. H. Roberts, L. A. Worl, D. D. Padilla, G. Baca, V. Contreras, M. Devolder, D. Harradine, D. Hill, R. Martinez, J. McFarlan, R. McFarlan, E. Martinez, M. Mitchell, C. Prenger, J. Roberts, M. Sedillo, K. Veirs, "Hydrothermal Processing Unit for Actinide Contaminated Combustible Wastes—FY96 94-1 R&D Final Report," Los Alamos National Laboratory report LA-UR-96:4730 (1996).

TRU Waste Segregation and Compaction

Background

The CST analytical chemistry groups at the Los Alamos National Laboratory have generated an average of 85 drums per year of transuranic (TRU, > 100 nCi/g) waste over the past 18 years. Out of these waste drums, 2/3 of them are potentially compactable TRU wastes. Currently these TRU wastes are not compacted due to the safeguards and security requirements. The instrumentation (Segmented Gamma Scans or SGS) that is used to perform non-destructive assay of the TRU waste drums cannot verify the plutonium content accurately if the wastes are compacted and materials are too dense in the drums. In 1996, analytical chemistry groups generated about 50 drums of compactable TRU waste. The average loading of these TRU waste drums was less than 0.5 g of plutonium. With an expected in increase nuclear material activities at LANL, the amount of compactable and non-compactable TRU wastes generated annually will at least double from the 1996 figures (100 drums versus 50 drums) in the next few years.

In the summer of 1996, the LANL Pollution Prevention Program Office provided the CST-8 Inorganic Elemental Analysis Group the funding to perform the TRU Waste Segregation and Compaction Project for the CMR building. The analytical chemistry groups generate approximately 80% of the total TRU waste in the CMR building. We are currently setting up a high purity germanium (HPGe) based detection system to quantitatively measure the radionuclides content in the TRU waste packages prior to placing them in the drum and compaction. With the proposed process, a sizable fraction of the low-level waste (< 100 nCi/g) can be segregated from currently declared TRU waste. An estimate of ~25% reduction of TRU waste will be achieved through this process.[1] The remaining actual TRU waste packages will be volume reduced by a factor of four through compaction.

Another benefit from the waste package measurement system will be determining whether changes in design or procedures for glovebox operations are effective at minimizing TRU waste generation. The system will also help the waste generators identify operations that routinely produce LLW as opposed to TRU waste. This will provide a strong technical basis for using knowledge of process (KOP) judgment to segregate and minimize TRU waste at the start of waste generation.

Current Practice

The compactible wastes generated from the CST analytical chemistry laboratories are collected in 4-L plastic bags and then placed directly into standard 55-gallon drums. The Pu content of these waste drums are measured by SGS at the CMR Waste Assay Facility. Then these drums are shipped to TA-54 for interim storage. Almost all the waste generated in the gloveboxes and some from the open-front boxes are disposed of as TRU wastes, but ~25% of it is actually below 100 nCi/g. The waste generators have little information available to declare their wastes as TRU or LLW and hesitate to segregate the wastes.

Proposed Segregation and Compaction of TRU Waste

The proposed process will help the waste generators to segregate their waste as TRU or LLW at the generation points. A HPGe gamma-ray based measurement

A. S. Wong
L. L. Jacobson
R. S. Marshall
A. P. Lovell
Los Alamos National Laboratory

system is used to determine the TRU concentration (nCi/g) in each 4-L waste package. If the waste packages have an activity level below 100 nCi/g, then they are segregated and disposed of as LLW in the standard 2 ft³ cardboard boxes for subsequent handling and disposal as LLW at TA-54. If the waste packages are TRU waste, then they are compacted with a compactor system housed in a glovebox. The expected compaction ratio is 4 to 1.

Before this process can be used for routine waste disposal, the measurement system must be certified to meet the safeguards requirements. We need to ensure the special nuclear material content are accurately stated, and the drums do not provide a diversion pathway.

Cost-Effectiveness Analysis

Based on a cost-effectiveness analysis,[2] the return of investment (ROI) for this project considering only local shipping, handling, and storage costs of the TRU waste is 68% for the first year (with initial investment of $271,000). After that, the expected LANL operational saving is $185,000 per year based on 50 drums of TRU wastes. If the WIPP costs (transportation, handling, and storage) are added to the analysis, an estimate of 257% ROI or $697,000 per year will be the savings to the taxpayers. The risks for the TRU waste compaction are small since the measurement method is based on proven technology, and the concept of trash compaction is a mature industrial process.

Summary

In this paper, the CST-8 waste package measurement system and TRU waste compaction system will be described, and the operational experiences will be presented. The proposed procedure expected to be implemented in the summer of 1997. We hope this process will be is part of the routine operation for waste disposal when the expected increase of weapon-related activities occurs at Los Alamos. Then the realized savings may approach $1 million per year from the 100+ waste drums generated per year.

References

1. A. S. Wong, T. Voss, R. S. Marshall, the final report to LANL Pollution Prevention Program Office on "Upstream Segregation of Low Level Waste and TRU Waste," CST-896-180 (September 30, 1996).

2. B. Drake, "TRU Waste Segregation and Compaction—Cost Effectiveness Analysis," a report to EM-P30 (August 20, 1996).

Isotopes/
Nuclear Fuels

Concept of Utilizing Weapon-Grade Plutonium in Channel-Type Water-Graphite Reactors RBMK-1000

This paper sets forth the concept of utilizing Russian weapon-grade plutonium Pu_{weap} in channel-type water-graphite reactors RBMK-1000. The main options considered include:

- utilization of Pu_{weap} in MOX fuel based on depleted uranium

- utilization of Pu_{weap} in MOX fuel based on recycling of the spent fuel from RBMK-1000 reactors

- utilization of Pu_{weap} in nonbreeding fuel

The paper focuses on the computational studies of physical and dynamic characteristics of RBMK-1000 reactors, with the core partially or fully charged with Pu_{weap}-based fuel. The studies involved optimization of the fuel composition, including use of burnable poison. The effect of the method and extent of reprocessing of the spent fuel from RBMK-1000 reactors on the characteristics of the fuel containing Pu_{weap} were analyzed.

The research was performed with the use of the three-dimensional neutronic-thermohydraulic code SADCO developed at RDIPE. Comprehensive neutronic calculations involved the WIMS-D4, MCU, and MCNP codes. The calculation results have found application in the ongoing preparation of the few-group library of macrocross-sections of the core cells. Primary emphasis in the studies on the physical and dynamic characteristics of the reactor was placed on the analysis of in-pile fuel behavior. The key parameters for the analysis include:

- maximum power of fuel assemblies
- fuel and cladding temperatures
- void effect of reactivity
- CPS rod worth
- subcriticality of the shutdown reactor

The paper discusses the possibilities for improving the RBMK-1000 fuel cycle by increasing fuel burnup and minimizing the size of the spent fuel storage. The conceptual study involved comparison of the RBMK-1000 fuel cycle characteristics for the following fuels:

- pre-Chernobyl fuel (UO_2, 2% enrichment)
- post-Chernobyl fuel (UO_2, 2.4% enrichment)
- experimental fuel with burnable poison ($UO_2 + Er_2O_3$, 2.6% enrichment)
- fuel made from depleted uranium and weapon-grade plutonium
- fuel made from weapon-grade plutonium and reprocessed spent fuel of RBMK-1000s

The paper dwells upon the costs and benefits of the use of weapon-grade plutonium fuel in RBMK-1000 reactors.

E. O. Adamov
V. K. Davidov
P. B. Kuznetsov
V. M. Panin
M. I. Rozhdestvenskyi
Yu. M. Cherkashov

Research and Development Institute of Power Engineering (RDIPE), Russia

Fabrication of CANDU MOX Fuel at AECL

F. C. Dimayuga
Atomic Energy of Canada Limited, Canada

Atomic Energy of Canada Limited's mixed-oxide (MOX) fuel fabrication activities are conducted in the Recycle Fuel Fabrication Laboratories (RFFL) at the Chalk River Laboratories (CRL). The RFFL facility is designed to produce experimental quantities of CANDU MOX fuel for reactor physics tests or demonstration irradiations. From 1979 to 1987, several fabrication campaigns were run in the RFFL, producing various quanitities of fuel with different compositions. About 150 bundles, containing over three tonnes of MOX, were fabricated in the RFFL before operations in the facility were suspended. In August 1996, a project to rehabilitate and recommission the RFFL was completed, and MOX operations were resumed. An up-to-date description of the facility, including the fabrication process and the associated equipment, as well as the upgraded safety system and laboratory services, will be presented.

The first fabrication campaign after rehabilitation of the RFFL consisted of the production of thirty-seven 37-element $(U,Pu)O_2$ bundles destined for void reactivity measurements in the ZED-2 reactor at CRL. A summary of this recently concluded fabrication campaign will be given. The fabrication process used to manufacture the fuel from the starting powders to the finished elements and bundles will be presented. Fabrication data including production throughputs and fuel characterization results will be discussed.

A brief overview of AECL's MOX fuel irradiation program is also given in this paper. Post-irradiation examination results of two major irradiation experiments involving several $(U,Pu)O_2$ fuel bundles are highlighted. One experiment involved bundles irradiated to burnups ranging from 18 to 49 GWd/te H.E. in the Nuclear Power Demonstrations (NPD) reactor. The other experiment consisted of several $(U,Pu)O_2$ bundles irradiated to burnups of up to 21 GWd/te H.E. in the National Research Universal (NRU) reactor.

The paper also outlines the status of current MOX fuel irradiation tests, including the irradiation of various $(U,Pu)O_2$ and $(Th,Pu)O_2$ bundles.

Automation in Plutonium Processing Environments

Introduction

At Los Alamos National Laboratory's (LANL's) Plutonium Facility, one of the primary missions is to process radioactive legacy waste materials into stable forms that can be safely stored. Historically, plutonium operations have been performed by manually processing these materials through various stations or locations in gloveboxes specifically designed for manual operations. Reduction of exposure to the operations staff performing these processes is typically accomplished by minimizing attended processing times and maximizing distance between the operator and the process. With the Department of Energy mandating ALARA as the determining guideline for all future processing exposures, the Nuclear Weapons Complex (NWC) has been forced to address exposures to operators while processing. Automation has been identified as a solution to the issue identified above; however, the glovebox environment that supports plutonium processing more often than not precludes the use of standard industrial solutions. This paper will outline the approach for implementing automated systems into plutonium processing that has been developed by LANL's Nuclear Materials Technology Division and Sandia National Laboratories' (SNL) Intelligent Systems and Robotics Center.

The characteristics that typically preclude the use of automation range from physical constraints dictated by the glovebox environment to costs associated with modification to infrastructure already in place in the plutonium processing facility. The glovebox environment has typically been the major constraint. Here, the introduction of automation into plutonium processing faces space utilization constraints, range of motion issues, weight and seismic constraints, and approval of penetrations into the glovebox. All of these issues are driven by safety analysis and review. Also, of major concern is the issue of Reliability, Availability, and Maintainability (RAM) of automation in the environment.

Environments which are normally found in plutonium processing include high humidity combined with corrosives such as hydrochloric acid, ionizing radiation and particulate contamination in the form of radioactive materials. Determining how automation will respond in these environments and assessing the effectiveness of implementing that automation into the plutonium processing environment requires the development of a knowledge/experiential database in automation RAM that does not exist. To this end LANL and SNL have agreed to pursue automation in a process identified as the Strategic Implementation of Automation Into Plutonium Processing Lines.

Description of Work

Strategic Implementation of Automation Into Plutonium Processing Lines is a structured approach to automation. The outline below identifies the process and the data that will be collected. These implementation steps are being used to bring automation to the processing of plutonium and other unique, high-exposure, nuclear materials. The information and experience gained while prototyping systems at LANL will be combined with existing experience to begin creating the experiential database.

 The following outline identifies the implementation process:

Plutonium Process Review: In this phase of the project, the candidate processes will be screened for potential automation success. Screening criteria will include

M. Dinehart
Los Alamos National Laboratory

G. R. McKee
Sandia National Laboratories

M. Evans
Los Alamos National Laboratory

historical data on radiation exposure, waste stream identification, waste generation, manual processing effectivity; and process environment suitability. In some cases, the processes are selected by the plutonium facilities staff and passed to the next phase of the implementation process because they have been identified as high-exposure processes in need of automation.

Evaluation of Process for Automation: When the candidate processes have been identified and accepted as potential candidates, the process will then be evaluated in terms of potential success. The success criteria include processing glovebox size and location and matching robotic capabilities to process requirements. Service and maintainability of the automation hardware and off normal processes that require manual operations to be performed will be reviewed to assure that they are capable of being performed within the existing infrastructure.

Simulation of Automated Process: Processes that are deemed to be solid candidates for automation will be simulated using software capabilities developed and used by SNL. These simulations will determine if the current processing environments will support the proposed automation. Both automated and manual processes will be simulated to assure the successful implementation of automation.

Radiation Exposure Analysis if Applicable: In many cases, a radiation exposure analysis will be performed to determine what exposures are present for both the automated and the manual processes. The radiation exposure analysis is performed on the simulation that was generated in the previous step. This simulation tool was developed at SNL and is used extensively to determine whole body and extremity exposures to staff performing the nuclear processes such as pit processing and plutonium materials handling. It generates exposure data based on time and distances from point sources (i.e., buttons, neutron sources, and cans of materials) as well as exposure maps of the work cell.

Design of Automation for the Process: In this step, the automation for the process is finalized and documented. Hardware selection will be based on the existing experience database. Design requirement documents for hardware and control software are generated and approved.

Implement Automation: The hardware is realized and installed in this phase of the implementation plan. The initial testing and evaluation is performed and documented into the experiential database. The system is installed in a cold environment for this testing and then transferred to the hot site customer for final installation.

Evaluate Automation and Incorporate into Experience Data: The evaluation of the full automation project will be performed at this point for archiving into the experiential database. The development of accurate data for this is imperative, and this phase of the implementation process is the most critical to future success.

Results

Currently, three automated systems have been identified for delivery into the plutonium processing facility at LANL. The first program is delivering an automated plutonium container packaging system into the ARIES Demonstration Line in FY 1998, the second program starts in FY 1998 and will deliver a Neutron Source Unpacking System into building PF-4 in mid FY 1999 and the third program will deliver an Automated Neutron Source Recovery process in FY 1999. It is anticipated that the experiential database will begin being assembled and available for use in the program beginning in FY 1999.

The International Science and Technology Center (ISTC) and the ISTC Projects Related to Plutonium Problems

The ISTC—History and State-of-the-Art Perspectives

A. Gerard
L. V. Tocheniy
International Science and Technology Center (ISTC), Russia

The ISTC is operating under the auspices of an intergovernmental agreement between the Russian Federation, European Union, Japan, and the United States. The Center started operation March 2, 1994. Since then, Finland and Sweden have acceded as Funding Parties. CIS respresentation has expanded to join Georgia, Belarus, Armenia, Kazakhstan, and Kyrgzia.

All work of the ISTC is aimed at the following goals defined in the ISTC Agreement:

- To give CIS weapons scientists, particularly those who possess knowledge and skills related to weapons of mass destruction and their delivery systems, the opportunities to redirect their talents to peaceful activities

- To contribute to solving national and international technical problems

- To support the transition to market-based economies

- To support basic and applied research

- To help integrate CIS weapons scientists into the international scientific community

The ISTC engages in a variety of activities aimed at meeting these goals:[1]

- Providing support to scientific research and development

- Stimulating collaboration of CIS institutes with foreign institutes, industries and universities. The parties make great efforts to seek foreign partners that are interested in the proposed projects, and to support meeting of the project recipients with foreign collaborators and their participation in scientific conferences

- Organizing of the ISTC Seminar Program on subjects of national and international interest

The projects may be funded both through governmental funds of the Funding Parties specified for the ISTC, and by organizations, nominated as Funding Partners of ISTC. According to ISTC Status, approved by appropriate national organizations, funds used within the ISTC projects are exempt from CIS taxes. Projects range from solving environmental problems related to nuclear industries and nuclear safety to the development of new vaccines for contagious diseases.

As of March 1997, above 1100 proposals had been submitted to the Center, of which 391 approved for funding, for a total value of approximately US$136 million. The number of scientists and engineers participating in the projects number more than 17,100.

Plutonium Problems in the ISTC Projects

A study of possible technical approaches to nuclear fuel cycles and technologies for utilization or for annihilation of plutonium (both weapon-grade and power one) is being carried out and suggested within a set of more than 30 of ISTC's

projects and proposals. One group of projects has a particularly close relationship because the projects are all dealing with the use of plutonium as fuel for civil power nuclear reactors, and so they focus on specific reactor aspects. The other group attacks a problem with an alternative approach on the basis of using sub-critical nuclear systems (blankets) driven by an accelerator of charged particles.

ISTC favors the coordination of the projects flow through participation at the joint project workshops, seminars, and so on.

Reactor Approach

Project #369 would contribute to general stagies for the use of weapon pluto-nium in Russia. It relates to studies of the technological and economical feasibility of the use of plutonium in some definite scenaria of fuel cycles based on both fast and thermal reactors and both existing and developing fuel manufacture tech-nologies.

Neutronics Reactor Concepts and Nuclear Safety

Two Projects (#116 and #271) have as their objective the development of methods, codes, data, and an experimental base for theoretical and experimental investiga-tions of neutronics, physical characteristics, and nuclear safety parameters of LWR (VVER) cores loaded by Pu-content fresh fuel (#271) and fuel corresponding to the mid-burnup state (#116).

Experimental, engineering, and analytical study of nuclear safety parameters of advanced sodium-cooled fast reactors with renovated oxide, carbide, nitride, and metallic Pu-content fuels has been developed in the framework of Project #220. In-core tests and continuation of these investigations are planned within the next stage of activity, Project #650.

The conceputal designs of deterministically safe power fast reactor have been suggested for burning Pu and minor actinides, computer and experimental analy-sis of reactor parameters, and self-regulating features of reactors cooled by helium (#269) and heavy-metal (lead, #071).

The options of uranium-thorium fuel cycles with specific branches for weapon plutonium burning are in Proposals #313 and #723.

Experimental modeling of thermo-hydraulics and study of some other extremely high physical parameters of a plutonium burner-reactor with melted-fuel core are under way in Project #134.

Neutron cross sections and data for actinides which are very important for pluto-nium fuel cycle are being updated in the experiments of Projects #304 and #305.

Fuels and Fuel Elements

Project #534 plans to update analytically and experimentally parameters of MOX fuels (mechanica, therma, radiation, and so on) to verify models of fuel elements and to predict their behavior under working loads.

Project #290 would develop and test at a laboratory level a new compact and low dusty technology to convert metallic plutonium to MOX form.

Projects #173 and #721 deal with the development of a technology, both non-irradiation and in-core tests, of new U and Pu fuel elements for LWR (VVER)-type reactors based on metallic or silicide dispersion fuel for extremely high burnup—up to 150,000 MW-d/tHM.

Project #272's goal is to develop a concept of nuclear reactor and fuel cycle for plutonium and actinides transmutation based on vibro-packed plutonium fuel.

Methods for extraction of fission products from plutonium oxide fuel are developed by Project #279.

Project #565 plans to investigate properties of U-Pu-Zr metal fuel and fuel elements for reactors when steady and non-stationary load take place.

Environment

Project #273 is the result of an investigation of the radioactivity of MOX fuel. It will define data necessary to examine the out of core impact of MOX on the environment during fuel fabrication and reprocessing.

Project #281's goal is to recommend approaches to improve the reprocessing technologies and to minimize technological radioactive wastes after reprocessing of spent nuclear fuel.

Project #330 develops a technology for removing plutonium and other transuranium elements from silt in radioactive waste storage ponds.

Decomissioning

The radioactive parameters of some components of the Russian Pu-production reactors after their decommissioning will be measured and processed (Project #561). Project #779 will develop the reprocessing technology for sodium in the primary loop of decommissioned BR-10 fast reactor.

Proposal #538 suggests to develop technology for compacting the non-reprocessed part of spent fuel from different types of reactors for long-term environmentally safe storage.

Storage

For a feasibility study of methods and approaches to store large masses of weapon-grade plutonium and uranium was developed in Project #332/1 and will continue in #332/2.

Others

The study of the behavior of war-head plutonium after a submarine accident in a water media may be carried out within Project #859. Development of a Training center for the plutonium research reactor in NIIAR is planned by Project #838.

Acclerator-Driven Subcrital Blanket Approach

General aspects of the blanket, target, and fuel cycle for incineration of plutonium, actinides, and some fission products has been developed mainly by Project #017. The Project has been competed and the results have been presented at an international conference (Sweden, June 1996). New proposals of this kind have been submitted to ISTC, including #559–design and tests of a lead-bismuth target; #442–reconstruction of an experimental heavy water reactor into the subcritical unit and the study of control system; #698, #747, #A-088–development of molten salt technology; and also #B-70–modeling of a target-blanket system using a neutron generator as a neutron source.

Reference

1.   ISTC Annual Reports - ISTC, Moscow, Russia (1994, 1995).

Conception of a VVER Reactors with Coated Particles

Introduction

The accident at the Chernobyl Nuclear Power Plant has sharply reduced the competitiveness of nuclear power. The construction of new NPPs was stopped. This process coincides with the process in the U.S.A after the Three-Mile Island accident.

Is it possible to rehabilitate nuclear power? The main reason for the modern NPP instability to severe accidents is the use of zirconium alloys for fuel rods in VVER reactor core. Zirconium alloys were chosen as a material for fuel cladding in the 1950s basically because of their good neutronic characteristics. Zirconium alloys are quite corrosion-stable in normal operation (300 to 350°C), and they are a rather bad protective barrier for radioactivity, accumulated in the fuel rods in emergency operation. They are quickly destroyed with the release of all accumulated activity even during short-term heating up to higher than 400°C. Besides, at the temperature of 800°C the steam-zirconium reaction begins with the formation of hydrogen and an intensive heating rate owing to chemical reactions. The hydrogen release creates the danger of powerful explosions, which almost destroyed the containment at the Three-Mile Island NPP.

So far, to provide safety the NPP designers have created repeatedly duplicated systems for reliable cooling of the reactor core and systems for localization of accident consequences. All this was done because the first barrier for radioactivity is very unstable to the action of high temperature. The safety systems and containment for traditional VVER provide safety on the probability level, and the efficiency of these safety system has to be proved with the probability methods. However, all severe accidents passed under the scripts not foreseen by the designs. For instance, at Three-Mile Island NPP there was no break of a large-diameter pipeline or a blackout, but the consequences have appeared worse than in a design-basis accident. Chernobyl-type reactors were evaluated by designers rather steadily for severe accidents. The long-term experience of channel-type reactor operation for plutonium fabrication testified to that.

Therefore, the probability methods for safety valuations cannot provide the procedure for severe accidents beyond the design basis. Also, there is a desire to approach NPP safety to the level, when the reactivity leakage is not possible, i.e., at which an "all-forgiving" (error of staff, designers, assemblers, and etc.) reactor design is achieved .

The ceramic cladding technologies have been developed in nuclear engineering.[1] These claddings effectively keep accumulated activity at a temperature of about 2000°C and even higher.[2] Such technology was applied in gas-cooled high-temperature reactors, successfully maintained in the U.S.A, France, and England. In Russia, the construction of such reactors was planned for power technology purposes.[3,4]

It is interesting to consider the combination of high-temperature reactor technology and technology of VVER. The application of fuel in the form of coated particles (CP) will considerably increase safety, first of all, at the expense of stability to severe accidents of the Chernobyl and Three-Mile Island type accidents. It is the ceramic cladding of CP that will ensure that accumulated activity practically at any accidents is held, including for instant vessel and containment failure. Such failures, for example for a VVER, are not considered even as hypothetical.

E. I. Grishanin
L. N. Phalkovsky
All-Russia Nuclear Power Engineering Research and Development Institute (VNIIAM), Russia

In Russia preliminary studies are conducted. They show that it is possible to use the CP without change of reactor design, including their application in working NPPs with VVER.[5] It is especially important that neutronic and thermal-hydraulic characteristics of the reactor core are quite acceptable and on some parameters they are better than for traditional reactor cores.

This technical decision will give the greatest effect for out-of-date NPPs, which do not meet the requirements of the current normative. The safety level in such plants with CP will be higher than at current NPPs with powerful safety systems.

The analysis of VVER with CP has shown that the activity release does not occur even at the heaviest accident, including reactor vessel destruction, since their temperature does not exceed 1500 to 2000°C. The relative radioactivity release from the CP cannot exceed 10^{-5}.

The CP fuel assembly has the same overall dimension as a fuel assembly VVER, including design of the tail and the top. The CP is directly cooled by water.

Design Description

The VVER-1000 design with CP does not differ from serial-type reactor design except for a CP-fuel assembly design. The CP fuel assembly has the same overall dimension as fuel assembly VVER, including design of the top and the tail. The CP are located in the CP-layer and directly cooled by water. The CP-layer are located between the inlet and outlet collectors. The gap between the neighboring fuel assembly is the outlet collector. The inlet collector is the conical tube.

Inlet and outlet collectors have a Z-shape and a passing section changing along the height. Accordingly, the vertical coolant rate is constant in the collectors. The coolant velocity distribution is approximately uniform at the entrance of CP layer (in lateral direction) along the height of the fuel assembly. More precise coolant distribution along the height of the CP layer is achieved by the perforation densities and according to the heating rate shape.

The CP consists of UO_2-pellets with a spherical shape (diameter 1160 mkm) and multi-layer clad. The CP has the first layer made of pyrocarbone (thickness 70 mkm, density 1 g/cm³), second layer pyrocarbone (thickness 50 mkm, density 1.8 g/cm³). For a water cooled reactor, the outer corrosion-resistant layer is made of SiC (thickness 50 mkm).

It is supposed to use stainless steel 12 by 18 H10 T as a construction material for CP-fuel assembly at the present stage of development. Use of other materials for CP clads (ceramics, composite materials) is possible and can be considered in further development. These materials should save serviceability at heating higher than 1500°C.

Neutronic and Thermal-Hydraulic Characteristics

The volumetric composition of the reactor core with CP does not essentially differ from the traditional one (Tables 1 and 2). The main differences of the new reactor core are as follows:

• the fuel temperature is close to the coolant temperature.

Name	Density	VVER-1000	VVER with CP
1. Uranium dioxide	10.0	28.2	26.3
2. Water	0.72	55.5	52.3
3. Zr-1Nb	6.4	11,2	–
4. Steel	7.9	2,4	2.3
5. Graphite	1.6	–	18.0
6. SiC	3.5	–	1.1
7. He	–	2.7	–

Table 1. Volumetric composition of the core, %.

Name	VVER-1000	VVER with CP
1. Diameter of CP core, cm	0.76 (cylinder)	0.116
2. Thickness of clad, cm	0.65	0.017
3. Temperature of water, °C	300	300
4. Average temperature of fuel, °C	850	350
5. Type of fuel lattice	triangular with pitch 12.75 mm	free CP filling with porosity 35%

Table 2. Reactor core characteristics.

- The neutronic characteristics of a VVER with CP are not worse in comparison with these characteristics of traditional VVER-1000, and some parameters can be essentially better (reactivity coefficients, reactivity margin for burnup).

- The fuel temperature effect is ten times less than this effect in the traditional VVER. Therefore, the water temperature effect and the reactivity density effect will be stabilizing factors. These effects will be realized reasonably quickly because the time of thermal delay in CP is 0.03 s. The time of thermal delay for serial-type VVER is 5 sec. As a result of this property the chain reaction can be stopped even without scram. It is possible to stop the chain reaction by the water temperature increase and the reduction of its density.

Such opportunity was realized for high-temperature reactors. The reactor shut-down could be realized only by cutting off the blowers. The reactors are shut down at the expense of the temperature effect of the graphite moderator, and further, by falling in the "iodine pit." The same effect can take place for the VVER reactor core with CP.

The main losses of pressure in CP-fuel assembly are stipulated by the resistance of the collectors. Because resistance of the CP layer is rather small even at a diameter ≈ 1 mm. The limiting factor in choosing the geometrical sizes of collectors is the maximum velocity allowable from the point of view of erosion wear and accepted equal to 15 m/s. The pressure losses in the CP-fuel assembly are accepted equal to 0.15 MPa.

Conclusion

The neutron and thermal-hydraulic caracteristics of a VVER with CP are not worse than that of a traditional VVER reactor.

The application of the CP fuel assembly in the VVER allows development of an enhanced safety reactor, so-called an "all-forgiving" reactor. It is a necessary condition for rehabilitation of nuclear power. Therefore, the VVER with CP is our hope.

References

1. D. Bedening, *High Temperature Gas Cooled Reactors*, M. Atomisdat (1975). (Russian)

2. Y. Dergaltsev, I. Mosevitsky, N. Ponomarev-Stepnoy, A. Smirnov et al., "Experimental Investigation for Coolant Technology and Fuel Elements of HTGR on Helium Loop PG-100 and Ampoule Channels" in *Atomic-Hydrogen Energy and Technology.* M. Energoatomizdat, (1983), Vol. 5, pp. 185–193. (Russian)

3. A. Chernikov, Y. Koshelev, Z. Shokina, "Manufacturing and Facility Control of Microfuel Particals, Fuel Elements and Fuel Assemblies for HTGR," *Atomic-Hydrogen Energy and Technology,* M. Atomizdat, (1979), Vol. 2, pp. 160–177. (Russian)

4. A. Chernikov, V. Kolesov, L. Permyakov, Y. Koshelev, L. Mihailichenko, "Design and Main Parameters of HTGR Fuel Elements," *Atomic-Hydrogen Energy and Technology,* M. Atomizdat, (1979), Vol. 2, pp. 207-213. (Russian)

5. E. Grishanin, S. Vigovski, L. Phalkovski, "Concept of Highly Safe Pressure-Vessel Water-Cooled Reactor with Spherical Fuel Elements," in *The Raw Material and Waste Activity Balance in the Projected Nuclear Power of Russia*, VNIIAM report N 6496. (Russian)

Steam-Water Cooled Power Plant
Using Weapons Plutonium and Actinides

A major goal of the nuclear power engineering of the near future is the disposal of weapons plutonium and actinides of radioactive waste from nuclear power plants.

Two proposals are being made:

* using plutonium for fueling PWR-type reactors

* burning up actinides in fast sodium-cooled reactors

This work presents design and performances of the reactor cooled with steam-water mixture (SWPR), in which weapons plutonium and actinides can be used as effectively as in fast reactors.

Development of SWPR was one of the areas of upgrading reactors in the USSR in the 1980s. It has a breeding ratio of more than 1, the efficiency of 49%, and the capital costs are 15% lower those for a nuclear power plant with a VVER-1000 reactor.

The SWPR concept is based on cooling the core with a steam-water mixture of 16MPa pr essure and an inlet mass steam quality of 35%. At the reactor outlet, the overheated steam has the temperature 400°C. Cooling of the core due to evaporation of water in the steam-water mixture at constant and relatively low temperature equal to the saturation temperature requires several times lower power for pumping as compared with pressurized water or dry steam. The temperature of fuel assembly claddings with this method of cooling does not exceed 450°C, which is 250°C lower than in sodium-cooled reactors. To preclude a dry-out in fuel elements, steam-water mixture with above-criticality mass steam quality is delivered to the core inlet. For the pressure of 16 MPa, the inlet steam quality is assumed to be 35%.

The SWPR design is identical to the design of a BWR-type boiling reactor with built-in jet pumps, but the vessel dimensions are the same as in the Russian reactor VVER-1000.

The feedwater at a pressure of 18 MPa is delivered from the high-pressure heater to the inlet of jet steam compressors which suck in part of the overheated steam from the core outlet and form a steam-water mixture with mass steam quality of 35% at a pressure of 16.5 MPa.

This mixture is fed to the core inlet, the water in the mixture evaporates and the steam is overheated to 400°C and directed to jet compressors (1/3 of the flow) and to the turbine (2/3 of the flow). Unlike BWR, recirculation of steam, rather than of water occurs within the SWPR reactor vessel. The fuel elements of SWPR are made of pipes of 6.8 by 0.4 mm in diameter with pellets of MOX fuel (weapons plutonium, depleted uranium, and actinides). The material of the fuel element claddings is radiation-resistant steel of ferrite-martensite class 450. It is produced by the Russian industry for the core of the BN-600 reactor of the 3-d unit of the Beloyarsk NPP.

The neutron and physical characteristics of SWPR are determined by the spectrum of neutrons which is very close to the spectrum of fast reactors. The dependence of

E. I. Grishanin
P. N. Alexeyev
P. A. Fomichenko
L. N. Phalkovsky
S. A. Subbotin
All-Russia Nuclear Power Engineering Reasearch and Development Institute (VNIIAM)

reactivity on coolant density is indicated in Table 1: a very small reactivity margin with respect to burnup, no xenon poisoning, and deep subcriticality during filling the core with water without boric acid—all this ensures a high safety standard as compared with PWR and BWR-type reactors. All known types of reactors have a large reactivity margin in cold conditions and active methods such as using shim rods, boric acid solution, and other ways are required to prevent reactivity to be realized. The SWPR is the only exception: it has no reactivity margin in the cold condition. This is achieved by addition of gadolinium oxide to the fuel.

Density kg/ m^3	0	25	50	80	130	170	260	300
Reactivity %	–0.35	–0.1	0	0	0	–0.1	–0.5	–0.7

During development of SWPR in Russia, a large volume of experimental work has been completed including the studies of:

• heat exchange and hydraulic performances of an electrically heated model of a fuel assembly at nominal parameters of the coolant and specific heat flux on the surface of fuel element simulators more than 1.5 MW/m²

• characteristics of jet steam compressors

• corrosion resistance of the materials in the steam-water environment

• heat-hydraulic stability of the steam-water mixture in parallel channels

SWPR development will rely on a wealth of the experience of design and operation of VVER-1000 (Table 2) and BWR-type reactors and BN-600 reactor with respect to fuel elements and the core.

**Table 2. Key
performances of
SWPR as compared
with the Russian
reactor VVER-1000.**

Performance	VVER-1000	SWPR
Electric power, MW	1000	1000
Heat output , MW	3000	2500
Coolant parameters:		
Pressure, MPa	16	16
Inlet/outlet temperature, °C	289/322	347/400
Inlet mass steam quality, %	–	35
Coolant flow rate, kg/s	16000	3500
Core characteristics:		
Fuel	UO$_2$	Pu$_2$+ actinides oxides
Core height/diameter, cm	350 / 312	150 / 270
Fuel element diameter, mm	9.1×0.65	6.8×0.4
Fuel element trigonal lattice pitch, mm	12.75	7.8
Linear power (max), kWt/m	45	21
Max. temperature of fuel element cladding, °C	350	450
Mean fuel enrichment, %	4.4	12
Max. burnup depth	4.0	10
Capital costs, %	100	80

The performances of SWPR suggest that this reactor can become a basis for upgrading PWR and BWR with the idea to improve their performances and effectively use plutonium and actinides.

The Role of Chemical Reactions in the Chernobyl Accident

E. I. Grishanin
O. V. Konovalova
L. N. Phalkovsky
All-Russia Nuclear Power Engineering Research and Development Institute (VNIIAM), Russia

In the literature, much attention has been given to the first phase of the accident at the 4-th unit of the Chernobyl nuclear power plant–the uncontrollable power rise in the reactor. Yet, the processes occurring after reaching 100 rated powers have not received due consideration.

The study of the damaged 4-th unit with the use of boreholes has revealed astonishing facts, namely: there is no graphite stack and fuel in the reactor, and concrete structures from the wrecked drum-separator compartment can be seen without any indications of high-temperature effects, whereas compartments under the reactor contain not more than 10% of fuel in the form of lava-type fuel-containing masses.

Also, no adequate explanation has been given to some documented features of the accident such as a comparative "dormancy" during 20 hours after the explosion; a sharp increase in the radioactivity release after 20 hours, the intense graphite burning, and an increase in the radioactivity release from May 1 to 6 by a factor of 6; a decrease in the radioactivity release on May 6 by millions of times; and a repeated increase in the neutron flux in the sarcophagus: detection of short-lived fission products up to September 1986.

The present work aims to explain events at the 4-th unit of the Chernobyl NPP with consideration of chemical reactions. In the course of the reactor runaway the coolant evaporated and was overheated, the temperature of the fuel elements grew to 1000°C and a vigorous steam-zirconium reaction was initiated with the formation of hydrogen.

As the reactor power continued to grow, the temperature of the overheated steam reached 1000°C and the high-pressure pipes lost their integrity. The steam and hydrogen began to enter the graphite stack in which the endothermic reaction occurred $H_2O + C = CO + H_2$.

At that time the reactor was working as a gigantic gas- generator with a nuclear heat source. When the excessive pressure in the graphite stack became more than 3.5 kg/cm,^{2} the reactor vessel collapsed. This was the first (steam) explosion resulting in a release of part of the fuel and graphite. Hydrogen and CO in the amount of 1000 m^3 entered the central hall from the reactor and on mixing with the air, they formed an explosive mixture. The mixture ignited from the graphite pieces having the temperature 500°C.

This was the second (volume-type) explosion which has led to a distinctive destruction of the reactor premises.

The reactor was accelerating rather slowly (as compared to the nuclear bomb) and that is why the first explosion destroyed only part of the core and the part remaining in the reactor became subcritical. By our estimation, not less than 50% of the fuel and graphite remained in the reactor. Prior to the explosion the reactor was in the state of xenon poisoning and 20 hours after the explosion the maximum excessive reactivity of 2.9% was released in the core.

However, as soon as 10 hours after the explosion the reactor was operating again. The power level was determined by the excessive reactivity and the air flow through the damaged reactor lines due to natural convection. By our estimates, the air inflow to the reactor was 40 kg/s.

The reactor was operating in cycles with pauses of 20 hours between the cycles, which can be explained by the fact that xenon and iodine were building up during the work and as a result the power fell to zero. In this period the following reactions occurred:

$$2C + O_2 = 2CO \text{ and } 2CO + UO_2 = U + 2CO_2$$

(the direct contact of fuel and graphite was inhibited by the high-pressure pipes and fuel elements).

It should be emphasized that the remaining heat of the core is not enough for the above chemical reactions, primarily endothermic, to happen. After complete oxidation and destruction of the zirconium pipes and claddings in the graphite channel itself, the pellets of UO_2 and fragments of ZrO_2 occurred as free haphazard fills (occurred in a haphazard fashion).

This change which, by our estimation, happened approximately on April 30 brought about a new increase in the reactivity, fuel temperature, and a sharp increase in the radioactivity release. In fact, on reaching the rated power the reactor worked as a blast furnace melting metallic uranium, plutonium, and fission products.

The reduced U (melting temperature 1100°C) was running off from the graphite stack to the lower steel coolant delivery pipes and solidified there (that is where it should be sought). When the process of U reduction was over, the fission chain reaction stopped and the activity release decreased first by a factor of 1000 and then after the graphite finished burning by a million times.

The metallic plutonium at the temperature of about 1100°C was sublimated and that is why it is not to be found in the lava-type fuel-containing masses.

In the south-east sector of the reactor the first explosion damaged the reactor support and the coolant delivery lines. Therefore, the reduced U was running off to the lower compartments where it interacted with concrete at the temperature of 1100°C and formed lava-type fuel-containing masses. The amount of U in these masses correlates with its content in the overheated part of the core destroyed by the first explosion. Our estimates of the time length of the processes occurring after the explosion are in good agreement with the actual data on the duration of the process.

Conclusions:

1. Chemical reactions played a major role during the disaster at the 4-th unit of the Chernobyl NPP in the pre-explosion, explosion, and after-explosion phases.

2. The type of destruction of the reactor hall indicates that there was a volume explosion of the mixture of the air with hydrogen and carbon monoxide.

3. After the explosion, not less than 50% of the fuel and graphite remained in the reactor.

4. The decay of xenon and iodine led to resumption of the fission chain reaction, from which the heat went for the reduction of uranium oxide and plutonium oxide.

5. The metallic uranium occurred in the lower metal structures feeding water to the reactor, whereas the metallic plutonium was sublimated leading to the contamination of the 30-km zone around the Chernobyl NPP.

The Application of Plasma-Chemical Technology for the Manufacture of Homogeneous Oxide Mixture Aimed at the Production of Uranium-Plutonium Fuel

G. P. Khandorin
N. V. Dedov
E. N. Maly
V. A. Matyukha
V. G. Sapozhnikov
Siberian Group of Chemical Enterprises, Russia

At the Siberian Group of Chemical Enterprises, plasma-chemical technology has been developed for the one-step manufacture of uranium and plutonium or their homogenous mixtures of different compositions from oxides solutions for nuclear fuel preparation.

The advantage of this approach is the high output of the equipment, reduction of the technology line, no precipitation operations and no usage of reactants-precipitators, absence of waste solutions, high chemical activity of obtained materials, formation of solid solutions in plasma-chemical reactor as well as improvement of labor conditions.

The technological line includes solution preparation, plasma-chemical denitration, oxide isolation, and gas purification.[1]

Theoretical and design development has been performed for special equipment of nuclear safe geometry, which is able to operate effectively for a long time at plasma temperature.

High-frequency inductive plasmatrons with metal discharge chambers and a capacity of 60 kW have been developed for plasma generation.

The effect of geometric sizes and construction features of plasmatrons on their operation reliability and energy effectiveness has been studied. At inner and outer discharge chamber diameters of 0.06 m and 0.074 m correspondingly and power transmitted by a generator to plasmatron of 25 to 50 kW and flow of heat-transport gas of $(2 \text{ to } 5) \times 10^{-3}$ kg/s, the coefficient of energy transmission from inductor to discharge is 0.92 to 0.95 and heat efficiency is 80%. Parameters of heat-transport gas are the following:

- enthalpy is up to $(16 \text{ to } 17) \times 10^{-4}$ kJ/kg
- mass-mean temperature is 5500 to 6000 K
- overall length of the plasmatron is 0.4 m, mass is 4.5 kg

While developing units operationally, the circuits and devices for its (plasmatron) remote run have been developed. Discharge initiation and plasmatron brining up to design operational conditions took not more than 5 sec.

On the results of math processing of experimental data on plasmatron energetic efficiency, the construction of plasma-chemical reactor has been developed, where solutions are decomposed to oxides. The construction has been designed and developed for a classic single-pass pattern. What were studied are reactor channel configuration, point and direction of sprayed solution input, and pneumatic sprayers quantity.

The plasma-chemical reactor is recommended for operation on plutonium-containing solutions and for industrial (commercial) implementation, where thermal resistance of materials is provided and the possibility of condensed substances sediment on the walls of the blending chamber is excluded.

To analyze potential reactor possibilities and to find out possible disadvantages, the methods of math simulation were applied to modeling the disperse particles behavior in high-temperature gas flows. Solving differential and algebraic equations characterizing movement and heat mass exchange of a polydisperse liquid drop system in high-temperature gas flow (with consideration of empirical

relations and distribution function of liquid drops in drop size in a spray plume, and other calculations), allowed the discovery of optimal constructive performances of a plasma-chemical reactor and determined that the temperature of steam-gas flow in the area of dispersed solution present before its absolute vaporation changes within the range of 1200 to 1800 K, moreover vaporation area does not exceed 0.7 m length. Design (estimated) time of the denitration process is 0.05-0.1 sec. Reactor performances are as follows:

- solution flow—up to 5.6×10^{-3} kg/s;
- heat efficiency—80% K;
- maximum inner diameter—0.12 m;
- overall length—0.83 m, mass—25 kg

Design data are confirmed by the absence of fused particles and aggregates in powders as well as high specific surface and chemical activity.

Development of intensive processes of thermal heterogeneous-system processing required looking for new approaches in filter purification of high-temperature gas flows containing fine particles. The best readings were obtained using wire fabric (grid) for filtration, precipitation efficiency is 99.0 to 99.9%.

During technological testing of the pilot facility, about 20 kg of plutonium dioxide and 40 kg of mixed uranium-plutonium waste were obtained. Oxide powders are in the form of fine-disperse submicron-sized particles. X-ray-structural analysis demonstrated that plutonium dioxide has a cubic grid of fluorite type with $\alpha=5,396\pm0.02$ Å corresponding to stoichiometric composition.[2] The specific surface square, measured with the dynamic BET method on argon thermal desorption, was approximately 40 m²/g. One plutonium dioxide pellet sintering during two hours at a temperature of 1600°C, reached the density of 11.0 g/cm³.

Plasma uranium-plutonium mixed oxides were well pressed for preparing pellets and "bushes" (pellets with holes), and then their sintering was finished at the temperature of 1400°C in a reducing environment with the formation of a single-phase solid solution with a grid parameter $\alpha=5,459$ Å.

Product density was 10,7 to 10,85 g/cm³. Fuel elements, manufactured by means of this method from plasma powders containing 20% of plutonium dioxide and 80% of uranium dioxide with 9 w.p. of [235]U, were successfully tested in a nuclear reactor.

Applying preliminary pelletization (granulation) of reduced powders, the bushes with chambers were manufactured from plasma uranium-plutonium oxide powders containing 25 mass % of plutonium for metal sum. The sintered bush material density was 10.4 to 10.6 g/cm³, and the oxygen coefficient was 1.96 to 1.99. Alpha-radiography of bushes demonstrated good homogeneity. Six commercial fuel elements were manufactured from bushes for BN-600.

Also the technology has been developed for the production of enriched uranium oxide powders with the necessary (2.3) oxygen coefficient for the plasma chemical reactor.

References

1. N. V. Dedov, F. A. Dorda, V. P. Korobtcev, E. M. Kutyavin, A. I. Soloviev, "Plasma-Chemical Method for Production of Ultra-Disperse and Fine Metal Oxides Powders and Areas of their Application," *New Commercial Technologies*, **issue 1** (261), 38–42 (1994).

2. N. V. Dedov, V. F. Bagryantcev, "The results of X-Rayography Analysis of Plutonium Dioxide Samples Obtained by Means of Plasma-Chemical Method," *Radiochemistry* **38** (issue I), 27–29 (1996).

Social and Psychological Causes of the Chernobyl Accident

This paper attempts to find the social and psychological rather than technological sources of the Chernobyl accident. The author believes that this accident is to a greater extent a natural consequence of the way that nuclear power developed historically than the result of a technical error.

First, the peaceful nuclear power is a side product of the military industry. The Ministry of Energy (ME) was engaged in the NPP construction and operation, but the reactor was developed by the Ministry of Mechanical Engineering (MME), which produced the nuclear weapon. The military developments were naturally taken as a basis. They were adapted to peaceful purposes and their similarity with a prototype was advantageous and was an important positive criterion for military experts.

Second, the command-administrative system of management and taking decisions has predominated in the USSR. Technical decisions were taken to the level of the Minister and even the highest party leaders were out of any criticism for scientific and technical society. It was especially evident in the area of the nuclear power. Here the experts' opinion and arguments did not have any significance compared to the leaders' opinion.

In the USA, a PWR developed by admiral Rickover for the "Nautilus" submarine was taken as a basis for peaceful nuclear power. In the USSR along with PWR, a uranium-graphite reactor developed for production of military Pu was used for peaceful nuclear power. The consequences in both cases were similarly grievous: the Three-Mile Island accident in the USA and Chernobyl accident in the USSR.

The possibility to use for the RBMK development the experience of the creation and operation of reactors for the weapon Pu production aroused enthusiasm in the MME leaders.

All technical decisions that would have seemed impossible to solve (welding of zirconium with stainless steel, manufacturing of large constructions with very high accuracy) have been successfully solved mainly due to the enthusiasm of the highly qualified experts with military directions.

In 1968 the MME experts developed a technical project of NPP with RBMK with 1000 MWe.

The MME leaders and Minister E. P. Slavskiy personally liked the project very much. They saw familiar technical decisions in the reactors as for the weapon Pu production: graphite laying with channels of zirconium instead of aluminum, piping system, etc. This child of the military industry could produce energy for peaceful purposes. The external similarity of RBMK and military reactors, for which the branch leaders were granted with rewards, government awards, and high status, filled them with belief in its reliability. It is an important psychological moment in the history of the Chernobyl accident.

But the impression of the reliability based on the external similarity was deceptive.

The following changes of parameters played the principal role:
- coolant (water) pressure was increased from 1 to 100 bar
- coolant boiling developed that can provide instabilities of various types
- fuel burnup depth was increased from fractions of percent to 2%
- reactor thermal power was increased almost 10 times, while the content of fission fractions almost 1000 times

O. V. Konovalova
All-Russia Nuclear Power Engineering Research and Development Institute (VNIIAM), Russia

- the reactor dimensions were increased to such an extent that the instability effects not foreseen by the designers became possible

These changes of parameters have increased the possibility of an accident and its radiological consequences many orders of magnitude.

As mentioned earlier, ME was engaged in the NPP construction and operation in the USSR. The technical project of NPP with RBMK was considered at the Interdepartment Council with participation of ME. It followed from the ME experts' conclusion that RBMK did not satisfy the nuclear power because it required larger expenses compared to a reactor of vessel type, constructed at NovoVoronezh NPP, and there was no technical possibility to ensure safety (in particular, it was impossible to build containment for a reactor of such a size as RBMK). On the basis of this conclusion, ME strongly rejected the development and construction of NPP with RBMK. But RBMK was a favorite child of MME and E.P. Slavskiy issued an order by which he charged his design and construction organizations (MME) with the development of the design and construction of NPP with RBMK. That is how in 1974 the Leningrad-1 (LNPP) with RBMK was built and this reactor type was "granted," or better to say, thrusted on Soviet nuclear power.

The RBMK constructed at LNPP and all subsequent RBMKs (a total of 15 units) have no containment and 200 ton of uranium as well as more than a ton of radioactive fission products was literally in the open air because the reactor hall roof was less stiff than the roof of a usual dwelling house.

During the RBMK first unit operation in 1974, a spatial instability of the neutron flux provided by the positive feedbacks not predicted by the reactor designers was found. The great difficulty of control of such a reactor has become a reason for the serious accident at the RBMK first unit in 1975 that can be considered a rehearsal for the Chernobyl accident. It can be reckoned that since that time the principal difference between RBMK and a reactor for Pu production that are externally similar has became evident.

But it was psychologically impossible for the MME leaders and experts to accept the fact that the RBMK was a danger. Even the fact of the accident at the LNPP first unit itself was hidden from society. By the decision of the government committee on the basis of the analysis of the accident at LNPP, the MME specialists have developed a set of measures for eliminating reasons of the RBMK instability. However, this set was not introduced and was implemented only after the Chernobyl accident in April 1986. The reason for the delay was the unwillingness of the MME leaders to worsen the characteristics of the RBMK fuel cycle.

Conclusions

1. The conducted analysis of the social and psychological sources of the Chernobyl accident shows that it was inevitable and natural.

2. The social source of the accident is the command-administrative system of management and taking decisions predominate in the branch.

3. The psychological source predetermining the accident was a confidence of the RBMK designers in the fact that it would be as reliable as a reactor for military Pu production.

The Calculation of Thermodynamic and Kinetic Characteristics of Component Redistribution in U-Pu-Zr Alloys

E. A. Smirnov
A. A. Shmakov
Moscow Engineering Physics Institute, Russia

Increased interest in metallic fuel for fast nuclear reactors has prompted a re-examination of our previously reported thermodynamic and transport properties of the U-Pu-Zr system.[1]

Clearly, an understanding of isothermal interdiffusion processes in fuel alloy is a necessary condition to predict real in-pile redistribution of its components. To achieve this understanding, the interdiffusion coefficients ($\tilde{D}_y^n$) for uranium rich BCC alloys were determined using the calculation method based on the principles of irreversible processes theory:[2]

$$\tilde{D}_{kl}^{n} = \sum_{m=1}^{n-1} \left[\, \delta_{km} \cdot D_m^* - C_k \cdot \left(D_m^* - D_n^* \right) \, \right] \cdot \frac{C_m}{C_l} \cdot g_{ml} \qquad (1)$$

where $D_i^*(i=1,2,3)$—the component diffusion coefficients in alloys;

$$g_{ml} = C_l \cdot \frac{\partial \ln C_m}{\partial C_l} + \frac{C_l}{RT} \cdot \frac{\partial F_m^E}{\partial C_l} \text{—thermodynamic multipliers.}$$

The relations for the D_i^* were derived by extension of results[2] on case of the ternary systems:

$$D_i^*(c) = (D_i^{*1})^{C1} \cdot (D_i^{*2})^{C2} \cdot (D_i^{*3})^{C3} \cdot \exp\left(\frac{F^E}{RT} \right) \qquad (2)$$

In (2): D_i^{*i}—the self-diffusion coefficients of γ-U, ε-Pu, and β-Zr, which are governed quite correctly by the expressions from;[3,4] D_i^{*j}—the impurity diffusion coefficients.

Empirical relations for the D_i^{*j} has been obtained in terms:

$$\lg\left(\frac{D_i^{*j}}{D_j^{*j}} \right) = (-0.497\pm0.006) - (0.140\pm0.054) + \left(\frac{T_{mj}}{T} \right)[(0.309\pm0.006) +$$

$$+ \quad (0.252\pm0.005) \cdot \left(\frac{T_{mj}}{T} \right)] \cdot \left(\frac{R_i}{R_j} \right)^{-6} \qquad (3)$$

by generalization of literature data for impurity diffusion in γ-U, ε-Pu, β-Zr, β-Th, and β-Ti.[5,6] In (3): T_{mj}—the melting point of matrix (j-component); R_i and R_j—the equivalent atomic radiuses of i and j components at 298 K.

The excess Gibbs free energy (F^E) and thermodynamic multipliers (g_{ml}) were calculated by the Kohler method using thermodynamic data for corresponding binary limiting systems of ANL investigators.

The full matrix of the $\tilde{D}_{ij}^{\,n}$ was determined by the (1-3) for the following concentration and temperature regions:

$$0.7 \leq C_U \leq 0.9, \quad 0.05 \leq C_{Pu,Zr} \leq 0.25, \quad 1073 \leq T \leq T_{sol},$$

where C_i—atomic fractions of i-component, T_{sol}—the solidus temperatures of corresponding ternary alloys, K. For example, the dependencies of diagonal interdiffusion coefficients are represented as:

$$\lg(\tilde{D}_{11}^{\,3}) = (-2.71\pm0.10)-(4.71\pm0.09)\cdot\left(\frac{T_{sol}}{T}\right), \tag{4}$$

$$\lg(\tilde{D}_{22}^{\,3}) = (-3.73\pm0.12)-(3.38\pm0.10)\cdot\left(\frac{T_{sol}}{T}\right)$$

where index 1 corresponds Zr, 2 - Pu and 3 - U.

In all, the results (4) have satisfactory agreement with the available experimental data as against previous theoretical evaluations.[1]

The very narrow interval (22 to 25 Kcal/mol) for Arhenius activation energy $\tilde{Q}_{22}^{\,3}$ in foregoing concentration region is noted, but the magnitude of $\tilde{Q}_{11}^{\,3}$ has strong dependence from alloys composition and is 24,5 Kcal/mol for alloy (C_U=0.7, C_{Pu}=0.25, C_{Zr}=0.05) and 35 Kcal/mol for alloy (C_U=0.7, C_{Pu}=0.05, C_{Zr}=0.25). It is easy to see that the calculated values of $\tilde{Q}_{11}^{\,3}$ have good agreement with experimental interdiffusion data ($\tilde{Q}$= 26 to 32 Kcal/mol) for corresponding binary system U-Zr.[7]

Besides, the anomality of interdiffusion processes in the BCC phase of the U-Pu-Zr system are analyzed.

References

1. E. A. Smirnov, I. E. Fedorova, "The Interdiffusion and Thermodynamic Properties of the U-Pu-Zr System," Intern. Conf. Actinides-93, Santa Fe, New Mexico, 1993, p. 87.

2. *The Processes of Interdiffusion in Alloys,* K. P. Gurov Ed., (Moscow, 1973, in Russian).

3. E. A. Smirnov, K. E. Smirnov, "The Diffusion Processes in BCC Phases of Actinides," Preprint of Moscow Engineering Physics Institute document 013-92 (1992, in Russian).

4. E. A. Smirnov, A. G. Mikhin, J. N. Osetsky, "The Point Defects and Mechanisms of Diffusion Processes in Zirconium and Titanium," Preprint of Moscow Engineering Physics Institute document 003-93, (1993, in Russian).

5. G. B. Fedorov, E. A. Smirnov, *Diffusion in Reactor Materials*, (Oxonian Press PVT.LTD, New Deli, 1984).

6. I. C. Okafor, "Diffusion and Electrotransport of Some Transition Elements in (bcc) Thorium," *J.Acta.metall.* **35**, 759,(1987).

7. Y. Adda, J. Philibert, "Etude de La Diffusion Uranium-Zirconium en Phase Gamma," *J.Compt. Rend. Acad. Sci.* **242**, 3081 (1956).

MOX Fabrication Experience at BELGONUCLEAIRE

Introduction

BELGONUCLEAIRE is part of the TRACTEBEL group, which shares equity of the company with the Belgian state. Its two main activities are MOX fuel supply and nuclear engineering. Since 1972, BELGONUCLEAIRE is operating a 35 HM ton/year MOX plant (PO) in Dessel (Belgium). BELGONUCLEAIRE has recently completed the design of a new plant (P1), a MOX plant based on the PO operation experience, that could be built in the US, as an option to transform surplus weapons-grade plutonium.[1]

The MIMAS Process

MIMAS was developed by BELGONUCLEAIRE in the 1980s to produce MOX pellets made of a solid solution Of UO_2/PuO_2 dispersed in a UO^2-matrix. Specificities of the MIMAS process are two blending steps (a primary blend also called *MAS*ter blend and a secondary blend), ball milling (*M*icronisation) of the master blend, and sintering of the green pellets under an atmosphere of hydrogen, argon, and moisture.[2]

J. van Vliet
E. Pelckmans
A. Vandergheynst
BELGONUCLEAIRE, Belgium
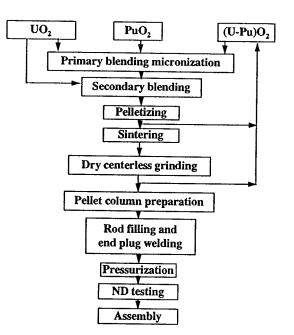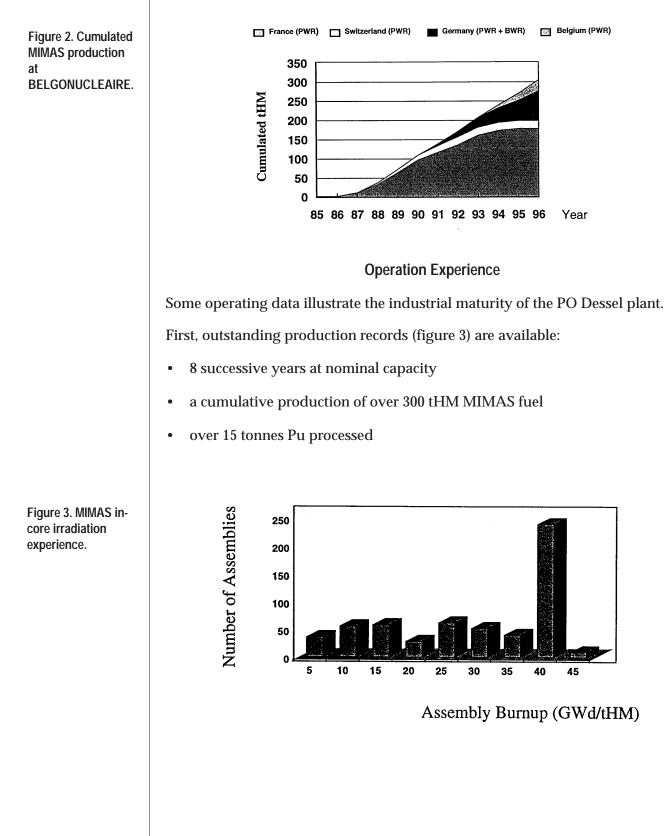
Figure 1. MIMAS process.

The remainder of the process is close to the UO_2 production process; only the technology is different for reasons of alpha-toxicity, criticality prevention, and waste limitation. For these purposes, BELGONUCLEAIRE has developed a totally dry technology: dry scrap recycling, dry pellet grinding, and contamination-free pellet loading and rod welding.

The MIMAS Product

Figure 2 illustrates the large irradiation experience gained with the MIMAS fuel in European commercial PWR's and BWR's reactors.[3] More than 600 fuel assemblies have already been loaded in French, German, Swiss, and Belgian reactors. Fabrication of the first reloads for Japan is contemplated in 1997.

Figure 2. Cumulated MIMAS production at BELGONUCLEAIRE.

Operation Experience

Some operating data illustrate the industrial maturity of the PO Dessel plant.

First, outstanding production records (figure 3) are available:

- 8 successive years at nominal capacity

- a cumulative production of over 300 tHM MIMAS fuel

- over 15 tonnes Pu processed

Figure 3. MIMAS in-core irradiation experience.

Assembly Burnup (GWd/tHM)

Second, the PO plant also presents outstanding operating records:

*   high flexibility (yearly production of 5 reloads according to various PWR/BWR fuel design and specifications)

*   no significant safety incident from its start up

*   occupational exposure conform to the ICRP 60 recommendations

*   scrap inventory under control

*   limited generation of solid contaminated waste (< 20 liter/kg Pu)

*   operation under satisfactory supervision of both IAEA and EURATOM

Conclusion

With the operation of its PO plant and its MIMAS process, BELGONUCLEAIRE proposes a unique experience of prime importance for the design, construction, and operation of new MOX plants.

This experience has been utilized for the French MELOX plant (capacity 100 to 160 tHM/y), that is also using the MIMAS process.

Within the coming years, this experience could be utilized by the U.S. for its domestic MOX fuel plant.

References

1.   D. Haas, Y. Vanderborck, Cl. Vandenberg, J. van Vliet, "Disposition of Plutonium from Dismantled Warheads: BELGONUCLEAIRE's Proposal," Washington, D.C., November 10–15, 1996.

2.   A. Vandergheynst, M. Debauche, "Key Issues of MOX Fuel Plants Engineering," Kyoto, Japan, April 1995.

3.   D. Haas, J. van Vliet, "Industrial Demonstration of the MOX Option for Light Water Reactor-Fuels," Seoul, Korea, April 11–12, 1996.

The AIDA/MOX 1 Program: Results of the French-Russian Study for Peaceful Use of W-Pu

The French-Russian studies conducted from 1993 to 1996 under the AIDA/MOX 1 program established the advantages and technical feasibility of the W-Pu MOX option in certain existing nuclear reactors within the Russian Federation.

Broadly speaking, the PWR-MOX and FR-MOX options for using excess dismantled weapons plutonium for peaceful commercial nuclear power generating purposes—like the CANDU-MOX and HTR-MOX options—offer several advantages over the remaining options (interim storage, disposal in vitrified form, etc.) notably from a nonproliferation standpoint:

- high radioactivity of the final product, a spent MOX fuel assembly: making any addition of radioactivity unnecessary

- fission of a significant fraction of the initial weapons plutonium: in the PWR-MOX scenario, some 30% of the W-Pu is converted into fission products after irradiation on the order of 40 GWd·t^{-1}

- plutonium accountancy: the W-Pu is processed in an industrial cycle in facilities under permanent surveillance by the international organizations responsible for nonproliferation safeguards (IAEA)

- isotopic denaturing of the residual plutonium (around 70%): the ^{239}Pu fraction diminishes and that of the even number isotopes (^{238}Pu, ^{240}Pu, and ^{242}Pu) increases

- conservation of natural resources: 50 metric tons of weapons-grade plutonium are capable of producing some 350 TWh of electric power

- no additional nuclear waste (e.g., vitrified plutonium): the spent MOX fuel assembly replaces a spent UOX fuel assembly

Compared with the other MOX options, the PWR-MOX and FR-MOX options also offer the following major advantages:

- the LWR-MOX and FR-MOX options are the only ones implementing proven technology: over 400 metric tons of PWR and BWR-MOX fuel have already been fabricated in Europe, and 19 European reactors have been using MOX for a number of years; over 100 metric tons of FR-MOX fuel have been fabricated to date in Europe

- the PWR-MOX and FR-MOX options are the only ones compatible with existing Russian reactors capable of using large quantities of W-Pu and known to be economically viable

Concerning the implementation of this option by the Russian Federation, the joint French-Russian studies carried out under the AIDA/MOX 1 program have led to the following conclusions:

1) Using 30% MOX fuel is feasible in certain VVER 1000 reactors, after implementation of design changes similar to those made in France in the 1980s and 1990s when EDF began recycling 30% MOX fuel in its 900 MW PWRs. These modifications are currently the subject of preliminary studies by the Russian and French parties, and will be covered in detail in the subsequent phase (1997 to 1998) proposed under the AIDA/MOX 2 program. This option ould enable dispositioning of 270 kg of W-Pu annually per VVER 1000 reactor.

N. N. Yegorov
E. Koudriavtsev
MINATOM, Russia

V. Poplavsky
IPPE, Russia

A. Polyakov
VNIINM, Russia

X. Ouin
Ministry of Industry, Russia

N. Camarcat
B. Sicard
H. Bernard
CEA, France

2) Using 100% MOX fuel in the BN 600 fast reactor without breeding blankets is certainly the most promising option in a reasonable time frame (even though further studies are necessary to validate it) and should therefore be assigned medium-term priority. In the short term, the easily implemented BN 600 hybrid core solution should make it possible for the disposition of 240 kg of W-Pu per year.

3) The processes investigated for converting W-Pu into MOX fuel have led to the definition of a reference process and two possible variants for a future facility or plant to be built in Russia. The reference process chosen by the French and Russian specialists is as follows:

- dissolution of plutonium alloy in HNo_3 + HF

- purification by extraction of plutonium nitrate

- Pu oxalate precipitation and PuO_2 production

- MOX fabrication using the COCA and MIMAS processes

4) The capacity of a MOX facility to be constructed in Russia was determined by the possibility of consuming MOX fuel in existing Russian VVER 1000 and BN 600 reactors:

- BN 600 hybrid core option (=> 240 kg of W-Pu per year), as the first step toward the final objective of 100% MOX fuel in the BN 600 reactor core (1310 kg of W-Pu per year) and gradual removal of all the blankets

- four VVER 1000 reactors at the Balakovo NPP (=> 4×270 kg of W-Pu per year) hence a total capacity of around 1300 kg of W-Pu for the TOMOX 1300 facility, i.e., approximately 30 metric tons of MOX per year.

5) Preliminary design work on the TOMOX 1300 facility implementing glovebox handling technology is under way in Russia with French participation. A detailed design proposal (planned under the AIDA/MOX 2 program) will be necessary in 1997 and 1998 before construction of the facility in Russia; allowance will be made for the basic facilities already in place at Russian nuclear sites, including Chelyabinsk 65 and Krasnoyarsk 26.

Abbreviations and Acronyms

W-Pu: Weapons Plutonium, derived from dismantled nuclear weapons

MOX: Mixed OXide (U + Pu)

LWR: Light Water Reactor

PWR: Pressurized Water Reactor

BWR: Boiling Water Reactor

FR: Fast neutron Reactor

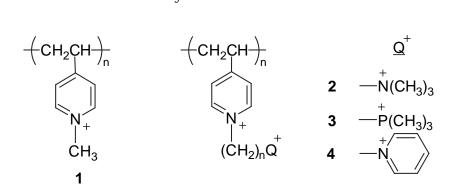CANDU: CANadian Deuterium-Uranium Reactor

HTR: High-Temperature Reactor

Separations

New Bifunctional Anion-Exchange Resins for Plutonium Separations

The most frequently used process for the recovery of plutonium from a wide range of impure nuclear materials is anion exchange. The most stable oxidation state of plutonium in nitric acid, Pu(IV), readily forms an anionic hexanitrato complex that is strongly retained by anion-exchange resins.[1] Since the Pu(IV) nitrate complex is very strongly sorbed and few other metal ions form competing anionic nitrato complexes, anion exchange is attractive for separating plutonium.[2] The primary disadvantage of this process has been the unusually slow rate at which the Pu(IV) nitrate complex is sorbed by the resin.[3]
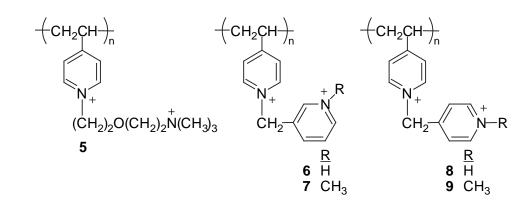
Compared with polystyrene-based anion-exchange resins, vinylpyridine polymers are more resistant to radiolytic degradation and chemical attack by nitric acid.[4] In 1988, Reilly Industries, Inc. began production of Reillex™ HPQ (**1**), a macroporous copolymer of partially N-methylated 4-vinylpridine and divinylbenzene, which is utilized in the full-scale plutonium recovery process at Los Alamos National Laboratory.

R. A. Bartsch
J. S. Kim
J. Nam
Texas Tech University

S. F. Marsh
G. D. Jarvinen
Los Alamos National Laboratory

To explore the reason for the unusually slow rate of Pu(IV) nitrate complex sorption, nuclear magnetic resonance (NMR) and extended x-ray absorption fine structure (EXAFS) were used to identify the plutonium complexes involved in the anion-exchange process.[5,6] The investigation indicated that the uncharged tetranitrato complex of Pu(IV) is most likely involved in interaction with the anion-exchange resin, even though this neutral complex must acquire two additional nitrate groups to become a divalent anion during the sorption process. It was postulated that the rate of Pu(IV) sorption by an anion-exchange resin might be enhanced for a bifunctional resin that would provide two anion-exchange sites separated by a fixed distance. The two anion-exchange sites could simultaneously deliver nitrate ions to the uncharged tetranitrato complex of Pu(IV) thereby enhancing the sorption rate compared with resins which possess only a single anion-exchange site per repeat unit.

We have tested this concept by preparing three series of bifunctional anion-exchange resins **2**-**4** by alkylation of the pyridine nitrogen of commercial Reillex™ 402 poly(4-vinylpyridine). In these resins, the identity of the second anion-exchange site is systematically varied from trimethylammonium (in **2**) to trimethylphosphonium (in **3**) to pyridinium (in **4**). For resins **2** and **4**, the number of carbon atoms in the spacer between the two positively charged sites in each repeat unit was varied from two to six, and for resins **3** from two to five. In addition, resin **5** was synthesized to determine the influence of enhanced flexibility in the spacer unit resulting from the incorporation of an oxygen atom. Finally resins **6**-**9** were prepared to assess the effect of a more fixed relationship of the two anion-exchange sites.

$$+CH_2CH+_n \qquad +CH_2CH+_n \qquad +CH_2CH+_n$$

Structure 5:
$$(CH_2)_2O(CH_2)_2\overset{+}{N}(CH_3)_3$$
5

Structures 6, 7:
$$CH_2 \quad \overset{+}{N}-R$$

	R
6	H
7	CH_3

Structures 8, 9:
$$CH_2 \quad \overset{+}{N}-R$$

	R
8	H
9	CH_3

Each resin was evaluated by measuring the distribution coefficients (Kd values in mL/g) of Pu(IV) from 1, 3, 5, 7, and 9 M nitric acid with contact periods of 0.5, 2, and 6 hours.

Resins **2** to **4** gave low Kd values (0.6 to 2.2) for sorption from 1 M nitric acid and high Kd values (several hundred to several thousand) for sorption from 5 to 9 M nitric acid. Thus they possess the potential for effective Pu(IV) sorption from 5 to 9M nitric acid and then desorption by changing to a less acidic medium.

For all three series, the highest Kd values for Pu(IV) sorption from 5 to 9 M nitric acid were reached with a five-carbon spacer between the two anion-exchange sites. Resin **5** in which the five-atom spacer includes an oxygen atom gave somewhat higher Pu(IV) sorption from 5 to 9 N nitric acid than did resin **2** with n = 5. Resins **6** to **9** were found to be less efficient in Pu(IV) sorption than analogous resins **4** which have a more flexible linkage between the two anion-exchange sites.

Compared with Reillex HPQ™ resin (**1**), essentially all of the new bifunctional resins **2** to **5** exhibited more rapid Pu(IV) sorption from 7 to 9 M nitric acid and the attainment of higher Kd values.

Thus we have established the validity of using bifunctional anion-exchange resins to facilitate the recovery of Pu(IV) from nitric acid solutions. Further investigation of the influence of structural variations within the bifunctional anion-exchange resins is in progress.

References

1. J. L. Ryan and E. J. Wheelwright, "The Recovery, Purification, and Concentration of Plutonium by Anion Exchange in Nitric Acid," U.S. Atomic Energy Commission report HW-55893(del) (1959).

2. J. P. Faris and R. F. Buchanan, "Applications of Anion-Exchange Spectrographic Procedures in Nitric Acid Medium," U.S. Atomic Energy Commission report TID-7606 (1960), p. 185 .

3. M. Streat, *Reactive Polymers* **2,** 79 (1984) .

4. S. F. Marsh, "The Effects of *In Situ* Alpha-Particle Irradiation on Six Strong-Base Anion Exchange Resins," Los Alamos National Laboratory report LA-12055 (April 1991).

5. S. F. Marsh, R. W. Day, and D. K. Veirs, "Spectrophotometric Investigation of the Plutonium Nitrate Species Sorbed by Ion Exchange Resins," Los Alamos National Laboratory report LA-12070 (June 1991).

6. D. K. Veirs, C. A. Smith, J. H. Berg, B. D. Zwick, S. F. Marsh, P. Allen, and S. D. Conradson, "Characterization of the Nitrate Complexes of Pu(IV) Using Absorption Spectroscopy, ^{15}N NMR, and EXAFS," *J. Alloys Compounds* **213/214**, 328 (1994).

Effects of Coprecipitation on Uranium and Plutonium Concentrations in Alkaline Salt Solutions

D. T. Hobbs
Westinghouse Savannah River Company

Introduction

The chemistry of uranium and plutonium in conjunction with the storage, retrieval, and treatment of high-level nuclear waste (HLW) has been the subject of increasing scrutiny due to concerns with nuclear criticality safety. Previous studies focused on determining the solubilities of plutonium and uranium in alkaline salt solutions that encompass the compositions present during storage and evaporation of fresh and aged BLW.[1,2] Recent studies extend the chemistry to include the effects of coprecipitation on the liquid phase concentrations of plutonium and uranium. Particle size, morphology and identification of crystalline phases in the precipitated solids as well as the plutonium and uranium dissolution characteristics upon dilution of the liquid phases were also determined.

Description

Four acidic solutions were prepared simulating Purex high-activity waste (Purex-HAW), Purex low-activity waste (Purex-LAW), HM high-activity waste (HM-HAW), and HM low-activity waste (HM-LAW) solutions at the Savannah River Site (SRS). The simulated wastes were comprised of varying amounts of iron, aluminum, manganese, nickel, and uranyl nitrate salts dissolved in 2.0 molar nitric acid solution. The source of plutonium was a nitric acid solution of Pu(IV). Three additional solutions containing uranium only (U-Blank), plutonium only (Pu-Blank), and plutonium and uranium only (Pu/U-Blank) were prepared as blanks. Concentrated sodium hydroxide solution (50 wt %) was added to portions of the acidic waste solutions to provide a final liquid phase hydroxide concentration of 1.2 molar. This hydroxide concentration is the target concentration used by the separations operations prior to transfer of the HLW to the waste storage tanks.

The resulting mixtures were mixed for one hour, then allowed to stand with periodic shaking at ambient laboratory temperature. Periodically, samples of the slurry were taken and filtered through a 0.20 μm pore size filter. The filtrate was analyzed for plutonium and uranium content. A portion of the precipitated solids from each waste type was isolated and analyzed for plutonium and uranium content, identification of crystalline phases by x-ray diffraction (XRD) and particle size and morphology by scanning electron microscopic (SEM) analyses. Portions of each alkaline slurry were also diluted with varying amounts of water to simulate the washing operation during pretreatment of the HLW for disposal. The diluted mixtures were agitated once daily and periodically sampled for determination of the plutonium and uranium content in the liquid phase.

Results and Discussion

Solid phases precipitated and settled upon addition of sodium hydroxide to the acid solutions. Slurries containing high iron concentrations did not settle to as high a solids concentration as the blank and high aluminum-containing slurries. The precipitated solid particles were generally irregularly shaped and ranged in size from about 1 to 50 mm in diameter.

In general, the XRD patterns of the dried solids exhibited broad peaks of low intensity indicative of the solids consisting primarily of amorphous, non-crystalline solids.

Crystalline phases identified included $Na_2U_2O_7$, $Al_2O_3 \cdot 3H_2O$ (gibbsite and bayerite) $NaNO_3$ and $\alpha\text{-FeOOH}$.

The plutonium and uranium concentrations in the four waste simulants and the three blank solutions were determined periodically over 59 days. There were no discernible relationships between time and the plutonium and uranium concentrations for any of the solutions. Therefore, all of the sample results were averaged. The average concentrations of plutonium and uranium in the alkaline solutions are provided in Table 1.

| Simulant | Concentrations (mg/L) | |
	Plutonium	Uranium
Purex-HAW	6.8 ± 1.8 E-4	4.1 ± 1.4
Purex-LAW	1.1 ± 0.56 E-3	4.7 ± 2.0
HM-HAW	0.35 ± 0.14	2.4 ± 0.13
HM-LAW	not determined	0.70 ± 0.31
Pu Blank	0.20 ± 0.16	0.041 ± 0.023
U Blank	not determined	4.5 ± 1.3
Pu/U Blank	8.4 ± 4.8 E-4	6.5 ± 1.8

Plutonium is effectively removed from simulated Purex and HM waste solutions upon the addition of sodium hydroxide by coprecipitation with iron and uranium, but not with aluminum. This results in alkaline salt solutions that are unsaturated in plutonium. Uranium was observed to be saturated in all alkaline salt solutions except that simulating HM-LAW waste. Thus, only in the HM-LAW waste solution is there a sufficiently high molar ratio of iron to uranium for coprecipitation to occur. Addition of water to the alkaline slurries that simulates dilution of the waste during sludge washing results in dissolution of small amounts of uranium and plutonium in Purex waste slurries, but not in HM waste slurries. The amounts of plutonium and uranium that dissolve are not sufficient to saturate the solution in either plutonium or uranium.

References

1. C. H. Delegard, *Radiochim. Acta* **41**, 11–21 (1987).

2. D. T. Hobbs and D. G. Karraker, *Nuclear Technology* **114,** 318–324 (1996).

Plutonium Purification from Americium by Vacuum Distillation Method when Heating by Electron Beam

G. P. Khandorin
V. M. Kondakov
E. N. Maly
V. G. Sapozhnikov
G. G. Shadrin
L. L. Ugrinsky
Siberian Group of Chemical Enterprises, Russia

When storing weapon-grade or energetic plutonium for a long time, it accumulates Am^{241} that forms during the β-decay of Pu^{241} isotope. Great amounts of the new element that is being accumulated in plutonium reduce its worth for further application because of neutron physical characteristics degradation; its storage becomes more expensive because of the constant increase of gamma field levels that is connected with intensive γ-radiation (59,5 keV) accompanying α-decay of Am^{241} that complicates the radiation situation of any technological equipment.

Therefore, a "dry" technology of deep plutonium purification from americium was developed at the Siberian Chemical Combine using the vacuum distillation method when heating by electron beam. At the present time, growing interest in the issue of Pu purification from Am becomes high priority in connection with possible commercial use of plutonium in nuclear reactors.

In the future, Pu isotopes separation by the laser method presumes preliminary Pu purification from Am.

The main advantage of the proposed method in comparison with the chemical (liquid) way of Pu purification from Am is the significant reduction of gamma-active waste solutions number. Their total mass is reduced by 3...5 exponents.

Certain physical characteristics were taken as a basis for the developed technological process—volatility of Am vapors in a vacuum in a wide temperature range is by 3...4 exponents higher than of Pu. The most convenient way to implement the distillation purification method is electron beam refining of a plutonium blend in a vacuum (Figure 1).

A vacuum chamber with a volume up to 1,5 m^3 is pumped out up to a pressure of 3×10^{-5} torr. The most expedient temperature range is 1400 to 1500 °C. With electron beam refining, such temperatures are created in a thin surface layer of melted Pu blend in the crucible. Temperature can be controlled both by forced heat removed with water cooling and by special disposition of equipment elements—crucible with liquid metal, chamotte heat insulating screens, heat exhausting stands (refrigerators)—when heat flow creates a temperature gradient up to 70 to 100°C/mm.
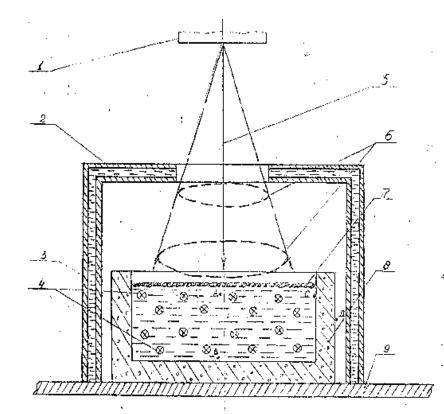
Crucible metal ceramic walls on the base of TiO ensure that the inner surface gets a thin layer of a separating self-sustaining coating from PuO_2 that protects safely a volume of liquid Pu from contamination by the crucible material.

This technology's wastes are condensates of evaporated metals (Pu, Am, Ga) mainly. Their mass and relative composition are determined on the whole by temperature conditions of process management and liquid bath surface square.

Melting parameters control is performed by a change of equipment construction, energy consumption, admixtures to Pu blend, and disposition in liquid bath of the PuO_2 layer, whose border of "opening" is controlled, and Am can be evaporated through the clean surface.

The condensation unit for metal fumes to collect (Pu + Am, possibly Ga and other easy flammable components of Pu blend—Pb, Zn, Mg ...) is manufactured from Rermeta and is cooled by an independent device.

Figure 1. Unit for Pu
blend melting and
Pu and Am metal
fumes condensation
using the vacuum
distillation method
when heating by an
electron beam.

1. electron beam gun
2. water cooling condenser of metal vapors
3. liquid metal
4. impurities molecules
5. electron beam
6. circular path of electron beam
7. oxides layer at liquid metal surface
8. crucible from cermet
9. heat removing support

Five safety barriers exist in order to perform all the activities by the operator's hands without mechanical arms. Chamber rubber gloves with filler reducing γ-radiation and a small sized integral dosimeter of operative control were specially developed.

While producing 200 g of Am^{241} at the experimental facility an operator received γ-radiation dose for hands less than 10 mSv/year. While performing industrial scale works, the total dose load is expected to be much less.

Specifications:

- coefficient of Pu purification from Am: 1000

- energy expenses: 10,000 kJ per 1 kg of purified Pu

- high-level wastes mass: up to 400 g per 100 kg of Pu

The technology is applicable for purification of mass qualities of returned Pu. It is environment and radiation safe.

The proposed technology will allow the production of isotopic and chemical pure Am^{241} for application in peaceful purposes.

Conversion of Weapon-grade Plutonium into an Oxide Powder Suitable for MOX Fuel Manufacturing by a Pyrochemical Method.

Introduction

A. Osipenko
A. Bychkov
O. Skiba
SSC RIAR, Russia

J. Lacquement
J. M. Adnet
P. Brossard
CEA/DCC, France

Among the processes which have been proposed to convert weapon grade plutonium into PuO_2 suitable for MOX fuel manufacturing, pyrochemical methods offer substantial interests compared to aqueous ones. The main advantages are a compact technology and the production of small radioactive waste volumes.

As part of the AIDA/MOX program, French and Russian teams have studied the chemical conversion in molten chlorides media.

The process in a NaCl-KCl molten salt includes:

- plutonium alloy dissolution and purification from gallium by chlorine bubbling

- plutonium dioxide precipitation and purification from americium by oxygen bubbling

This paper describes both dissolution and precipitation stages and their applications to conversion of Pu-Ga alloy into PuO_2. Pyrochemical experiments have been carried out in the Atalante Laboratory in Marcoule to convert about 175 g of Pu-Ga alloy into PuO_2 powder. The ain results, such as residual gallium concentration in PuO_2 and conversion yield, are presented in tables. Further sintering tests should be performed in the Plutonium Laboratory in Cadarache to confirm the powder ability to be manufactured into MOX fuel.

Summary

Since the 1960s the R.I.A.R (Research Institute of Atomic Reactors in Dimitrovgrad) performs scientific research in using molten salts systems in the nuclear fuel cycle. The provided pyroelectrochemical knowledge in molten chlorides media has allowed the creation of a compact technology for UO_2 and MOX fuel production and spent fuel reprocessing.

The Russian-French AIDA/MOX program launched in 1992 schedules to convert the excess dismantled weapons plutonium into MOX fuel. One topic jointly lead between R.I.A.R and C.E.A (French Atomic Energy Commission) consists of applying the Russian pyrochemical technology to this conversion.

Following basic studies at the Dimitrovgrad Laboratory, experiments have been recently carried out in the French Atalante Laboratory. The starting material was metallic plutonium having up to 4 wt % of gallium. Its complete conversion in PuO_2 has been proved.

Basis of the Pyrochemical Conversion

The pyrochemical process includes two stages. First, plutonium alloy is poured into molten NaCl-KCl salt under a chlorine stream. The alloy chlorination produces Pu(IV) by autocatalysis:

$$PuCl_3 + 1/2\ Cl_2 => PuCl_4$$

$$3\ PuCl_4 + Pu => 4\ PuCl_3$$

Initial Pu(III) results from alloy corrosion in a molten bath:

$$Pu + 3\ MeCl => PuCl_3 + 3\ Me\uparrow \text{ where } Me = Na \text{ or } K$$

Gallium is oxidized up to Ga(III) and released from the bath by $GaCl_3$ volatilization:

$$Ga + 2\ PuCl_4 => GaCl_2 + 2\ PuCl_3$$

$$GaCl_2 + \_\ Cl_2 => GaCl_3 \uparrow$$

During the second stage, oxygen bubbling precipitates plutonium dioxide while americium remains in the molten salts:

$$PuCl_4 + O_2 => PuO_2 \downarrow + 2Cl_2$$

Experimentals

Experiments take place in a quartz vessel. A water cooler is used to trap the gallium trichloride while the chlorine excess is trapped in sodium carbonate solutions. 85 g of equimolar NaCl-KCl mixture are loaded into a pyrographite crucible.

After vessel closing, the salts are fused under a chlorine stream (2.5 l/h) up to 720°C. When salts are melted, special devices (thermocouple, reference electrode, gas introduction tube, and alloy introduction vessel) are put down into the molten salts. The plutonium alloy is then loaded into the crucible using a spread introduction vessel. The plutonium dissolution is controlled by measuring the potential between the crucible and a reference electrode.

Alloy batches represented about 17.5 g to 26.5 g. Chlorine flow rates were 5, 7.5 and 10 l/h and dissolution lasted from 50 up to 90 minutes, although chlorination generally carried on 40 to 60 minutes longer for complete gallium removing.

After the dissolution stage, all devices are put up over the molten bath and salts are cooled down under chlorine (2.5 l/h). When the salts are solid, the chlorine atmosphere is replaced by an argon atmosphere and the introduction vessel by an oxygen selective electrode. Salts are fused one more time under an argon stream (5 l/h). Pure oxygen is added (5 l/h) to precipitate plutonium dioxide from molten salts. Plutonium precipitation is controlled by measuring the decreasing potential between the selective and the reference electrodes.

Precipitation lasted for 120 minutes. An additional 30 minutes under an argon stream allowed a complete settling of the powder.

Then the vessel is cooled down to room temperature. PuO_2 powder is removed from the saline block using a hammer, washed with 0.1 M nitric acid and then water. After drying, the PuO_2 powder is weighted to determinate the plutonium conversion yield. Sampling is performed to undergo the chemical and radiochemical analysis (ICP/MS for Ga and α-counting for Am).

Main results

175.5 g of Pu-Ga alloy have been processed in eight experiments. Experimental results are listed in Tables 1 and 2. The produced powder is black with some green reflectance. The powder seems to be very fine (under 1 μm grain size) and precise measurements are under way at the Cadarache Plutonium Laboratory.

Experiment	Alloy Sample Weight (g)	Pu Conversion Yield (wt. %)[1]
1	17.51	81.3
2	17.48	70.2
3	17.59	68.5
4	17.48	74.9
5	26.49	68.9
6	26.44	72.1
7	26.26	86.2
8	26.58	78.6

[1] Measured as the total plutonium converted into oxide.

Experiment	Gallium (ppm)
1	16.5
2	26.3
3	29.2
4	34.0
5	74.6
6	46.1
7	19.8
8	22.5

The plutonium concentration in the molten salts after the precipitation and settling stages does not exceed 0.5 wt %.

After each precipitation stage some PuO_2 powder is laid down on the experimental quartz devices. The plutonium dioxide is periodically removed from quartz by scrapping with a metallic blade. All the PuO_2 slag has been dissolved by chlorination and re-precipitated without quartz devices. Concerning the overall plutonium to plutonium dioxide conversion campaign an average yield of 95 wt % has been obtained.

Gallium concentration in the PuO_2 powder is always less than the 100 ppm limit which is the currently allowed fraction. Am concentration is also very low (always less than 100 ppm). Further characterization is under way to measure other elements such as chlorine and carbon.

Conclusion

The pyrochemical conversion of gallium alloyed plutonium into a pure plutonium oxide powder has been demonstrated at the laboratory scale (200 g). Further tests will be carried out in Cadarache in order to specify grain size and specific area of the produced powder. Sinterability tests will confirm or not the opportunity to select such a process for MOX fuel manufacturing.

Solid/Gas Phase Catalytic Reduction for the Clean Separation of Gallium from Gallium Oxide/Plutonium Oxide

C. V. Philip
W. W. Pitt, Jr.
K. Chung
R. G. Anthony
Texas A&M University

Gallium present in weapons plutonium has to be removed before it can be used for the production of MOX fuel rods since Ga is expected to react corrosively under the nuclear reactor conditions. The preliminary studies conducted at Texas A&M University resulted in the invention of a new process which could be developed as a process for the separation of gallium from a gallium oxide/plutonium oxide matrix. The new process is cleaner, simpler, and more efficient than those based on existing techniques under evaluation.

Gallium has a melting point of 29.78°C and a boiling point of 2403°C. Gallium trioxide is nonvolatile. Gallium suboxide sublimes at temperature < 500°C. Heating Ga_2O_3 in a reducing atmosphere causes the volatilization of Ga_2O which at higher temperatures decomposes to metallic Ga and Ga_2O_3 which are nonvolatile. A clean separation of Ga from a Ga_2O_3/PuO_2 mix is not achieved by heating in a reducing atmosphere. The use of wet techniques produce liquid wastes. This invention could be used to develop a new 'dry process' for the clean separation of gallium from plutonium oxide without any deposition of gallium or its oxide on any part of the reactor and vent assemblies and any waste streams. Since the reaction temperature is relatively low, after the separation, the change in the surface area and the granular size of plutonium oxide will be minimal and will meet the feed specifications for MOX fuel.

Since Texas A&M does not have a certified facility for conducting experiments with plutonium dioxide, and cerium oxide is a good surrogate of plutonium oxide, several experiments were conducted using a gallium oxide/cerium oxide matrix. The experiments demonstrated a clean separation of gallium from cerium oxide matrix. The separation of gallium from plutonium oxide matrix will be tested later either at Los Alamos National Laboratory or any other suitable facility.

Currently there is no process for the separation of gallium from a plutonium oxide matrix. Researchers at Los Alamos National Laboratory were able to remove most of the gallium from plutonium oxide by heating the mixture in 6% H_2/Ar at 1400°C. Loss of surface area, increase in granular size of plutonium oxide, the deposition gallium and gallium oxide on the walls of the reactor, and the vent are the major drawbacks of the process. Wet processes using the selective extraction of plutonium complexes from a solution containing Ga and Pu are also being tested, however, the waste fluids from these processes is of great concern.

This invention has been demonstrated using a simple apparatus composed of a quartz 'U' tube in which gallium oxide/cerium oxide is held with the help of two quartz wool plugs in one side and the catalyst on the other side. When the reactor is then heated at 700 to 900°C passing a reducing gas using the side with the oxide as the inlet and side with catalyst as the outlet, the continuous deposition of droplets of metallic gallium only on the catalyst surface is observed.

The new process uses a lower temperature, and the effect of temperature on the surface area and the granular size is less drastic. The plutonium oxide after the gallium removal will meet the feed specifications for MOX fuel. The process is clean and does not produce any liquid waste and keeps the processing unit and the lines clean. The existing processing units can easily be modified for use with

the new process. Although the process has not been tested using plutonium oxide, it is expected that plutonium oxide will behave like cerium oxide.

Only few experiments have been conducted at Texas A&M and the potential this invention has not been fully investigated. Some of the details of the experiments will be presented at the meeting.

Plutonium Solubility and Speciation
Under Hydrothermal Waste Treatment Conditions

Operations at DOE facilities have created a large legacy of combustible wastes that are contaminated with transuranic compounds, other radioactive elements, and strong oxidizers such as nitrates. Hydrothermal oxidation is one of several technologies being studied for the destruction of residues and wastes.[1] Hydrothermal oxidation completely oxidizes a wide variety of organic and other hazardous materials. Understanding the speciation and solubility of actinides during and after hydrothermal treatment is crucial for the design of post-processing effluent separations, and ultimately for the deployment of this technology for nuclear waste reduction and residue stabilization. Such a strongly oxidizing environment will generate plutonium(VI); and upon destruction of organics, hydrothermal reactor effluent solutions will likely be concentrated in carbonate. Depending upon the pH, salts present, and total Pu(VI) and carbonate concentration in the process effluent, a number of solution and solid state species may be present. We are investigating the structure, solubility, and stability of each of these species.[2]
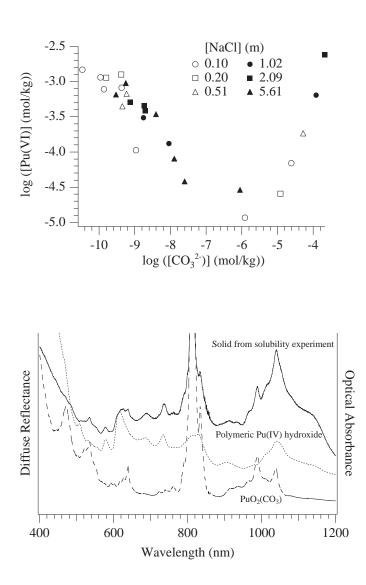
We have collected spectrophotometric titration data on the plutonyl carbonate system. Based upon a preliminary fit of these data, we have calculated formation constants for the tris- and biscarbonato complexes to be, $\log \beta_{130}=17.7$ and $\log \beta_{120}=13.6$, r espectively. These values are in excellent agreement with those calculated from the solubility of plutonium carbonate in $NaClO_4$, $\log \beta_{130}=17.4$ and $\log \beta_{120}=13.4$. [3] The tris- and biscarbonato species have much smaller formation constants than the analogous uranyl species, $\log \beta_{130}=21.8$ and $\log \beta_{360}=48.6$.[4] These formation constants indicate that under conditions relevant to the hydrothermal process effluent, $PuO_2CO_3(aq)$ is the predominant species over a large pH range. Thus, our initial focus is the solubility of the corresponding solid, PuO_2CO_3. We have prepared and characterized the plutonyl carbonate, PuO_2CO_3, and verified that it is isostructural with UO_2CO_3 using powder XRD and EXAFS analysis. We determined the solubility product of PuO_2CO_3 to be $\log Ksp=-12.9$ in 0.1 m NaCl (Figure 1). This value compares well with the solubility product determined for UO_2CO_3, $\log Ksp=-13.3$ in 0.1 m NaCl [5] and the two literature values for the solubility product of PuO_2CO_3 in 0.1 m $NaClO_4$, $\log Ksp=-13.4$ [3] and -13.98.[6] We have also determined the solubility product of plutonyl carbonate at higher concentrations of NaCl. Based upon our results and the few data available in the literature, we find that plutonyl carbonate is significantly more soluble in NaCl than in $NaClO_4$. This difference is due to the formation of chloro complexes $PuO_2Cl_x^{2-x}$.

Solutions from the solubility experiments show that Pu(VI) is reduced to Pu(V), which in turn disproportionates to yield polymeric Pu(IV) hydroxide. We have monitored this behavior using optical absorbance spectroscopy. The solid phase changes from an initial tan color to green after aging for several months. Characterization of the aged solid by diffuse reflectance spectroscopy shows that it is a mixture of the starting PuO_2CO_3 solid and polymeric Pu(IV) hydroxide (Figure 2). The rate of the transformation depends on the chloride concentration. At low NaCl concentrations, Pu(VI) is reduced within hours in the absence of an oxidizing agent; whereas in concentrated NaCl (5.6 m) Pu(VI) is stable for several days. Concentrated NaCl appears to stabilize the higher oxidation state via chloro complexation and radiolytic production of hypochlorite.

We will present the synthesis, characterization, stability, and solubility of plutonium(VI) carbonato and chloro species.

S. D. Reilly
M. P. Neu
W. H. Runde
Los Alamos National Laboratory

Figure 1. Initial results on the solubility of Pu(VI) in NaCl solution as a function of free carbonate concentration.

Figure 2. Diffuse reflectance spectrum of PuO_2CO_3 solid aged in 0.1 M NaCl for 4 months compared to diffuse reflectance spectrum of pure PuO_2CO_3 solid and optical absorbance spectrum of polymeric Pu(IV) hydroxide.

References

1. (a) M. Modell, *Standard Handbook of Hazardous Waste Treatment and Disposal*; H. M. Freeman, Ed. (McGraw-Hill, New York, New York, 1989), pp. 8.153–8.168. (b) J. W. Tester, H. R. Holgate, F. J. Armellini, P. A. Webley, W. R. Killilea, G. T. Hong, H. E. Barner, *Emerging Technologies in Hazardous Waste Management III;* D. W. Tedder and F. G. Pohland, Eds. (ACS Symposium Series 518, American Chemical Society, Washington, DC, 1993), p. 35.

2. M. P. Neu, S. D. Reilly, W. H. Runde, *Material Research Society Symposium Proceedings Series, II. Scientific Basis for Nuclear Waste Management XX*, Vol. 465 (in press).

3. P. Robouch, P. Vitorge, *Inorg. Chim. Acta* **140**, 239 (1987).

4. I. Grenthe, J. Fuger, R. J. M. Konings, R. J. Lemire, A. B. Muller, C. Nguyen-Trung, H. Wanner, *Chemical Thermodynamics of Uranium* (North-Holland, Amsterdam, Holland, 1992), Vol. 1.

5. W. H. Runde, Ch. Lierse, B. Eichhorn (to be published in *Geochim. Cosmochim. Acta.*).

6. I. Pashalidis, W. Runde, J. I. Kim, *Radiochim. Acta* **61**, 141 (1993).
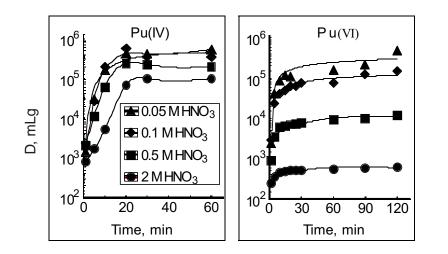
Pu Sorption and Extraction
by the 1,2-hydroxypyridinone Based Agents

Plutonium is among the radioactive species of most concern in the long-term storage of nuclear waste. As a result of processing and purifying Pu for nuclear weapons over the past decades, wastes containing both high and low concentrations of plutonium and other actinides currently exist at many Department of Energy sites in the U. S. Efficient pretreatment for removal of Pu and other radionuclides from the waste solutions could minimize their volume and facilitate their disposal, thus decreasing health risks and the cost of waste management. Solvent extraction and ion exchange are among the technologies which are most suitable for this purpose. However, only a small fraction of the waste, by weight, is made up of radionuclides. Typical wastes have low concentrations of heavy metals and radionuclides, along with normal or elevated levels of common non-toxic or low-toxicity cations and anions, sometimes with organic complexing agents. To optimize waste pretreatment, the resins and extractants to be used should have high selectivity and efficiency for the targeted cations.

Chelating ion exchange resins and solvent extraction agents designed for the efficient and preferential Pu(IV) removal from aqueous solutions are being evaluated for Pu(IV) and Pu(VI) extraction from nitric acid media. Results for the chelating ion exchange 1,2-HOPO Resin and the 1,2-HOPO octylcarboxamide extractant for solvent extraction based on 1-hydroxy-2-(1H)-pyridinone ligand (1,2-HOPO) will be presented.

We have shown that 1,2-HOPO Resin and a solution of 1,2-HOPO octylcarboxamide in octanol extract both Pu(IV) and Pu(VI) from acidic and neutral media. The selectivity of 1,2-HOPO agents was significantly higher for Pu(IV) than for Pu(VI) (Figures 1and 2). In general, the kinetics of metal removal from aqueous phase by chelating ion exchangers are relatively slow in comparison with other types of resins. However, the Pu uptake by 1,2-HOPO resin was very fast. Usually an equilibrium can be reached within 20 minutes (Figure 1). Conditions for stripping of Pu species have been examined.
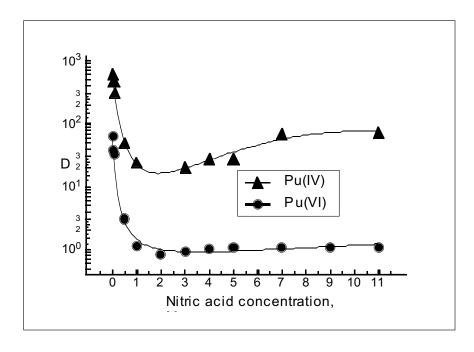
Our results show that 1,2-HOPO agents are highly selective and efficient for Pu(IV) uptake over a wide range of solution compositions. We anticipate that molecular modeling can be used to design and synthesize sequestering agents for uranyl, neptunyl, and other actinide ions based on modification[1] of natural siderophores or their analogs.

V. V. Romanovski
P. Zhao
D. C. Hoffman
D. W. Whisenhunt Jr.
G. T. Seaborg Institute for Transactinium Science, Lawrence Livermore National Laboratory

D. White
X. Jide
K. N. Raymond
University of California, Berkeley

Figure 1. Pu sorption by 1,2-HOPO resin from nitric acid.

Figure 2. Distribution
coefficients of Pu(IV)
and Pu(VI) between
0.003 M 1,2-HOPO
octylcarboxamide in
octanol and nitric
acid.

Figure 2. Distribution coefficients of Pu(IV) and Pu(VI) between 0.003 M 1,2-HOPO octylcarboxamide in octanol and nitric acid.

References

1.   D. W. Whisenhunt, Jr., M. P. Neu, Z. Hou, J. Xu, D. C. Hoffman, and
      K. N. Raymond, "Specific Sequestering Agents for the Actinides. 29. Stability of the
      Thorium(IV) Complexes of Desferrioxamine B(DFO) and Three Octadentate
      Catecholate or Hydroxypyridinonate DFO Derivatives: DFOMTA, DFOCAMC, and
      DFO-1, 2-HOPO. Comparative Stability of the Plutonium(IV) DFOMTA Complex,"
      Inorganic Chemistry **35**(14), 4128–4136 (1996).

Environmental and Biosphere Chemistry

Plutonium in Damaged Nuclear Fuel at the Chernobyl NPP Accident

S. Bogatov
A. Borovoi
S. Gavrilov
Russian Research Centre "Kurchator Institute," Russia

At the Chernobyl NPP accident in 1986 active core formed that has to be destroyed totally. This accident directly contacted with the environment more than 200 t of irradiated nuclear fuel. The fuel contained 2.1 kg of ^{238}Pu, 411.4 kg of ^{239}PU, 206.3 kg of ^{240}Pu, and 47.1 kg of ^{241}Pu.

It seemed possible after 10 years of investigations carried out both inside and nearby the damaged Unit to clarify the species of transuranics in the damaged fuel (fuel containing silicates melt and fuel dust) and to study its behavior in various environments: soil, air and water. On the basis of the studies, one can assess the radiological significance of plutonium in the environment.

Direct investigation into the chemistry of plutonium at Chernobyl is difficult, but it is reasonable to use the similarity of chemical properties of plutonium and uranium. If, before the accident, both uranium and plutonium were present in nuclear fuel as stechiometrical dioxides (UO_2, PuO_2), then as a result of accidental transformations the following forms were generated: uranium zirconium eutectic (average composition may be described as $UO_2 \cdot 7ZrO_2$), crystal formations like $(Zr,U)SiO_4$ as a result of the interaction of U-Zr-O eutectic and silicates melt, UO_x (changed stechiometry) with Zr admixtures, low (reduced by graphite during the accident) and high oxides. The latter are at present practically dissolved. It can be asserted that from 215 t of fuel (UO_2) about 10% occurred to be finely dispersed ("fuel dust") and 40% formed silicates "lava" under reactor rooms. The remaining fuel is covered at upper levels of the Unit, presumably as active core fragments with initial chemical composition.

Roughly, about one third of the dispersed fuel is now dissolved, one third is practically insoluble and, the remaining part is being dissolved slowly with kinetics similar to uranium dioxide.

As a result of urgent decontamination by means of upper soil layer excavation and subsequent burial into shallow trenches, a significant amount of fuel was in direct contact with soil and, sometimes, with subsoil water. Two to three tons of fuel are buried within so called "Sites of Temporal Radioactive Waste Localization" near the ChNPP site, about 700 kg of fuel has remained at the site after cleanup, and the amount of fuel buried in containers nearby the "Sarcophagus" walls is unknown. Most contamination of subsoil water is discovered where it immediately contacts with waste buried and contains high organics. However, even under these conditions plutonium contamination is about at the permissible level.

Analysis of plutonium air contamination at the site and the release out of openings in the encasement shows that contamination of the air environment becomes lower with time and is now less than 0.1 of the permissible level.

Plutonium contamination of water inside the damaged Unit varies broadly and can achieve dozens of Bq/l.

Cooling the fuel-containing "lavas" made possible their impregnation with water. Under the influence of weathering, the "lavas" have lost their "monolith" outward appearance and crumble into macro fragments.

Dose Formation from Transuraniums to the Population Living at the Chernobyl Alienation Zone

Potential dose formation from transuranic elements (TUE) by different pathways at the late stage of the Chernobyl accident is the least studied issue in the whole post-Chernobyl dosimetry. On the other hand, the long-term radiation situation at the Chernobyl Alienation Zone will be determined by TUE of the Chernobyl fallout. This paper considers probable ways to form and quantitatively estimate doses from transuraniums to the population living at the contaminated territory of the Alienation Zone to maintain radiation safety for further activities at this Zone.

It is shown by means of modeling that there is a definite relationship between deposition and excretion of plutonium. Thus the daily plutonium contents in urine of a local inhabitant gives the possibility to restore the plutonium contents in the skeleton for chronical peroral intake. An estimation of expected urine excretion levels of plutonium for the local inhabitants are presented. These calculations were made using the standard metabolic ICRP model and are based on the actual levels of soil plutonium contamination. The following comparison of these estimations to the actual data on plutonium contents in urine for the local inhabitants serves as ground for discussion of probable sources of plutonium intake.

A research expedition was conducted at July 1996 on the territory of the Alienation Zone. The research covered three former villages (south-south-east) where people are still living: Otashev (24 people), Opachichi (60), and Kupovatoe (80). Samples were taken from families having been living permanently at the Zone, running their own farms and owning a dairy cow. For these people internal irradiation doses from transuraniums are assessed. It is shown that a major factor (from all taken into account) of transuranium intakes following the Chernobyl accident was likely inhalation from the primary cloud.

Historically the most studied isotopes among TUE after the Chernobyl accident were alpha emitting plutonium isotopes. However, a comparative analysis of the accumulation dynamics of ^{241}Am and the sum of alpha emitting isotopes of plutonium in the skeleton show that americium becomes a most significant dose forming factor among transuraniums at the late stage of the accident.

O. A. Bondarenko
Radiation Protection Institute, Ukraine

Experimental and Modeling Studies of the Cycling of Plutonium in a Monomictic, Freshwater Reservoir

S. B. Clark
S. M. Loyland
Washington State University

Understanding the natural mechanisms controlling radionuclide cycling in contaminated ecosystems is important for prioritizing remediation needs and designing clean-up strategies. For example, contaminants might be bound in a refractory form and unavailable for cycling into the geosphere. Such a situation would pose a minimal risk to the public and should reduce the priority for remediation. Natural processes can also result in the transport of contaminants to drinking water, presenting a direct pathway for human ingestion. These kinds of contamination problems require immediate attention. Understanding the mechanisms by which natural processes increase or decrease the mobility of a contaminant should allow prediction of the consequences of remedial actions, and such knowledge may be exploited to facilitate remediation.

The seasonal cycling of ^{137}Cs and isotopes of Pu have been modeled for a contaminated lake at the Department of Energy's Savannah River Site, and modeling results have been compared to reported field observations. The system is a monomictic, 87 hectare impoundment contaminated with 5.7 TBq ^{137}Cs and undocumented quantities of actinides, including Pu. During the summer, the lake stratifies, creating anoxic conditions in the deeper portions of the lake, which increases concentrations of ^{137}Cs and Pu in the water column. Field results show that ion exchange between the NH_4^+ (produced in the lower levels of the lake during anoxia) and ^{137}Cs dominates the geochemical behavior of Cs in this system. However, observations concerning the cycling of Pu during anoxia are conflicting. Although concentrations of Fe and Mn also increase in the water column during the summer, the data do not support Pu mobilization from dissolution of Fe/Mn oxides within the sediments.

The geochemical modeling code MINTEQA2 coupled with an actinide-specific thermodynamic database has been used to describe this system during oxic and anoxic cycles. The model can adequately predict the behavior of ^{137}Cs using ion exchange as the controlling mechanism. The cycling of Fe and Mn can also be adequately described compared to field observations. For Pu, we have coupled its redox with Fe and Mn dissolution from the sediments. During oxic periods, Pu is modeled as the PuO_2^+ and PuO_2^{2+} species, whereas its valence is tetravalent and trivalent during anoxia. Allowing Pu mobilization from the sediments along with Fe and Mn during anoxia overpredicts the observed plutonium concentrations for the water column. On the other hand, allowing redox to control cycling of suspended particulates gives estimated Pu concentrations closer to the field observations. Also, considering Pu complexation by organic matter gives estimated concentrations consistent with field observations.

Based on these results, we are using large-scale laboratory systems to mimic the conditions observed in the reservoir. These mesocosms contain well characterized lake sediments and synthetic freshwater. We are using tracers for chemical analogs of Pu, while also introducing Pu into the systems in known oxidation states. The chemical analogs used are Eu(III) for trivalent Pu, Th(IV) for tetravalent Pu, NpO_2^+ for PuO_2^+, and UO_2^{2+} for PuO_2^{2+}. After introducing the tracers of Pu and the analogs, the mesocosms are cycled between oxic and anoxic systems, similar to the natural cycling of the reservoir. The partitioning of Pu within the system is compared to the partitioning of the chemical analogs to provide a basis for assigning oxidation state(s) to the Pu. These experiments are providing a scientific basis for our modeling efforts. Our modeling and experimental results to date will be presented and discussed.

An Overview of the Redox, Aqueous, and Solid Phase Speciation of Uranium in the Drainage Water Evaporation Ponds of the San Joaquin Valley, California

M. C. Duff
Los Alamos National Laboratory

C. Amrhein
University of California at Riverside

P. M. Bertsch
D. B. Hunter
University of Georgia's Savannah River Ecology Laboratory

D. E. Morris
J. A. Musgrave
Los Alamos National Laboratory

Introduction

Elevated levels of uranium (up to 22 mg L^{-1}) are found in the agricultural drainage water evaporation basins of the San Joaquin Valley (SJV), California. These basins or ponds sustain wildlife and are potential sources of U toxicity via food chain transfer. Periodically, the basins are filled with drainage waters and evaporated to dryness—which influences redox processes. The ponds vary in size from 10 to 1800 acres and are generally shallow (~1.5 m in depth). The ponds support algae (such as the green alga *Chlorella*[1]), which have been shown to sorb U(VI) to their outer surface.[2,3] Upon drying, the algae become incorporated in the sediment often, as layers of organic material (OM). The OM promotes anaerobic conditions facilitate the chemical and/or biological reduction of sediment U.

This presentation is a synopsis of over four years of research (from October 1991 to May 1995) which was conducted to determine the processes controlling U speciation and distribution in the SJV evaporation ponds.[4-8] Recently conducted and on-going research (from August 1995 to present) as described below will be presented in detail.[9] Prior to this research, the geochemistry of U in the ponds of the SJV remained largely unstudied and poorly understood.

Conducted Research

Several studies were done with regard to the processes controlling U geochemistry in the SJV evaporation ponds.[4-8] The first of these studies was performed to determine the influence of pH, carbonate alkalinity, PCO$_2$, salinity on U(VI) adsorption on an SJV soil and the mineral goethite.[4,5] Several SJV evaporation pond sediments, surface waters, ground waters, and surface salt crusts were sampled to identify the factors governing U speciation in the aqueous and solid pond phases.[5,6] Some of the factors of concern were carbonate alkalinity, salinity, drainage water U concentrations, and the dissolved Ca^{2+}: CO$_3^{2-}$ ratio in the pond water. A method, developed to separate U(VI) and U(IV) oxidation states using ion exchange chromatography in saline waters, was used to determine the redox speciation in a water in contact with reducing sediments.[7,8] Pond sediments (consisting of the surface depositional layers, 0 to 5 cm) were subjected to changes in redox status and monitored for changes in soluble U(IV) and U(VI) over time.[8] Surface sediment containing the depositional layers (11 layers were easily separated by hand) was analyzed for U(VI)/(IV) ratios with respect to depth using x-ray absorption near edge spectroscopy (XANES). The U(VI)/(IV) ratios of collected anaerobic surface sediments were measured before and after being subjected to oxidizing conditions.[8]

In the fall of 1996 and in 1997, time-resolved laser induced luminescence techniques were used to characterize fluorescent forms of U(VI) in the surface sediment layers with respect to layer depth.[9,10] The subsurface sediments (from approximately 100 cm below the pond surface) were also examined with time-resolved luminescence techniques at room and low temperature. One of the surface sediment layers was extracted for U (or treated) with various solutions, such as (NH$_4$)$_2$CO$_3$, NaHCO$_3$, H$_2$SO$_4$, a solution of 0.1 N H$_2$SO$_4$, 16.4 mM FeSO$_4$ 7H$_2$O and 8.3 mM MnO$_2$, in addition to various oxidizing agents such as Na$_2$O$_2$ and NaOC1). The solutions were analyzed by kinetic phosphorescence

analysis (KPA), and the amount of U leached was determined. The extracted sediments were examined with time-resolved laser induced luminescence. The pond surface sediment layers were equilibrated with synthetic and natural drainage waters which contained approximately 10 mg U L^{-1} in the presence of potential reducing agents. The three potential reducing agents and various conditions were *Chlorella* (in the presence of light, nutrients, vitamins, and air), sucrose (under N$_2$) and ground alfalfa (under N$_2$). The sediment-water mixtures were equilibrated with the sediments for three weeks. The sediment was separated from the waters by centrifugation. The supernatants were analyzed for dissolved U and the sediments U(VI)/(IV) ratios were determined. Scanning electron microscopy with energy dispersive analysis (SEM-EDX) and x-ray powder diffraction (XRD) were conducted to investigate the heterogeneity of the surface sediment layers.

Results

Uranium reduction was only observed in the sediments treated with alfalfa (38 and 54% of the sediment U was U(VI) for the natural and synthetic drainage water equilibrations, respectively. It was thought that U may be reduced by *Chlorella* because the alga has been shown to reduce Se(VI),[1] however, this was not observed with our system. Dissolved U was below 250 mg U L^{-1} in the alfalfa-treated equilibration whereas the other treatments had U concentrations at or slightly below that of the originally added U concentration.

Three forms of luminescent solids were observed in one of the pond sediments. In the surface sediment layers, one of the species resembled a synthetic U(VI) ternary carbonate salt. The spectra of a second resolved species was similar to mineral schoepite or synthetic hydroxycarbonate solid. The ternary carbonate salt is likely to be $Na_4UO_2(CO_3)_3$. This conclusion is also supported because the ponds contain waters which have high dissolved Na and because considerably less U was extracted in the 0.5 M Na_2CO_3 than in the 0.5 M $(NH_4)_2CO_3$ equilibrations. In the deeper, subsurface sediment, a broad unstructured species, which was distinctively different from that of the species found in the surface layers, was observed. Preliminary results from the examination of the extracted sediments suggest basic non-oxidizing solutions do not influence the luminescence behavior of the U(VI) in the sediment. The layers were found to be very homogeneous with respect to U and with respect to mineralogy. Uranium was very finely dispersed in the sediment layers.

References

1. T. W-M. Fan, A. N. Lane, and R. M. Higashi, "Selenium transformations by a Euryhaline Microalga Isolated from a Saline Evaporation Pond," *Environ. Sci. Technol.* **31**, 569–576 (1997).

2. T. Horikoshi, A. Nakajima, and T. Sakaguchi, "Uptake of Uranium by *Chlorella Regularis*," *Agric. Biol. Chem.* **43**, 617–623 (1979).

3. H-H Liu and J-T. Wu, "Uptake and Recovery of Americium and Uranium by Anacystis Biomass," *J. Environ. Sci. Health* **A28**(2), 491–504 (1993).

4. M. C. Duff, and C. Amrhein., "Uranium(VI) Adsorption on Goethite and Soil in Carbonate Solutions," *Soil Sci. Soc. Amer. J* **60**, 1393–1400 (1996).

5. M. C. Duff, "Trace Element Chemistry in the Agricultural Evaporation Basins of the San Joaquin Valley, CA: Emphasis on Uranium," Ph.D. dissertation, University of California, Riverside (1995).

6. M. C. Duff, C. Amrhein, and G. Bradford, "Nature of Uranium Contamination in the Agricultural Drainage Water Evaporation Ponds of the San Joaquin Valley, California, USA," (to be published in *Canadian J. Soil Sci.*, August issue).

7. M. C. Duff, and C. Amrhein, "Method for the Separation of Uranium(IV) and (VI) Oxidation States in Natural Waters," *J. Chrom.* A **743**, 335–340 (1996).

8. M. C. Duff, et al., "The Chemistry of Uranium in a San Joaquin Valley, California, USA, Evaporation Pond Sediment Using X-Ray Fluorescence and XANES Techniques," *Geochim. Cosmochim. Acta.* **61**, 73–81 (1997).

9. M. C. Duff, D. E. Morris, C. Amrhein, P. M. Bertsch, D. B. Hunter, and J. A. Musgrave, "Speciation of Uranium(VI) in an Evaporation Basin Sediment Using Luminescence Spectroscopy and Factors Influencing Uranium Redox Chemistry Pond Sediment" (in preparation).

10. D. E. Morris, et al., "Speciation of Uranium in Fernald Soils by Molecular Spectroscopic Methods: Characterization of Untreated Soils," *Environ. Sci. Technol.* **30**, 2322–2331 (1996).

Human Health Issues for Combined Exposures to Plutonium and Chemicals: An Experimental Toxicology Approach

G. L. Finch
C. H. Hobbs
D. L. Lundgren
J. M. Benson
F. F. Hahn
K. J. Nikula
W. C. Griffith
M. D. Hoover
E. B. Barr
S. A. Belinsky
B. B. Boecker
J. L. Mauderly
Lovelace Respiratory Research Institute

Introduction

Workers throughout the DOE complex may be exposed to combinations of various agents. The possibility that chemicals and/or radiation may interact in producing deleterious effects in exposed individuals has been recognized for some time. Although there is a substantial body of knowledge on how specific interactions influence various biological endpoints, no comprehensive framework exists that allows one to reliably predict health effect outcomes from combined exposures. As a result, regulators have relied on simple additive models for setting exposure standards.

An Experimental Toxicology Approach

Using laboratory studies in rodents, we are investigating how combinations of exposures interact to modify the risks of adverse health effects, compared to risks predicted by additive models of the agents acting individually. Specific experiments have been designed to determine the general classes of toxic agents, exposure conditions, and mechanisms of interaction which are likely to be synergistic, additive, or less than additive. Combinations chosen for study were based on commonly encountered combinations of chemical and radioactive agents found in the nuclear workplace. Experiments are focused around inhaled ^{239}Pu, thus drawing upon our extensive knowledge of the health effects of this radionuclide alone. Multi-species and molecular studies are included as a basis for understanding the mechanisms of disease development in order to better extrapolate the results of the animal studies to humans.

This ongoing project is centered around life-span carcinogenicity studies in F344 rats exposed to inhaled ^{239}PuO$_2$ combined with either (1) chronically inhaled cigarette smoke, (2) an injected organic chemical carcinogen (the tobacco-specific nitrosamine, NNK), (3) external, whole-body x-ray exposure, or (4) inhaled beryllium metal, a suspected human carcinogen. Sub-chronic studies are examining combinations of inhaled ^{239}Pu(NO$_3$)$_4$ and CCl$_4$. Each carcinogenesis study uses some 800 to 5,000 rodents to provide sufficient statistical power to identify carcinogenesis from each agent alone, and to analyze interaction terms. These studies are either still under way or are being analyzed and reported.

Results can be placed into three general categories: (1) dose-modifying interactions; (2) carcinogenic interactions; and (3) multiple species and mechanistic evaluations. Regarding dose modifications, the clearance of ^{239}Pu from the lung is retarded by either cigarette smoke or metallic beryllium, and the uptake and retention of ^{239}Pu in the liver are enhanced by CCl$_4$ inhalation. In the case of cigarette smoke, animals chronically inhaling 250 mg total particulate matter/m^3 have lifetime radiation doses from ^{239}Pu approximately twice those in animals inhaling ^{239}PuO$_2$ alone. Dose-modifying effects were also observed in the CCl$_4$ experiment, in which exposure to CCl$_4$ did not alter the pulmonary clearance of the ^{239}Pu or tracer particles in either rats or Syrian hamsters, but compared with rats, the hamsters had decreased uptake and retention of ^{239}Pu in the liver with higher CCl$_4$ doses, due to CCl$_4$-induced toxicity in that organ.

A pronounced synergism in lung tumor formation results from combined exposures to ^{239}PuO$_2$ and cigarette smoke. Prevalences of benign or malignant lung

tumors in rats exposed for at least 12 months to low or high cigarette smoke concentrations without $^{239}PuO_2$ are similar to values in controls (prevalences range from 0 to 3%), except for a statistically significant increase in female rats exposed to the high level (prevalence of 7%). However, prevalences in groups of rats exposed to only $^{239}PuO_2$ or to $^{239}PuO_2$ combined with low or high cigarette smoke levels are 27, 55, and 73%, respectively. The extent to which this interaction is due to increased radiation dose from smoke-induced lung clearance reduction is being examined. In addition, preliminary data indicate that inhaled $^{239}PuO_2$ and metallic beryllium also interact synergistically in producing lung tumors in the rat. In contrast, the carcinogenic interaction between $^{239}PuO_2$ and x-rays is no greater than additive. X-irradiation, however, was shown to significantly reduce the median life-span of exposed rats. This life-span shortening effect necessitates an evaluation of age-specific tumor prevalences in the study groups before final conclusions can be made.

To support efforts to extrapolate results to humans, other species are being studied, and molecular changes within exposure-induced tumors are being examined. Multi-species studies are demonstrating that (1) whereas metallic beryllium is a potent lung carcinogen in rats, at comparable lung burdens metallic beryllium is either non-carcinogenic or weakly carcinogenic to the lungs of either of two strains of mice (A/J or C3H/HeJ), and (2) differences exist in the liver toxicity of inhaled CCl_4 between rats and hamsters, and these toxicity differences translate into differences in hepatic disposition of ^{239}Pu inhaled as $^{239}Pu(NO_3)_4$. One mechanistic study employs a special animal model, heterozygous transgenic p53$^{+/-}$ knockout mice having one of the two p53 tumor suppressor gene alleles inactivated, and is demonstrating that neither inhaled $^{239}PuO_2$ or metallic beryllium is a lung carcinogen in this model, suggesting that the p53 gene might not play a significant role in lung carcinogenesis from these materials. Other mechanistic studies are examining mutations to the gene targets p53, K-ras, and c-raf-1 in rodent lung tumors induced by the agents being studied either alone or in combination.

Conclusion

The goal of this work is to understand how hazardous materials, particularly ^{239}Pu and the other agents being studied, interact in causing lung cancer. Carcinogenic interactions observed range from simple additivity to certain cases in which synergism is being seen. This information can aid in setting appropriate, scientifically justified workplace exposure standards for (1) routine radiological work, (2) ongoing and future plant decontamination and decommissioning, and (3) environmental cleanup activities. Additional work is required to (1) complete the experiments described here, (2) further our understanding of how the results can be extrapolated to humans, and (3) identify and conduct additional studies pertinent to the DOE complex in this important area.

Column Tests to Study Selected Mechanisms for Plutonium Transport in Sedimentary Interbed at the INEEL Site

In previous laboratory column studies in crushed basalt and in sedimentary interbed, we have observed a fraction of the plutonium to be transported rapidly through the columns. These "high mobility fractions" ranged from 10% to 70% in crushed basalt and from 0.1% to 1% in interbed. Experiments are currently being conducted to study plutonium transport in interbed in more detail. The specific objectives are (1) to characterize the transport of Pu(IV) and Pu(V) in simulated perched water at the INEEL, (2) to isolate the conditions under which high mobility fractions are observed, and (3) to suggest mechanisms that may be responsible for high mobility fractions.

A simulated perched water will be produced in which the concentrations of bicarbonate, sulfate, fluoride, EDTA, fulvic acid, and humic acid exceed those which are observed in field samples. These constituents were selected based on their potential to form soluble complexes with plutonium. The simulated perched water will be spiked with either Pu(IV) or Pu(V) and tritium. Tritium is used as a non-partitioning tracer to evaluate column dynamics and check for channeling. A column experiment is performed by introducing one pore volume of the spiked simulant and eluting with 1000 to 2000 displaced pore volumes of unspiked simulant. The eluate is collected in discrete fractions and analyzed by liquid scintillation counting. The method of moments is used to determine retardation factors of both the high mobility fraction and the other fraction, if observed. If all of the plutonium is not recovered, the soils in the columns are fractionated and analyzed to locate the remainder. For modeling purposes, distribution coefficients are calculated from retardation factors.

The importance of colloidal mechanisms in high mobility transport will also be studied by conducting experiments in the presence and absence of colloids. A base-line study for Pu(IV) and Pu(V) will be conducted with the simulated perched water in the presence of colloids (i.e., an unwashed or chemically altered column). In subsequent experiments, the colloids and chemical constituents will be systematically removed to isolate factors affecting high mobility transport of plutonium.

R. A. Fjeld
J. T. Coates
A. W. Elzerman
Clemson University

J. D. Navratil
D. K. Jorgensen
Lockheed Martin Idaho Technologies Company

Microbial Transformations of Actinides

A. J. Francis
Brookhaven National Laboratory

The actinides in wastes and contaminated soils are present in various forms, such as elemental, oxide, coprecipitates, inorganic and organic complexes, and naturally occurring minerals. Of the actinides, Th, U, Pu, Am, and Np are of primary concern because of the potential for migration from the waste repositories and contamination of the environment. Microorganisms play a major role in the transformation of the actinides which affect the solubility, bioavailability, and mobility. Under appropriate conditions, dissolution or precipitation of actinides is brought about by the direct enzymatic or indirect actions of microorganisms. These include (1) oxidation-reduction reactions, (2) changes in pH and Eh, (3) chelation or production of specific sequestering agents, (4) biosorption by biomass and biopolymers, (5) formation of stable minerals, and (6) biodegradation of actinide-organic complexes. Fundamental information on the biotransformation of actinides under various microbial process conditions will be useful in developing appropriate remediation and waste management strategies as well as predicting the microbial impacts on the long-term performance of the waste repositories. Among the actinides, transformation of uranium by microorganisms has been extensively studied. We have only limited information on the biotransformation of other actinides. Initial results on the dissolution, precipitation, and biosorption of inorganic and/or organic complexes of the ^{238}U, ^{232}Th, ^{239}Pu, ^{243}Am, and ^{237}Np by pure and mixed cultures of bacteria isolated from wastes and from hypersaline environments will be presented. In addition, the mechanisms of biotransformation of several forms of uranium, i.e., ionic, inorganic- and organic-complexes, and mixed metal-organic complexes commonly present in wastes and contaminated sites under various microbial process conditions, will be discussed.

Worker Protection Issues for Monitoring Airborne Plutonium

A technically defensible air monitoring program is essential to protecting workers in plutonium facilities. Adequate monitoring for routine and accidental releases of plutonium requires basic knowledge about potential source terms and suitable techniques for providing an early warning of unusual aerosol concentrations in the workplace. This paper summarizes recent progress in the qualification and use of alpha continuous air monitors (CAMs) to protect workers from airborne plutonium.

M. D. Hoover
G. J. Newton
B. R. Scott
Lovelace Respiratory Research Institute

Qualification of New Continuous Air Monitors

Qualification tests at our institute and other locations have been under way to determine the aerosol collection efficiency, detection efficiency, minimum detectable activity, and other operating characteristics of alpha CAMs. Equipment to perform the aerosol qualification tests includes aerosol wind tunnel systems; aerosol generators for inert tracer particles, radon progeny, and plutonium; optical scanners for determining the homogeneity of particle collection on filters; and radiation detection and radiochemistry systems for verifying the actual collection of radioactivity. Instrument type-testing equipment has also been used to determine the sensitivity of CAMs to temperature, humidity, vibration, radiofrequency interference, and other environmental effects. Criteria have been developed for the uniformity of radioactivity on NIST-traceable, electroplated sources used for calibration of alpha CAMs. For sources with a diameter of 25 mm or 47 mm, we recommend that each 10 mm^2 area of the source have an activity concentration within 10% of the mean concentration. Acceptable characteristics for collection filters include high collection efficiency, good front-surface collection capabilities for alpha spectroscopy, rugged construction to avoid damage, low pressure drop to allow adequate flowrates, and suitability for chemical dissolution, as needed. The Fluoropore 5-μm pore size filter from Millipore Corporation (Bedford, MA) provides excellent performance in a teflon membrane, and the Millipore AW-19 filter is an excellent alternative in a mixed-cellulose ester filter suitable for chemical dissolution. The Fluoropore filter is now made with a black-fiber backing to differentiate the support side from the collection side. The collection efficiency for these filters is greater than 99.9% at the most penetrating particle size of 0.3 μm aerodynamic diameter. Dorrian and Bailey[1] have reported that the typical aerosol size distribution for radioactive particles in the workplace has an activity median aerodynamic diameter of about 5 μm with a geometric standard deviation of 2.5.

The Role of Continuous Air Monitoring

Use of CAMs in the workplace has been emphasized in regulatory requirements such as the U.S. Department of Energy's rule for Occupational Radiation Protection (10CFR835).[2] Along with visual indicators of problems and direct detection of contaminated hands, feet, clothing, or work surfaces, CAMs are intended to provide a realtime, early warning of problems. According to the DOE rule, for the airborne radioactive material that could be encountered, realtime air monitors shall have alarm capability and sufficient sensitivity to alert potentially exposed individuals that immediate action is necessary to minimize or terminate inhalation exposures. In addition, the false alarm rate must be tolerable because excessive numbers of false alarms will reduce the CAM's credibility as an early warning device in the eyes of the worker. It is recommended that false alarms should not exceed one per month per unit. The recommended sensitivity is 8 Derived-Air-Concentration-hours (8 DAC-h) under laboratory conditions of low

dust interference and low radon concentrations. Hoover and Newton[3] have described laboratory conditions as involving less than 10 μg/m³ dust concentrations and ^{218}Po concentrations greater than 0.1 pCi/L. Assuming a typical indoor equilibrium factor of 50% for radon and its decay products, that concentration of ^{218}Po is equivalent to 0.2 pCi/L radon. Typical indoor radon concentrations are about 0.2 to 0.4 pCi/ L, but can be substantially higher for poorly ventilated areas with concrete construction. Most modern alpha CAMs have well-designed sampling inlets, use alpha spectroscopy to discriminate between plutonium and ambient radon progeny radionuclides, and allow adjustments to the sample integration time and the algorithm for background subtraction to meet the sensitivity requirement. Actual conditions of ambient dust and radon concentrations may require that the alarm be raised to a setpoint such as 24 DAC-h. Dust concentrations less than 0.2 mg/m³ over an 8-h period cause negligible attenuation of the collected alpha radioactivity. In any case the conditions and alarm setpoint are to be documented.

Other Considerations

Scott et al.[4] have noted that sampling for the high-specific-activity isotopes of plutonium such as ^{238}Pu may be problematic because the particle number concentration can be very small at the allowed radioactivity concentration for worker exposure. The specific activity of ^{238}Pu is about 280 times greater than that of ^{239}Pu, and many thousands of breaths may be required before a worker inhales a particle of ^{238}Pu when the airborne radioactivity concentration is less than 100 DAC.

Proper placement of the instruments has also been a concern. The traditional thought has been that the best location for air monitors is near the exhaust vents, unless there are obvious locations of potential release. Recent work by Whicker et al.[5] have shown that other locations in the room may provide a shorter response time, and thereby minimize potential exposures to workers.

Conclusion

A balanced worker protection program includes a well-trained staff, strict adherence to adequate operating procedures, frequent monitoring of surfaces for radioactivity, and proper storage of materials and waste. Although concerns such as low particle number concentration and proper placement of CAMs will remain problematic, an improved understanding of the behavior of workplace aerosols and the performance requirements for CAMs is improving our ability to protect workers.

References

1.   M. D. Dorrian and M. R. Bailey, "Particle Size Distributions of Radioactive Aerosols Measured in Workplaces," *Radiation Protection Dosimetry* **60** (2), 119–133 (1995).

2.   U.S. Department of Energy, *Occupational Radiation Protection; Final Rule*, Title 10, Code of Federal Regulation, Part 835, December 14, 1993.

3.   M. D. Hoover and G. J. Newton, "Calibration and Operation of Continuous Air Monitors for Alpha-Emitting Radionuclides," *Proceedings of the 1993 DOE Radiation Protection Workshop*, Las Vegas, Nevada, April 13–15, 1993.

4. B. R. Scott, M. D. Hoover, and G. J. Newton, "On Evaluating Respiratory Tract Intake of High Specific Activity Alpha Emitting Particles for Brief Occupational Exposure," *Radiation Protection Dosimetry* **69** (1), 43–50 (1997).

5. J. J. Whicker, J. C. Rodgers, C. I. Fairchild, R. C. Scripsick, and R. C. Lopez, "Evaluation of Continuous Air Monitor Placement in a Plutonium Facility," *Health Physics J.* **72** (5), 734–743 (1997).

Thermodynamic Simulation of Possible Solubility Limits of Pu(IV) and (III) Oxides and Fluorides in Modeling Underground Waters

The code GBFLOW developed in the Department of Geochemistry of the Moscow State University has been used to model the migration of plutonium in geological media. It has an advantage in comparison with other codes for minimization of free energy of the chemical system as it can account for changes in compositions of both solid and solution phases during the rock/water interaction. It uses the concept of successive known Helgeson reactions which are useful for describing the dynamics of the solubility process as a function of the water/rock interaction at various times throughout the history of the geologic repository.

The subsequent behavior in the "far" field after leaving the backfill barrier must include first of all hydrolytic and complexation by such anionic species as CO_3^{2-}, F^-, Cl^-, and SO_4^{2-} which are present. The special database of stability constants for Pu inorganic complexes was compiled with the use of data by Allard (1982) for hydroxide, fluoride, and sulfate species, Fuger (1983) for chlorides, and Fuger et al. (1992) for carbonates. Thermodynamic properties were taken from Barin (1989) for solid plutonium oxides and fluorides and from Brookins (1988) for solid $Pu_2(CO_3)^3$.

As a major result, three types of models evaluating solubility limits of plutonium solids and solution speciation are presented and compared. They reflect physical-chemical situations in the following bedrocks from sites considered for geological repositories:

1. Finnsjon Sweden granite and Boom clay from Belgium with underground waters of bicarbonate type (220–250 mg/l HCO_3^-);

2. Hanford basalt with waters arranging high contents of chloride (148 mg/l), fluoride (37–52 mg/l) and sulfate (108 mg/l);

3. Bottstein Swiss granite with thermal sulfate-chloride waters of high (13274 mg/l) total mineralization (Grindrod et al., 1995).

This set of ground water compositions allows us to evaluate the speciation and migration ability of plutonium in very different "far" field situations.

G. R. Kolonin
United Institute of Geology, Geophysics and Mineralogy, Russia

G. R. Choppin
Florida State University

Batch Sorption Results for Americium, Neptunium, Plutonium, Technetium, and Uranium Transport through the Bandelier Tuff, Los Alamos, New Mexico

Quantifying the migration of radionuclides through the Bandelier Tuff is essential in conducting the Performance Assessment for Material Disposal Area-G, Technical Area-54, Los Alamos National Laboratory. This investigation was conducted as part of the Performance Assessment and Composite Analysis for Technical Area-54 (the current solid low-level radioactive waste disposal area) to satisfy DOE Order 5820.2A, Radioactive Waste Management (September 1988). The purpose of this investigation is to provide the results of batch-sorption experiments of Am(III), Np(V), Pu(V), Tc(VII), and U(VI) performed on the Bandelier Tuff.[1] Results obtained from these experiments are required for solute-transport calculations and serve as input to the mass-heat transfer model FEHM (Finite Element Heat and Mass Transfer).[2]

The sorption of radionuclides on Bandelier Tuff is controlled by (1) the surface area and mineralogy of the tuff and (2) by the water chemistry of the solution in contact with the tuff. The dominant adsorbents within the Bandelier Tuff are inferred to include glass, hematite, smectite, amorphous $Fe(OH)_3$, kaolinite, and possibly calcite. Water Canyon Gallery ground water, discharging from the Bandelier Tuff, was used in the batch sorption experiments. This ground water is relatively oxidizing and is characterized by a calcium-sodium-bicarbonate ionic composition with a total dissolved solids content less than 130 mg/L. The distribution coefficients for radionuclides measured on the Bandelier Tuff, at a pH value of 7.3, decrease in the following order: Am(III) >> Pu(V) > U(VI) >> Np(V) > Tc(VII). The median distribution coefficients, using Water Canyon Gallery ground water, for Am(III), Np(V), Pu(V), and U(VI) are 141, 0.25, 20.4, and 5.14 ml/g, respectively. The distribution coefficients for Tc(VII) are all negative and therefore, they are assumed to be zero.

Vadose-zone pore water was extracted from the Bandelier Tuff using an Unsaturated/Saturated Flow Apparatus.[3] The pore water is characterized by a sodium-carbonate-bicarbonate solution with a total dissolved solids content of greater than 1300 mg/L. The pH values of the pore water samples range from 9.2 to 9.8, and the solutions are oversaturated with respect to calcite. The distribution coefficients for radionuclides measured on the tuff samples using the synthetic pore water, at a pH value of 9.8, decrease in the following order: Am(III) >> Pu(V) > U(VI) > Np(V) > Tc(VII). The median distribution coefficients, using a synthetic pore water, for Am(III), Np(V), Pu(V), and U(VI) are 2359, 1.88, 8.06, and 2.44 ml/g, respectively. The distribution coefficients for Am(III) and Np(V) using synthetic pore water are higher than the distribution coefficients for these two actinides using Water Canyon Gallery ground water.

Geochemical modeling, using the computer code MINTEQA2[4] that contains the most appropriate thermodynamic data for the actinides of interest,[5–9] was performed to evaluate solute speciation and solid phase saturation. Results of the computer simulations suggest that the dominant aqueous complexes of Am(III) and Np(V) for the synthetic pore water-Bandelier Tuff system are $Am(CO_3)_3^{3-}$ and $NpO_2(CO_3)_3^{5-}$, respectively. In addition, the aqueous complexes of Pu(V) and U(VI) in this system are predicted to include PuO_2^+, PuO_2OH^0, and $UO_2(CO_3)_3^{4-}$. The synthetic pore water is predicted to be undersaturated with respect to $Am(OH)_3(s)$, $Am(OH)_3(am)$, $AmOHCO_3$, $PuO_2OH(am)$, $NPO_2OH(am)$, $NPO_2OH(aged)$, $NaNpO_3 \cdot 3.5H_2O$, $NaNpCO_3$, and $UO_2(OH)_2$. Enhanced sorption

P. Longmire
C. R. Cotter
I. R. Triay
J. J. Kitten
A. I. Adams
Los Alamos National Laboratory

of Am(III) and Np(V) carbonato complexes on calcite is possible through surface exchange with carbonate and bicarbonate functional groups present on the calcite surface in the vadose zone.

Results of the batch sorption experiments were used as input to solute transport calculations for the Performance Assessment of Technical Area-54. The maximum dose for the ground water pathway including receptors downgradient of Technical Area-54, calculated over the 1,000 year compliance period, is 3.5×10^{-5} mrem/year. The performance objective for groundwater protection is 4 mrem/year. These batch experimental results confirm that sorption of actinides onto Bandelier Tuff at Technical Area-54 is a significant geochemical process that controls the migration of contaminants in the subsurface.

References

1. P. Longmire, C. R. Cotter, I. R. Triay, J. J. Kitten, C. Hall, J. Bentley, D. J. Hollis, and A. I. Adams, "Batch Sorption Results for Americium, Neptunium, Plutonium, Technetium, and Uranium Transport Through the Bandelier Tuff, Los Alamos, New Mexico," Los Alamos National Laboratory report LAUR-96-4716 (1996), p. 41.

2. G. A. Zyvoloski, Z. V. Dash, and S. Kelhar, "FEHM: Finite Element Heat and Mass Transfer Code," Los Alamos National Laboratory report LA-1 1224-MS (1988).

3. J. Conca, and J. Wright, "Find Transport Data Faster," *Soil and Groundwater Cleanup*, (December 1995), pp. 14–26.

4. J. D. Allison, D. S. Brown, and K. J. Novo-Gradac, "MINTEQA2/PRODEFA2, A Geochemical Assessment Model for Environmental Systems: Version 3.0 User's Manual," U.S. Environmental Protection Agency report EPA/600/3-91/021 (1991).

5. I. Grenthe, J. Fuger, R. J. M. Konings, R. J. Lemire, A. B. Muller, C. NguyenTrung, and H. Wanner, "Chemical Thermodynamics of Uranium," Nuclear Energy Agency Thermochemical Data Base Project (Saclay: OECD Nuclear Energy Agency, 1992), pp. 29–62.

6. J. F. Kerrisk and R. J. Silva, "A Consistent Set of Thermodynamic Constants for Americium(ill) Species with Hydroxyl and Carbonate," in *Proceedings of the Workshop on Geochemical Modeling* (Fallen Leaf Lake, California, 1986), pp. 167–175.

7. R. J. Lemire, "An Assessment of the Thermodynamic Behavior of Neptunium in Water and Model Groundwater from 25 to 150°C," Atomic Energy of Canada Limited report AECL-7817 (1984).

8. R. J. Lemire, and P. R. Tremaine, "Uranium and Plutonium Equilibria in Aqueous Solutions to 200°C," *Jour. Chem. Eng. Data.* **25** (1980), pp. 361–370.

9. H. Nitsche, R. C. Gatti, E. M. Standifer, S. C. Lee, A. Muller, T. Prussin, R. S. Deinhammer, H. Maurer, K. Becraft, S. Leung, and S. A. Carpenter, "Measured Solubilities and Speciations of Neptunium, Plutonium, and Americium in a Typical Groundwater (J-13) from the Yucca Mountain Region, Milestone Report 3010-WBS 1.2.3.4.1.3.1," Los Alamos National Laboratory LA-12562-MS (1993), p. 127.

Iron Oxide Colloid Facilitated Plutonium Transport in Ground water

Sorption of [239]Pu onto iron oxide colloids in ground water plays an important role for transport of Pu along potential flowpaths from actinide-contaminated areas and release to the accessible environment. A natural ground water (pH 8.25, alkalinity 20 meg/L) and a carbonate-rich synthetic ground water (pH 8.47, alkalinity 22.5 meg/L) , which were filtered through a 0.05-μm membrane, were used as media. Two iron oxides (e.g., synthetic hematite and synthetic geothite) and two oxidation states of [239]Pu, including Pu(IV) which is a polymer with particle size of 100 Å and Pu(V) which is a soluble form, were used in this study. We performed laboratory batch sorption experiments to evaluate: (1) sorption of Pu as a function of two different iron oxide colloids; (2) sorption of Pu as a function of two different oxidation states; and (3) sorption kinetics of Pu(IV) and Pu(V) onto these iron oxide colloids.

The preliminary results show that sorption of Pu is a rapid process. After a 10 minute period of sorption, hematite sorbed 46.7% to 90% of Pu(V) and sorbed 79% to 96% of Pu(IV); geothite sorbed 21% to 70% of Pu(V) and sorbed 39% to 44% of Pu(IV)(see Table 1). Thereafter, the amounts of Pu adsorbed increased with time, except the sorption of Pu(IV) on to hematite in synthetic ground water which did not change with time. After 24 hours, hematite sorbed 76% to 96% of Pu(V) and 82% to 96% of Pu(IV); geothite sorbed 57% to 82% of Pu(V) and 51% to 76% of Pu(IV). Hematite sorbed more Pu(IV) than Pu(V), whereas geothite sorbed more Pu(V) than Pu(IV). Iron oxide colloids sorbed more Pu in the synthetic ground water than in the natural ground water. Pu oxidation state and Pu-carbonate or Pu-bicarbonate complexes may influence sorption rate. The results also show that hematite colloids sorbed more Pu than geothite. This was due to the difference of their crystal structure, surface structure, particle shapes, and potential surface charge. During this experimental duration, precipitation of Pu(V) and Pu(IV) in the initial solution did not occur.

To confirm the results from these experiments, three additional batch experiments are being conducted to examine: (1) sorption of Pu onto iron oxide colloids, in nanopure deionized water, under carbon dioxide free environments; (2) desorption of Pu from iron oxide to look at how strong Pu binds to iron oxide colloidal particles; and 3) stability of hematite and geothite in natural ground water and synthetic ground water.

Time	Fe_2O_3J13. Pu(V) %	Fe_2O_3J13. Pu(IV) %	Fe_2O_3SY. J13.Pu(V) %	Fe_2O_3SY. J13.Pu(IV) %	FeOOH. J13.Pu(V) %	FeOOH. J13.Pu(IV) %	FeOOH.SY. J13.Pu(V) %	FeOOH.SY. J13.Pu(IV) %
10 min	46.7	78.5	90.3	96.2	20.6	39.3	69.8	43.8
30 min	48.5	81.2	92.9	96.3	22.0	42.9	69.5	42.9
1 h	51.5	82.4	91.9	95.7	25.2	62.2	70.5	70.1
4 h	58.6	82.4	96.2	95.6	38.2	55.6	75.5	70.0
6 h	63.3	82.4	96.0	95.9	43.4	53.7	77.3	76.7
24 h	75.5	82.4	95.7	95.6	57.1	51.4	82.0	76.2

Table 1. Percentage of [239]Pu adsorbed onto hematite and geothite colloids in a natural ground water and a synthetic ground water as a function of time.

N. Lu
C. R. Cotter
H. D. Kitten
I. R. Triay
Los Alamos National Laboratory

Sensitivity of the Consequences of Severe Accidents in Mixed-Oxide-Fueled Reactors to Actinide Release and Transport

Introduction

E. S. Lyman
Nuclear Control Institute

The Department of Energy (DOE) has decided to pursue a "two-track" approach for disposition of excess weapons plutonium: immobilization of a fraction of the excess with high-level waste in glass or ceramic, and conversion of the remainder to mixed-oxide (MOX) fuel and irradiation in existing reactors, most likely U.S. light-water reactors (LWRs).

For two reasons, a thorough characterization of the incremental environmental, health, and safety impacts associated with the substitution of MOX fuel for uranium oxide fuel in existing reactors will be essential for determination of the viability of the MOX track for plutonium disposition. First, with regard to compliance with the National Environmental Policy Act (NEPA), an accurate comparison of these incremental risks to risks associated with the immobilization alternative will be necessary to inform further decision-making. Second, during the course of the licensing process for use of MOX in reactors, the Nuclear Regulatory Commission (NRC) will have to determine whether such use will increase the probability or consequences of a reactor accident, and if so, whether such increases will be "significant."

The concentrations of actinides at any point in the reactor operating cycle will be several times greater in weapons-grade MOX cores than in uranium oxide cores.[1] Therefore, a quantitative assessment of the incremental consequences of severe accidents will depend on a detailed understanding of actinide release and transport mechanisms, which depend on the chemical speciation of actinides in the MOX-fueled reactor core, in the containment atmosphere, and in the external environment. However, there are considerable uncertainties in the current understanding of core melt chemistry, and estimates of actinide release fractions vary over several orders of magnitude.[2] To clarify this issue for regulatory purposes, these uncertainties should be reduced.

The common assumption that the incremental consequences associated with MOX will be marginal and do not require consideration, because of the low probability of accidents of severity great enough to mobilize refractory elements such as the actinides, is inaccurate from both regulatory and technical perspectives.

Source terms for beyond-design-basis accidents play a role in a number of regulatory functions, including determination of the sizes of emergency planning zones for nuclear plants and risk determinations in plant environmental impact statements. The source term recently adopted for use by the NRC, NUREG-1465, does assume release of a small fraction (approximately 0.5%) of the low-volatile radionuclide inventory in such accidents.[3]

Under some conditions, higher actinide release fractions can occur. For example, it is now estimated that 3.5% of the actinide inventory was released during the Chernobyl accident.

Description of Work

This paper consists of two parts. The first is an analysis, using the MACCS code, of the sensitivity to actinide release fractions of the incremental severe accident consequences (aggregate health effects and acute and chronic individual doses) associated with MOX use. The second is a literature review which identifies chemical and physical phenomena that may affect actinide release fractions, describes uncertainties in current understanding, and outlines future work that may be necessary to resolve outstanding questions.

Results

Preliminary results indicate that under some circumstances, actinide releases can contribute significantly to the consequences of severe accidents in MOX-fueled reactors, increasing both acute and chronic individual exposures in the plume path by as much as 50% (note: this is work in progress and results are being refined). However, uncertainties in actinide release fractions, as well as in calculated radionuclide inventories, lead to wide variations in these predictions.

Use of the NUREG-1465 source term tends to minimize the incremental consequences of MOX use. However, the intent of this source term is to provide values that are "representative or typical, rather than conservative or bounding." In particular, it does not fully account for accidents that create highly reducing conditions in the core, a situation that can greatly enhance actinide releases.

Moreover, there are indications that NUREG-1465, which was developed for uranium fuel, is not appropriate for MOX and underestimates the low-volatile release fraction. NUREG-1465 may not be applicable to high-burnup uranium oxide fuel because of recent information that such fuel is prone to violent failure during reactivity insertion accidents (RIAs), leading to release of a significant fraction of the fuel in a highly fragmented or powdered form.[3] This should hold even more strongly for high-burnup MOX fuel, because of recent indications that it is more vulnerable than uranium oxide fuel of the same burnup to RIAs.[4]

Moreover, NUREG-1465 is based primarily on fission product release tests involving irradiated uranium oxide fuel and does not account for either the greater fission gas release from high-burnup MOX fuel (up to seven times greater than uranium oxide) or microstructural differences that may affect low-volatile releases.

For these reasons, development of a regulatory source term specific to weapons-grade MOX fuel is advisable.

References

1. See for example, *Study of Plutonium Disposition Using Existing GE Advanced Boiling Water Reactors*, GE Nuclear Energy report NEDO-32361 (June 1, 1994).

2. H. P. Norubakhsh, "Estimates of Radionuclide Release Characteristics into Containment Under Severe Accidents," United States Nuclear Regulatory Commission report NUREG/CR-5747 (November 1993).

3. "Accident Source Terms for Light-Water Nuclear Power Plants," United States Nuclear Regulatory Commission report NUREG-1465 (December 1994).

4. Institut De Protection Et De Surete Nucleaire (IPSN, France), "Nouveau Test de l'IPSN Sur la Tenue du Mox a Haut Taux de Combustion," IPSN press release (January 30, 1997).

The Distribution and Physicochemical Characterization of Uranium in U-Contaminated Soils after Leaching with Sodium Bicarbonate

Introduction

During the summer of 1996, a pilot remedial action was performed at Technical Area-33 (TA-33), Los Alamos. The area at TA-33 had been used for firing uranium projectiles resulting in a contaminated earth catch box. Nine rectangular containers, each holding one ton of uranium (U) contaminated soil, were leached with sodium bicarbonate using an unsaturated flow system. This resulted in U removal of about 90% of the initial contamination through the formation of the soluble tris carbonate uranyl species, $UO_2(CO_3)_3^{2-}$ as follows:

$$UO_2^{2+} + 3HCO_3^- = UO_2(CO_3)_3^{2-} + 3H^+$$

These results have been reported elsewhere.[1]

By comparing the pre- and post-leach characteristics of the soil, details about the process are revealed including the effect of the lixiviant on the residual uranium and on the soil profile. Additional effects include: preferential flow pathways, solubilities of initial uranium minerals, changes in surfaces of solid uranium phases, pore water content, migration rates, and particle size distribution of the soil's components.

The objectives of the research described here are to:

1. Identify the distribution and characterization of the residual uranium
2. Determine the distribution of uranium as a function of soil particle size
3. Determine the transport rate of the clay-sized particles

The results obtained will improve the performance of future remedial actions, and help define the optimization of conditions. In addition, they define some of the parameters governing the solubility of uranium species. Information about the movement of clay minerals and other colloids in the subsurface is of generalized importance as several radionuclides (^{137}Cs, ^{238}Pu, ^{239,240}Pu, ^{241}Am) adsorb strongly onto clays.

The study reports the pre- and post-leach physico chemical characterization of the soil.

Description of the Work

Composited samples of the U-contaminated soil were taken prior to leaching. One of the nine containers was subject to 0.5 M sodium bicarbonate for 21 days at a flow rate of 0.1 cc/min. After 21 days, nine core units were drilled (center, corners, and middle of sides), and samples taken at measured intervals along the core. Following sample collection, these core samples were dried, separated into sand, silt, and clay-sized materials, and analyzed for total U using a Kinetic Phosphorescence Analyzer (KPA).

C. F. V. Mason
N. Lu
H. D. Kitten
M. Williams
P. Longmire
B. Thomson
W. R. J. R. Turney
Los Alamos National Laboratory

Results

The characterization of the original soil before leaching is shown in Table 1.

Table 1. Characterization representative U-contaminated soils prior to leaching.

pH	6.9
Gravel	46.4%
Sand	38.3%
Silt	9.3%
Clay	6.0%
Organic matter	1.6%
Moisture content	9.8%
Characterization by X-ray-diffraction	schoepite $(UO_3 \cdot 2H_2O)$
ΣU concentration by delayed neutron activation analysis	17,141 mg U/kg

Preliminary results of the pre- and post-leached soils suggest uniform residual uranium distribution, implying uniform flow of lixiviants without preferential pathways. However the results also indicate migration of the smaller soil particles to the base of the leach container.

These results will be discussed in detail.

Reference

1.   W. R. J. R. Turney, C. F. V. Mason, N. Lu, M. C. Duff, and D. Dry, "Pilot Treatment Project for the Remediation of Uranium-Contaminated Soil at a former Nuclear Weapons Development Site at the LANL," Waste Management '97, Tucson, Arizona, Los Alamos National Laboratory document LA-UR-96-3914.

Human Health Issues for Plutonium Inhalation: Perspectives from Laboratory Animal Studies

Introduction

Since the first production of plutonium in the 1940s, potential health effects from plutonium have been a concern for humans. The few people exposed to plutonium and the relatively small intakes that have occurred, at least in the western world, have resulted in very little direct information from human population studies. The Manhattan Project workers have been followed for decades and few health effects observed. The situation is similar for the population of workers at the Rocky Flats facility. Some information is now being released from the former Soviet Union on selected worker populations who show biological effects, primarily pulmonary fibrosis and some increase in lung cancers.

Information From Studies With Laboratory Animals

Due to the lack of human data until very recently, animal studies were conducted to provide information of the metabolism and toxicity of plutonium. Early studies showed that plutonium is poorly absorbed from the gastrointestinal tract and through the intact skin. From these data, inhalation or penetrating skin wounds were clearly the most important exposure routes for potential human exposure. For this reason, studies were initiated at the Lovelace Respiratory Research Institute on the toxicity of inhaled plutonium. These studies were directed at several important health issues: (1) the toxicity of inhaled plutonium isotopes $^{239}PuO_2$ and $^{238}PuO_2$; (2) the importance of the homogeneity of the distribution of dose within the lung; (3) interspecies comparison of the toxicity of inhaled plutonium; and (4) the ef fect of age at the time of exposure.

The early effects observed from the inhalation of high activity levels of plutonium were radiation pneumonitis, inflammation and scaring of the lung, and a decrease in the numbers of lymphocytes in the blood. At lower activity levels and at much longer times after inhalation, lung cancer was the primary effect observed, especially from $^{239}PuO_2$. Bone and liver cancers were also observed from $^{238}PuO_2$. It was found that the differences in the biological behavior of these two isotopes of plutonium were due to the breakup of the crystalline structure of the $^{238}PuO_2$ particles from the high specific activity of ^{238}Pu. This resulted in larger surface areas and thus increased solubility.

In these studies, the plutonium aerosols were delivered as monodisperse particles. That made it possible to alter the distribution of local dose within the lung using many small particles or a few large particles. Similar risks of developing lung cancer were found in both cases. The "hot particle theory" had proposed that the high dose around larger particles would pose higher cancer risks than from the lower doses around smaller particles. This theory was shown to be false.

Studies in multiple species, primarily dogs, rats, and mice, showed similar biological effects and cancer risks. This finding has provided increased confidence in the extrapolation of the animal data predicting health risks to people. The studies on the effect of age at the time of exposure are still in analysis, but early indications are that old dogs may be more sensitive to plutonium dioxide than young adults and juveniles. The old dogs developed lung injury at lower doses and shorter time intervals than the younger dogs. No increased sensitivity to inhaled plutonium dioxide for the development of biological effects by juveniles has been

B. A. Muggenburg
F. F. Hahn
R. A. Guilmette
J. A. Diel
B. B. Boecker
D. L. Lundgren
M. D. Hoover
Lovelace Respiratory Research Institute

found so far, but the data are still being analyzed. A list of the publications that have been completed is available.[1]

Conclusion

In summary, inhaled plutonium dioxide was shown to cause serious biological effects in a dose-related fashion in the organs that received the largest doses. Because of differences in the tissue distribution of $^{238}PuO_2$ versus $^{239}PuO_2$, some differences in the biological effects were observed. The uniformity of dose distribution in the lung did not affect the probability of developing a cancer, and the probability of developing lung cancer from inhaled $^{239}PuO_2$ was similar among several laboratory animal species. Age at exposure was important, and older animals were more sensitive for developing biological effects. Based on the similar results obtained among laboratory animal studies, extrapolation of these results to humans appears to be reasonable.

Reference

1.   Inhalation Toxicology Research Institute, *Publications of the ITRI Nuclear Toxicology Program: 1960 – 1996*, ITRI-149, Lovelace Respiratory Research Institute, Albuquerque, NM (December 1996).

Plutonium Explosive Dispersal Modeling Using the MACCS2 Computer Code

The purpose of this paper is to derive the necessary parameters to be used to establish a defensible methodology to perform explosive dispersal modeling of respirable plutonium using Gaussian methods. A particular code, MACCS2, has been chosen for this modeling effort due to its application of sophisticated meteorological statistical sampling in accordance with the philosophy of USNRC Regulatory Guide 1.145, "Atmospheric Dispersion Models for Potential Accident Consequence Assessments at Nuclear Power Plants." A second advantage supporting the selection of the MACCS2 code for modeling purposes is that meteorological data sets are readily available at most DOE and NRC sites. This particular MACCS2 modeling effort focuses on the calculation of respirable doses and not ground deposition.

More sophisticated plume modeling approaches exist for explosive dispersal modeling, such as the ERAD (Explosive Release Airborne Dispersion) code developed at Sandia National Laboratories (Boughton and DeLaurentis, 1987, 1992). However, as currently implemented, the code is difficult to use because meteorological data cannot be easily obtained as input, and final consequence statistics cannot be easily derived.

Once the necessary parameters for the modeling are developed, the model is benchmarked against empirical test data from the Double Tracks shot of project Roller Coaster (DASA-1644, Shreve,1665) and applied to a hypothetical plutonium explosive dispersal scenario. The actual amount of plutonium involved in this test is still classified, so the mass of respirable plutonium used as the originating source term in the MACCS2 benchmark is 1 kg after the fashion of Dewart, Bowen, and Elder (1982).

Further modeling with the MACCS2 code is performed to determine a defensible method of treating the effects of building structure interaction on the respirable fraction distribution as a function of height. These results are related to the Clean Slate 1 and Clean Slate 2 bunkered Roller Coaster test results.

An efficient method is presented to determine the peak 99.5% sector doses on an irregular site boundary in the manner specified in NRC Regulatory Guide 1.145 (1983). Parametric analyses are performed on the major analytic assumptions in the model to define the potential relative errors that are possible in using this methodology.

C. M. Steele
T. L. Wald
D. I. Chanin
Department of Energy, Los Alamos Area Office

Detection
and Analysis

Determination of Actinides in WIPP Brines
by Inductively Coupled Plasma Mass Spectrometry

S. L. Bonchin
J. A. Eyre
L. A. Gallegos
T. M. Yoshida
Los Alamos National Laboratory

The Actinide Source-Term Waste Test Program (STTP) considers radionuclide release via groundwater mobilization. The goal is to identify factors influencing the mobility of the actinide elements in transuranic (TRU) waste immersed in brine. The concentrations of these actinides can be as low as 10^{-10} M in solutions containing 45 wt % or more total dissolved solids (TDS). We have investigated several approaches for analyzing actinides in brines centered around inductively coupled plasma mass spectrometry (ICP-MS).

ICP-MS is the method of choice for trace elemental analysis. The low detection limits (ppt-ppq) make it an obvious choice for the detection of the low levels of actinides expected in the STTP samples. However, the most common method for sample introduction to the plasma, solution nebulization, can only tolerate on the order of 1% TDS. A method for actinide analysis in brines has been developed for solution nebulization ICP-MS which requires a 1:100 dilution of the sample. Even with this dilution, severe matrix effects necessitate the use of internal standards, and the salt deposition on the torch, cones, and lens stack is problematic. Plasma instability has also been observed.

Solution nebulization is only on the order of 2% efficient in the transport of the analyte from the nebulizer to the plasma. Incorporating electrothermal vaporization (ETV) introduces the sample in gaseous form directly into the torch, with resulting efficiencies greater than 60%. ETV also allows the analysis of samples that have elevated levels of matrix constituents, by providing a temporal separation of these components from the analyte of interest prior to their detection. This is also beneficial for samples containing large amounts of dissolved solids, such as the brine solutions investigated in this study. Another advantage of ETV is the ability to handle very small sample volumes, on the order of microliters. This improves the absolute detection limits (low femtograms) where sample volume is limited. Further, the use of chemical modifiers and physical carriers can improve sensitivity for some elements, i.e., halogens and halocarbons serve as volatilization aids for some refractory elements. Several ETV parameters have been optimized for the analysis of actinides in brines, including argon carrier gas flow rate, sample volume, ashing temperature, vaporization temperature, and drying time. Other factors, such as chemical modifiers and physical carriers, have also been investigated.

While ETV eliminates some of the problems associated with analyzing samples with high total dissolved solids by ICP-MS, there are still difficulties. If the ashing step used to drive off the matrix constituents is not harsh enough, some remain and affect the signal. If it is too harsh, some of the analyte may be lost. The transport of the vaporized analyte to the plasma is also difficult to achieve with a high degree of precision. We have investigated the use of small, polymeric, chelating beads to preconcentrate the analyte and eliminate the brine matrix. An automatic preconcentration/matrix elimination system was used to investigate the preconcentration of actinides in synthetic brine solutions. The sample is mixed with very small (< 0.2 μm diameter) chelating polymeric beads which are derivatized to bind specific classes of elements. These are injected into a hollow fiber bundle where matrix elements are forced out of the fibers while retaining the beads and any bound elements. The beads are recovered in a small volume. The two types of suspended particle reagent (SPR) studied were derivatized with iminodiacetate (IDA) functional groups and phosphonic acid resin functional groups. These bind most of the transition elements, REEs, and actinides. The

beads have been analyzed with both ETV and solution nebulization ICP-MS. The preconcentration/matrix elimination system produced preconcentration factors ranging from 7X to 9X for both kinds of suspended particle reagent studied with reasonable reproducibility (~7% RSD). It was seen that when the beads are introduced to the ICP via conventional solution nebulization, memory effects are severe, however, there were no memory effects using ETV.

Another sample introduction method for ICP-MS studied is ultrasonic nebulization (USN). Sensitivities are improved almost an order of magnitude with USN over conventional pneumatic solution nebulization due to the better aerosol quality and transfer efficiency. However, the amount of TDS the USN can tolerate is limited. We have investigated the improved sensitivity versus extra required dilution for the analysis of actinides in brines.

A Method for Size and Activity Measurement of Minute Alpha Emitting Particles of Dispersed Reactor Fuel

O. A. Bondarenko
Radiation Protection Institute, Ukraine

The practice of environmental monitoring with help of SSNTDs has shown two distinct forms of radioactivity distribution which are diffusive and aggregate in form. An example of the diffusive form can be observed in radon measurements. An aggregate form ("fuel particles") can be seen in contaminated soil, i.e., around the Chernobyl Nuclear Power Plant. Our work to date has concentrated upon the detection and analysis of hot particles from such contaminated ground.

Hot particles (tiny radioactive particles of dispersed burnt nuclear fuel) represent a potential hazard of which there are principally two aspects. Firstly, after deposition in (or on) the human body, hot particles produce huge local doses in spite of low average doses. This can lead to the risk of micro injury inside different organs as well as contribute to late (carcinogenic) effects.

Secondly, hot particles are "repositories" of a large amount of transuranic radioactivity which is encapsulated inside them. The solubility of hot particles and the degree of mechanical destruction determine the biologically accessible fraction of transuranic nuclides, which enter systemic circulation in the human body. For example, there is interesting evidence of strong dependence of the radionuclide soil-plant transform coefficient a distance from the 4th block of the Chernobyl nuclear power plant.

Simultaneous measurement of such parameters as activity and the size of a radioactive particle would have immense value for many applications in radiation protection and control of the environment. The most important results should be obtained from models of lung inhalation of hot particles during the first fortnight after the Chernobyl accident and also from the prediction of plutonium transfer in soil from an aggregate form to biologically accessible ones.

The algorithm and performance of multiple alpha track analysis is discussed concerning the identification of various parameters of the particle such as activity, physical size, and distance between the particle and the detector surface (air gap). Preliminary individual track processing of CR-39 (TASTRAK) has been performed with the use of an automated microscope scanning system. This system is capable of measuring individual track characteristics such as azimuthal angle, dip angle, range, and X, Y coordinates. The plastic detector TASTRAK (CR-39 type) used in this work is manufactured by Track Analysis System Ltd at the University of Bristol. The geometric parameters of etched nuclear particle pits were measured with the system for the automated analysis of nuclear particle tracks which has been developed at Bristol University.

In order to examine the proposed method in practice, two soil samples taken from Chernobyl and Bristol were exposed 1 week and 8 weeks, respectively, with the use of TASTRAK plastic detectors. The following processing of these detectors led to the conclusion that the method is sufficiently adequate and robust with regard to the estimation of the parameters size and alpha fluence.

A New Principle of Alpha Particle Spectrometry Using SSNTD

O. A. Bondarenko
Radiation Protection Institute, Ukraine

During the last decades, a new method for registration of charged particles with high stopping power (including alpha particles) was recognised. It uses solid-state nuclear track detection (SSNTD) and possesses certain advantages. These are (1)operational simplicity , (2) low production cost, (3) practically 100% protection from external sources of alpha radiation, (4) no need to use electronic equipment during exposition giving possibility to carry out long-term stable measurements, and (5) a high level of discrimination of nuclear particles different than alpha particles, i.e., gamma-quanta, neutrons, beta-particles, mu-mesons.

The SSNTD method is based on the property of plastic film (of the CR-39 type) to store latent destruction made by an alpha particle along its track. Consecutive etching of the plastic reveals these tracks as surface pits of different shapes. The shape of a pit is determined by many parameters of which most important are the type of plastic, the time and the temperature of etching, the energy, and the incident angle of an alpha particle. Automated analysis of a digitised microscopic image of etched out tracks gives the following information about an individual alpha particle: X and Y coordinates of an alpha particle incident on the detector surface, azimuthal, and incident angles.

A new principle of alpha particle spectrometry using SSNTD is advanced. It is based on the measurement of the end diameter of an etched out track. A simple linear ratio links the track end diameter and the range of an alpha particle in the detector. A special calibration procedure is worked out in order to compensate the track end diameter dependence on the alpha particle incidence angle. This procedure avoids direct measurement of etching rates Vt and Vb and makes attainable transfer to the energy scale.

As a result the energy resolution achieved so far is 2% within the energy range between 4 and 6 MeV. Additionally the method gets a high value of the absolute registration efficiency, i.e., up to 25%. It is explained that a few parts of the tracks are rejected in the course of analysis, namely these are almost vertical tracks and those which the incidence angle exceeds the critical angle.

The main factors determining the sensitivity of spectroscopy are the background, the energy resolution, and a possibility of a long-term exposition of samples. For example, providing measures for radon exclusion, a typical intrinsic background of a track detector TASTRAK (of CR-39 type, manufactured by TASL, Bristol, UK) is 10 to 100 count*cm–2*year–1. For the SSNT type of detectors, the productivity of the spectrometric equipment is determined by the processing time of the detector which takes about 15 minutes independently on the time of its exposition. Thus having increased the time of registration to one week, the lower limit of detection can be achieved at the level of 0.1 mBq.

Attainment of the good energy resolution for SSNT detectors combining with their naturally immanent advantages gives the possibility of their application in ultra-low activity measurement. That is especially essential when using semicon-ductor and ionisation types of detectors is not possible or inexpedient, i.e., in research of bioassay samples, measurement of different ultra-pure construction materials, etc. An important practical advantage of the given technique is the low cost of a single measurement of low and ultra-low radioactivity. The more samples needed to be measured, the lower the cost of a single measurement compared to a semi-conductor alpha-spectrometer.

Also the approach of using SSNTD alpha spectrometry looks very promising for the design of a personal radon alpha dosimeter. SSNTD alpha spectrometry would improve the overall performance, especially for radon/thoron simultaneous measurements. Another area of research where SSNTD alpha spectrometry would reveal its advantaves is in the measurements of alpha-emitting aerosols, especially hot particles. Additionally the total activity and the geometrical dimensions of the energy spectrum for an individual particle could be assessed.

Laser Ablation-Inductively Coupled Plasma-Mass Spectrometry for Trace Analyte Determination in Actinide and Actinide Contaminated Matrices

J. Cross
D. J. Figg
C. Brink
Los Alamos National Laboratory

We are currently setting up Laser Ablation-Inductively Coupled Plasma-Mass Spectrometry (LA-ICP-MS) in a glovebox for trace inorganic analyte determination in actinide containing samples. LA-ICP-MS is a direct solid, multielement analysis technique. It bypasses the dissolution of the sample and therefore does not generate the acid waste stream that is produced with traditional wet methods. A laser is used to vaporize a small portion of the solid sample. The vaporized portion is then transported to the ICP where the particles are dissociated, atomized, and ionized. The elemental ions are then drawn into the mass spectrometer where they are mass anlayzed. 90 to 95% of the elements can be fully quantitated within minutes. LA-ICP-MS can be used for the elemental analysis of soils, cements, metals, alloys, glass, polymers, food, plants, etc.

ICP-MS analysis of digested plutonium samples has been carried out in a glovebox for several years at Los Alamos. For the plutonium laser work, a new glovebox has been attached to the current glovebox that contains the ICP-MS (VG PlasmaQuad 2) used for the analysis of liquid plutonium samples. The laser system (Spectron SL282 Nd:YAG) is outside the gloveboxes, and only the laser beam is transported into the new laser ablation glovebox. A sample cell and x, y, and z motorized stages are housed in the new glovebox. A LabView program has been developed to manipulate the x, y, and z translational stages so that a sample can be moved under the focused laser beam. Schematics and pictures of the instrumentation will be shown.

Previously, we have experimented with 266, 532, and 1064 nm ablation on polished glass samples and have found the analytical conditions produced with 266nm ablation superior to those pr oduced with 532 and 1064 nm ablation.[1] UV ablation produces better signal precision and less elemental fractionation than 532nm or 1064 nm. 355 nm will be used for the glovebox system because it wears less on the optics and plenty of power can be generated.

The plutonium samples likely to be analyzed by the glovebox LA-ICP-MS are relatively pure, powdered PuO_2 samples. There could also be other types of actinide containing samples such as cemented TRU waste. The ultimate goal for LA-ICP-MS of such materials will be to achieve the analysis requirements of the customer with minimum sample preparation. Currently, to do good quantitative analysis with LA-ICP-MS one has to have matrix-matched standards and internal standards added to all of the samples. Adding an internal standard to a solid sample is difficult and time consuming. We are carrying out a different set of experiments to determine how to eliminate the addition of the internal standards to each sample. This would reduce sample analysis time and worker exposure. Results from nonradioactive cement samples will be discussed.

Reference

1. M. Kahr and D. Figg, to be published in *Applied Spectrosc.*

Analysis of Pu and U Materials for Trace Contaminants Using a CID Equipped ICP-AES Echelle Spectrometer

D. J. Gerth
Los Alamos National Laboratory

Introduction

Analysis of Pu and U metal, PuO_2, UO_2, and mixed Pu/U oxide (MOX) has traditionally been carried out by DC-Arc spectrography after performing a chromatographic separation to remove the Pu or U from the sample matrix. This separation was necessary due to the richness of the Pu and U emission spectra. The recent development of charge transfer devices (CCD, CID) as detectors for analytical atomic spectroscopy, coupled with an Echelle spectrometer, has resulted in high-resolution instruments capable of direct analysis of dissolved material without the need for separation. This is highly desirable from safety, waste minimization, and sample turnaround standpoints.

Experimental

All samples were analyzed using a Thermo Jarrell-Ash IRIS CID equipped Inductively Coupled Plasma Emission Spectrometer. This instrument features a solid state 512×512 pixel cryogenically cooled charge injection device detector and a moveable entrance slit for full wavelength coverage.

An interference study was performed by analyzing 1000 mg/L single element standards and observing the resulting intensity at each analyte wavelength. The method comparison study was performed by analyzing NIST standard U (CRM 123-2, CRM 123-7), and in-house Pu samples before and after the separation procedure. Each sample was also analyzed by ICP-mass spectrometry as a check.

Results
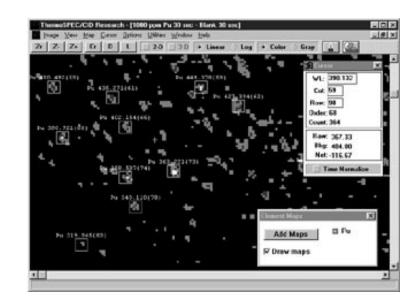
Pu Spectral Mapping

An image of the Pu spectrum was obtained by aspirating a 1000 mg/l solution of Pu in 2% HNO_3. The spectral image was enhanced by subtracting a 2% HNO_3 blank spectrum, and prominent emission line wavelengths assigned from their position on the chip. A Pu spectral atlas compiled by Edelson et al.[1] was used to positively identify each line. A spectral map was then assembled which allows the unambiguous identification of Pu in the sample matrix. A section of the map is shown in Figure 1.

Interelement Corrections

Spectral interferences were uncovered by analyzing 1000 mg/l single element standards and noting shifts in intensity at target analyte wavelengths. A novel interelement effects (IEs) identification algorithm was developed using Microsoft Excel which provides a statistical rationale for IE selection.

Figure 1. Detail of Pu emission spectrum obtained on the TJA IRIS ICP-AES.

NIST Standard and Sample Analysis

Two U CRMs, 123-2 and 123-7, were analyzed for eighteen constituents before and after ion exchange removal of the U. Results of the analyses and statistical data demonstrating no significant difference between the two sets (before and after separation) will be presented. The results of several Pu sample analyses (before and after Pu separation) and statistical data demonstrating no significant difference between the two will also be presented. As a result of this work, ion exchange separation of Pu or U from samples appears to be unwarranted; elimination of this step will greatly improve the efficiency of the analysis, reduce the hazards involved by eliminating the need for nitric acid treatment of the ion exchanger, and reduce waste.

References

1.   M. C. Edelson, E. L. DeKalb, R. K. Winge , V. A. Fassel, "Atlas of Atomic Spectral Lines of Plutonium Emitted by an Inductively Coupled Plasma," Ames Laboratory publication IS-4883 (September 1986).

Investigation and Automation of Sorbent Extraction Separations of Actinides by Flow Injection Analysis

J. W. Grate
Pacific Northwest National Laboratory

O. B. Egorov
Pacific Northwest National Laboratory and University of Washington

J. Ruzicka
University of Washington

Recently developed selective sorbents for radionuclide separations can be used to perform radionuclide separation in a format that is highly suitable for automation by flow injection techniques. Integrated with commercially available radioactivity detection instrumentation, automated radionuclide separations can be used to develop flow injection-based radionuclide analyzers or the flow injection instrument can be used to investigate and develop new separation procedures. Despite this potential, thus far there has been very little application of flow injection to radionuclide separation.

Recently we developed a rapid automated procedure for the determination of ^{90}Sr in aged nuclear waste. The procedure is based on a sequential injection analysis system which rapidly separates ^{90}Sr from interfering radionuclides on a minicolumn containing Sr-Resin™. Our most recent results demonstrate that flow injection can be successfully used in automation of substantially more difficult separations such as the separation of actinide elements. The chemically challenging separation of individual actinides can be performed in automated flow injection format, using a TRU Resin™ sorbent extraction column designed to selectively retain actinides under particular conditions. Separations are achieved through multiple eluent changes and actinide specific oxidation-reduction reactions performed on-line. The separation column functions as a reactor designed to selectively retain a group of analytes under given conditions, while rapidly and selectively releasing individual species upon the appropriate change of the eluent-analyte-sorbent chemistry.

We have now demonstrated that it is possible to separate gross actinides from the matrix as a group; transuranic elements from the matrix and from uranium; Am and Pu; and several actinides individually. The separation of Am and Pu is based on the fact that trivalent actinides are not retained on the TRU-Resin column in hydrochloric acid, whereas tetravalent and higher valence state actinides are retained. After loading a reduced sample on the column, the Pu valence state is adjusted to Pu(IV), which is then retained while trivalent species such as AM(III) are eluted with hydrochloric acid. Pu separation is then achieved by reducing the Pu(IV) back to Pu(III) and eluting it from the column. Since the redox adjustment is selective for Pu, efficient separation from other actinides such as Th, Np, and U can be achieved. Typically, hydroquinone is used as the reducing agent as it is known to provide fast reduction kinetics in homogeneous solutions. Our investigation of the procedure for Am and Pu separation revealed a number of previously unknown features of on-column redox reactions with TRU Resin. One such result is that reduction with hydroquinone is not very effective. The rate is slow, elution of Pu(III) shows substantial tailing, and recovery of Pu as Pu(III) is incomplete. We investigated a number of alternative reducing reagents and found that fast efficient reduction and elution of Pu(III) could be obtained using TiCl$_3$ instead. Therefore, knowledge derived from homogeneous reactions should be used with caution when applied to on-column reaction format. We also found that the oxidation of Pu from Pu(III) to Pu(IV) with nitrite, normally done before Am(III) elution and the subsequent reduction of Pu(IV) back to Pu(III), has a substantial effect on the subsequent behavior of Pu on the column. This arises from two effects. First, some of the nitrite interacts irreversibly with the column. This bound material (exact chemical speciation unknown) adversely affects subsequent reductions of Pu with reducing agents such as hydroquinone. Second, nitrite is

retained by the organic phase on the column. Using typical procedures with 2 mL columns, the retained nitrite is not fully eluted before the later reduction step is begun. Therefore, the reducing agent must consume the remaining nitrite before the Pu(IV) is fully reduced to Pu(IV) and eluted. This results in slower elution of the Pu(III) than might be expected. With this additional understanding, analytical separation procedures can be optimized.

Our flow injection system provides precise control over fluidic conditions and the ability to change the experimental parameters from computer keyboard, while monitoring the progress of the separation in real time. This facilitates the investigation and "fine tuning" of radionuclide separations. Experiments that are too tedious to be performed in a manual format can be easily done in a flow format so that new information can be obtained. In terms of radiochemical analysis, the advantages of the new automated separation methodology include faster and more efficient separations, reduced waste generation, reduced personnel exposure, and fully automated unattended operation.

Neutron Source Processing—Managing Radiation without Using a Hot Cell

D. W. Gray
Los Alamos National Laboratory

The Plutonium Facility at the Los Alamos National Laboratory has routinely received and destroyed neutron sources since its opening in 1978. This work has been part of the Laboratory's effort to "reduce the nuclear danger," and is part of the wealth of plutonium handling experience that exists at Los Alamos. The Neutron Source Project is part of that vast experience base, and I will present various efforts made to reduce the dose to all personnel while still processing neutron sources for the Nation to as I mentioned previously, "reduce the nuclear danger."

The Neutron Source Prjoect was reorganized in 1992 to adapt to the changing needs of the Department of Energy (DOE). DOE recognized the importance of removing these neutron emitting devices from the public domain, and funded a separate project to allow the team to streamline the shipping of the sources into the facility, reduce the dose received by personnel, and maintain a source processing capability.

We achieved our goals through a dynamic team organization that broke the processing tasks down into manageable subtasks, and them improved then significantly. The subtasks included shielding of the glovebox, hard automation of the decladding process where the stainless steel is removed and then the tantalum crucible is breached, and lastly, the dissolution process, which actually eliminates the (α, n) reaction that has been occurring between the actinide and beryllium or other light metal. The actinides are then processed and stored for future disposition.

For the shielding of the glovebox, we doubled the volume of shielding by increasing the height and thickness. This was successful because we altered the decladding process from a manual one to a remotely operated one. This eliminated the need for routine glovebox access. The remote operations and the camera viewing system removed the operator from the front of the glovebox, reducing operator dose even further. And finally, remotely operating the dissolution process by watching the neutron count rate decline from a source rate down to background essentially eliminated the dose received from this operation.

The Neutron Source Project achieved its goals, and it is in this regard which I believe that managing the radiation associated with receiving, processing, and safely storing alpha-emitting actinides can be done efficiently and promptly in a glovebox line rather than a Hot Cell. Future processing requirements, lower personnel dose, smaller and or larger sources are all problems that can be addressed and handled at the Los Alamos National Laboratory's Plutonium Facility.

Figure 1. Old shielding arrangement 4 inches thick, 9.3 cubic feet.

Figure 2. New shielding arragement 5.25 inches thick, 19.8 cubic feet.
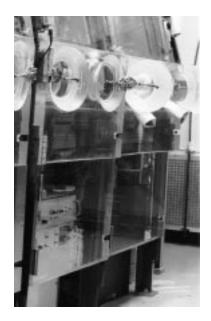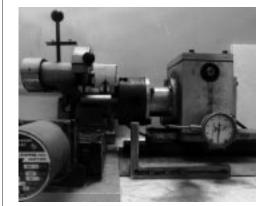

Figure 3. Manual decladder carbide abrasive saw.

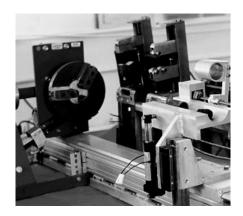Figure 4. Remotely operated decladder simple pipe cutter.

Figure 5. Incremental aqueous dissolution.

Figure 6. Remotely operated dissolution simple computer-controlled pump.

Characterization of Plutonium Irreversibly Bound to Ion Exchange Resins Using X-Ray Absorption Spectroscopy

D. K. Veirs
C. A. Smith
S. D. Conradson
M. P. Neu
L. A. Morales
Los Alamos National Laboratory

Ion exchange resins that have been used in processing plutonium always contain some plutonium that cannot be easily removed. Remediation technologies for spent ion exchange resins must address the fate of this irreversibly bound plutonium. The chemical nature of this form of plutonium and why it is intransigent to normal processing chemistry is unknown. We have characterized plutonium on spent ion exchange resin using x-ray absorption spectroscopy techniques with the goal of elucidating the chemical form of the irreversibly bound plutonium so that remediation efforts can be efficiently directed.

An ion exchange resin that had been stored in the TA-55 vault for four years was studied. The resin had been used at TA-55 to remove impurity metals from hydrochloric acid solutions. The resin was washed with a weak hydrochloric acid solution prior to storage in order to remove any soluble actinides. The resin was stored in a galvanized paint can within a plastic bag-out bag. When the item was removed from the TA-55, vault it was found that the bottom third of the paint can had been corroded. A small sample was removed from the containing resin mixed with small metal fragments from the corroded can. The sample was loaded directly into a sample holder for x-ray absorption analysis with no sample preparation. The resin sample was estimated by NDA to contain 1 part plutonium in 600 by weight.
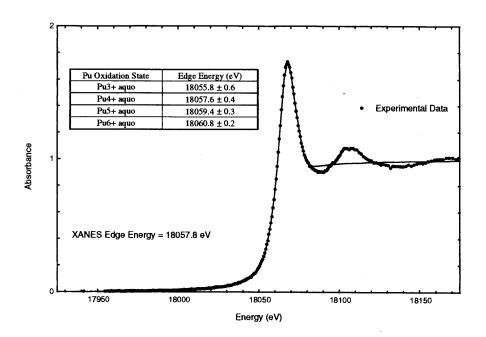
X-ray absorption data of the L_{III} edge of plutonium (17555 to 18551 eV) was collected at the Stanford Synchrotron Radiation Laboratory using experimental conditions described previously.[1] The zirconium edge at 17999 eV was used for energy calibration. The sample was cooled to liquid nitrogen temperature during data collection.

The XANES edge was examined in order to ascertain the oxidation state of the plutonium irreversibly bound to the resin. The location of the XANES edge was determined using the approach described by Conradson et al.[2] The energy region from 17950 to 18175 eV was fit to the sum of an arctangent and two Gaussian functions. The XANES edge and the fit are shown in Figure 1. The position of the arctangent was found to be 18057.8 eV. The results of [1] indicate that the XANES edge for plutonium IV is 18057.6 eV with a difference in energy between oxidation states of nearly 1.7 eV. The position of the XANES edge for the resin sample is consistent with an oxidation state of IV. Plutonium in oxidation states V and VI exhibit a strong shoulder on the white line feature in the XANES region which was not observed in the XANES of the resin sample indicating that the majority of the plutonium must be in lower oxidation states. From these observations we conclude that the majority of the plutonium must be in the IV oxidation state.

The EXAFS data was studied in order to elucidate the chemical form of the plutonium. The FT modulus of the EXAFS data from the resin sample was found to most closely resemble the FT modulus of the colloidal form of plutonium and to a lesser extent the FT modulus of plutonium oxide. Six oxygen shells and one plutonium shell were required to reasonably fit the EXAFS data. FEFF 7 was used to obtain the theoretical phases and amplitudes for each shell. The parameters obtained from the fit are shown in Table 1. The phase factor for chlorine is significantly different than the phase factor for oxygen and was used to confirm the absence of chlorine in any of the shells.

Figure 1. The plutonium L$_{III}$ absorption edge obtained from a sample of ion exchange resin used for processing plutonium hydrochloric acid solutions. The data have been fit to a sum of arctangent and two Gaussian functions. The correlation between the edge energy and the plutonium oxidation state is shown in the inset.

Pu Oxidation State	Edge Energy (eV)
Pu3+ aquo	18055.8 ± 0.6
Pu4+ aquo	18057.6 ± 0.4
Pu5+ aquo	18059.4 ± 0.3
Pu6+ aquo	18060.8 ± 0.2

XANES Edge Energy = 18057.8 eV

• Experimental Data

Table 1. The distance and number of atoms obtained from a fit of the EXAFS data for plutonium irreversibly bound on an ion exchange resin.

Atom	Distance (Å)	Number
Oxygen	2.25	7.53
Oxygen	2.40	1.87
Oxygen	2.85	2.02
Oxygen	3.06	3.25
Oxygen	3.31	5.61
Oxygen	3.53	2.9
Plutonium	3.79	2.7

The results of the fit are very similar to the results of a fit to the EXAFS data for plutonium colloids.[3] The number of shells required to fit the data are the same and the distances the shells are observed at vary in the range 0.04 to -0.04 Å. The principal difference lies in the number of atoms observed in each shell. In general the number of oxygen atoms in shells two through six are less in the aged resin sample than in the freshly prepared colloids. The EXAFS data for the resin sample are less similar to EXAFS data for plutonium oxide powder. The distance of the first oxygen shell differs from the oxygen shell in PuO_2 by 0.08 Å, and the plutonium shell differs from the plutonium shell in PuO_2 by 0.04 Å. The number of plutonium atoms is much less in the resin sample than in PuO_2.

It is found from the x-ray absorption data that the plutonium irreversibly bound to this sample of ion exchange resin which has been aged for four years is principally in the form of a plutonium colloid. The number of oxygens appear to be less in the outer oxygen shells than in the freshly prepared colloids. In this respect the plutonium on the aged resin could be aging towards a plutonium oxide form which would be more difficult to remove chemically from the resin.

References

1. P. G. Allen, D. K. Veirs, S. D. Conradson, C. A. Smith, and S. F. Marsh, "Characterization of Aqueous Plutonium(IV) Nitrate Complexes by Extended X-ray Absorption Fine Structure Spectroscopy," *Inorg. Chem.* **35**, 2841 (1996).

2. S. D. Conradson, I. Al Mahamid, D. L. Clark, N. J. Hess, E. A. Hudson, M. P. Neu, P. D. Palmer, W. H. Runde, C. D. Tait, "X-Ray Absorption Edges of Plutonium in Different Oxidation States," (submitted to *Inorg Chem.*).

Novel Plutonium/ Actinide Compounds and Complexes

Spectroscopic Investigations of Np, Pu, and Am in Selected Immobilization Glasses

The science of immobilizing materials for nuclear waste has been an active topic for decades and many widely varying studies have been performed with regard to this subject. Such studies have varied from examining the different physical properties of the materials to sophisticated attempts for modeling long-term behaviors. The latter are frequently given in time frames up to 10^6 years and the modeling parameters must depend heavily on valid, fundamental scientific information for these long-term estimations. Our experimental efforts have been aimed at addressing and acquiring such information.

As part of these efforts, we have pursued some of the fundamental solid-state chemistry and materials science of 4f- and 5f-elements in selected glasses and other immobilization materials. Glasses studied to date have included two high-temperature (850° and 1400°C melting points) silicate-based glasses and a glass prepared via a sol-gel technique. Optical spectroscopy (fluorescence, Raman, and luminescence) was the principal investigating tool, although other techniques have also been employed in the work.

One aspect of our work with glasses has been to determine the oxidation states exhibited by the f-elements in these matrices, as well as the factors that control and/or alter these states. With the high-temperature silicate-based glasses, we have noted that a correlation exists between the oxidation state of the f elements in the products with the elements' high-temperature oxide chemistries. We have prepared and studied all of the individual 4f elements, except Pm, in such glasses and the 5f elements from Np through Es.

We report here detailed studies carried out on Np, Pu, and Am in these glasses matrices but minor references will be made to results obtained with these other f-elements.

The correlation noted between oxidation states(s) of the f-elements exhibited in the glasses and those exhibited in their oxide chemistry seems plausible given the silica-based network encountered in the glasses. One exception to this correlation was noted with americium: americium behaves similarly to its 4f-element homolog, europium, in the glasses but differently from europium in its formation of oxides in air.

In silicate-based glasses exhibiting oxide-based networks, a primary concern with regard to the behaviors of materials is whether they have dissolved homogeneously or are dispersed heterogeneously in the host matrix. Such differences would be expected to significantly affect several aspects and properties of the products. In glass products formed via a sol-gel technique, the inserted materials should, in principle, be homogeneously dispersed, uniformly bonded, and also avoid affects arising from the higher temperatures encountered in the dissolution/dispersion processes with the molten glass preparations. Thus, several fundamental aspects of the inserted f-element's chemistry in glasses can be explored by establishing correlations and controlling the formation parameters of these different host materials. A special aspect of the sol-gel preparation is certain oxidation states of plutonium and neptunium which cannot normally be obtained via dissolution in molten glasses at high temperatures.

Z. Assefa
R. G. Haire
Oak Ridge National Laboratory

N. Stump
Winston-Salem State University

We have examined the behavior of americium and plutonium in these glass hosts as a function of the particular glass employed as well as of the preparation and/or annealing temperatures. We have also considered americium's oxidation state observed in the glasses with the comparable states obtained with other 4f-elements and other 5f-elements. In attempting to understand better the particular behavior of neptunium, plutonium, and americium in these glass matrices, we engaged in spectroscopic (luminescence, Raman, and fluorescence) studies of these glass materials. A specific aspect of the studies was to ascertain the local environment, complexation, and bonding nature of the actinides in these matrices.

In spectroscopic experiments with these glass materials, it has been found that the actinides' environment in the low-temperature (e.g., sol-gel glasses) is more "solution-like" than in the glasses prepared by dissolution of the actinides in molten glasses, where the actinides appeared to be more "complexed" or present in multi-sites within the silicate matrices. Thermal treatments of the low-temperature glasses resulted in different spectral responses, which were more in accord with those observed with the high-temperature preparations. We shall discuss the spectral features observed for these materials in terms of proposed complexation, crystal field effects, etc. and offer some interpretations of these features. In addition, the significance and importance of these findings for technological applications will also be offered.

Ionic Strength and Acid Concentration Effects on the Thermodynamics and 5f Electronic Structure of Plutonium(IV) Nitrate and Chloride Complexes in Aqueous Solution

Introduction

Plutonium cations in solution form coordination complexes with solvent molecules and with neutral or anionic solute species. Separations chemistry involving at least one solution phase is partially controlled by the thermodynamics of these complexation reactions. Visible and near-infrared absorption spectroscopy reveals changes in the ground and excited electronic states of $5f^n$ manifold that can be used to infer the stoichiometries of these complexes and to quantify their formation under a wide range of solution conditions. The results of the present studies demonstrate the power of this technique to study equilibrium systems of multiple complexes, five or more in the case of Pu(IV)/nitrate in acidic aqueous solution. We use these results to measure and model how the formation constants of Pu(IV) nitrate and chloride complexes vary with ionic strength. We also discuss observed perturbations of the spectra by non-complexing solution components, and the implications for modeling multicomponent equilibria over a wide range of ionic strengths.

Description of the Actual Work

We have completed a series of studies quantifying the complexation of Pu(IV) by nitrate and chloride in acidic solution under widely varying ionic strength conditions using both pure acids and mixed acids and salts as background electrolytes. This builds upon earlier work focusing on lower ionic strengths or using other spectroscopic techniques.[1,2]

Complexation has been probed by the following changes in the intra-5f electronic absorption spectra of the plutonium ion as it is titrated with nitrate or chloride in the presence of a constant ionic strength background electrolyte. The results are analyzed by fitting the full spectra from each titration series to an equilibrium model containing apparent formation constants for nitrate complexes as parameters adjusted by a non-linear least squares fitting routine. The absorption coefficients for each of the complexes at each sampled wavelength are included as parameters fit by a linear least squares for each trial set of formation constants tested by the non-linear fitting routine.

Titrations were conducted at twelve different ionic strengths and in both pure acid electrolytes and in several different constant-ratio mixtures of acid and sodium salt. In all cases perchlorate was used to adjust ionic strength because it is a non-complexing anion. The concentrations of the complexing anions, NO_3^- and Cl^-, were varied from 0 to 100% of the electrolyte concentration. Corrections for incomplete dissociation of these strong acids were necessary to model the data collected at the highest ionic strengths.

Results

Each series of spectra from a constant-I titration showed evidence of formation of series of discrete inner-sphere complexes of Pu(IV) with the titrant anion. In the case of nitrate, a minimum of five discrete complexes are formed between 0 and 19 mol/kg nitrate molality. The formation of the first two complexes has been fit

J. M. Berg
R. B. Vaughn
M. R. Cisneros
D. K. Veirs
Los Alamos National Laboratory

to a straightforward equilibrium model by the method described earlier. Their apparent formation constants vary with ionic strength in a manner that suggests several ion-ion interactions between the reactants and the electrolyte components become important at high ionic strength. However, the ionic strength dependences follow the simple equations of specific ion interaction theory (SIT) when formation constants are calculated in terms of the free nitrate concentrations taken from Raman measurements by Sampoli et al.[3] This result is somewhat unexpected since SIT typically does not work well above 2 to 5 molal ionic strength. The measured formation constants are listed in Table I.

Table 1. Logarithms of the overall formation constants β_1 and β_2 for each ionic strength. Also shown are the degree of dissociation (α) of nitric acid in a perchloric acid from the data in Reference 3, and the logarithms of the overall formation constants adjusted for the amount of free nitrate ion available to complex Pu.

I (mol/kg)	$log\beta_1$ ((mol/kg)$^{-1}$)	$log\beta_2$ ((mol/kg)$^{-2}$)	a	$log(\beta_1/\alpha)$	$log(\beta_2/\alpha^2)$
2	0.48	1.08	0.98	0.49	1.10
5	0.72	1.63	0.89	0.78	1.74
9	1.14	2.46	0.53	1.42	3.02
11	1.29	2.90	0.32	1.78	3.88
13	1.26	2.93	0.17	2.04	4.48
15	1.27	2.91	0.083	2.35	5.07
17	1.27	2.92	0.040	2.66	5.71
19	1.30	2.93	0.020	3.00	6.33

For weakly complexing ligands such as nitrate and chloride, ligand concentrations must be quite high before higher complexes are formed. Once ligand concentration becomes significant relative to the ionic strength of the solution, the activity coefficients of the reactants and products in the complex-forming reactions can no longer be assumed to be constant. This presents some problems in modeling data where activity coefficients of major electrolyte components are not known in the specific mixed electrolytes being used.

As is typical in using visible/NIR absorption spectroscopy to probe complexation equilibria, we started with the assumption that only inner-sphere complexation changes will perturb the spectra significantly enough to be observed. However, at the high ionic strengths to which this study extends, we have observed significant shifts in absorption maxima energies that cannot be explained by complexation by the titrant anion. The shifts are smaller than is typical for inner sphere complexation, but could be due to changes in the outer coordination sphere, or due to changes in the properties of the inner-sphere ligands due to large differences in their solvation in high ionic strength as compared to low ionic strength solutions. These effects and their possible interpretations will be further discussed in our presentation.

References

1.   D. K. Veirs, C. A. Smith, J. M. Berg, B. D. Zwick, S. F. Marsh, P. G. Allen, and S. D. Conradson, *J. Alloys and Compounds*, **213/214**, 328 (1994).

2.   P. G. Allen, D. K. Veirs, S. D. Conradson, C. A. Smith, and S. F. Marsh, *Inorg. Chem.*, **35**, 2841 (1996).

3.   M. Sampoli, A. De Santis, N. C. Marziano, F. Pinna, and A. Zingales, *J. Phys. Chem.*, **89**, 2864 (1985).

Synthesis and Structural Characterization of Uranium (IV,VI) and Plutonium (IV,VI) Phosphates

Phosphate coordination plays a significant role in actinide chemistry. Concentrated phosphoric acid-nitric acid solutions being studied at Savannah River National Laboratory for the destruction of organic process wastes may contain soluble actinide complexes. On the other hand, in the concepts for underground storage of high-level radioactive waste phosphate minerals have been considered as potential secondary barriers or backfill materials to reduce actinide solubility and to enhance adsorption of radionuclides. Despite the importance of actinide phosphates, surprisingly little is known about the structure, bonding, stability and spectroscopic properties of the pure compounds.
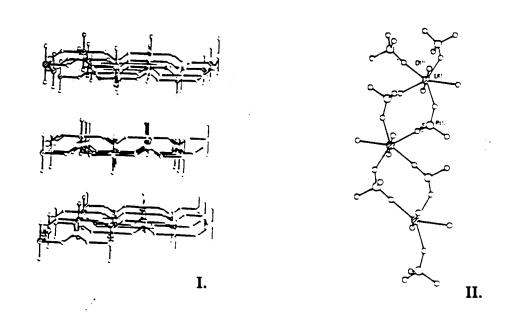
Well-characterized pure compounds are required for solubility studies. Synthetic compounds studied to date have been obtained by precipitation from aqueous solutions under atmospheric conditions. The compounds can be grouped into two general categories: binary phases described by varying ratios of actinide (or actinyl) and phosphate and ternary phases described by varying ratios of actinide (or actinyl), phosphate, and M, where M is an alkali or alkaline-earth ion. At this time, only a few plutonium phosphate compounds have been isolated as single crystals. The structural, chemical and spectroscopic characterization of these compounds and others prepared as microcrystalline solids remains incomplete. It must be noted that the structural and chemical diversity within these compounds is quite remarkable, due to the various actinide coordination numbers (6 to 9) and oxidation states (+III to +VI), and the h^1 and h^2 binding modes of the phosphate ligands that occupy lattice sites to generate one-, two-, and three-dimensional frameworks. These varying structural properties will influence a wide range of physical properties such as solubility, leachability, and radiation-resistance. Our objective is to develop a fundamental knowledge of plutonium phosphate chemistry in order to understand the mechanism of plutonium phosphate formation in waste streams, the disposition of plutonium in the solid state phosphate matricies and to develop a predictive understanding of chemical behavior under radiolysis and aqueous conditions. Well-characterized plutonium phosphate compounds produced in this work will be used for plutonium solubility studies.

Studies performed in our lab on the $UO_2(NO_3)_2 \cdot xH_2O$ - H_3PO_4 - H_2O system serve as background for the study of plutonium phosphate chemistry. Thermodynamically stable compounds in the $UO_2(NO_3)_2 \cdot xH_2O$ - H_3PO_4 - H_2O system have been prepared by conventional techniques including precipitation from and hydrothermal treatment of aqueous solutions. Our data support the existence of three hydrated compounds in the system, $(UO_2)_3(PO_4)_2 \cdot xH_2O$, $UO_2HPO_4 \cdot xH_2O$ **(I)** and $UO_2(H_2PO_4)_2(H_2O) \cdot 2H_2O$ **(II)**, and suggest that the total phosphate concentration in the mother liquors from which these solids precipitate may play a more critical role than the acidity of said liquors. The compounds are accessible via a number of synthesis routes. Data from single crystal X-ray diffraction (XRD), X-ray powder diffraction (XRPD), and extended X-ray absorbance fine-structure (EXAFS) analyses allowed us to identify the solids. We employed these techniques as well as ^{31}P NMR, solid-state NMR , FT-IR, Raman, diffuse reflectance and X-ray absorption spectroscopy where applicable, to fully characterize the solids and solutions.

Once studied, the chemistry of plutonium phosphate complexes can be compared to the known uranium systems; we anticipate both similarities and differences. These studies provide us with increased understanding of the basic science of actinide phosphates and phosphate-mediated actinide migration in waste streams.

J. A. Danis
Los Alamos National Laboratory and The University of Maryland

H. T. Hawkins
W. H. Runde
D. K. Veirs
Los Alamos National Laboratory

B. W. Eichhorn
The University of Maryland

I.

II.

Electronic Structure and Phase Stability of Pu-Ga Alloys

Introduction

Plutonium metal has six different crystallographic allotropes from room temperature until it melts just above 600°C. The room-temperature α phase is monoclinic with 32 atoms per unit cell (an α phase with 16 atoms per cell also exists), which is the lowest-symmetry crystal structure known of any pure element. In fact, only the high-temperature δ (fcc) phase of Pu possesses one of the traditional close-packed structures. The low-symmetry and small lattice constants of the lowest-temperature phase of the light actinides can be used as an argument for f-bonding in these materials. The large volume increase in Pu in going from the α to the δ phase has been argued on phenomenological grounds to be the result of decreased f-bonding.

In addition, XPS data have been obtained for both the α and the δ phases. Both sets of data show the presence of a peak below the Fermi level (E_F). This peak is 2.0 eV wide in the δ phase and 3.0 eV wide in the δ phase. The XPS intensity calculations (for the two phases) which treat the f-electrons as bonding states agree with the measurements of the α phase spectra, but not with those of the δphase. The calculated spectr um shows a narrow f-peak pinned at E_F instead of the wide f-peak below E_F seen in the XPS spectra. It can be argued that the wide spectra seen experimentally are due to the multiplet structure of localized f-states that do not participate very actively in the bonding.

In spite of the difference in the properties of the α and δ phases of Pu (for example α-Pu is brittle while δ-Pu is ductile), it is not difficult to retain either phase by alloying. Indeed, it is often desirable to retain the ductile δ phase for engineering purposes, by alloying, for example, Pu with Al, Ga, or Si.

Description of Work
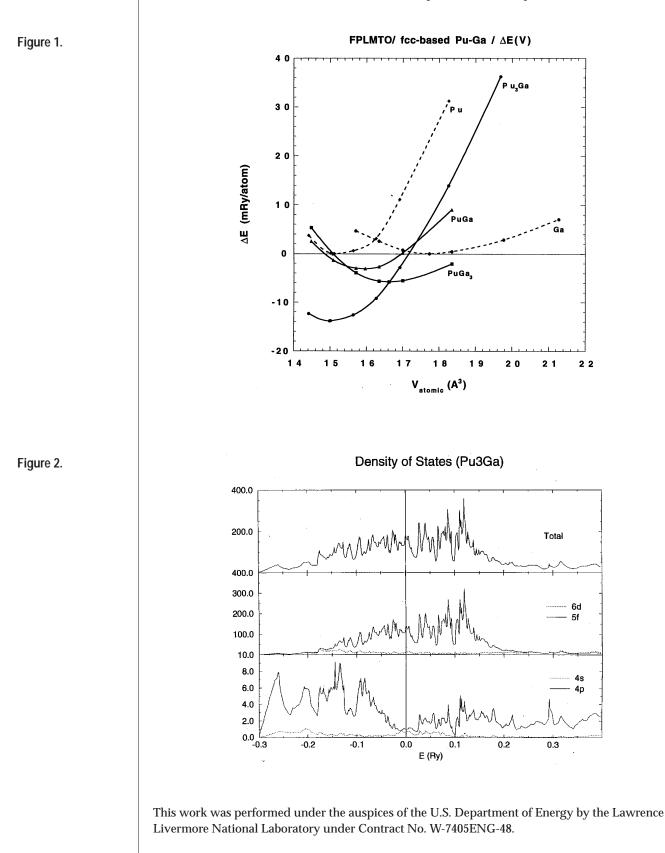
We report on the results of the first-principles electronic structure calculations based on the full-potential LMTO (FP-LMTO) method for pure Pu as well as for Pu-Ga alloys. The aim of these calculations is to determine the energetics of PuGa alloys, the bonding between impurity and host atoms, the relevant atomic interactions between atoms of different species and, ultimately, the phase-stability tendencies of Pu-Ga alloys. We use the Connolly-Williams method for determining these interactions through the study of ordered configurations of the alloy at stoichiometric concentrations, with the aim of eventually using methods based on the coherent-potential approximation (CPA) which can be carried out at arbitrary concentrations.

Results

Figure 1 shows the energy of mixing as a function of atomic volume for Pu-Ga alloys at three Ga-concentrations. The main result that can be read from this figure is the tendency of the alloy to form at any composite (mixing energy negative). The density of states (DOS), shown in Figure 2, of the alloy Pu_3Ga in the LI_2 (of
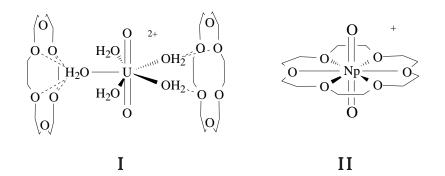
A. Gonis
P. E. A. Turchi
Lawrence Livermore National Laboratory

N. Kioussis
California State University

Cu$_3$Au-type) structure together with the bonding charge density (not represented here) indicate that the presence of Ga modifies the electronic properties of pure Pu. In particular, we find that in the (100) plane the nature of the bonding tends to be ionic in character, with charge being transferred from Pu to Ga cells. The effect of these modifications on the stability of Pu-Ga alloys will be discussed.

Figure 1.

FPLMTO/ fcc-based Pu-Ga / ΔE(V)

Figure 2.

Density of States (Pu3Ga)

Crown Ether Complexation of Transuranic Ions (Np, Pu).
Factors Influencing Inner-Sphere Versus Outer-Sphere Complexation

Crown ether ligands have been studied as potential actinide extractants for many years,[1] and have been shown to influence actinide partitioning in aqueous biphasic systems. There are many examples of crown ether ligands affording actinide extraction in hydrocarbon-water systems, and many of these invoke a standard cavity size argument to explain the observed results.[2-4] However, examples of actinide crown ether complexes wherein the actinide ion is actually coordinated to the crown ether moiety by one or more donor atoms of the crown are exceedingly rare, and limited to uranium.[5] It has been argued that synthesis of inclusion complexes of crown ether ligands necessitates the use of weakly coordinating anions, nonaqueous conditions, and proper choice of cavity size.[5] Indeed, the majority of reports on actinide crown ether complexes reveal second-sphere hydrogen bonding between the crown ether oxygen atoms and water molecules coordinated to the actinide metal center.[6] Well-known examples would include $[UO_2(H_2O)_5][ClO_4]_2 \cdot 2(18\text{-crown-}6) \cdot H_2O \cdot CH_3CN$[7] and $[UO_2(H_2O)_5][CF_3SO_3]_2 \cdot (18\text{-crown-}6)$,[8] depicted qualitatively in **I**.

D. W. Keogh
D. L. Clark
P. D. Palmer
B. L. Scott
C. D. Tait
G. T. Seaborg Institute for Transactinium Science, Lawrence Livermore National Laboratory, and Los Alamos National Laboratory

I   **II**

We find that NpO_2^{2+} and NpO_2^+ ions react with crown ether ligands in acidic aqueous solution to produce inner-sphere Np(V) crown complexes, such as $NpO_2(18\text{-crown-}6)^+$ (**II**) with ClO_4^-, $CF_3SO_3^-$, and even NO_3^- counter ions. Single crystal x-ray diffraction revealed that the NpO_2^+ ion is completely encapsulated by the crown ether with Np=O = 1.799(5), and Np-O = 2.589(9) Å. This is the first example of a structurally characterized transuranic crown ether complex. The Np=O bond is unusually short for a Np(V) ion, and Raman spectroscopy confirmed that the shortening is accompanied by an increase in the O=Np=O ν_1 stretch to 767 cm^{-1}, the highest energy stretching mode ever observed for a Np(V) ion. In order to confirm the identity of the ν_1 stretching mode, the Np(V) complex was labeled with ^{18}O and showed the expected red-shifting of the Raman resonance. This same reduced product was also obtained under highly oxidizing conditions, i.e., bubbling O_3 through the Np(VI) stock, and in the presence of better coordinating anions, i.e., NO_3^-.

However, switching to a non-aqueous environment such as MeCN, precluded the redox chemistry and resulted in the formation of outer sphere Np(VI) crown complexes. This is best illustrated through the synthesis and structural characterization of the outer sphere complex $NpO_2(NO_3)_2(H_2O)_2 \cdot H_2O \cdot 18\text{-crown-}6$, which was crystallized from a 60% MeCN solution. With these results, we have begun to test the conditions (cavity size, solvent system, and anionic ligand choice) that
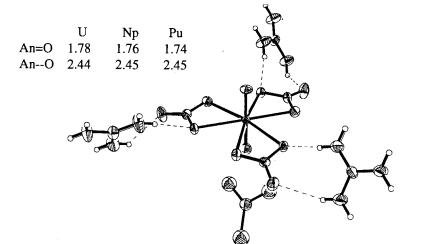
govern the formation of inner-sphere crown complexes, and we will present the synthesis and full characterization of a series of the first examples of Np and Pu crown ether complexes in oxidation states IV, V, and VI. An understanding of the factors controlling crown ether complexation of actinides may lead towards the development of actinyl separation methods using crown ethers.

References

1. M. Lemaire, A. Guy, R. Chomel, J. Foos, *J. Chem. Soc., Chem. Commun.* 1152 (1991).

2. K. L. Nash, *Solvent Extr. Ion Exch. 11*, 729 (1993).

3. W. J. Wang, Q. Sun, *J. Radioanal. Nucl. Chem. 98*, 11 (1986).

4. C. M. Wai, H. S. Du, Y. Meguro, Z. Yoshida, *Anal. Sci., 7 (Suppl., Proc. Int. Congr. Anal. Sci., 1991) pt. 1 pp.* 41–44.

5. P. Thuéry, N. Keller, M. Lance, J. D. Vigner, M. Nierlich, *New J. Chem. 19*, 619 (1995).

6. R. D. Rogers, A. H. Bond, W. G. Hipple, A. N. Rollins, R. F. Henry, *Inorg. Chem. 30*, 2671 (1991).

7. R. D. Rogers, L. K. Kurihara, M. M. Benning, *Inorg. Chem. 26*, 4346 (1987).

8. L. Deshayes, N. Keller, M. Lance, M. Nierlich, J. D. Vigner, *Acta Cryst. C50*, 1541 (1994).

Plutonium Coordination Chemistry with Oxygen Donor Ligands

Speciation, thermodynamic, and characterization data are needed to understand the behavior of plutonium in chemical and separations processes and environmental systems. In order to identify Pu species in these non-ideal systems, we are using structural and spectroscopic features of pure complexes which we have prepared and fully characterized. We are drawing on the coordination chemistry of plutonium with the oxygen donor ligands, aquo, carbonato, hydroxo, polyaminocarboxylates, and others. For example, we have determined the coordination geometries of Pu(III–VI) aquo ions using EXAFS spectroscopy. Pu(III) is coordinated by 9 to 10 waters at a bond distance of 2.48 Å; Pu(IV) is coordinated by 9 waters at a bond distance of 2.39 Å; Pu(V) is coordinated by 2 -yl oxygens at 1.80 Å and 4 waters at a bond distance of 2.45 Å; Pu(VI) is coordinated by 2 -yl oxygens at 1.74 Å and 5 to 6 waters at a bond distance of 2.40 Å. The coordination environment for the carbonates compares well. The limiting Pu(IV) carbonate, $Pu(CO_3)_5^{6-}$, shows Pu bound by 10 oxygens at bond distance of 2.41 Å (by XRD and EXAFS). The limiting Pu(VI) carbonate $PuO_2(CO_3)_3^{4-}$ shows 2 -yl oxygens at 1.74 Å and 6 carbonate oxygens at a bond distance of 2.45 Å (Figure 1). The complexation of Pu(IV) by EDTA also yields a product where the Pu is bound by 9 or 10 oxygen donors. The coordination geometries of these and other Pu complexes and related U and Np species, determined using extended x-ray absorption fine structure and single crystal x-ray and diffraction, will be presented. Implications of these findings to general plutonium chemistry, environmental speciation, and waste issues will also be discussed.

M. P. Neu
D. L. Clark
S. D. Conradson
P. D. Palmer
S. D. Reilly
W. H. Runde
B. L. Scott
C. D. Tait
G. T. Seaborg Institute for Transactinium Science, Lawrence Livermore National Laboratory, and Los Alamos National Laboratory

	U	Np	Pu
An=O	1.78	1.76	1.74
An--O	2.44	2.45	2.45

Figure 1. ORTEP view of the single crystal x-ray diffraction structure of $[C(NH_2)_3]_6[(AnO_2)_3(CO_3)_6]$, isostructural for U, Np, and Pu.

Thermodynamic Studies of Nuclear Waste Ceramic Materials: Enthalpy of Formation for Zirconolite, $CaZrTi_2O_7$

R. L. Putnam
Princeton University/ University of California at Davis

A. Navrotsky
University of California at Davis

B. Ebbinghaus
Lawrence Livermore National Laboratory

M. A. Williamson
J. Y. Huang
Los Alamos National Laboratory

Introduction

With the end of the Cold War, a significant amount of weapons grade plutonium and uranium has been classified as "excess" material requiring disposition. In their present form excess materials can be easily utilized in weapons and pose a security risk. Disposition of these materials reduces the risk to a level similar to spent nuclear fuel and makes recovery of the material for weapons use difficult. Several alternatives have been proposed as ceramics for the disposition of uranium and plutonium among them are actinide substitution of Zr^{+4} in zircon $(ZrSiO_4)$[1] and zirconolite $(CaZrTi_2O_7)$.[2] Though PuO_2 and UO_2 have been shown to have significant solid solubility in these minerals indicating that each has promise as an immobilization material, little is known about the thermodynamic stability of actinide substitution in these minerals. Several determinations of the enthalpy of formation of zircon have been performed[3] making estimates involving actinide substituted zircon potentially more accurate. However no determinations have been performed on zirconolite. We report here the enthalpy of formation for end member zirconolite $CaZrTi_2O_7$.

Description

Using high-temperature oxide melt solution calorimetry, a technique that has been successfully and widely used in our laboratory,[4] we have recently been able to determine requisite thermodynamic quantities leading to the enthalpy of formation of end member zirconolite.

High-temperature oxide melt solution calorimetry uses an oxide melt at an elevated temperature to replace the aqueous acid solution in more conventional solution calorimetry. The sample is dissolved in the melt and the energetics of the dissolution are determined. The recent perfection of a gas flow mixing technique (bubbling) in our laboratory has made it possible for us to dissolve previously troublesome materials such as ZrO_2, TiO_2, CeO_2 and several additional refractory materials containing Ce, Ti, Zr, and Si. Bubbling solution calorimetry utilizes a slow flowing gas stream introduced at the bottom of the melt to form bubbles that then rise through the melt providing a controlled mixing of the solvent.

A sample of end member zirconolite slightly enriched in ZrO_2, composition 0.0824 $ZrO_2 + CaZrTi_2O_7$, was provided by Rich VanKonynenburg at Lawrence Livermore National Laboratory. Powder x-ray diffraction showed the sample to be zirconolite and electron microprobe analysis showed that the excess ZrO_2 was present as small single phase inclusions within the zirconolite grains, therefore the sample was considered to be a mechanical mixture of ZrO_2 and zirconolite. Using bubbling calorimetry and ~5 mg portions, we have dissolved zirconolite in lead borate $(2PbO \cdot B_2O_3)$ at 700°C while measuring the energetics of its dissolution.

Results

Using literature[3,5] and thermodynamic quantities previously obtained in our laboratory,[6] the enthalpy of formation of $CaZrTi_2O_7$ at 298 K has been determined to be -88.85 ± 4.293 kJ/mol from the oxides CaO, ZrO_2, and TiO_2 using equation 1. The standard enthalpy of formation from the elements can then be calculated from equation 2 and is -3713.74 ± 4.78 kJ/mol. The heat content from 298 to 974 K has

also been obtained for $CaZrTi_2O_7$ (171.017±1.31 kJ/mol) and can be used to calculate an average low-temperature heat capacity (252.98 J/Kmol). Additional heat content measurements from 298 K to 1046 K (199.27 ± 1.22 kJ/mol) allow the estimation of an average high-temperature heat capacity (332 J/Kmol).

Equation 1

$$CaO_{(sol, 974)} + 1.0824\ ZrO_{2(sol, 974)} + 2\ TiO_{2(sol, 974)} \rightarrow 0.0824\ ZrO_{2(cr, 298)} + CaZrTi_2O_{7\ (cr, 298)} \qquad -257.53 \pm 3.797[6]$$

$$1.0824\ ZrO_{2\ (cr, 974)} \rightarrow 1.0824\ ZrO_{2\ (sol, 974)} \qquad 1.0824(\ 24.25 \pm 0.71)[6]$$

$$1.0824\ ZrO_{2\ (cr, 298)} \rightarrow 1.0824\ ZrO_{2\ (cr, 974)} \qquad 1.0824(\ 45.29 \pm 0.73)[6]$$

$$2\ TiO_{2\ (cr, 298)} \rightarrow 2\ TiO_{2\ (sol, 974)} \qquad 2(\ 55.421 \pm 1.22)[6]$$

$$CaO_{\ (cr, 298)} + CO_{2\ (g, 298)} \rightarrow CaCO_{3\ (cr, 298)} \qquad -178.77 \pm 1.00[3]$$

$$CO_{2\ (g, 974)} \rightarrow CO_{2\ (g, 298)} \qquad -32.06[3]$$

$$CaCO_{3\ (cr, 298)} \rightarrow CaO_{\ (sol, 974)} + CO_{2\ (g, 974)} \qquad 193.4 \pm 0.70[3]$$

$$CaO_{\ (cr, 298)} + ZrO_{2\ (cr, 298)} + 2\ TiO_{2\ (cr, 298)} \rightarrow CaZrTi_2O_{7\ (cr, 298)} \qquad -88.85 \pm 4.293\ kJ/mol$$

Equation 2

$$CaO_{\ (cr, 298)} + ZrO_{2\ (cr, 298)} + 2\ TiO_{2\ (cr, 298)} \rightarrow CaZrTi_2O_{7\ (cr, 298)} \qquad -88.85 \pm 4.293$$

$$Ca_{\ (cr, 298)} + 1/2\ O_{2\ (g, 298)} \rightarrow CaO_{\ (cr, 298)} \qquad -635.09 \pm 0.88[3]$$

$$Zr_{\ (cr, 298)} + O_{2\ (g, 298)} \rightarrow ZrO_{2\ (cr, 298)} \qquad -1100.3 \pm 0.7[5]$$

$$2Ti_{\ (cr, 298)} + 2\ O_{2\ (g, 298)} \rightarrow 2\ TiO_{2\ (cr, 298)} \qquad 2(\ -944.75 \pm 1.26)[3]$$

$$Ca_{\ (cr, 298)} + Zr_{\ (cr, 298)} + 2Ti_{\ (cr, 298)} + 7/2\ O_{2\ (g, 298)} \rightarrow CaZrTi_2O_{7\ (cr, 298)} \qquad -3713.74 \pm 4.782\ kJ/mol$$

Use of the newly determined enthalpy of formation, the average heat capacities, and an estimated entropy $(S(CaTiO_3) + S(ZrTiO_4))$ at Lawrence Livermore National Laboratory in the FACT equilibrium code has resulted in the prediction that zirconolite is the stable phase at 1300°C and that in the presence of excess TiO_2 and decreasing oxygen fugacity, ZrO_2 and $CaTiO_3$ are the thermodynamically stable phases. These predictions are consistent with what is observed experimentally in the synthesis of zirconolite indicating that the enthalpy of formation obtained is reasonable.

Recent successes with a series of cerium aluminates indicate that the energetics of the substitution of Ce^{+4} (as an analog for Pu^{+4} and U^{+4} and other actinides) for Zr^{+4} in zirconolite can now be performed resulting in a significant improvement in the predictive capabilities of current and future process models.

Acknowledgements

References

1. R. C. Ewing, W. Lutze, W. J. Weber, "Zircon: A Host-Phase for the Disposal of Weapons Plutonium," *J Mater. Res.* **10** (2), 243–246 (1995).

2. W. Lutze, R. C. Ewing, *Radioactive Wasteforms for the Future* (Elsevier Science Publishing Company, Inc., New York, NY, 1988).

3 . D. D. Wagman, W. H. Evans, V. B. Parker, R. H. Schumm, I. Halow, S. M. Bailey, K.L. Chumey, R. L. Nuttall, "The NBS Tables of Chemical Thermodynamic Properties. Selected Values for Inorganic and C_1, and C_2 Organic Substances in SI units," *J Phys. Chem. Ref. Data* **11**, (supl. 2) (1982).
    R. A. Robie, B. S. Hemingway, and J. R. Fisher, "Thermodynamic Properties of Minerals and Related Substances at 298.15 K and 1 bar (10^5 Pascals) Pressure and at Higher Temperatures," United States Government Printing Office, Geological Survey Bulletin, 1452 (1976).
    M. W. Chase, Jr, C. A. Davies, J. R. Downey, Jr., D. J. Frurip, R. A. McDonald, A. N. Syverud, "JANAF Thermochemical Tables Third Edition." *J. of Phys. Chem. Ref Data* **14**, (supl. 1) (1985).

4. A. Navrotsky, "Recent Progress and New Directions in High Temperature Calorimetry," *Phys. Chem. Min.* **2**, 89–104 (1997).

    A. Navrotsky, "Recent Progress and New Directions in High Temperature Calorimetry Revisited," to be published in *Phys. Chem. Min.*

5. M. Bolech, E. H. P. Cordfunke, F. J. J. G. Janssen, A. Navrotsky, "Standard Enthalpy of Formation of Lanthanum Zirconate," *J. Am. Ceram. Soc.* **78** (8), 2257–58 (1995).

6. Laboratory results from this study and related studies, Princeton University Department of Geosciences and Princeton Materials Institute.
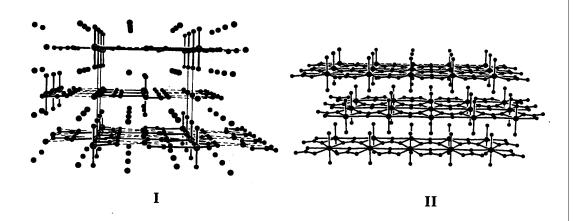
Characterization and Stability of Actinide (U, Np, Pu, Am) Carbonates

The solubility of actinides in aqueous solutions is primarily governed by the solubility product of the actinide bearing solid phase. The understanding of chemical and physical properties of these actinide solids is essential for understanding and predicting actinide solubilities in natural aquifer systems. The present work is directed toward determination of the chemical properties of the An(III), (V), and (VI) (An = U, Np, Pu, Am) carbonate solids and their stabilities in aqueous solutions. X-ray diffraction (XRD), extended x-ray absorption fine structure (EXAFS), differential thermal and thermogravimetric analysis, diffuse reflectance spectroscopy, and Raman spectroscopy have been employed to determine the structure and composition of these solids.

Three types of An(III) carbonate solids of formula $An(OH)(CO_3)$, $An_2(CO_3)_3$, and $NaAn(CO_3)_2$ have been investigated. These solids control the solubility of trivalent actinides under most natural conditions[1,2]. Their stability is dependent on ionic strength and CO_2 partial pressure: at low CO_2 pp the hydroxocarbonate is stable, but transforming into the normal carbonate at higher carbonate concentrations; the double carbonate is found to form in highly concentrated electrolyte solutions, such as saturated NaCl solutions and WIPP brines.

Two types of An(V) carbonates of the general formula $NaAnO_2(CO_3) \cdot xH_2O$ $Na_3AnO_2(CO_3)_2 \cdot xH_2O$ have been reported to form in aqueous solutions.[1,3] At higher sodium carbonate concentrations $Na_3AnO_2(CO_3)_2 \cdot xH_2O$ is stable. These solids consist of AnO_2CO_3 layers with the alkali ions localized between ($NaAnO_2(CO_3) \cdot xH_2O$) and also within the carbonate layer ($Na_3AnO_2(CO_3)_2 \cdot xH_2O$, **(I)**).

$PuO_2(CO_3)$ is isostructural with rutherfordine, $UO_2(CO_3)$.[4] The layered solids contain bidentate and monodentate carbonate groups in the equatorial plane around the actinyl ion (**II**). The actinyl monocarbonates are reported as the predominant solids in the An(VI) carbonate system. However, in highly concentrated sodium chloride solution, the formation of $Na_4AnO_2(CO_3)_3$ has been observed at $[CO_3^{2-}] > 10^{-5}$ M. At decreasing CO_2 partial pressure, the carbonate solids become less stable, and actinyl oxides are formed. The structure of the carbonate solids and the nature of the actinyl(VI) oxide/hydroxides will be discussed. The thermodynamic stability of actinide(III,V,VI) carbonates will be presented.

W. Runde
D. L. Clark
S. D. Reilly
M. P. Neu
P. D. Palmer
C. D. Tait
G. T. Seaborg Institute for Transactinium Science, Lawrence Livermore National Laboratory, and Los Alamos National Laboratory

B. W. Eichhorn
University of Maryland

I

II

References

1. J. Fuger, I. L. Khodakovsky, E. I. Sergeyeva, V. A. Medvedev, J. D. Navratil, *The Chemical Thermodynamics of Actinide Elements and Compounds. Part 12. The Actinide Aqueous Inorganic Compexes.* (IAEA, Vienna, Austria, 1992).

2. Runde, Meinrath, Kim, *Radiochim. Acta*, **58/59**, 93 (1992).

3. Runde, Neu, Clark, *Geochim. Cosmochim. Acta*, **60** (12), 2065 (1996).

4. Clark, Christ, *Am. Miner.*, **41**, 844 (1957).

Chloride Complexation of Actinide Ions (U, Np, Pu, Am)

Actinide solubilities in highly concentrated chloride solutions are about one order of magnitude higher than in similar inert electrolyte ($NaClO_4$) solutions.[1] This increased solubility is due to interactions between actinide and chloride ions. Contradictory results exist regarding the interaction mechanism between actinide and chloride ions. Specifically, both inner-sphere complex formation and ion pair association have been implicated in the interpretation of spectrophotometric and extraction data.[2,3] These techniques cannot differentiate between ion activity changes due to inner-sphere complexation or ion pairing effects. To address this controversy, we investigated the interaction between actinides in the (III), (IV), (V), and (VI) oxidation states and chloride ions using a multi-method approach. Spectroscopic techniques (Raman, UV-Vis absorption, EXAFS) were used to distinguish between changes in the inner coordination sphere of the Pu ion and effects of ion pairing. X-ray absorption spectroscopy and single crystal x-ray diffraction were used to determine structural details of the Pu chloro complexes formed in solution and solid state. Comparison of the Pu chloride complexation with that of analogous light actinides, U(VI), Np(V), and Am(III), is undertaken to determine the structures and stabilities of actinide chloro complexes and to verify the interaction mechanism.
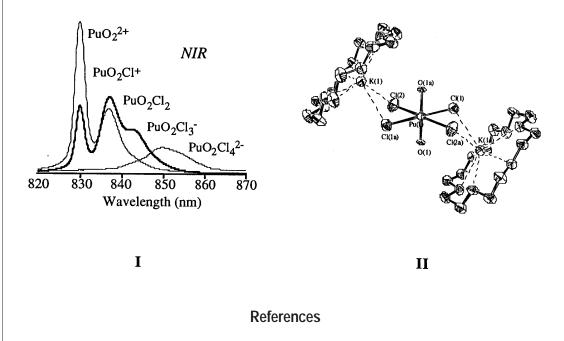
Chloro complexes of actinides are reported to be relatively weak ($\log \beta_1 = -0.1 \pm 0.1$, Am(III), I = 1),[2,3] and high concentrations of chloride are required to replace water molecules in the inner-coordination sphere to form $AnCl_n^{m-n}$ (m = 3,4) or $AnO_2Cl_n^{m-n}$ (m = 1,2) complexes. Recommended stability constants of actinide chloro complexes are used for species distribution calculation.[2] Only about 10 to 20% of the total amount of actinides in the oxidation states III, IV, V, and VI, in 5M NaCl solution should exist as the free aquo ion. Absorption spectra of Am(III) in 5M NaCl and 5M $NaClO_4$ show no significant difference in both the peak location (503.2 nm) and the peak shape. In addition, the fluorescence band of Am^{3+} at 687 nm (excitation wavelength 503.2 nm) is not influenced by the addition of NaCl up to 5 M suggesting an outer-sphere complexation of trivalent actinides with chloride. Similar to Am(III), the spectroscopic evidence for chloride complexation of tetra- and pentavalent actinides is limited. Addition of 5M KCl does not affect the main Np(IV) absorption bands at 723 and 959 nm. In contrast, the absorption spectra of Np(IV) show obvious changes due to the addition of carbonate and the formation of strong Np(IV) carbonato complexes.

Neptunium(V) solubility studies have shown an increase of solubility at $[CO_3^{2-}] < 10^{-3}$ mol kg^{-1} by about one order of magnitude in NaCl compared to that measured in inert electrolyte solutions ($NaClO_4$) at ionic strength I = 5M.[1] These differences in experimental solubility in NaCl and $NaClO_4$ suggest a chloride interaction with Np(V) aquo ion and Np(V) monocarbonato complex. However, the Np(V) absorbance at 980 nm is insignificantly shifted upon addition of NaCl, suggesting a weak outer-sphere interaction.

In contrast, addition of NaCl results in significant changes in the U(VI) and PU(VI) absorption spectra. The main UO_2^{2+} absorption peak at 413.3 nm is shifted to 423.4 nm, and in addition two absorption bands appear at 458.2 and 473.8 nm. An isosbestic point at 392.4 nm at [NaCl] < 1.5 m indicates the existence of only two species, UO_2^{2+} and UO_2Cl^+. At higher NaCl concentrations the absence of an isosbestic point in the absorption spectra indicates the existence of more than two uranyl species in solution, and further chloride complexation of the uranyl ion. The appearance of three new absorption bands centered at 837, 843, and 849 nm are consistent with the formation of $PuO_2Cl_n^{2-n}$ for n = 1-3 (**I**). A shoulder at about

W. Runde
M. P. Neu
D. L. Clark
P. D. Palmer
S. D. Reilly
C. D. Tait
G. T. Seaborg Institute for Transactinium Science, Lawrence Livermore National Laboratory, and Los Alamos National Laboratory

857 nm is observed only at very high chloride concentrations due to the formation of the tetrachloro complex, $PuO_2Cl_4^{2-}$. The limiting chloro species, $AnO_2Cl_4^{2-}$ (An = U, Pu) (**II**), was isolated after addition of 18-Crown-6.

Investigations on the spectroscopic characterization of Pu (III, IV, V) chloro complexes are ongoing to establish the formation of Pu chloro complexes at chloride concentrations relevant for natural aquifer systems (up to 5M [Cl⁻]). The structure and stability of these Pu chloro complexes will be presented and the impact for species distribution and modeling of Pu solubilities will be discussed.

I   **II**

References

1.   W. Runde, M. Neu, D. Clark, *Geochim. Cosmochim. Acta* **60** (12), 2065 (1996).

2.   J. Fuger, I. L. Khodakovsky, E. I. Sergeyeva, V. A. Medvedev, J. D. Navratil, *The Chemical Thermodynamics Actinide Elements and Compounds. Part 12. The Actinide Aqueous Inorganic Compexes* (IAEA, Vienna, Austria, 1992).

3.   I. Grenthe, J. Fuger, R. J. M. Donigs, R. J. Lemire, A. B. Muller, C. Nguyen-Trung, H. Wanner, *Chemical Thermodynamics of Uranium* (Elsevier Science Publishing Company Inc., North-Holland, 1992), Vol. 1.

Synthesis and X-Ray Investigation of New Compounds in the U-Nd-Au-Si System

P. S. Salamakha
L'viv State University, Ukraine

Introduction

With the wealth of information now available on the binary and ternary intermetallic compounds, greater attention should focus on the crystal structure investigation and physical properties study of the multicomponent alloys containing actinides and lanthanides which would have industrial applications. Some attempts have been already done earlier by the author[1,2] as well as by other researches.[3] In continuation of our research on the systematic investigation of intermetallic systems containing actinides and lanthanides as well as in order to accumulate experimental data on the physical properties of multicomponent systems with uranium and neodymium, this work is focused on the synthesis and crystal structure investigation of the quaternary uranium- and neodymium-containing alloys with further study of their physical characteristics.

Experimental Details

The samples were prepared by direct arc melting high-purity components, annealed at 870 K for two weeks in evacuated sealed quartz ampoules and quenched in cold water. Phase analysis was carried out using x-ray powder film data obtained by Debye-Scherrer technique. Lattice constants were determined from the powder patterns (diffractometer DRON-3M, CuK_α radiation). All calculations were performed using the LASY PULVERIX program.

Results

X-Ray Phase Analysis and Crystallographic Characteristics of the U-Au-Si and Nd-Au-Si Compounds

X-ray phase analysis was performed for the 8 alloys which contain 33.3 at. % of U and for the 12 samples which contain 33.3 at. % of Nd. A rather extended homogenous region was observed for the $NdAu_{0.2-0.5}Si_{1.8-1.5}$ compound. The crystallographic characteristics of the revealed compounds are presented in Table 1.

Compound	Structure Type	Space Group	Lattice parameters, nm	
			a	c
UAuSi	AlB_2	P6/mmm	0.4197(2)	0.3976(3)
U_2AuSi_3	AlB_2	P6/mmm	0.4149(4)	0.3994(4)
$UAu_{0.3}Si_{1.7}$	α-$ThSi_2$	$I4_1/amd$	0.4071(3)	1.4066(6)
NdAuSi	AlB_2	P6/mmm	0.4285(4)	0.4192(7)
$NdAu_{0.7}Si_{1.3}$	AlB_2	P6/mmm	0.4274(5)	0.4216(3)
$NdAu_{0.2-0.5}Si_{1.8-1.5}$	α-$ThSi_2$	$I4_1/amd$	0.41768(2)–0.4171(2)	1.39893(9)–1.4352(2)
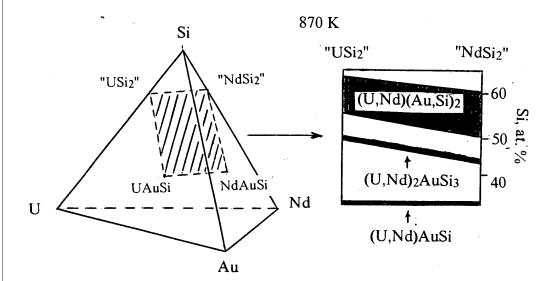
Table 1. Crystallographic data of the ternary U-Au-Si (33.3 at. % of U) and Nd-Au-Si compounds (33.3 at. % of Nd).

Partial Isothermal Section of the U-Nd-Au-Si at 870 K

We have investigated the "USi$_2$"-"NdSi$_2$"-NdAuSi-UAuSi region of the U-Nd-Au-Si at 870 K. A partial phase diagram is shown in Figure 1. Formation of the continuous solid solutions is observed between the ternary isostructural compounds. Crystallographic data for a series of selected quaternary alloys are presented in Table 2.

Compound	Structure Type	Space Group	Lattice parameters, nm	
			a	c
U$_{0.5}$Nd$_{0.5}$AuSi	A1B$_2$	P6/mmm	0.4290(1)	0.4075(4)
UNdAuSi$_3$	A1B$_2$	P6/mmm	0.4235(5)	0.4102(3)
U$_{0.5}$Nd$_{0.5}$Au$_{0.3}$Si$_{1.7}$	a-ThSi$_2$	I4$_1$/amd	0.4174(3)	1.4154(6)

References

1. O. Sologub, P. Salamakha, "Structural Chemistry of New Quaternary Germanides of Uranium," Actinides and the Environment, NATO ASI Advanced Study Institute, Crete, Greece, July 7–19, 1996 (in press).

2. P. Salamakha, O. Sologub, "Synthesis and Crystal Structure of New Quaternary Silicides of Uranium," Actinides and the Environment, NATO ASI Advanced Study Institute, Crete, Greece, July 7–19, 1996 (in press).

3. E. Caspi, M. Kuznetz, H. Ettedgui, H. Pinto, M. Melamud, and H. Shaked, Collected abstracts, 26[iemes] Journes des Actinides, Szklarska Poreba, Poland, April 10–14, 1996, pp. 125–126.

Determination of Thermodynamic Properties of Actinide Elements in Room Temperature Molten Salts

W. H. Smith
D. Costa
F. deRege
Los Alamos National Laboratory

Several processes used in the recovery and purification and of actinide elements are redox-based chemical processes carried out in high-temperature molten salt systems. In spite of the fact that these processes have been in use for many years, few direct measurements of the redox properties of the actinides have been made in these media. This is primarily due to the difficulty of maintaining a stable reference electrode system under the high-temperature conditions used and the corrosive nature of the salts, and due to convective mixing in the melts which upsets the diffusional mode of mass transport which is critical to making accurate thermodynamic measurements.

One way to circumvent these problems is to carry out thermodynamic measurements in room temperature rather that high-temperature molten salt systems. Room temperature molten salts (RTMS) consist of a mixture of aluminum trihalide in combination with an organic halide salt. The systems most studied to date are aluminum trichloride in combination with n-butyl pyridinium or methyl-ethyl-imidizolium chloride. These mixtures are liquid at or near room temperature, are highly conducting, have a very wide potential window, and are capable of establishing a very stable reference electrode. In addition, the acidity or basicity of the melts can be varied over a wide range by varying the aluminum salt to organic salt ratio. This is a distinct advantage over the high-temperature salt systems currently in use, and allows for an evaluation of the degree of chloride ion complexation of the actinide element under investigation. The RTMS systems also have an extremely wide spectroscopic window extending from the ultraviolet to the near infrared. This characteristic allows for spectroscopic characterization of the actinides in addition to electrochemical measurements.

Studies carried out in RTMS systems on actinide elements have been limited to neptunium[1] and uranium,[2–5] with the bulk on the work done on the latter element. This presentation summarizes the uranium/RTMS results obtained from work done in our lab and in previously published results.

The results of electrochemical measurements for selected starting uranium species in both acidic and basic melts is provided in Table I. The first entry, beginning with U^{4+} in an acidic melt, indicates one reversible reduction process to yield U^{3+} and two reversible oxidation processes to yield U^{5+} and U^{6+}, respectively. This behavior is in marked contrast to that observed in aqueous solution where the higher valent species react with solvent to produce the dioxygen adduct uranyl species: $U^{4+} - 2e^- + 2H_2O \Longleftrightarrow UO_2^{2+} + 4H^+$. Since there is no source of oxygen in the molten salt, the higher valent species exist only as solvated ions.

When uranium is added to an acidic melt in the form of UO_2^{2+}, the electrochemical behavior is notably different. First, the redox potentials are all shifted in the negative direction due to the presence of the oxygen ligands. The magnitude of this shift is a measure of the overall formation constant for the uranyl complex and gives an estimated value of $\sim 10^{16}$. Second, the reduction waves are all irreversible, indicating a fast chemical reaction following electron transfer. In this case the uranyl loses one or both oxygens on reduction, similar to behavior in acidic aqueous solution. In fact, even uranyl is not that stable in the acidic melt, reacting to first lose its oxygens to solvent, then undergoing an electron transfer reaction to ultimately produce U^{5+} over a period of several days. The solvent is sufficiently acidic to remove the oxygens in a Lewis type acid-base reaction: $UO_2^{2+} + 4Al_2Cl_7^- \Longleftrightarrow U^{6+} + 2AlOCl_2^- + 6AlCl_4^-$.

Table 1. Summary of uranium redox behavior in RTMS systems.

Melt Composition*	Acidic/Basic	Starting U Species	Redox Couple	Redox Potential**
2 AlCl$_3$: 1 n-BuPyCl	acidic	U^{4+}	U^{6+}/U^{5+}	+2.31
			U^{5+}/U^{4+}	+1.97
			U^{4+}/U^{3+}	+1.00
55 AlCl$_3$: 45 MEIC	acidic	UO$_2^{2+}$	UO$_2^{2+}$/UO$_2^{1+}$	+1.3
			UO$_2^{1+}$/UO$_2^{0}$ (?)	+1.0
			UO$_2^{0}$/UO$_2^{1-}$ (?)	+0.5
45 AlCl$_3$: 55 MEIC	basic	U^{4+}	U^{4+}/U^{3+}	−1.35
45 AlCl$_3$: 55 MEIC	basic	UO$_2^{2+}$	UO$_2^{2+}$/U^{4+}	−0.66
			U^{4+}/U^{3+}	−1.34

* n-BuPyCl = n-butylpyridinium chloride, MEIC = methyl-ethyl-imidazolium chloride.

** All potentials versus Al wire immersed in 2:1 acidic melt.

In basic melts U^{4+} exhibits a single reduction wave to yield U^{3+}. The measured potential for this process is ~ 2.3 volts more negative than the same reduction process in the acidic melt and is due to complexation by free chloride ion. The magnitude of this shift is in this case a measure of the ratio of the overall formation constants for the highest chloro complexes for the two oxidation states, and has an estimated value of ~ 10^{39}. A shift of similar magnitude is observed for the reduction of UO$_2^{2+}$ in the basic melt relative to its reduction potential in the acidic melt. The stability of UO$_2^{2+}$ is much greater in the basic melt than the acidic melt indicating that the acid-base reaction listed above is more favorable than a simple ligand exchange between the oxide dianion and free chloride in solution: UO$_2^{2+}$ + xCl$^-$ <==> UCl$_x^{(6-x)}$ + 2O^{2-}. As in the acidic melt, reduction of UO$_2^{2+}$ in the basic melt occurs with an overall addition of 2 equivalents of electrons and subsequent loss of the oxide ligands to form U^{4+}. In neither the acidic nor the basic melt is the U^{3+} to U^0 reduction observed and is believed to lie just beyond the cathodic solvent limit in both cases.

References

1. J. P. Schoebrechts and B. Gilbert, *Inorg. Chem.* **24**, 2105 (1985).

2. R. De Waele, L. Heerman, and W. D'Olieslager, *J. Electroanal. Chem.* **142**, 137 (1982).

3. P. B. Hitchcock, T. J. Mohammed, K. R. Seddon, J. A. Zora, C. L. Hussey, and E. H. Ward, *Inorg. Chim. Acta* **113**, L25 (1986).

4. L. Heerman, R. De Waele, and W. D'Olieslager, *J. Electroanal. Chem.* **193**, 289 (1985).

5. C. J. Anderson, M. R. Deakin, G. R. Choppin, W. D'Olieslager, L. Heerman, and D. J. Pruett, *Inorg. Chem.* **30**, 4013 (1991).

Synthesis and Structural Chemistry of New Quaternary Germanides and Silicides of Uranium

Introduction

O. L. Sologub
L'viv State University, Ukraine

The fascinating physical properties of lanthanides and actinides turned attention to their alloys, particularly those with transition metals and with elements of the fourth and fifth group of the Mendeleyev Table. A large number of new phases have been synthesized, exhibiting different stoichiometries and variety of crystal structure types. The results of systematic investigations of the RE-T-Ge systems are presented in our earlier paper.[1] Comparing the alloying behavior of neodymium and uranium with germanium and the corresponding transition metals, we have observed an existence of the isotypic series of compounds.[2]

Earlier investigations[3] of the phase equilibria in the uranium-iron (cobalt, nickel)-silicon systems reported on the formation of a variety of ternary compounds which show a manifold of structure types (18 ternary silicides were observed for the uranium-cobalt (nickel)-silicon combination and 13 ternary phases were found in the U-Fe-Si system). A common feature of the U-T-Si systems is the formation of ternary phases within a concentration region from 0 to 33.3 at. % U.

X-ray investigations of the alloys with the $(U_{1-x}Nd_x)T_2Ge_2$, $U_{0.5}Nd_{0.5}TGe$ and $UNdTSi_3$ compositions are the subject of this paper.

Experimental Details

The samples were prepared by direct arc melting high-purity components, annealed at 870 K for two weeks in evacuated sealed quartz ampoules and quenched in cold water. Phase analysis was carried out using x-ray powder film data obtained by Debye-Scherrer technique. Lattice constants were determined from the powder patterns (diffractometer DRON-3M, $CuK\alpha$ radiation). All calculations were performed using LASY PULVERIX program.

Results
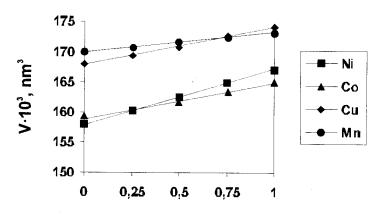
Formation and Crystallographic Characteristics of the $U_{1-x}Nd_xT_2Ge_2$ Compounds

With respect to the knowledge of the existence of the $(U_{1-x}Nd_x)Co_2Ge_2$ solid solution[4] and taking into account the formation of the ternary $U(Nd)T_2Ge_2$ compounds where $T \equiv Mn,Ni,Cu$ ($CeGa_2Al_2$-type), we made an attempt to synthesize the quaternary $(U_{1-x}Nd_x)T_2Ge_2$ alloys (x=0.25, 0.50, and 0.75). The results of the x-ray powder analysis with respect to the position and intensity of the reflections at the diffractograms in all cases confirmed the isotypism with the crystal structure of $CeGa_2Al_2$. The variation of volume of the $(U_{1-x}Nd_x)T_2Ge_2$ compounds versus concentration of Nd is presented in Figure 1. The substitution of uranium by neodymium alters the lattice dimensions and leads to the linear increase of the volume.

The $U_{0.5}Nd_{0.5}TGe$ Compounds

The results of x-ray powder diffraction analysis of the $U_{0.5}Nd_{0.5}TGe$ samples are listed in Table 1. Alloys with the nominal compositions $U_{0.5}Nd_{0.5}MnGe$, $U_{0.5}Nd_{0.5}FeGe$, $U_{0.5}Nd_{0.5}CoGe$, $U_{0.5}Nd_{0.5}AgGe$ resulted in a heterogenous multiphase mixture, i.e., no compound formation was observed.

Figure 1. Volume versus concentration of Nd for the $(U_{1-x}Nd_x)T_2Ge_2$ solid solutions with the $CeGa_2Al_2$-type, $T \equiv Mn, Co$ [4], Ni, Cu.

Legend:
- ■ — Ni
- ▲ — Co
- ◆ — Cu
- ● — Mn

(Y-axis: $V \cdot 10^3$, nm^3, ranging 150 to 175; X-axis: 0, 0.25, 0.5, 0.75, 1)

Formation and Structural Chemistry of the $UNdTSi_3$ Compounds

Phase analysis and crystal data for a series of selected quaternary alloys are presented in Table 1. The single phase samples were obtained in case neodymium and uranium form the isotypic compounds.

Table 1. Crystallographic characteristics of the $U_{0.5}Nd_{0.5}TGe$ and $UNdTSi_3$ compounds.

Compound	Structure type	Space group	Lattice parameters, nm		
			a	b	c
$U_{0.5}Nd_{0.5}NiGe$	TiNiSi	Pnma	0.7170(3)	0.4248(2)	0.762(2)
$U_{0.5}Nd_{0.5}CuGe$	LiGaGe	$P6_3mc$	0.4287(1)		0.7670(1)
$U_{0.5}Nd_{0.5}AuGe$	LiGaGe	$P6_3mc$	0.4433(1)		0.7872(3)
$UNdCoSi_3$	AlB_2	P6/mmm	0.3995(5)		0.4030(2)
$UNdNiSi_3$	AlB_2	P6/mmm	0.4009(3)		0.4055(4)
$UNdCuSi_3$	α–$ThSi_2$	$I4_1/amd$	0.4100(3)		1.3841(3)

References

1. P. S. Salamakha, O. L. Sologub, and O. I. Bodak, "Phase Equilibria and Crystal Chemistry in Ternary Rare Earth Germanium Systems with Metallic Elements," *Handbook on the Physics and Chemistry of Rare Earths*, K. A. Gschneidner Jr. and L. Eyring, Eds. (1997), Vol. 27 (in press).

2. A. M. Aslan, "Phase Equilibria and Crystal Structures of Compounds in the Ternary U-(Co,Ni)-Ge Systems," Ph. D. thesis, L'viv University, Ukraine, (1990), p. 17.

3. L. G. Akselrud, "Investigation on Crystal Chemistry of the Ternary Silicides of Uranium," Ph. D. thesis, L'viv University, Ukraine (1980), p. 17.

4. E. Caspi, M. Kuznetz, H. Ettedgui, H. Pinto, M. Melamud, and H. Shaked, Collected abstracts, 26[iemes] Journees des Actinides, Szklarska Poreba, Poland, April 10–14,1996 pp. 125–126.

X-Ray Absorption Spectroscopy of Plutonium in Different Oxidation States

C. D. Tait
D. L. Clark
S. D. Conradson
M. P. Neu
P. D. Palmer
S. D. Reilly
W. H. Runde
G. T. Seaborg Institute for Transactinium Science, Lawrence Livermore National Laboratory, and Los Alamos National Laboratory

Complete speciation of plutonium complexes include the identification of both the oxidation state and coordination sphere. Four oxidation states (III, IV, V, and VI) of Pu may coexist under environmentally relevant conditions. An efficient method to determine the oxidation state actually present in various matrices would enhance the ability to model the fate and transport of plutonium in process streams and in the environment. This abstract establishes that the L_3 x-ray absorption near edge structure (XANES) spectra of Pu are primarily determined by the valance state and the presence or absence of the trans dioxo moiety, consistent with previous U and Np XANES studies. The edge energies were observed to shift progressively to higher energy with increasing valence, with an average 1.68 eV increase per formal oxidation state increase. In addition, the general spectral shape of the (III) and (IV) species is clearly different from the dioxo-containing (V) and (VI) species, with the first maximum much larger and sharper for the (III) and (IV) spectra than for the (V) and (VI) spectra.

Plutonium L_3 Extended X-ray Absorption Fine Structure (EXAFS) spectra are capable of delineating the coordination sphere around the plutonium in well chosen, single component systems. EXAFS spectra for the aquo complexes of Pu(III, IV, V, and VI) will be presented and structural features will be discussed. In addition to determining the bond distance for the dioxo yl moiety in the V and VI complexes, the bond distance and coordination number of inner sphere water molecules is also examined for each of the oxidation states. With the XANES and EXAFS spectra taken together, a rather full structural picture of plutonium aquo ions is constructed.

Author Index

A

Adamov, E. O.—129, 199
Adams, A. I.—273
Adnet, JM.—239
Alexseyev, P.—213
Allen, P. G.—73, 143
Amrhein, C.—257
Anderson, E. B.—21, 99
Anthony, R. G.—243
Arko, A. J.—93
Assefa, Z.—307
Attrep, Jr., M.—179
Aumeier, S. E.—133

B

Bakel, A. J.—135
Banar, J. C.—171
Barr, E. B.—261
Bartsch, R. A.—233
Bates, J. K.—147
Beauvy, M.—15
Becker, J. D.—101
Beer, P. D.—95
Begg, B. D.—19
Belinski, S. A.—261
Benson, J. M.—261
Berg, J. M.—309
Bernard, H.—29, 229
Bertsch, P. M.—257
Boecker, B. B.—261, 281
Boesch, A.—49
Bogatov, S.—251
Bonchin, S. L.—287
Bondarenko, O. A.—253, 289, 291
Bonnerot, J. M.—15
Boone, S.—171
Borisov, L.—49
Borisov, G. B.—137
Borovoi, A.—251
Bourcier, W.—115, 119
Brainard, J. R.—63
Brandel, V.—23
Brink, C.—293
Bros, P.—49
Brossard, P.—49, 239

Bruno, J.—59
Bucher, J. J.—73, 143
Buck, E. C.—135, 139
Buelow, S. J.—191
Burakov, B. E.—21
Buscher, C. T.—169
Bychkov, A.—239

C

Calloway, R. B.—115
Camarcat, N.—229
Capelle, E.—49
Chamberlain, D. C.—147
Chanin, D. I.—283
Chassigneux, B.—23
Chen, Y. L.—113
Cherkashov, Yu. M.—199
Choppin, G. R.—71, 271
Chung, K.—243
Cisneros, M. R.—309
Clark, D. L.—87, 315, 317, 323, 325, 333
Clark, S. B.—121, 255
Coates, J. T.—263
Condit, R. H.—161
Conley, C. M.—165, 167
Conradson, S. D.—25, 87, 89, 181, 301, 317, 333
Cooper, B. R.—101
Costa, D.—329
Cotter, C. R.—273, 275
Coughlin, J.—115
Cox, L. E.—93, 101
Cremers, D.—163
Cremers, T. L.—177
Cross, J.—293
Curtis, P.—125

D

Dacheux, N.—23
Danis, J. A.—107, 311
Darab, J. G.—143
Davidov, V. K.—199
Day, R. A.—19

Dedov, N. V.—217
deRege, F.—329
Diel, J. A.—281
Dimayuga, F. C.—201
Dinehart, M.—203
Dodge, C. J.—61
Donohoe, R. J.—169
Drake, R.—163
Drew, M. G. B.—95
Duan, Y.—163
Duff, M. C.—257
Duriez, C.—15
Dzekun, E. G.—173

E

Ebbinghaus, B. B.—19, 125, 135, 319
Edelstein, N. M.—73, 143
Edwards, T. B.—117
Efurd, D. W.—67, 171
Egorov, O. B.—297
Eichhorn, B. W.—311, 323
Elliott, M. L.—115, 187
Elzerman, A. W.—263
Eriksson, O.—103
Evans, M.—203
Ewing, R. C.—21
Eyre, J. A.—287

F

Farmer, J.—115
Farr, J. D.—89, 181
Figg, D. J.—163, 293
Filippov, E. A.—173
Finch, G. L.—261
Fjeld, R. A.—121, 263
Fomichenko, P.—213
Forsberg, C. W.—41
Forsmann, J. H.—133
Fortner, J. A.—147
Francis, A. J.—61, 265
Frank, S. M.—111, 155
Friedrich, S. R.—77

G

Gallegos, L. A.—287
Ganev, I. Kh.—129
Gavrilov, S.—251
Genet, M.—23
Gerard, A.—205
Gerth, D. J.—295
Gervais, T.—15
Gibson, J. O.—165, 167
Gillow, J. B.—61
Glagovsky, E. M.—151
Gonis, A.—313
Grate, J. W.—297
Gray, D. W.—299
Griffith, W. C.—261
Grishanin, E.—209, 213, 215
Gruetzmacher, K.—153, 185
Guilmette, R. A.—281
Gurevitch, A.—189

H

Hahn, F. F.—261, 281
Haire, R. G.—11, 89, 307
Hambley, M. J.—19
Hanson, M.—155
Hardy, B. J.—159
Hart, K. P.—19
Hart, R. R.—105, 123
Havrilla, G. J.—79
Hawkins, H. T.—107, 311
Hecker, S. S.—xiii
Helean, K. B.—21
Hersman, L.—63
Hess, N. J.—25
Hill, D.—53
Hines, J. J.—77
Hobbs, C. H.—261
Hobbs, D. T.—235
Hobson, B.—115
Hoffman, D. C.—73, 247
Hoover, M. D.—261, 267, 281
Huang, J. Y.—109, 319
Hunter, D. B.—257